ISSN 2500-316X (Online)

RUSSIAN TECHNOLOGICAL JOURNAL

РОССИЙСКИЙ ТЕХНОЛОГИЧЕСКИЙ ЖУРНАЛ

Information systems.
Computer sciences.
Issues of information security

Multiple robots (robotic centers) and systems.
Remote sensing and nondestructive testing

Modern radio engineering and telecommunication systems

Micro- and nanoelectronics.
Condensed matter physics

Analytical instrument engineering and technology

Mathematical modeling

Economics of knowledge-intensive and high-tech enterprises and industries.
Management in organizational systems

Product quality management. Standardization

Philosophical foundations of technology and society

12+
www.rtj-mirea.ru

14(1) 2026

ISSN 2500-316X (Online)

RUSSIAN TECHNOLOGICAL JOURNAL

РОССИЙСКИЙ ТЕХНОЛОГИЧЕСКИЙ ЖУРНАЛ

- Information systems. Computer sciences. Issues of information security
- Multiple robots (robotic centers) and systems. Remote sensing and nondestructive testing
- Modern radio engineering and telecommunication systems
- Micro- and nanoelectronics. Condensed matter physics
- Analytical instrument engineering and technology
- Mathematical modeling
- Economics of knowledge-intensive and high-tech enterprises and industries. Management in organizational systems
- Product quality management. Standardization
- Philosophical foundations of technology and society

- Информационные системы. Информатика. Проблемы информационной безопасности
- Роботизированные комплексы и системы. Технологии дистанционного зондирования и неразрушающего контроля
- Современные радиотехнические и телекоммуникационные системы
- Микро- и наноэлектроника. Физика конденсированного состояния
- Аналитическое приборостроение и технологии
- Математическое моделирование
- Экономика наукоемких и высокотехнологичных предприятий и производств. Управление в организационных системах
- Управление качеством продукции. Стандартизация
- Мировоззренческие основы технологии и общества

Russian Technological Journal
2026, Vol. 14, No. 1

Russian Technological Journal
2026, том 14, № 1

https://www.rtj-mirea.ru

https://doi.org/10.32362/2500-316X

ISSN 2500-316X (Online)

Russian Technological Journal
2026, Vol. 14, No. 1

Publication date January 30, 2026.

The peer-reviewed scientific and technical journal highlights the issues of complex development of radio engineering, telecommunication and information systems, electronics and informatics, as well as the results of fundamental and applied interdisciplinary researches, technological and economical developments aimed at the development and improvement of the modern technological base.

Periodicity: six times a year.
The journal was founded in December 2013. The titles were «Herald of MSTU MIREA» until 2016 (ISSN 2313-5026) and «Rossiiskii tekhnologicheskii zhurnal» from January 2016 until July 2021 (ISSN 2500-316X).

Founder and Publisher:
Federal State Budget
Educational Institution of Higher Education
«MIREA – Russian Technological University»
78, Vernadskogo pr., Moscow, 119454 Russia.

The journal is included into the List of peer-reviewed science press of the State Commission for Academic Degrees and Titles of Russian Federation. The Journal is included in Russian Science Citation Index (RSCI), Russian State Library (RSL), Science Index, eLibrary, Directory of Open Access Journals (DOAJ), Directory of Open Access Scholarly Resources (ROAD), Google Scholar, Ulrich's International Periodicals Directory.

Editor-in-Chief:
Alexander S. Sigov, Academician at the Russian Academy of Sciences, Dr. Sci. (Phys.–Math.), Professor, President of MIREA – Russian Technological University (RTU MIREA), Moscow, Russia.
Scopus Author ID 35557510600, ResearcherID L-4103-2017, sigov@mirea.ru.

Editorial staff:
Managing Editor — Cand. Sci. (Eng.) Galina D. Seredina
Scientific Editor — Dr. Sci. (Eng.), Prof. Gennady V. Kulikov
Executive Editor — Anna S. Alekseenko
Technical Editor — Darya V. Trofimova
86, Vernadskogo pr., Moscow, 119571 Russia.
Phone: +7 (499) 600-80-80 (#31288).
E-mail: seredina@mirea.ru.

The registration number ПИ № ФС 77 - 81733 was issued in August 19, 2021 by the Federal Service for Supervision of Communications, Information Technology, and Mass Media of Russia.

The subscription index of *Pressa Rossii*: **79641**.

Russian Technological Journal
2026, том 14, № 1

Дата опубликования 30 января 2026 г.

Научно-технический рецензируемый журнал освещает вопросы комплексного развития радиотехнических, телекоммуникационных и информационных систем, электроники и информатики, а также результаты фундаментальных и прикладных междисциплинарных исследований, технологических и организационно-экономических разработок, направленных на развитие и совершенствование современной технологической базы.

Периодичность: 6 раз в год.
Журнал основан в декабре 2013 года. До 2016 г. издавался под названием «Вестник МГТУ МИРЭА» (ISSN 2313-5026), а с января 2016 г. по июль 2021 г. под названием «Российский технологический журнал» (ISSN 2500-316X).

Учредитель и издатель:
федеральное государственное бюджетное образовательное учреждение высшего образования «МИРЭА – Российский технологический университет»
119454, РФ, г. Москва, пр-т Вернадского, д. 78.

Журнал входит в Перечень ведущих рецензируемых научных журналов ВАК РФ, в которых должны быть опубликованы основные научные результаты диссертаций на соискание ученой степени кандидата наук и доктора наук, входит в RSCI, РГБ, РИНЦ, eLibrary, Directory of Open Access Journals (DOAJ), Directory of Open Access Scholarly Resources (ROAD), Google Scholar, Ulrich's International Periodicals Directory.

Главный редактор:
Сигов Александр Сергеевич, академик РАН, доктор физ.-мат. наук, профессор, президент ФГБОУ ВО МИРЭА – Российский технологический университет (РТУ МИРЭА), Москва, Россия.
Scopus Author ID 35557510600, ResearcherID L-4103-2017, sigov@mirea.ru.

Редакция:
Зав. редакцией — к.т.н. Г.Д. Середина
Научный редактор — д.т.н., проф. Г.В. Куликов
Выпускающий редактор — А.С. Алексеенко
Технический редактор — Д.В. Трофимова
119571, г. Москва, пр-т Вернадского, 86, оф. Р-108.
Тел.: +7 (499) 600-80-80 (#31288).
E-mail: seredina@mirea.ru.

Регистрационный номер и дата принятия решения о регистрации СМИ ПИ № ФС 77 - 81733 от 19.08.2021 г. СМИ зарегистрировано Федеральной службой по надзору в сфере связи, информационных технологий и массовых коммуникаций (Роскомнадзор).

Индекс по объединенному каталогу «Пресса России» **79641**.

https://www.rtj-mirea.ru

Editorial Board

Редакционная коллегия

Contents

Содержание

Information systems. Computer sciences. Issues of information security
Информационные системы. Информатика. Проблемы информационной безопасности

UDC 004.042
https://doi.org/10.32362/2500-316X-2026-14-1-7-18
EDN TAUPKU

RESEARCH ARTICLE

Methods for prioritizing the processes of transferring data to central storage

Daniil A. Pushkarev [1, @], Vladimir A. Bogatyrev [1, 2]

[1] *ITMO University, Saint Petersburg, 197101 Russia*
[2] *Saint Petersburg State University of Aerospace Instrumentation (SUAI), Saint Petersburg, 190000 Russia*
[@] *Corresponding author, e-mail: dpushkarev@itmo.ru*

• **Submitted:** 10.06.2025 • **Revised:** 28.07.2025 • **Accepted:** 12.11.2025

Abstract

Objectives. The efficient management of parallel ETL (Extract, Transform, Load) process execution in central data warehouses critically impacts overall processing time. Existing orchestration tools such as Apache Airflow, NiFi, Luigi employ simplified prioritization algorithms which ignore dependency graph topology and resource dynamics, leading to suboptimal scheduling. The objective of this work is to develop and validate a novel task prioritization method for ETL pipelines, aimed at minimizing their total duration through deep analysis of structural features of Directed Acyclic Graphs (DAGs), as well as the use of simulation modeling to evaluate various scheduling strategies under conditions of competition for limited concurrency slots.

Methods. The study proposed a Python simulation model, replicating ETL process execution in an environment with limited concurrency slots. The model generates a DAG which reflects the dependency structure of processes for building a central data warehouse and compares 9 prioritization algorithms. These include basic algorithms (prioritization by minimum/maximum average execution time), topological algorithms (prioritization by minimum/maximum layer level, maximization of dependency count), and hybrid algorithms (splitting slots into queues for minimum and maximum execution time). Experiments were conducted on graphs of a variety of topologies using the developed simulation model.

Results. The hybrid algorithm (slot allocation: 50% for tasks with maximum execution time, 50% for tasks with minimum execution time) demonstrated the highest level of efficiency. It reduced total execution time by 15–17%, when compared to basic algorithms, minimized task idle time by 20–25%, and showed resilience to graph topology variations. A linear combination of optimized coefficients (execution time being the most significant factor) ranked second in terms of efficiency.

Conclusions. Prioritization based on DAG topology analysis and hybrid strategies significantly reduces ETL pipeline execution time. The hybrid algorithm is recommended for implementation in orchestrators, since it balances minimizing pipeline duration and task idle time. A promising area for further study is the development of adaptive algorithms that account for real-time dynamic resource load.

Keywords: ETL orchestration, simulation modeling, dependency graphs, data warehouse, directed acyclic graph

For citation: Pushkarev D.A., Bogatyrev V.A. Methods for prioritizing the processes of transferring data to central storage. *Russian Technological Journal.* 2026;14(1):7–18. https://doi.org/10.32362/2500-316X-2026-14-1-7-18, https://www.elibrary.ru/TAUPKU

Financial disclosure: The authors have no financial or proprietary interest in any material or method mentioned.

The authors declare no conflicts of interest.

НАУЧНАЯ СТАТЬЯ

Методы приоритизации процессов переноса данных в центральное хранилище

Д.А. Пушкарев [1, @],
В.А. Богатырев [1, 2]

[1] *Национальный исследовательский университет ИТМО, Санкт-Петербург, 197101 Россия*
[2] *Санкт-Петербургский государственный университет аэрокосмического приборостроения, Санкт-Петербург, 190000 Россия*
[@] *Автор для переписки, e-mail: dpushkarev@itmo.ru*

• **Поступила:** 10.06.2025 • **Доработана:** 28.07.2025 • **Принята к опубликованию:** 12.11.2025

Резюме

Цели. Эффективное управление параллельным выполнением ETL[1]-процессов в центральных хранилищах данных критически влияет на общее время обработки. Существующие инструменты оркестрации Apache Airflow, NiFi, Luigi используют упрощенные алгоритмы приоритизации, игнорирующие топологию графов зависимостей и динамику ресурсов, что приводит к субоптимальному планированию. Целью данной работы являются разработка и валидация нового метода приоритизации задач в рамках ETL-конвейеров, направленного на минимизацию их общей длительности за счет глубокого анализа структурных особенностей направленных ациклических графов и использования имитационного моделирования для оценки различных стратегий планирования в условиях конкуренции за ограниченные слоты параллелизма.

Методы. Предложена имитационная модель на языке Python, воспроизводящая выполнение ETL-процессов в среде с ограниченными слотами параллелизма. Модель генерирует направленный ациклический граф, отражающий структуру связей процессов для формирования центрального хранилища данных, и сравнивает 9 алгоритмов приоритизации, включая базовые (приоритизация минимального/максимального среднего времени выполнения), топологические (приоритизация минимального/максимального уровня слоя, максимизация числа зависимостей) и гибридные (разделение слотов на очереди для минимального и максимального времени выполнения). Эксперименты проведены на графах различных топологий на основе полученной имитационной модели.

Результаты. Гибридный алгоритм (разделение слотов: 50% для задач с максимальным временем выполнения, 50% – с минимальным) показал наилучшую эффективность: снижение общего времени выполнения на 15–17% по сравнению с базовыми алгоритмами, минимизацию времени простоя задач на 20–25% и устойчивость к вариациям топологии графов. Линейная комбинация с оптимизированными коэффициентами (время выполнения – наиболее значимый фактор) заняла второе место по эффективности.

[1] Извлечение (extract), преобразование (transform) и загрузка (load) данных.

Выводы. Приоритизация на основе анализа DAG[2]-топологии и гибридных стратегий существенно сокращает время выполнения ETL-конвейеров. Гибридный алгоритм рекомендуется для внедрения в оркестраторы как балансирующий минимизацию длительности конвейера и времени простоя задач. Перспективное направление – адаптивные алгоритмы, учитывающие динамическую загрузку ресурсов в реальном времени.

Ключевые слова: оркестрация ETL-процессов, имитационное моделирование, графы зависимостей, хранилище данных, ациклический направленный граф

Для цитирования: Пушкарев Д.А., Богатырев В.А. Методы приоритизации процессов переноса данных в центральное хранилище. *Russian Technological Journal*. 2026;14(1):7–18. https://doi.org/10.32362/2500-316X-2026-14-1-7-18, https://www.elibrary.ru/TAUPKU

Прозрачность финансовой деятельности: Авторы не имеют финансовой заинтересованности в представленных материалах или методах.

Авторы заявляют об отсутствии конфликта интересов.

INTRODUCTION

Every year sees a growth in the amount of data passing through various applications. One of the main tasks facing data storage developers is to collect and store this data Central data warehouses (CDWs) [1, 2] have been proposed as a solution to this problem. These are distributed storage facilities which collect data from all services for further analysis, and provide additional information which businesses can use to their advantage. In this way, CDWs are becoming the center for all business decisions [3].

The repository is populated through the processes of extracting (Extract), transforming (Transform), and loading (Load) data—ETL [2, 4–7]. These processes are complex operations aimed at integrating data from a variety of sources, including relational databases, file systems, and web servers. The first stage involves data extraction which means collecting information from the specified sources. Next, the data undergoes a transformation process, during which it is structured, normalized, and cleaned, in order to improve the quality and consistency of the information. The final stage is loading the prepared data into the target storage to make it available for subsequent analysis and use.

In modern data processing systems, ETL processes play a key role in preparing information. However, with the increase in infrastructure scales and the number of such processes, the problem of effectively managing their execution arises. When dozens or hundreds of ETL tasks interact within a complex architecture, manually determining the order in which they are launched becomes not only labor-intensive, but also risks suboptimal results. The sequence of process execution directly affects the overall data processing time. Competition for computing resources, cascading delays due to dependencies between tasks, and suboptimal load distribution can multiply the execution time of the entire process pipeline. For example, a delay in a process which provides data for several subsequent stages can cause a chain reaction of downtime. In order to resolve this problem, not only do prioritization methods need to be implemented, but also the architecture of the ETL system needs to be clearly modeled.

Complex interrelationships between processes, including explicit data dependencies, in which the output of one task serves as the input for another, and hidden constraints (memory resources, network bandwidth), can be visualized using directed acyclic graphs (DAGs) [8].

Directed acyclic graphs are accepted as the standard tool for modeling data extraction, transformation, and loading processes. This is due to their key properties which ensure reliability, efficiency, and transparency of data processing [2, 7, 8]. The acyclic nature of the structure guarantees the absence of infinite cycles, critical for ensuring the completion of tasks in data processing pipelines, especially when working with large amounts of information. The graph data structure allows the execution of interdependent tasks to be controlled, which is important when building data warehouse filling processes (for example, data extraction always precedes data transformation). In addition, thanks to its structure a directed acyclic graph allows parallel tasks to be worked on efficiently. This also allows the dependencies between different stages of data processing to be visualized. Thus, the tasks represented in the graph are independent and can be performed simultaneously.

Orchestration tools such as Apache Airflow [9–11] provide basic mechanisms for defining dependencies, but effective prioritization requires more detailed analysis which takes into account dynamically changing loads, the criticality of business metrics, and which predict bottlenecks. Without a systematic approach to describing the architecture and formalizing the rules for ordering processes, there is a risk that they will be executed in a sequence which is far from optimal. This is particularly critical in the context of near real-time analytics.

[2] Directed acyclic graph – ориентированный ациклический граф.

Despite the significant practical importance of optimizing ETL pipelines, the number of specialized studies on task prioritization in this area remains limited. Most existing orchestrators[3, 4] (Apache Airflow, NiFi, Luigi) [6, 10–12] use simplified strategies such as first-in-first-out or static priorities set by the user based solely on their empirical experience. Significant achievements exist in the related field of real-time systems, in which the DAG model is also widely used [13]. These studies solve the problem of guaranteed adherence to strict deadlines for parallel tasks on multiprocessor systems, using the concept of parallel progression of selected paths in a graph with sub-task prioritization and complex worst-case response time analysis.

Despite their common foundation in directed acyclic graphs, the goals and conditions of ETL optimization differ fundamentally from real-time planning. Firstly, ETL focuses on minimizing the average pipeline execution time and task downtime with flexible parallelism, while real-time systems require guarantees of deadline compliance with strict resource allocation. The probability of completing requests within a given time and the readiness coefficient for completing requests within a given time can be used as metrics for real-time systems [14, 15]. Secondly, the performance metrics differ. For ETL, the total duration and resource utilization are critical, rather than worst-case analysis.

The direct application of methods for improving the efficiency of real-time systems (including path selection algorithms) in an ETL context is suboptimal. Their excessive complexity and reservation requirements lead to underutilization of resources, ignoring at the same time the specifics of data storage layers and the dynamic constraints of orchestrators. Static approaches to real-time assurance are poorly adapted to load changes, in which hybrid strategies are more efficient. Thus, despite the formal similarity of the models, the difference in operational requirements and metrics necessitates the development of specialized prioritization methods for ETL, which justifies this study.

An analysis of existing ETL prioritization methods [16, 17] reveals significant limitations in current approaches:

- The proposed algorithms do not take into account the topological characteristics of process graphs which negatively affects the efficiency of planning in distributed systems;
- The predominant method of prioritization remains static. It is based on user labels for individual tasks and does not take into account the dynamics of execution and the mutual influence of processes in the pipeline.

The aim of this work is to develop and justify a method for prioritizing ETL processes which minimizes the execution time of the entire data pipeline using system analysis and simulation modeling methods.

This study proposes a simulation model which enables ETL process management in complex architecture environments to be analyzed. The model recreates an environment in which a directed acyclic graph is generated, reflecting the chains of ETL task execution which form a theoretical data warehouse. Each directed acyclic graph models dependencies between processes and time constraints. A key feature of the approach is the ability to compare different prioritization algorithms under identical conditions, providing an objective assessment of their effectiveness. This allows not only the execution of processes to be visualized within a centralized data warehouse, but also the impact of the selected algorithm on the overall duration of the pipeline to be quantitatively assessed. For example, by varying the number of nodes, the depth of dependencies, or the duration of a single task, it is possible to determine which algorithm demonstrates the best results in which scenarios. The results of the model generate metrics for comparison such as average execution time and percentage of resource downtime, forming the basis for an informed choice of optimization method in real-world conditions. Thus, the simulation model serves as a tool for systematic analysis of ETL orchestration, minimizing the risks of implementing ineffective solutions in industrial systems.

1. FORMALIZATION OF THE TASK

As part of this work, we will formalize the task of orchestrating ETL processes and will also establish a number of constraints necessary for its solution. The orchestration task includes several key stages: defining priorities for tasks; controlling the number of processes running simultaneously; and managing changes in task statuses according to their current status.

It should be emphasized that the study will not analyze the load on the target computing system. Instead, a variable will be introduced to regulate the load on the system, in order to determine the maximum number of simultaneously active tasks–slots. This is a common approach in similar tools. For example, Apache Airflow has a parameter for the number of available computing slots[5], responsible for the total

[3] https://nifi.apache.org/. Apache NiFi. Apache Software Foundation. Accessed January 10, 2025.

[4] https://www.informatica.com/. Informatica. Informatica LLC. Accessed January 12, 2025.

[5] https://airflow.apache.org/docs/apache-airflow/stable/configurations-ref.html. Airflow Configuration Reference. Accessed January 20, 2025.

number of tasks which can be executed simultaneously across all processes. In addition, an additional restriction will be imposed. Once a specific process is started, its execution cannot be suspended until that process is completed. Resources will only become available once it has finished running.

Let us formulate the optimization problem for the orchestration process. Let **G** = (**V**, **E**) be a directed acyclic graph, in which **V** is a set of processes and **E** is a set of dependencies between them. In the case where the maximum number of simultaneously executing processes is limited to one, the problem can be solved using the classic method of topological sorting. Topological sorting is a linear ordering of the vertices of a directed acyclic graph, in which for each directed edge from vertex A to vertex B, the condition that A precedes B in this ordering is satisfied. Applying topological sorting to graph **G** allows us to obtain a sequence of process execution which satisfies all the established dependencies.

For this task, we can use the following notations: $\mathbf{P} = \{p_1, p_2, \ldots, p_n\}$ is the set of processes; $\mathbf{D}(p_i)$ set of processes upon which the process p_i depends; t_i is the execution time of each process.

The objective is to minimize the total execution time of all processes, taking their dependencies into account. This optimization problem can be written as follows:

$$\text{minimize}\, T_{\text{total}} = \sum_{i=1}^{n} t_i, \quad (1)$$

provided that for each process p_i the following condition holds: p_j is executed before p_i if $p_j \in \mathbf{D}(p_i)$.

However, with such a formulation of the problem, in which only one process can be launched at a time, we obtain a single solution. This is the sum of the execution times of all processes:

$$T_{\text{total}} = \sum_{i=1}^{n} t_i.$$

If N processes can be run simultaneously (in parallel), this solution may not be unique. Given this formulation, the new optimization problem can be described as follows:

1. Let us define a set of active processes $\mathbf{A}(t)$ which can be launched at time t.
2. Let $C(t) \le N$ be the number of processes which can be launched at time t.
3. The execution time of all processes will now depend on the parallelism of their execution.

The general objective remains the same—minimizing the total execution time (1).

2. SIMULATION MODELING OF ORCHESTRATION

Comparing different prioritization algorithms upon real data in a computing cluster can be challenging for several reasons. Firstly, individual experiments can take several hours to complete. Secondly, running multiple parallel processes requires significant cluster computing power. Therefore, it makes sense to consider a simulation model which would reproduce the behavior of a similar system while minimizing time and computational resources.

The simulation of parallel execution of tasks with a limited number of slots was implemented using a discrete-event modeling approach with a custom event scheduler based on a priority queue, implemented in Python. Python was chosen for implementing the simulation model due to its combination of advantages, corresponding to the specifics of the research problem. This programming language provides a well-developed ecosystem of scientific libraries which significantly simplify model implementation. Furthermore, Python's integration with visualization tools and data processing capabilities simplifies model validation and interpretation of experimental metrics.

The operation algorithm includes four key stages. First, a list of running tasks is generated. At this stage, the program analyzes the directed acyclic graph and adds processes to the queue, the dependencies of which are already fulfilled (for example, parent nodes in the graph are completed or missing). The current priority of these processes is the highest among available tasks. This is implemented by checking the status of nodes in a directed acyclic graph and sorting them according to specified prioritization rules (for example, based on the layer value at which the process is running). Second, the minimum execution time among all active tasks in the list is determined: this is the time it takes for at least one of the tasks to complete. Third, this value is added to the total pipeline execution time, thus moving the system forward in time by this amount. Finally, for all running tasks, their remaining execution time is reduced by the calculated minimum value. Completed processes are marked as completed, updating the dependency graph for subsequent iterations. This approach effectively emulates the concurrent execution of tasks, taking into account both the logical dependencies between them and the dynamics of resource allocation, providing flexibility for testing various prioritization algorithms within a single model.

Let us consider the data upon which the experiments will be conducted. A classic data warehouse has a layered structure [1, 7, 18, 19].

Operational data storage. Stores operational, often current, detailed data which has not yet been aggregated. This layer serves as a source of operational information for reporting and can be directly used to build higher-level layers.

Detailed data layer. A centralized repository of integrated data collected from one or more disparate sources. The data is structured specifically for querying and analysis.

Data marts. A subset of a data storage focused on a specific area of activity or team. Data maps are developed with specific needs or analysis in mind.

There are situations in which the number of layers may exceed three. This parameter is determined by the specific application conditions. However, the most common implementation option is three-layer architecture: the architecture proposed by Ralph Kimball [1] and the medallion architecture [13, 20].

In this study, directed acyclic graphs were generated to ensure maximum coverage of diverse scenarios. The generation was performed using the following methodology:

- Number of layers is 3. This number is most common when forming a data storage.
- The total number of nodes (processes) for each graph was generated according to a uniform distribution in the range from 250 to 400.
- The nodes were distributed among the layers in accordance with Table 1.
- Additionally, links were added within the layers of the detail layer and data marts to model complex transformations. Each node had up to two random predecessors within its layer (the probability of establishing a link was 0.1, the Pareto distribution for the number of links). After generating the links, a check for cycles was performed in order to exclude links that could cause a given cycle. The total number of links per node does not exceed 10.
- The execution time of each node was assigned independently, and uniformly distributed in the range from 100 to 5000 s. No relationship was established between execution time, layer, or node degree.

Table 1. Percentage of tables relative to the layer

Layer	Share of tables
Source data storage	30–40%
Integrated repository of a structured data ready for analysis	30–40%
Specialized subset focused on a specific subject area	20–30%

In order to evaluate the performance of nine prioritization algorithms, each algorithm was run on each generated directed acyclic graph. Experiments were conducted for varying numbers of parallelism slots to assess the impact of increasing this parameter on the performance of the algorithm.

3. PRIORITIZATION ALGORITHMS

Task prioritization is a process in which the priority level of each individual task is determined based upon its characteristics and relationships with other tasks. This priority level can be random or determined based on the parameters of a specific task, its position, and its relationships with other elements. Let us consider several possible prioritization algorithms.

Random selection. This algorithm operates on the principle of equal priority. This means that any process that can be launched at a given moment will be activated with equal probability. This solution is not optimal and is more of a baseline solution used for comparison with alternative approaches.

Minimum execution time. Processes with the shortest execution time are executed first.

Maximum execution time. Processes with the longest execution time are executed first.

Maximizing the number of dependencies. The algorithm is based on the number of processes dependent on each process.

Hybrid time algorithm. This approach divides the available computing slots of the ETL system into two parts. The first part is allocated to execute the tasks with the highest priority according to the maximum execution time strategy. The second part is allocated to execute the tasks with the highest priority according to the minimum execution time strategy.

Recursive maximization of the number of dependencies. An algorithm which takes into account the number of dependent tasks not only of the current process, but also of all downstream processes that depend on this one.

Minimum layer level. An algorithm based on the layer level within which a given ETL process is executed. The operational layer corresponds to level 0, the detailed layer to level 1, and the data mart layer to level 2. If there are more layers, they are classified similarly according to the graph topology.

Maximum layer level. An algorithm which prioritizes processes at a higher layer level.

Linear combination. This approach integrates all parameters into a single model. For prioritization, a linear combination of features and their corresponding coefficients is constructed. The following criteria are selected as parameters: execution time, number

of dependent processes, and layer level. The resulting linear combination has the following form:

$$t_i x_1 + p_i x_2 + l_i x_3,$$

wherein x_1, x_2, x_3 are constants, l_i is the layer level of the ith process.

When using this combination, the appropriate coefficients need to be selected. For this purpose, optimization algorithms were used, in which each iteration runs the simulation model with a new parameter vector **X**, resulting in the overall execution time of the model. This time must be minimized.

4. EXPERIMENTAL RESULTS

Based on the requirements described above, 50 graphs were generated representing the different architectures of ETL processes which fill the data storage.

Let us consider the process of selecting coefficients for an algorithm based on a linear combination. In order to determine the optimal values for these coefficients, N graphs were selected, which were run with predetermined coefficients x_i. The objective of the optimization model is to minimize the total execution time of all N graphs. Thus, the coefficients are selected not for a specific model, but rather generalized for various graph topologies. This approach is necessary because in real-world applications of the algorithm it may be impossible to select such parameters.

The following methods were selected as optimization algorithms for solving this problem: Powell's algorithm; the COBYLA method (from Constrained Optimization BY Linear Approximations); the Nelder–Mead algorithm; and the Conjugate Gradient (CG) method. The implementation of these algorithms is taken from the SciPy library, optimize module[6]. The results of the optimization algorithms are presented in Table 2.

Table 2. Results of solving the optimization problem for a linear combination

Model	Iterations	Execution time	Coefficients
Powell	193	32282	2.58792896, 2.66311897, −1.85081307
CG	43	32385	$2.10667215 \cdot 10^{-5}$, $4.67212040 \cdot 10^{-5}$, 0
COBYLA	26	32274	1.1580144, 0.80662082, 1.44364821
Nelder–Mead	**109**	**30193**	**−3.68735705, 0.75631002, 0.5**

The best result was obtained using the Nelder–Mead algorithm. Based on the coefficients obtained, it can be concluded that this algorithm identified execution time as the most influential parameter for process prioritization.

The algorithm was applied to a set of graphs not included in the training set. The result was the total processing time of all processes in these graphs for various values of the number of available slots parameter (Fig. 1).

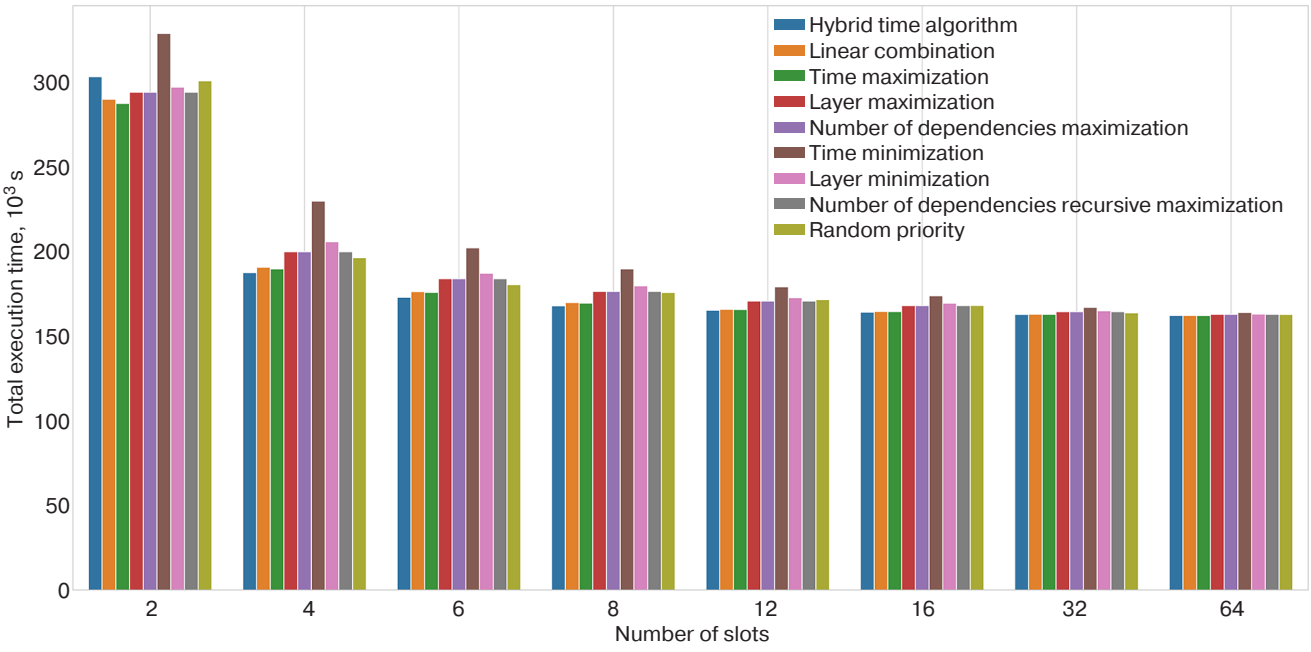

Fig. 1. Orchestration results of the presented algorithms (colors are indicated in order from left to right)

[6] https://docs.scipy.org/doc/scipy/reference/generated/scipy.optimize.minimize.html. Accessed January 27, 2025.

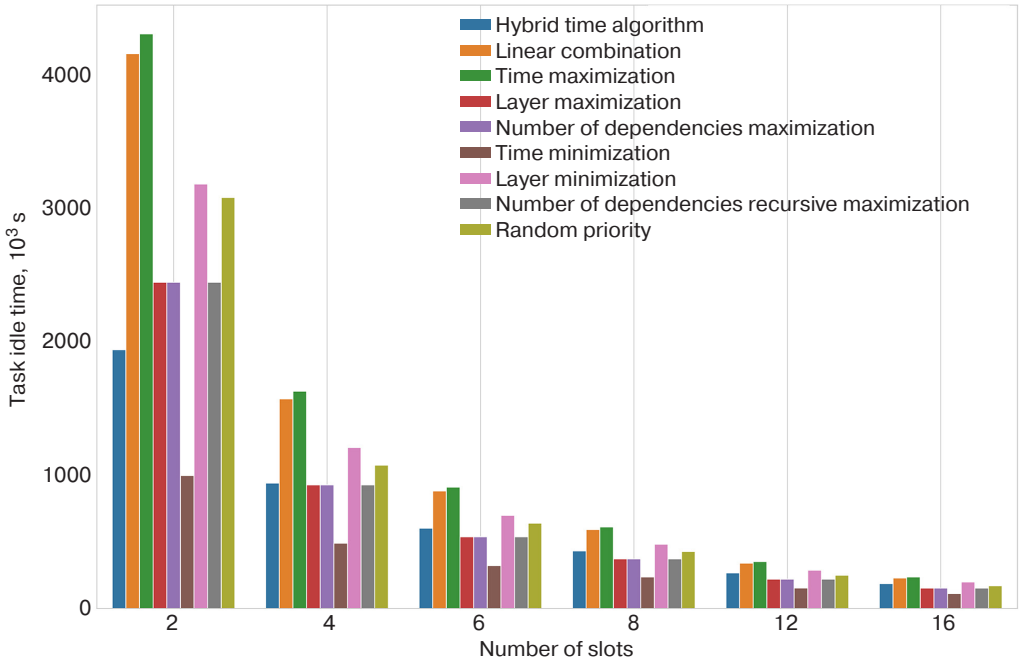

Fig. 2. Tasks idle time for different algorithms

To assess the efficiency of task servicing in the queue, we introduce an additional metric—task idle time. It is calculated as the total time spent in the queue by tasks ready to run. The results of this metric are presented in Fig. 2.

The results of the study demonstrate that the algorithm for prioritizing tasks with maximum execution time provides the best overall execution time for ETL processes only under conditions of limited parallelism. This is when the number of concurrently executing tasks (slots) is no more than two. Under such conditions, this algorithm minimizes the impact of long-running tasks as bottlenecks, preventing their blocking effect on the completion of the entire queue.

However, as the degree of parallelism increases, the hybrid algorithm, which divides the queue into two equal parts—one for tasks with minimum and one for maximum execution time—outperforms the algorithm which maximizes execution time based on total execution time. This is due to the ability of the hybrid approach to efficiently allocate resources. Dedicated slots for short tasks enable the queue to be quickly cleared of small operations, while slots for long-running tasks ensure their continuous execution without downtime. Furthermore, the hybrid algorithm significantly reduces the idle time of tasks in the queue, when compared to the time-maximizing algorithm. However, it is inferior in this respect to the algorithm that prioritizes tasks with minimum execution time.

The discrepancy regarding idle time, where minimizing time yields the lowest values and maximizing time yields the highest, can be explained by the fundamental difference in their optimization goals. An algorithm which prioritizes tasks with the shortest execution times ensures their rapid completion. This dramatically reduces the waiting time for most tasks in the queue. An algorithm which prioritizes tasks with the longest execution times starts processing the longest tasks, forcing short operations to accumulate and remain idle for the entire duration of long processes. For example, if a queue contains one 10-h task and twenty 1-min tasks, prioritizing long processes will cause all short tasks to wait for the entire duration of the 10-h operation, creating colossal cumulative idle time.

Thus, an algorithm which prioritizes long-running processes optimizes the overall queue completion time by concentrating resources on long-running operations, while an algorithm which prioritizes tasks with minimal execution time sacrifices the processing speed of long-running tasks in order to minimize the waiting time for most operations. A hybrid algorithm mitigates this tradeoff, achieving a balance between the two metrics while demonstrating the best result in terms of the duration of the entire pipeline of tasks.

CONCLUSIONS

This article proposes a combination of a methodological approach and tool solutions for optimizing ETL pipelines adapted to dynamic execution conditions. Unlike classical studies which focus on static prioritization or isolated algorithm analysis, the proposed model integrates task execution simulation, while taking into account resource constraints and the topological

characteristics of the process chain which generates the data warehouse's content.

The study demonstrated that prioritization based on the topology of process links is feasible and can reduce the overall execution time of a data pipeline. Thus, the optimal choice of prioritization algorithm can significantly reduce overall idle time. This will impact the overall duration of processes, as demonstrated by a hybrid algorithm that divides the queue into a queue of tasks with the shortest execution time and those with the longest execution time.

The results of the study have significant practical value for optimizing the design and operation of ETL processes in modern data warehouses and data lakes. The developed hybrid prioritization algorithm demonstrated experimental results which reduced the overall execution time of data pipelines by 15–17% compared to alternative algorithms. A key advantage for its practical implementation is the architectural flexibility of the algorithm. It can be implemented as a custom component for popular open-source orchestration systems, such as Apache Airflow. This integration enables increased efficiency in the utilization of cluster computing resources with minimal modifications to the existing infrastructure.

A promising area for further research is the development and evaluation of adaptive prioritization algorithms capable of dynamically accounting for the current load of centralized data storage computing resources in real time. While a strategy based on maximum task duration has proven effective under static conditions, ETL pipeline performance largely depends on the actual availability of resources such as computer cores, memory, disk subsystem bandwidth, and network capacity, which can fluctuate significantly during execution. Integrating resource monitoring systems and using these dynamic metrics as additional input parameters for the prioritization algorithm will pave the way for more flexible and responsive systems. This approach will potentially enable the optimization of task allocation not only at the planning stage but also during execution. This will also promptly increase the priority of tasks, the execution of which can be accelerated by a temporary surplus of a particular resource, or by downgrading resource-intensive tasks during peak load periods. This will thereby minimize overall execution time and reduce the risk of downtime due to resource shortages. The study of the effectiveness of various strategies for combining predicted task durations with actual resource metrics is of significant scientific and practical interest.

Authors' contributions

D.A. Pushkarev—conceptualization, methodology, software, validation, writing—original draft preparation, visualization.

V.B. Bogatyrev—conceptualization, methodology, writing—review and editing, supervision.

All authors have read and approved the published version of the manuscript.

REFERENCES

1. Kimball R., Ross M. *The Data Warehouse Toolkit: The Definitive Guide to Dimensional Modeling.* 3nd ed. Kimball group. Wiley; 2013, 608 p.
2. Simitsis A., Skiadopoulos S., Vassiliadis P. The History, Present, and Future of ETL Technology. In: *DOLAP, CEUR Workshop Proceedings*. 2023;3369:3–12.
3. Tian W. Enhancing Financial Decision-Making Through Automated Business Intelligence Systems. *Int. J. e-Collaboration* (*IJeC*). 2025;21(1):1–20. Available from URL: https://www.igi-global.com/article/enhancing-financial-decision-making-through-automated-business-intelligence-systems/367575. Accessed January 20, 2025.
4. El-Sappagh S.H.A., Hendawi A.M.A., El Bastawissy A.H. A proposed model for data warehouse ETL processes. *Journal of King Saud University – Computer and Information Sciences* (*J. King Saud Univ.*). 2011;23(2):91–104. https://doi.org/10.1016/j.jksuci.2011.05.005
5. Wijaya R., Pudjoatmodjo B. An overview and implementation of extraction-transformation-loading (ETL) process in data warehouse. In: *2015 3rd International Conference on Information and Communication Technology* (*ICoICT*). 2015. P. 70–74. https://doi.org/10.1109/ICoICT.2015.7231399
6. Kuzmina Yu.V., Kubanskikh O.V. Brief description of the ETL process. *Uchenye Zapiski Bryanskogo Gosudarstvennogo Universiteta = Scientific Notes of the Bryansk State University.* 2017;1(5):33–36 (in Russ.). https://www.elibrary.ru/zmwlez
7. Dhaouadi A., Bousselmi K., Gammoudi M.M., Monnet S., Hammoudi S. Data Warehousing Process Modeling from Classical Approaches to New Trends: Main Features and Comparisons. *Data*. 2022;7(8):113. https://doi.org/10.3390/data7080113
8. Vassiliadis P., Simitsis A., Skiadopoulos S. Graph-Based Modeling of ETL Activities with Multi-level Transformations and Updates. In: Tjoa A.M., Trujillo J. (Eds.). *Data Warehousing and Knowledge Discovery. Part of the book series*: *DaWaK 2005*. *Lecture Notes in Computer Science*. 2005. V. 3589. P. 43–52. https://doi.org/10.1007/11546849_5
9. Yasmin J., Wang J.A., Tian Y., Adams B. An empirical study of developers' challenges in implementing Workflows as Code: A case study on Apache Airflow. *J. Syst. Software.* 2024;219(5):112248. https://doi.org/10.1016/j.jss.2024.112248

10. Mikhailov A.N. Using Apache Airflow for Data Processing Orchestration. *Vestnik Nauki.* 2024;10(79):783–787 (in Russ.). https://www.elibrary.ru/ijihms
11. Gromov N.D., Platoshin A.I., Panov A.V. Comparative analysis of tools and platforms for automation of ETL processes in modern data warehouses. *Mezhdunarodnyi zhurnal gumanitarnykh i estestvennykh nauk = International Journal of Humanities and Natural Sciences.* 2023;11-4(86):46–48 (in Russ.). https://doi.org/10.24412/2500-1000-2023-11-4-46-48
12. Zhdanov D.E. Building ETL Processes Based on Cron and Luigi Task Orchestrator. *Aktual'nye issledovaniya = Current Research*. 2023;46-1(176):63–68 (in Russ.). https://www.elibrary.ru/nenikj
13. Ueter N., Günzel M., Brüggen G., Chen J. Parallel Path Progression DAG Scheduling. *IEEE Transactions on Computers*. 2023;72(10):3002–3016. https://doi.org/10.1109/TC.2023.3280137
14. Bogatyrev V.A., Bogatyrev S.V., Bogatyrev A.V. Assessment of the readiness of a computer system for timely servicing of requests when combined with informational recovery of memory after failures. *Nauchno-tekhnicheskii vestnik informatsionnykh tekhnologii, mekhaniki i optiki = Scientific and Technical Journal of Information Technologies, Mechanics and Optics.* 2023;23(3):608–617 (in Russ.). https://doi.org/10.17586/2226-1494-2023-23-3-608-617
15. Bogatyrev V.A., Bogatyrev S.V., Bogatyrev A.V. Recovery of Real-Time Clusters with the Division of Computing Resources into the Execution of Functional Queries and the Restoration of Data Generated Since the Last Backup. In: Vishnevskiy V.M., Samouylov K.E., Kozyrev D.V. (Eds.). *Distributed Computer and Communication Networks: Control, Computation, Communications*. Book series: *Lecture Notes in Computer Science* (*including subseries Lecture Notes in Artificial Intelligence and Lecture Notes in Bioinformatics*). 2024. V. 14123. P. 236–250. https://doi.org/10.1007/978-3-031-50482-2_19
16. Karagiannis A., Vassiliadis P., Simitsis A. Scheduling strategies for efficient ETL execution. *Inform. Syst.* 2013;38(6): 927–945. https://doi.org/10.1016/j.is.2012.12.001
17. Topcuoglu H., Hariri S., Min-You Wu. Performance-Effective and Low-Complexity Task Scheduling for Heterogeneous Computing. *IEEE Trans. Parallel Distrib. Syst*. 2007;13(3):260–274. https://doi.org/10.1109/71.993206
18. Strengholt P. *Building Medallion Architectures*. 1st ed. Sebastopol (CA): O'Reilly Media; 2024, 209 p.
19. Serra J. *Deciphering Data Architectures*. 1st ed. Sebastopol (CA): O'Reilly Media; 2024, 146 p.
20. Blažić G., Poščić P., Jakšić D. Data warehouse architecture classification. In: *2017 40th International Convention on Information and Communication Technology, Electronics and Microelectronics* (*MIPRO*). 2017. P. 1491–1495. https://doi.org/10.23919/MIPRO.2017.7973657

СПИСОК ЛИТЕРАТУРЫ

1. Kimball R., Ross M. *The Data Warehouse Toolkit: The Definitive Guide to Dimensional Modeling.* 3nd ed. Kimball group. Wiley; 2013, 608 p.
2. Simitsis A., Skiadopoulos S., Vassiliadis P. The History, Present, and Future of ETL Technology. In: *DOLAP, CEUR Workshop Proceedings*. 2023;3369:3–12.
3. Tian W. Enhancing Financial Decision-Making Through Automated Business Intelligence Systems. *Int. J. e-Collaboration* (*IJeC*). 2025;21(1):1–20. URL: https://www.igi-global.com/article/enhancing-financial-decision-making-through-automated-business-intelligence-systems/367575. Дата обращения 20.01.2025. / Accessed January 20, 2025.
4. El-Sappagh S.H.A., Hendawi A.M.A., El Bastawissy A.H. A proposed model for data warehouse ETL processes. *Journal of King Saud University – Computer and Information Sciences* (*J. King Saud Univ.*). 2011;23(2):91–104. https://doi.org/10.1016/j.jksuci.2011.05.005
5. Wijaya R., Pudjoatmodjo B. An overview and implementation of extraction-transformation-loading (ETL) process in data warehouse. In: *2015 3rd International Conference on Information and Communication Technology* (*ICoICT*). 2015. P. 70–74. https://doi.org/10.1109/ICoICT.2015.7231399
6. Кузьмина Ю.В., Кубанских О.В. Краткое описание процесса ETL. *Ученые записки Брянского государственного университета*. 2017;1(5):33–36. https://www.elibrary.ru/zmwlez
7. Dhaouadi A., Bousselmi K., Gammoudi M.M., Monnet S., Hammoudi S. Data Warehousing Process Modeling from Classical Approaches to New Trends: Main Features and Comparisons. *Data*. 2022;7(8):113. https://doi.org/10.3390/data7080113
8. Vassiliadis P., Simitsis A., Skiadopoulos S. Graph-Based Modeling of ETL Activities with Multi-level Transformations and Updates. In: Tjoa A.M., Trujillo J. (Eds.). *Data Warehousing and Knowledge Discovery. Part of the book series*: *DaWaK 2005*. *Lecture Notes in Computer Science*. 2005. V. 3589. P. 43–52. https://doi.org/10.1007/11546849_5
9. Yasmin J., Wang J.A., Tian Y., Adams B. An empirical study of developers' challenges in implementing Workflows as Code: A case study on Apache Airflow. *J. Syst. Software.* 2024;219(5):112248. https://doi.org/10.1016/j.jss.2024.112248
10. Михайлов А.Н. Использование Apache Airflow для оркестрации процессов обработки данных. *Вестник науки*. 2024;10(79):783–787. https://www.elibrary.ru/ijihms
11. Громов Н.Д., Платошин А.И., Панов А.В. Сравнительный анализ средств и платформ для автоматизации ETL процессов в современных хранилищах данных. *Международный журнал гуманитарных и естественных наук.* 2023;11-4(86):46–48. https://doi.org/10.24412/2500-1000-2023-11-4-46-48
12. Жданов Д.Е. Построение ETL процессов на базе Cron и оркестратора задач Luigi. *Актуальные исследования*. 2023;46-1(176):63–68. https://www.elibrary.ru/nenikj
13. Ueter N., Günzel M., Brüggen G., Chen J. Parallel Path Progression DAG Scheduling. *IEEE Transactions on Computers*. 2023;72(10):3002–3016. https://doi.org/10.1109/TC.2023.3280137

14. Богатырев В.А., Богатырев С.В., Богатырев А.В. Оценка готовности компьютерной системы к своевременному обслуживанию запросов при его совмещении с информационным восстановлением памяти после отказов. *Научно-технический вестник информационных технологий, механики и оптики.* 2023;23(3):608–617. https://doi.org/10.17586/2226-1494-2023-23-3-608-617
15. Bogatyrev V.A., Bogatyrev S.V., Bogatyrev A.V. Recovery of Real-Time Clusters with the Division of Computing Resources into the Execution of Functional Queries and the Restoration of Data Generated Since the Last Backup. In: Vishnevskiy V.M., Samouylov K.E., Kozyrev D.V. (Eds.). *Distributed Computer and Communication Networks: Control, Computation, Communications*. Book series: *Lecture Notes in Computer Science* (*including subseries Lecture Notes in Artificial Intelligence and Lecture Notes in Bioinformatics*). 2024. V. 14123. P. 236–250. https://doi.org/10.1007/978-3-031-50482-2_19
16. Karagiannis A., Vassiliadis P., Simitsis A. Scheduling strategies for efficient ETL execution. *Inform. Syst.* 2013;38(6): 927–945. https://doi.org/10.1016/j.is.2012.12.001
17. Topcuoglu H., Hariri S., Min-You Wu. Performance-Effective and Low-Complexity Task Scheduling for Heterogeneous Computing. *IEEE Trans. Parallel Distrib. Syst*. 2007;13(3):260–274. https://doi.org/10.1109/71.993206
18. Strengholt P. *Building Medallion Architectures*. 1st ed. Sebastopol (CA): O'Reilly Media; 2024, 209 p.
19. Serra J. *Deciphering Data Architectures*. 1st ed. Sebastopol (CA): O'Reilly Media; 2024, 146 p.
20. Blažić G., Poščić P., Jakšić D. Data warehouse architecture classification. In: *2017 40th International Convention on Information and Communication Technology, Electronics and Microelectronics* (*MIPRO*). 2017. P. 1491–1495. https://doi.org/10.23919/MIPRO.2017.7973657

About the Authors

Daniil A. Pushkarev, Postgraduate Student, Lecturer, Faculty of Software Engineering and Computer Systems, ITMO University (49, bldg. A, Kronverkskii pr., St. Petersburg, 197101 Russia). E-mail: dpushkarev@itmo.ru. RSCI SPIN-code 5781-0210, https://orcid.org/0009-0003-2688-0093

Vladimir A. Bogatyrev, Dr. Sci. (Eng.), Professor, Faculty of Software Engineering and Computer Systems, ITMO University (49, bldg. A, Kronverkskii pr., St. Petersburg, 197101 Russia); Professor, Department of Information Security, Saint Petersburg State University of Aerospace Instrumentation (SUAI) (67, bldg. A, Bolshaya Morskaya ul., St. Petersburg, 190000 Russia). E-mail: vabogatyrev@itmo.ru. Scopus Author ID 7006571069, RSCI SPIN-code 3310-8044, https://orcid.org/0000-0003-0213-0223

Об авторах

Пушкарев Даниил Александрович, аспирант, преподаватель, факультет программной инженерии и компьютерной техники, ФГАОУ ВО «Национальный исследовательский университет ИТМО» (Университет ИТМО) (197101, Россия, Санкт-Петербург, Кронверкский пр., д. 49, лит. А). E-mail: dpushkarev@itmo.ru. SPIN-код РИНЦ 5781-0210, https://orcid.org/0009-0003-2688-0093

Богатырев Владимир Анатольевич, д.т.н., профессор факультета, факультет программной инженерии и компьютерной техники, ФГАОУ ВО «Национальный исследовательский университет ИТМО» (Университет ИТМО) (197101, Россия, Санкт-Петербург, Кронверкский пр., д. 49, лит. А); профессор кафедры информационной безопасности, ФГАОУ ВО «Санкт-Петербургский государственный университет аэрокосмического приборостроения» (ГУАП) (190000, Россия, Санкт-Петербург, ул. Большая Морская, д. 67, лит. А). E-mail: vabogatyrev@itmo.ru. Scopus Author ID 7006571069, SPIN-код РИНЦ 3310-8044, https://orcid.org/0000-0003-0213-0223

Translated from Russian into English by Lyudmila O. Bychkova
Edited for English language and spelling by Dr. David Mossop

Information systems. Computer sciences. Issues of information security
Информационные системы. Информатика. Проблемы информационной безопасности

UDC 004.056.53
https://doi.org/10.32362/2500-316X-2026-14-1-19-30
EDN TXHMHW

RESEARCH ARTICLE

Identification of the message flow between two subscribers in multi-agent systems based on the analysis of its contextual characteristics

Maxim O. Tanygin,
Ilya O. Mishin [@],
Elena A. Kuleshova,
Alexey V. Kiselev

Southwest State University, Kursk, 305040 Russia
[@] Corresponding author, e-mail: mishin.ilya46@yandex.ru

• **Submitted:** 28.04.2025 • **Revised:** 01.07.2025 • **Accepted:** 17.11.2025

Abstract

Objectives. The paper examines the problem of improving the accuracy of identifying the message flow between two subscribers in multi-agent systems. This is done by analyzing the contextual characteristics of the overall message flow in the communication channel. Situations may arise during the process of source identification and verification of authenticity in which authentication codes for two or more messages collide. One way to resolve such conflicts is to isolate the message flow between two subscribers by leveraging its unique statistical characteristics which differ from the characteristics of the general message flow within the system. The aim of the paper is to develop a method which reliably identifies the target message flow even in cases of authentication code collisions.

Methods. The contextual characteristics of messages are used, in order to analyze and highlight patterns of agent behavior in the message flow. These characteristics include frequency of sending, message size, timestamps, and historical interaction data. The method involves the formation of statistical characteristics of the message flow between two agents in a multi-agent system, such as skewness and kurtosis, as well as distribution parameters for the number of messages sent between events from the target source along with their classification by means of logistic regression.

Results. During experiments, the method developed has been found to demonstrate a Precision metric value in the range of 0.81–0.85. This is 40–50% higher than existing methods based on the analysis of inter-packet time intervals, indicating that 81–85% of the messages classified as belonging to the target source are actually such. ROC[1] analysis confirmed the high efficiency of the model and acceptable classification quality.

Conclusions. The results of the study show that the use of contextual characteristics and statistical analysis enables the accurate identification of target flows in multi-agent systems with a total number of agents ranging from 70 to 110. This method can be used in low-bandwidth communication channels where it is essential to minimize the size of the transmitted batch header and computational costs associated with authentication procedures.

[1] Receiver operating characteristic.

Keywords: multi-agent systems, contextual characteristics, binary classification, logistic regression, skewness, kurtosis, ROC analysis

For citation: Tanygin M.O., Mishin I.O., Kuleshova E.A., Kiselev A.V. Identification of the message flow between two subscribers in multi-agent systems based on the analysis of its contextual characteristics. *Russian Technological Journal.* 2026;14(1):19–30. https://doi.org/10.32362/2500-316X-2026-14-1-19-30, https://www.elibrary.ru/TXHMHW

Financial disclosure: The authors have no financial or proprietary interest in any material or method mentioned.

The authors declare no conflicts of interest.

НАУЧНАЯ СТАТЬЯ

Выделение потока сообщений между двумя абонентами в многоагентных системах на основе анализа его контекстуальных характеристик

М.О. Таныгин,
И.О. Мишин [@],
Е.А. Кулешова,
А.В. Киселев

Юго-Западный государственный университет, Курск, 305040 Россия
[@] Автор для переписки, e-mail: mishin.ilya46@yandex.ru

• **Поступила:** 28.04.2025 • **Доработана:** 01.07.2025 • **Принята к опубликованию:** 17.11.2025

Резюме

Цели. В статье исследуется задача повышения точности выделения потока сообщений между двумя абонентами в многоагентных системах на основе анализа контекстуальных характеристик общего потока сообщений в канале связи. При проведении процедур определения источника и установления его подлинности могут возникать коллизии кодов аутентификации двух и более сообщений. Одним из способов разрешения подобных ситуаций является выделение потока сообщений между двумя абонентами на основе его статистических характеристик, отличающихся от характеристик общего потока сообщений в системе. Цель работы – разработка метода, позволяющего надежно идентифицировать целевой поток в случае возникновения коллизий кодов аутентификации.

Методы. Для анализа и выделения паттернов активности агентов в потоке сообщений использованы контекстуальные характеристики сообщений: частота отправки, размер, временные метки и исторические данные взаимодействий. Метод включает формирование статистических характеристик потока сообщений между двумя агентами многоагентной системы (коэффициенты асимметрии и эксцесса, параметры распределения количества сообщений между событиями целевого источника) и их классификацию с помощью логистической регрессии.

Результаты. В ходе проведенных экспериментов было установлено, что разработанный метод демонстрирует значения метрики Precision (полнота) в диапазоне 0.81–0.85 (от 81% до 85% сообщений, классифицированных как принадлежащие целевому источнику, действительно являются таковыми), что на 40–50% превышает показатели существующих методов, основанных на анализе межпакетных интервалов времени. ROC[2]-анализ подтвердил высокую эффективность модели и приемлемое качество классификации.

[2] Receiver operating characteristic – рабочая характеристика приемника.

Выводы. Результаты исследования показали, что использование контекстуальных характеристик и статистического анализа позволяет точно выделять целевые потоки при общем числе агентов в многоагентных системах от 70 до 110. Метод может применяться в каналах связи с низкой пропускной способностью, где необходимо минимизировать размер заголовочных частей передаваемых пакетов данных и вычислительные затраты на выполнение процедур аутентификации.

Ключевые слова: многоагентные системы, контекстуальные характеристики, бинарная классификация, логистическая регрессия, асимметрия, эксцесс, ROC-анализ

Для цитирования: Таныгин М.О., Мишин И.О., Кулешова Е.А., Киселев А.В. Выделение потока сообщений между двумя абонентами в многоагентных системах на основе анализа его контекстуальных характеристик. *Russian Technological Journal*. 2026;14(1):19–30. https://doi.org/10.32362/2500-316X-2026-14-1-19-30, https://www.elibrary.ru/TXHMHW

Прозрачность финансовой деятельности: Авторы не имеют финансовой заинтересованности в представленных материалах или методах.

Авторы заявляют об отсутствии конфликта интересов.

INTRODUCTION

A multi-agent system (MAS), often referred to as a self-organized system, represents an advanced distributed computing network composed of numerous interacting agents. Each agent operates with a degree of autonomy and the capacity to adjust to its surroundings. MAS is used in a variety of fields including robotics, resource management, intelligent transportation, and e-commerce. The effectiveness of MAS systems relies significantly on the reliability and safety of interactions between agents, thereby making authentication a vital factor to consider [1].

In MAS, authentication focuses on verifying the identity of data sources, known as network agents. This process is essential for safeguarding the trustworthiness and privacy of data during transmission. With the escalation of cybersecurity threats, the development of adaptable and resilient authentication methods is increasingly crucial.

In MAS, multiple authentication techniques are employed, each with its own influence on the security and operational efficiency of the system.

Cryptography is a common approach to authentication in MAS. The use of both symmetric and asymmetric cryptographic algorithms enables trustworthy data security and agent identification [2]. Symmetric approaches, exemplified by the advanced encryption standard (AES), deliver rapid processing speeds, although they require a secure key exchange. Asymmetric encryption techniques such as Rivest–Shamir–Adleman (RSA) and elliptic-curve cryptography circumvents the challenges of key distribution. In resource-limited environments, they might prove less efficient [3].

A variety of authentication protocols have been specifically designed for MAS. For example, challenge-response protocols enable agents to verify their identity while keeping their secret keys private. These protocols may be enhanced with timestamp mechanisms to defend against replay attacks [4, 5].

Multifactor authentication (MFA), also employed in MAS systems, demands confirmation through multiple factors, in order to validate the identity of an agent. While MFA significantly enhances security within MAS, implementation introduces complexity to the authentication procedure and potentially increases system response times. It is important to acknowledge that design or implementation shortcomings in the authentication protocols can result in vulnerabilities and performance problems. Study [6] explores the challenge of identifying weaknesses in MFA protocols by means of a structured analytical approach. The authors establish a comprehensive set of criteria to evaluate security, encompassing both established and novel factors. The paper further examines the applicability of MFA across diverse sectors and pinpoints potential vulnerabilities. The study also uncovers critical flaws in ten prominent MFA protocols and offers solutions to mitigate these risks.

Dynamic authentication is another noteworthy aspect of MAS which uses fluctuating parameters to verify agent identities. This can include temporary passwords or unique codes generated through specific algorithms. This method significantly reduces the vulnerabilities arising from compromised static credentials. For example, in article [7] the author examines passwords as a form of authentication. Despite advancements in authentication methods, this technique remains the primary authentication approach in numerous systems. When heightened security is necessary, it is often used together with other authentication methods, creating a two-factor or multi-factor authentication setup. This research highlights the drawbacks of the current authentication method and suggests an alternative of a time-based one-time password (TOTP) system. TOTP generates unique access codes which are only valid for a specific timeframe. This approach, along with dynamic passwords and a hybrid system blending one-time passwords with traditional passwords, offers solutions for both user authentication and peer-to-peer (P2P) authentication.

In MAS, where agents interact with each other under uncertain conditions, reputation-based authentication plays a crucial role. This process enables agents to evaluate the reliability and trustworthiness of other agents based on their past interactions. The approach not only allows for the authentication of agents but also fosters the development of trust relationships within the system. Study [8] proposes a method for message authentication using blockchain technology. This method relies on a reputation assessment mechanism, in order to authenticate messages. Blockchain is employed to manage identities and certificates in this context, while identity authentication and certificate revocation are facilitated through smart contracts. A reputation mechanism is devised in the aims of evaluating the credibility of messages. This can be integrated with message authentication, in order to ensure effective verification of message reliability. The performance analysis conducted in the study demonstrates that the proposed approach is more efficient than the traditional signature-based authentication method. This has been determined by comparing the following characteristics: computational power requirements, message latency, and data loss rate. The findings of the authors indicate that the solution proposed offers an acceptable level of protection against various well-known types of cyberattacks.

With the advancement of blockchain technology, it is now possible to use decentralized authentication methods in MAS. Blockchain provides for both transparency and the immutability of records, enabling agents to exchange sensitive information securely. This approach has the potential to significantly enhance security and reduce risks associated with centralized management. Study [9] proposes a novel (MFA) strategy to enhance security in dynamic environments, utilizing blockchain technology. The research also introduces a consensus model based on the Raft algorithm for selecting a trusted host, ensuring fast and reliable authentication. The analysis demonstrates that this approach effectively mitigates cyberattacks which target authentication systems.

The analysis also indicates that selecting an authentication method for MAS largely hinges on the particular needs for security, performance, and scalability. Integrating multiple approaches can result in more resilient and secure systems, capable of operating efficiently in dynamic environments prone to potential threats.

OVERVIEW OF AUTHENTICATION COLLISION PROTECTION METHODS

Each message in MAS can be assigned a unique identifier, enabling it to be distinguished from other messages and preventing duplication. However, one issue which arises during the processes of source verification and authenticity validation in MAS is the occurrence of identifier collisions. For the purpose of this discussion, a collision refers to the matching of test sequences for two or more distinct messages [10]. Numerous methods exist to safeguard against such collisions. Let us examine the primary approaches.

Using unique message identifiers as verification sequences helps to prevent collisions during the authentication process. These identifiers can be generated using time stamps, random numbers, or a combination of both [11].

One effective method for guarding against collisions is the implementation of cryptographic hash functions with robust properties to mitigate the likelihood of generating identical hash outputs for distinct messages [12]. Prominent examples of such hash functions include SHA-256 and SHA-3 (Secure Hash Algorithm) [13]. The same category of applications also incorporates digital signature algorithms across various domains, in order to establish links between these algorithms and their scenarios [14]. The authors have conducted comparative analyses of widely-used digital signature algorithms such as RSA, Lamport, Elliptic Curve Digital Signature Algorithm (ECDSA), and Edwards-Curve Digital Signature Algorithm, in terms of their performance. Study [15] also analyzes existing encryption techniques and proposes a multi-layered encryption strategy. This strategy uses AES for data encryption, RSA for key protection, and role-based encryption for access control. This hierarchical method significantly raises the computational difficulty of unauthorized access attempts. Integrating these technologies has led to a 50% reduction in key compromise risks and an improvement in data integrity by leveraging MAS verification.

At the same time, when considering an MAS class where communication occurs over low-bandwidth channels, such as sensor networks, industrial Internet systems, or the Internet of Things, the algorithms mentioned above are not applicable. This limitation arises due to the restricted size of the transmitted batch header. In such cases, the likelihood of collisions is influenced more by the identifier size than the cryptographic function properties. This mechanism offers protection against spoofing and collisions, since altering the message results in a hash mismatch [16]. The paper addresses both the confidentiality of message content and the role of digital signatures in verifying its authenticity and integrity. These mechanisms not only shield the message from unauthorized access but also confirm that it has been sent by the specific agent associated with the signature.

Enhancing the reliability of flow separation—identifying the source of each message in a communication

flow—can be achieved by incorporating the contextual characteristics of the messages into the authentication process. Contextual details such as message timing, agent location, message type, and content contribute to more precise assessments of risks and subsequent actions during authentication. For example, the research outlined in [17] addresses inter-operability issues in MAS related to communication, coordination, and adaptability in dynamic environments. The study emphasizes strategies designed to elevate communication within MAS by focusing on protocols, reward structures, learning algorithms, and trust-building mechanisms. Standardized message formats and the implementation of context-aware communication approaches can greatly enhance both the clarity and relevance of exchanged information. Furthermore, integrating reinforcement or deep learning algorithms enables agents to adapt dynamically and develop cooperative behaviors over time. Applying these strategies in MAS results in more efficient and dependable performance within complex and ever-changing environments.

In a dynamic MAS environment, it is recommended to implement adaptive authentication mechanisms which adjust parameters according to the characteristics of messages and the context of interactions. For example, if a message appears to be suspicious, the system could require extra layers of authentication or verification. The research outlined in [18] introduces a solution which incorporates risk assessment with a platform-based MFA system. This approach can be seamlessly integrated into applications, enabling the delegation of the authentication process to an external resource while preserving the internal security of the system.

Combining various methods enhances the accuracy of the flow identification. For example, statistical analysis can be employed for preliminary data filtering [19], followed by the application of machine learning algorithms to improve classification accuracy [20].

MATERIALS AND METHODS

In order to address the challenge of identifying a specific message flow between two participants from a shared communication channel, a method which relies on analyzing the contextual characteristics of the shared message flow within the communication channel is proposed.

Using the previously referenced sensor network as an example of an MAS, the following characteristics can be identified as contextual for distinguishing message flows from multiple sensors at the gateway [21]:

- the frequency of sending messages serves as a quantitative parameter which measures the intensity of data transmission from individual sensor agents. It is determined by calculating the ratio between the number of messages sent by a sensor and a specified time interval.
- the message size represents the amount of data transmitted by the sensor, encompassing both the average and maximum sizes of messages sent. Given that sensors of the same type often transmit messages with uniform sizes, this characteristic can be used to identify and classify devices within the network.
- the message types categorize messages based on their content or purpose, such as requests, responses, or notifications. Since sensors of similar types typically send messages for analogous purposes, this parameter enables specific data flows from individual sources to be isolated and their activity evaluated.
- the send time refers to the time at which messages are transmitted, utilizing timestamps for analysis. This parameter makes it possible to detect activity patterns of sensors. However, data interpretation may require caution due to potential distortions caused by packet losses stemming from interference.
- the historical data comprises previous interaction records related to the source, including successful and failed authentication attempts.

The method is proposed, in order to address issues related to the collision of message identifiers. This approach relies on determining the source by counting the number of messages exchanged through the communication channel between two specific messages, thus testing the hypothesis that they originate from the same source. The method assumes that the contextual characteristics of agents remain relatively stable over time, enabling historical data to be used to analyze and distinguish message flows effectively. It takes into account that an originating agent may produce messages for a given target based on interactions with other agents, such as transmitting messages after a fixed or calculated number of exchanges with other MAS agents. This implies that the agent has the ability actively to manage the stability of its message flow contextual characteristics. The proposed solution offers notable benefits, including simplicity in implementation: a key consideration for devices with low computational capabilities and autonomous power supplies. Furthermore, this method can be executed independently on either the sender or the receiver side, since such meta-information does not need to be transmitted within service messages.

Several mechanisms can be employed to evaluate the statistical characteristics of message flow at the receiver during the processes of authentication and data flow identification:

1. Statistical analysis techniques such as clustering and regression analysis are effective in identifying patterns within the data and isolating the target flow.

Clustering allows for messages to be grouped around similar attributes, thus facilitating the distinction of message groups related to specific subscribers [22].

2. Machine learning algorithms, such as decision trees, neural networks, and support vector machines, can be trained on historical data to classify messages and identify the desired flow. For training purposes, structured data regarding interactions between specific subscribers can serve as a training dataset [23].
3. Time series analysis enables temporal dependencies in the data to be considered. This aids in the detection of anomalies which may signify the start or end of particular message flows. Techniques such as autoregressive models and moving average models can be applied to predict future messages based on past trends [24].

When relying on only one contextual characteristic, clustering is inadequate for decision-making due to the potential for a significant number of type I and type II errors, especially when similar characteristics appear in different flows. In addition, data derived from time series analysis can be heavily affected by the specific communication protocols in use. In fact, this has led the authors to abandon the continuous-time model [19], adopting instead a discrete-time approach based on counting messages transmitted in MAS. Consequently, a more suitable method for analyzing the resulting data involves machine learning. Logistic regression in this method serves as an efficient tool for reducing computational complexity during decision-making: an essential consideration for highly autonomous sensor devices in the MAS class under review.

A model is proposed for generating analyzed samples representing the number of messages transmitted in MAS between dataflow messages from a single source to a single receiver (Fig. 1).

This scenario contains a specific sequence of messages, $S_{i-1}, S_i, S_{i+1}, S_{i+l-1}, ..., S_{i+l}, S_{i+l+1}, S_{i+l+2}$, sent by the network target agent, alongside multiple messages, $\mathbf{D}_{i-1}, \mathbf{D}_i, \mathbf{D}_{i+1}, ..., \mathbf{D}_{i+k-1}, \mathbf{D}_{i+k}$, originating from other network agents and transmitted accordingly. The count of these messages from other agents within the system is measured between pairs S_{i-1} and S_i, S_i and S_{i+1}, ..., S_{i+l-1} and S_{i+l}. Let $n_{i-1}, n_i, n_{i+1}, ..., n_{i+k-1}, n_{i+k}$ denote the cardinalities of the associated sets. Using these values, a sequential dataset is constructed to represent the number of messages exchanged before, during, and after each message in the sequence sent by the target agent.

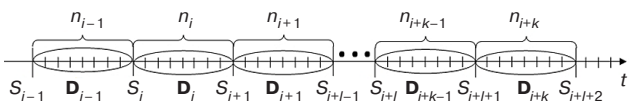

Fig. 1. A scheme for sampling statistical characteristics of the message flow depending on the message arrival time

Using fixed or calculated message values in MAS poses significant risks from an information security perspective. The inherent predictability allows an external observer to easily identify such message flows. As a consequence, the MAS structure becomes vulnerable and can be mapped by an attacker, even without directly analyzing the content of the transmitted data. However, introducing randomness in defining the sizes of sets $\mathbf{D}_{i-1}, \mathbf{D}_i, \mathbf{D}_{i+1}, ..., \mathbf{D}_{i+k-1}, \mathbf{D}_{i+k}$—where the distribution law and its parameters act as a shared secret between the sender and receiver—significantly enhances security. This approach complicates an attacker's ability to isolate messages from the source in the overall MAS message flow. Such increased unpredictability requires prolonged monitoring efforts, making unauthorized analysis much more challenging.

The message flow process operates as follows: once the source transmits a message, it waits for other MAS agents to send a random number of messages. This number can either remain constant or be calculated, as previously noted. In the study, a source is implemented where its messages are produced based on a count subordinate to the Poisson distribution. Randomizing the intervals allows for the messages from each specific source to be masked. This effectively conceals the MAS structure and the contextual details of the information flows from individual sources.

In the given scenario, unique message identifiers serve as verification sequences transmitted by a specific agent during a collision event (Fig. 2). Let us consider a sequence of messages, S_{i-1}, S_i, S_{i+1}, S_{i+l-1}, ..., S_{i+l}, S_{i+l+1}, S_{i+l+2}, generated by the target agent with inter-message intervals, $n_{i-1}, n_i, n_{i+1}, ..., n_{i+k-1}, n_{i+k}$, which are random values distributed according to the Poisson distribution in this scenario. Now, let us assume that the message S_{ab} is received between messages S_{i-1} and S_{i+1}. Upon verification of its identifier, it is determined to be a target agent-generated message appearing between two authentic messages. Since the unique parameters used to generate testing sequences are not known to the attacker, and any coincidence of these sequences in S_{ab} and S_i is entirely random, the message ID within the message sequence $n_{i-1} + n_i$ in MAS adheres to a random distribution. Therefore, the value of n_{ab} is uniformly distributed in the interval $n_{i-1} + n_i$.

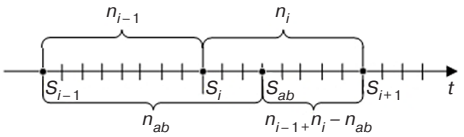

Fig. 2. Model for generating intervals in the case of a collision of unique verification sequences for two different messages

The task of the receiver involves analyzing two sets of paired values, (n_{i-1}, n_i) and $(n_{ab}, n_{i-1} + n_i - n_{ab})$, in order to calculate the probability that pair 1 follows the Poisson distribution, accounting for the generation of corresponding messages by the target agent. Meanwhile, pair 2 does not conform to this distribution, allowing message S_i to be excluded from consideration. These pairs can be enhanced by integrating a series of random values distributed according to the Poisson law. They represent the number of messages in MAS exchanged between different target source messages preceding or succeeding a collision. This approach considers not only a sequence of three messages where a collision takes place but also a broader sample of messages generated by the agent. However, the size of such a sample may not be large *a priori*. Expanding it excessively would lead to delays in determining which message caused the collision or require storing a substantial history of messages. Such scenarios would negatively impact the overall performance of the agents, especially their autonomy.

As highlighted in [25], skewness and kurtosis are effective tools for identifying the type of distribution. These coefficients, indicating variations in agent activity patterns, can serve as features for classifying message flows. However, when working with small sample sizes, the application of these coefficients requires caution. Their high sensitivity to extreme values makes them less reliable for small samples ($n < 50$), since standard coefficient errors tend to increase with decreasing n. This, in turn, diminishes the reliability of normality tests [26].

EXPERIMENTAL

The paper examines message flows in MAS to be identified using specific parameters for generating messages by the source and analyzing them at the receiver:

- M_chain = 11 refers to the number of messages from target agents analyzed, during which an ID collision occurred for one specific message.
- K = 70–110 represents the Poisson allocation parameter (accessible to the receiver), used by the source to define intervals between successive messages. In the context of MAS, this parameter corresponds to the ratio of message generation rates of all MAS agents to that of the source over a unit of time. It can also be understood as the total number of agents in MAS, assuming equal message generation rates among all agents.

Binary classification is used to assess the quality of the classification process using a message flow identification technique based on the individual statistical characteristics of each subscriber.

For each simulation cycle on the test dataset, the following steps are performed:

1. Create empty arrays to store information about messages and their properties.
2. Generate data:
   a) generate time intervals for the message sequence using the Poisson distribution (sequence A_1: $n_1, ..., n_9, n_{10}$).
   b) generate time intervals for the message sequence (sequence A_2: $n_1, ..., n_{ab}, n_9 + n_{10} - n_{ab}$, where n_{ab} is the evenly distributed number in the interval $n_9 + n_{10}$).
   c) calculate the skewness a and kurtosis e for two data sets, A_1 and A_2.
   d) assign labels to the input datasets, $f(e_1, a_1, e_2, a_2) = 1$, $f(e_2, a_2, e_1, a_1) = 0$, using labels from the interval $\{0, 1\}$.

Next, training and testing datasets are created from the generated dataset, in order to train the logistic regression model. Then the accuracy of the model classification on the testing dataset is assessed. Based on the values of type I and type II errors obtained, a classification matrix is constructed and ROC[3] analysis is performed to evaluate the model performance.

Logistic regression is used for binary classification. The likelihood of event Y occurring given the values of X is described by the following equation:

$$P(Y = 1 \mid X) = \frac{1}{1 + e^{-(\beta_0 + \beta_1 X_1 + \beta_2 X_2 + ... + \beta_n X_n)}}, \quad (1)$$

wherein $\beta_0, \beta_1, ..., \beta_n$ represent the model coefficients.

The following metrics are commonly employed to evaluate the performance of binary classification models:

1. Specificity (True Negative Rate) is calculated using the following formula:

$$TNR = \frac{TN}{TN + FP}, \quad (2)$$

wherein TN represents the number of true negatives while FP denotes the number of false positives.

2. Accuracy measures the degree to which the predicted outcomes match the actual results, expressed as follows:

$$Accuracy = \frac{TP + TN}{TP + TN + FP + FN}, \quad (3)$$

wherein TP stands for true positives, FN for false negatives, TN for true negatives, and FP for false positives.

[3] Receiver operating characteristic.

3. Precision is described using the following formula:

$$\text{Precision} = \frac{\text{TP}}{\text{TP} + \text{FP}}. \quad (4)$$

4. Recall (or sensitivity) is calculated as follows:

$$\text{Recall} = \frac{\text{TP}}{\text{TP} + \text{FN}}. \quad (5)$$

5. $F1$ score is the harmonic mean of Precision and Recall, which is defined as follows:

$$F1 = 2 \cdot \frac{\text{Precision} \times \text{Recall}}{\text{Precision} + \text{Recall}}. \quad (6)$$

The $F1$ score ranges from 0 to 1, where a score of 1 signifies perfect precision and recall, while a score of 0 indicates no correct predictions.

In multi-class classification tasks, the following approaches are commonly used to aggregate metrics like Precision, Recall, and $F1$ score:

1. Macro average is an average value associated with aggregated or general indicators. It is used to compare the performance of a model across all classes, regardless of the size of each class:

$$\text{Macro avg} = \frac{1}{N}\sum_{i=1}^{N} M_i, \quad (7)$$

wherein N represents the total number of classes while M_i is the metric value for class i.

2. Weighted average calculates the average metric value for each class, taking into account the number of instances in each class:

$$\text{Weight avg} = \frac{\sum_{i=1}^{N} M_i \omega_i}{\sum_{i=1}^{N} \omega_i}, \quad (8)$$

wherein ω_i represents the number of instances (or weight) for class i.

RESULTS AND DISCUSSION

The studies reveal that the metric values (Precision, Recall, $F1$) for each of the two classes (0; 1) with $K = 70$–110, vary between 0.81 and 0.85. These metrics are derived by analyzing the contextual characteristics of information flows from individual sources. A method is used which identifies message flows based on these contextual attributes. The Precision metric signifies that 81% to 85% of messages classified as belonging to the target source actually originate from it. Similarly, the Recall metric shows that 81% to 85% of all messages from the target source are correctly identified. The $F1$ score reflects the balance of the model, and demonstrates its effectiveness in minimizing both false positives and false negatives.

The Accuracy metric represents the overall percentage of messages correctly classified, indicating that 81% to 85% of all messages in the system (both target and irrelevant) are assigned to their correct categories. The alignment of the Macro average and Weighted average values suggests that there is no class imbalance. This is crucial because, in real-world scenarios, a balanced distribution of target and irrelevant messages makes analysis more straightforward and enhances method reliability.

The identical values for classes 0 and 1 can be attributed to the balanced data and the use of optimized feature selection, derived from the statistical characteristics of message flow.

Figure 3 illustrates the ROC curve for the logistic regression model at $K = 90$. The x-axis depicts the false positive rate, while the y-axis shows the true positive rate. The area under the curve (AUC) is calculated to be 0.83, suggesting that the model exhibits high sensitivity and effectively distinguishes between target and non-target messages, delivering satisfactory performance.

The experimental results indicate that the model operates reliably, even with a high value of K. Here, K represents the ratio of the total number of messages in MAS per unit of time to the number of messages from the target agent during the same time period.

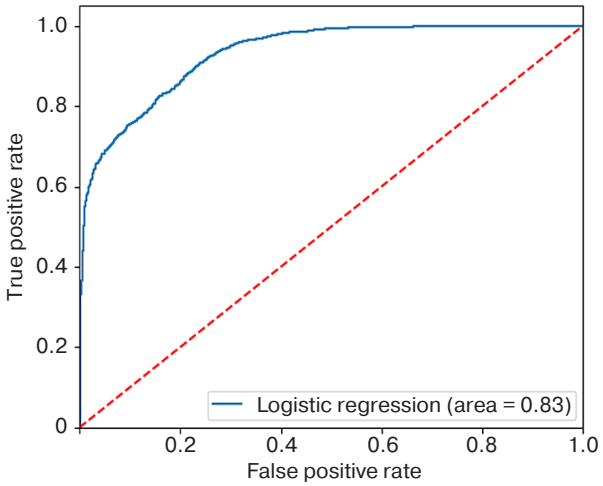

Fig. 3. ROC curve for the logistic regression model with $K = 90$ (solid blue line). The red dashed line represents a random classifier (AUC = 0.5)

Study [19], previously examined, introduces a methodology for identifying the origin of messages through statistical analysis of inter-packet interval times. It incorporates an evaluation of skewness and kurtosis, in which the defining rules are expressed as linear relationships between these parameters.

However, the study does not account for the impact of interference on the communication channel or delivery time. This omission is justified by disregarding the inter-packet interval time in the given context, allowing the influence of such interference to be reasonably overlooked.

The application of advanced statistical analysis, as opposed to the algebraic comparison of skewness and kurtosis, enables higher Precision metric values to be achieved than those reported in [19]. For example, with the same predefined message sequence length of M_chain = 11, a Precision metric in the range of 0.3–0.4 is achieved in [19].

When comparing the results of this study to the aforementioned method, it can be concluded that under comparable communication system parameters the Precision metric shows an improvement, increasing by 0.4–0.5.

CONCLUSIONS

The study of the hypothesis presented in this paper regarding the use of skewness and kurtosis in identifying the distribution type of random variables has demonstrated its potential for distinguishing differences in the activity patterns of agents based on their contextual characteristics.

Through simulation of the operation of the message flow identification subsystem in the event of a collision of unique message identifiers, satisfactory values for binary classification quality metrics have been achieved using a method for identifying message flows based on information flow characteristics from specific sources.

The approach described, which involves calculating the total number of messages exchanged between all MAS elements for a given target agent, is notable for its simplicity of implementation. This aspect is particularly important for low-performance devices which rely on autonomous power supplies. In addition, the method enables such counting to be performed independently on both the sender and receiver sides. The classification accuracy achieved by this approach ranges between 0.81 and 0.85.

The research findings demonstrate that leveraging contextual characteristics and statistical analysis facilitates accurate identification of target flows in MAS containing 70 to 110 agents. This method is especially suitable for low-bandwidth communication channels, in which it is crucial to minimize the size of transmitted batch headers and reduce the computational costs associated with authentication procedures. A particularly promising avenue for further development involves integrating adaptive mechanisms capable of handling dynamically changing traffic congestion, where the effective number of agents in MAS may vary widely.

Authors' contributions

M.O. Tanygin—concept development, methodology development, approval of the final version.

I.O. Mishin—conducting research, writing the draft, preparing and editing the text.

E.A. Kuleshova—conducting research, analyzing data, preparing and editing the text.

A.V. Kiselev—conducting research, analyzing data.

REFERENCES

1. Öztürk G., Saran N., Doğanaksoy A. Modified Attribute-Based Authentication for Multi-Agent Systems. *Int. J. Inform. Security Sci.* 2023;12(3):1–13. https://doi.org/10.55859/ijiss.1294580
2. Kuleshova E.A., Maruhlenko A.L., Dobritsa V.P., Tanygin M.O., Plugatorev A.V. A variant of the algorithm for generating pseudorandom binary sequences based on the properties of linear cellular automata. *Prikaspiiskii zhurnal: upravlenie i vysokie tekhnologii = Caspian Journal: Control and High Technologies.* 2021;54(2):62–70 (in Russ.). https://doi.org/10.21672/2074-1707.2021.53.1.062-070
3. Tanygin M.O., Kuleshova E.A., Mitrofanov A.V., Gladilina E.U. Increasing the speed of error detection when forming data block chains based on the analysis of the number of hash matches. *Prikaspiiskii zhurnal: upravlenie i vysokie tekhnologii = Caspian Journal: Control and High Technologies.* 2022;1(57):85–93 (in Russ.). https://doi.org/10.54398/2074-1707_2022_1_85
4. Yuan J., Yang J., Zhou S., Wang C. Efficient Group Authentication with Multiple Authentications on Resource-Limited Devices. *J. Supercomput.* 2025;81:929. https://doi.org/10.1007/s11227-025-07404-6
5. Gopirajan P.V., Mani K. Secure Multi-Authentication using BlockchainTechnology in Cloud based Internet of Things. *Telematique*. 2022;21(1):6640–6650.
6. Wee A.K., Chekole E.G., Zhou J. Excavating Vulnerabilities Lurking in Multi-Factor Authentication Protocols: A Systematic Security Analysis. *arXiv Cornell University*. 2024;2407(20459):1–24. https://doi.org/10.48550/arXiv.2407.20459
7. Chenchev I. Framework for Multi-factor Authentication with Dynamically Generated Passwords. In: Arai K. (Ed.). *Advances in Information and Communication. FICC 2023. Lecture Notes in Networks and Systems*. Springer; 2023. V. 652. P. 563–576. https://doi.org/10.1007/978-3-031-28073-3_39
8. Li H., Han D. Blockchain-assisted secure message authentication with reputation management for VANETs. *J. Supercomput.* 2023;79(17):19903–19933. https://doi.org/10.1007/s11227-023-05394-x
9. Xu Y., Jian X., Li T., Zou S., Li B. Blockchain-Based Authentication Scheme with an Adaptive Multi-Factor Authentication Strategy. *Mobile Inform. Syst.* 2023;2023:4764135. https://doi.org/10.1155/2023/4764135

10. Liu J., Mu Q., Che R., et al. Multi-participant quantum anonymous communication based on high-dimensional entangled states. *Physica Scripta*. 2024;99(9):095109. https://doi.org/10.1088/1402-4896/ad69d9
11. Kuleshova E.A., Tanygin M.O. Study of characteristics of modern generators of pseudorandom sequences. *Telekommunikatsii = Telecommunications*. 2023;7:28–39 (in Russ.). https://doi.org/10.31044/1684-2588-2023-0-7-28-39
12. Tanygin M.O. Restoring the order of information packets based on hash sequence analysis. *Izvestiya Yugo-Zapadnogo gosudarstvennogo universiteta = Proceedings of the Southwest State University*. 2020;24(1):175–188 (in Russ.).
13. Alamgir N., Negati S., Bright C. SHA-256 Collision Attack with Programmatic SAT. *arXiv Cornell University.* 2024;2406.20072. https://doi.org/10.48550/arXiv.2406.20072
14. Fang Y. A research on different digital signature schemes. *Appl. Comput. Eng.* 2023;16(1):27–35. http://doi.org/10.54254/2755-2721/16/20230855
15. Phatangare S., Jadhav S., Kawane S., Holkar P., Gaikwad P. Multi-Level Encryption System using AES and RSA Algorithms. *Int. J. Res. Appl. Sci. Eng. Technol.* 2024;15(5):4043–4051. https://doi.org/10.22214/IJRASET.2024.62420
16. Tanygin M.O., Alshaeaa H.Y., Kuleshova E.A. A method of the transmitted blocks information integrity control. *Radio Electronics, Computer Science, Control.* 2020;1:181–189.
17. Tao M., Li Q., Yu J. Multi-Objective Dynamic Path Planning with Multi-Agent Deep Reinforcement Learning. *J. Marin. Sci. Eng.* 2025;13(1):20. https://doi.org/10.3390/jmse13010020
18. Morais D., Zuquete A., Mendes A. Adaptive, Multi-Factor Authentication as a Service for Web Applications. In: *2023 7th Cyber Security in Networking Conference* (*CSNet*). 2023. P. 74–80. http://doi.org/10.1109/CSNet59123.2023.10339695
19. Plugatarev A.V. Model for determining the message source by statistical analysis of metadata in an open communication channel. *Prikaspiiskii zhurnal: upravlenie i vysokie tekhnologii = Caspian Journal: Control and High Technologies.* 2022;4(60):30–37 (in Russ.).
20. Dharrao D., Gaikwad P., Gawai S.V., Bongale A.M., Patel K., Singh A. Classifying SMS as spam or ham: Leveraging NLP and machine learning techniques. *Int. J. Saf. Secur. Eng.* 2024;14(1):289–296. https://doi.org/10.18280/ijsse.140128
21. Placzek B. A Multi-Agent Prediction Method for Data Sampling and Transmission Reduction in Internet of Things Sensor Networks. *Sensors*. 2023;23(20):8478. https://doi.org/10.3390/s23208478
22. Vedmiediev D., Shapoval N. Text Message Clustering. *Electronics and Control Systems.* 2023;4(78):16–20.
23. Katwal S., Sharma N., Kumar K. A Deep Learning Approach for Throughput Enhanced Clustering and Spectrally Efficient Resource Allocation in Ultra-Dense Networks. *IEEE Trans. Netw. Service Manag*. 2025;22(1):582–591. https://doi.org/10.1109/TNSM.2024.3470235
24. Huang X., Zhou S. QMNet: Importance-Aware Message Exchange for Decentralized Multi-Agent Reinforcement Learning. *IEEE Trans. Mobile Comput*. 2023;23(5):4739–4751. https://doi.org/10.1109/TMC.2023.3296726
25. Goloveshkin V.A., Zhukova G.N., Ulyanov M.V., Fomichev M.I. The estimation of the complexity of solving a particular travelling salesman problem by quantile-based measures for skewness and kurtosis. *Int. J. Open Inform. Technol.* 2016;4(12):7–12 (in Russ.). https://elibrary.ru/xetabh
26. Tanygin M.O., Dobritsa V.P., Mitrofanov A.V., Ahmat Kh.I. Mathematical interpretation of the results of cognitive analysis of network packets metadata. *Izvestiya Yugo-Zapadnogo gosudarstvennogo universiteta = Proceedings of the Southwest State University*. 2023;27(3):66–78 (in Russ.).

СПИСОК ЛИТЕРАТУРЫ

1. Öztürk G., Saran N., Doğanaksoy A. Modified Attribute-Based Authentication for Multi-Agent Systems. *Int. J. Inform. Security Sci.* 2023;12(3):1–13. https://doi.org/10.55859/ijiss.1294580
2. Кулешова Е.А., Марухленко А.Л., Добрица В.П., Таныгин М.О., Плугаторев А.В. Вариант алгоритма генерации псевдослучайных двоичных последовательностей, основанный на свойствах линейных клеточных автоматов. *Прикаспийский журнал: управление и высокие технологии.* 2021;54(2):62–70. https://doi.org/10.21672/2074-1707.2021.53.1.062-070
3. Таныгин М.О., Кулешова Е.А., Митрофанов А.В., Гладилина Е.Ю. Повышение скорости обнаружения ошибок при формировании цепочек блоков данных на основе анализа числа совпадений хешей. *Прикаспийский журнал: управление и высокие технологии.* 2022;1(57):85–93. https://doi.org/10.54398/2074-1707_2022_1_85
4. Yuan J., Yang J., Zhou S., Wang C. Efficient Group Authentication with Multiple Authentications on Resource-Limited Devices. *J. Supercomput.* 2025;81:929. https://doi.org/10.1007/s11227-025-07404-6
5. Gopirajan P.V., Mani K. Secure Multi-Authentication using BlockchainTechnology in Cloud based Internet of Things. *Telematique*. 2022;21(1):6640–6650.
6. Wee A.K., Chekole E.G., Zhou J. Excavating Vulnerabilities Lurking in Multi-Factor Authentication Protocols: A Systematic Security Analysis. *arXiv Cornell University*. 2024;2407(20459):1–24. https://doi.org/10.48550/arXiv.2407.20459
7. Chenchev I. Framework for Multi-factor Authentication with Dynamically Generated Passwords. In: Arai K. (Ed.). *Advances in Information and Communication. FICC 2023. Lecture Notes in Networks and Systems*. Springer; 2023. V. 652. P. 563–576. https://doi.org/10.1007/978-3-031-28073-3_39
8. Li H., Han D. Blockchain-assisted secure message authentication with reputation management for VANETs. *J. Supercomput.* 2023;79(17):19903–19933. https://doi.org/10.1007/s11227-023-05394-x
9. Xu Y., Jian X., Li T., Zou S., Li B. Blockchain-Based Authentication Scheme with an Adaptive Multi-Factor Authentication Strategy. *Mobile Inform. Syst.* 2023;2023:4764135. https://doi.org/10.1155/2023/4764135
10. Liu J., Mu Q., Che R., et al. Multi-participant quantum anonymous communication based on high-dimensional entangled states. *Physica Scripta*. 2024;99(9):095109. https://doi.org/10.1088/1402-4896/ad69d9

11. Кулешова Е.А., Таныгин М.О. Исследование характеристик современных генераторов псевдослучайных последовательностей. *Телекоммуникации*. 2023;7:28–39. https://doi.org/10.31044/1684-2588-2023-0-7-28-39
12. Таныгин М.О. Восстановление порядка следования информационных пакетов на основе анализа хеш-последовательностей. *Известия Юго-Западного государственного университета*. 2020;24(1):175–188.
13. Alamgir N., Negati S., Bright C. SHA-256 Collision Attack with Programmatic SAT. *arXiv Cornell University.* 2024;2406.20072. https://doi.org/10.48550/arXiv.2406.20072
14. Fang Y. A research on different digital signature schemes. *Appl. Comput. Eng.* 2023;16(1):27–35. http://doi.org/10.54254/2755-2721/16/20230855
15. Phatangare S., Jadhav S., Kawane S., Holkar P., Gaikwad P. Multi-Level Encryption System using AES and RSA Algorithms. *Int. J. Res. Appl. Sci. Eng. Technol.* 2024;15(5):4043–4051. https://doi.org/10.22214/IJRASET.2024.62420
16. Tanygin M.O., Alshaeaa H.Y., Kuleshova E.A. A method of the transmitted blocks information integrity control. *Radio Electronics, Computer Science, Control.* 2020;1:181–189.
17. Tao M., Li Q., Yu J. Multi-Objective Dynamic Path Planning with Multi-Agent Deep Reinforcement Learning. *J. Marin. Sci. Eng.* 2025;13(1):20. https://doi.org/10.3390/jmse13010020
18. Morais D., Zuquete A., Mendes A. Adaptive, Multi-Factor Authentication as a Service for Web Applications. In: *2023 7th Cyber Security in Networking Conference* (*CSNet*). 2023. P. 74–80. http://doi.org/10.1109/CSNet59123.2023.10339695
19. Плугатарев А.В. Модель определения источника сообщений на основе статистического анализа метаданных в открытом канале связи. *Прикаспийский журнал: управление и высокие технологии.* 2022;4(60):30–37.
20. Dharrao D., Gaikwad P., Gawai S.V., Bongale A.M., Patel K., Singh A. Classifying SMS as spam or ham: Leveraging NLP and machine learning techniques. *Int. J. Saf. Secur. Eng.* 2024;14(1):289–296. https://doi.org/10.18280/ijsse.140128
21. Placzek B. A Multi-Agent Prediction Method for Data Sampling and Transmission Reduction in Internet of Things Sensor Networks. *Sensors*. 2023;23(20):8478. https://doi.org/10.3390/s23208478
22. Vedmiediev D., Shapoval N. Text Message Clustering. *Electronics and Control Systems.* 2023;4(78):16–20.
23. Katwal S., Sharma N., Kumar K. A Deep Learning Approach for Throughput Enhanced Clustering and Spectrally Efficient Resource Allocation in Ultra-Dense Networks. *IEEE Trans. Netw. Service Manag*. 2025;22(1):582–591. https://doi.org/10.1109/TNSM.2024.3470235
24. Huang X., Zhou S. QMNet: Importance-Aware Message Exchange for Decentralized Multi-Agent Reinforcement Learning. *IEEE Trans. Mobile Comput*. 2023;23(5):4739–4751. https://doi.org/10.1109/TMC.2023.3296726
25. Головешкин В.А., Жукова Г.Н., Ульянов М.В., Фомичев М.И. Использование квантильных коэффициентов асимметрии и эксцесса для оценки сложности решения задачи коммивояжера. *Int. J. Open Inform. Technol.* 2016;4(12):7–12. https://elibrary.ru/xetabh
26. Таныгин М.О., Добрица В.П., Митрофанов А.В., Ахмат Х.И. Математическая интерпретация результатов когнитивного анализа метаданных сетевых пакетов. *Известия Юго-Западного государственного университета.* 2023;27(3):66–78.

About the Authors

Maxim O. Tanygin, Dr. Sci. (Eng.), Associate Professor, Dean of the Faculty of Fundamental and Applied Informatics, Southwest State University (94, 50 Let Oktyabrya ul., Kursk, 305040 Russia). E-mail: tanygin@yandex.ru. Scopus Author ID 19640649200, ResearcherID N-7689-2016, RSCI SPIN-code 2639-4800, https://orcid.org/0000-0002-4099-1414

Ilya O. Mishin, Postgraduate Student, Department of Information Security, Southwest State University (94, 50 Let Oktyabrya ul., Kursk, 305040 Russia). E-mail: mishin.ilya46@yandex.ru. ResearcherID MXJ-7912-2025, RSCI SPIN-code 6911-3642, https://orcid.org/0009-0006-8883-1731

Elena A. Kuleshova, Cand. Sci. (Eng.), Associate Professor, Department of Information Security, Southwest State University (94, 50 Let Oktyabrya ul., Kursk, 305040 Russia). E-mail: lena.kuleshova.94@mail.ru. Scopus Author ID 57216349335, ResearcherID AAI-9214-2021, RSCI SPIN-code 9607-8582, https://orcid.org/0000-0002-8270-564X

Alexey V. Kiselev, Cand. Sci. (Eng.), Associate Professor, Computer Engineering Department, Southwest State University (94, 50 Let Oktyabrya ul., Kursk, 305040 Russia). E-mail: kiselevalexey1990@gmail.com. Scopus Author ID 57337411000, ResearcherID S-9914-2018, RSCI SPIN-code 2016-7550, https://orcid.org/0000-0001-7228-0281

Об авторах

Таныгин Максим Олегович, д.т.н., доцент, декан факультета фундаментальной и прикладной информатики, ФГБОУ ВО «Юго-Западный государственный университет» (305040, Россия, Курск, ул. 50 лет Октября, д. 94). E-mail: tanygin@yandex.ru. Scopus Author ID 19640649200, ResearcherID N-7689-2016, SPIN-код РИНЦ 2639-4800, https://orcid.org/0000-0002-4099-1414

Мишин Илья Олегович, аспирант, кафедра информационной безопасности, ФГБОУ ВО «Юго-Западный государственный университет» (305040, Россия, Курск, ул. 50 лет Октября, д. 94). E-mail: mishin.ilya46@yandex.ru. ResearcherID MXJ-7912-2025, SPIN-код РИНЦ 6911-3642, https://orcid.org/0009-0006-8883-1731

Кулешова Елена Александровна, к.т.н., доцент, кафедра информационной безопасности, ФГБОУ ВО «Юго-Западный государственный университет» (305040, Россия, Курск, ул. 50 лет Октября, д. 94). E-mail: lena.kuleshova.94@mail.ru. Scopus Author ID 57216349335, ResearcherID AAI-9214-2021, SPIN-код РИНЦ 9607-8582, https://orcid.org/0000-0002-8270-564X

Киселев Алексей Викторович, к.т.н., доцент, кафедра вычислительной техники, ФГБОУ ВО «Юго-Западный государственный университет» (305040, Россия, Курск, ул. 50 лет Октября, д. 94). E-mail: kiselevalexey1990@gmail.com. Scopus Author ID 57337411000, ResearcherID S-9914-2018, SPIN-код РИНЦ 2016-7550, https://orcid.org/0000-0001-7228-0281

Translated from Russian into English by Kirill V. Nazarov
Edited for English language and spelling by Dr. David Mossop

Modern radio engineering and telecommunication systems

Современные радиотехнические и телекоммуникационные системы

UDC 621.391.82
https://doi.org/10.32362/2500-316X-2026-14-1-31-42
EDN UDTTHY

RESEARCH ARTICLE

Investigation of multipath compensation efficiency in communication channels using filters with inverse impulse response

Yuriy A. Polevoda [@], **Gennady V. Kulikov**

MIREA – Russian Technological University, Moscow, 119454 Russia
[@] *Corresponding author, e-mail: polevoda@mirea.ru*

• **Submitted:** 21.04.2025 • **Revised:** 19.06.2025 • **Accepted:** 10.11.2025

Abstract

Objectives. A key challenge when transmitting data in modern communication systems is the multipath propagation of signals caused by reflections from various obstacles. Various methods have been developed to address this issue including: directional antennas; diversity reception; adaptive filtering; and the choice of effective modulation methods. One promising approach is the use of filters with impulse response (IR) inverse to IR channel. This allows for compensating delayed signals. The effectiveness of such filters depends on the accuracy of their parameter settings. The paper aims to develop guidelines for effectively using filters with inverse IR to compensate for multipath. Additionally, it aims to evaluate the impact of various channel parameters, such as time delays and reflected signal intensities, on the bit error rate (BER) and to determine the energy gain.

Methods. The methods of statistical radio engineering, the theory of optimal signal reception and mathematical modeling were used.

Results. The results of a study on the effectiveness of multipath compensation in communication channels when using filters with inverse IR to that of the channel at the receiving side are presented. A multipath communication channel model was developed in the *Simulink* software environment, consisting of six beams with different time delays and intensities. Discrete information reception was simulated using different modulation methods: 16-QAM (quadrature amplitude modulation), 8-PSK (phase-shift keying), and 8-FSK (frequency-shift keying). The BER value was estimated depending on the signal-to-noise ratio and multipath channel parameters, including time delays and reflected beam intensities. It was shown that the use of filters with inverse IR can significantly reduce BER and improve communication quality. The change in the BER value is estimated for deviations of filter parameters from the ideal ones.

Conclusions. The results demonstrate that the use of compensating filters is effective in combating multipath distortion, especially under strong interference conditions. The data obtained can be used for the design and optimization of modern communication systems operating in complex signal propagation conditions.

Keywords: multipath communication channel, impulse response, filter with inverse impulse response, multi-position modulation, bit error probability, signal-to-noise ratio

For citation: Polevoda Yu.A., Kulikov G.V. Investigation of multipath compensation efficiency in communication channels using filters with inverse impulse response. *Russian Technological Journal.* 2026;14(1):31–42. https://doi.org/10.32362/2500-316X-2026-14-1-31-42, https://www.elibrary.ru/UDTTHY

Financial disclosure: The authors have no financial or proprietary interest in any material or method mentioned.

The authors declare no conflicts of interest.

НАУЧНАЯ СТАТЬЯ

Исследование эффективности компенсации многолучевости в каналах связи при использовании фильтров с инверсной импульсной характеристикой

Ю.А. Полевода [@], **Г.В. Куликов**

МИРЭА – Российский технологический университет, Москва, 119454 Россия
[@] *Автор для переписки, e-mail: polevoda@mirea.ru*

• **Поступила:** 21.04.2025 • **Доработана:** 19.06.2025 • **Принята к опубликованию:** 10.11.2025

Резюме

Цели. При передаче данных в современных системах связи одной из ключевых проблем является многолучевое распространение сигналов, вызванное отражениями от различных препятствий. Для борьбы с этим эффектом используются разные методы, такие как направленные антенны, разнесенный прием, адаптивная фильтрация и выбор эффективных методов модуляции. Одним из перспективных подходов является применение фильтров с импульсной характеристикой (ИХ), инверсной ИХ канала, которые позволяют компенсировать задержанные сигналы. Эффективность таких фильтров зависит от точности настройки их параметров. Цель работы состоит в выработке рекомендаций для обеспечения эффективной компенсации многолучевости при использовании фильтров с инверсной ИХ, оценке влияния параметров канала (временных задержек и интенсивностей отраженных сигналов) на вероятность битовой ошибки (bit error rate, BER) и определении энергетического выигрыша.

Методы. Использованы методы статистической радиотехники, теории оптимального приема сигналов и математического моделирования.

Результаты. Представлены результаты исследования эффективности компенсации многолучевости в каналах связи при использовании на приемной стороне фильтров с ИХ, инверсной ИХ канала. В программной среде *Simulink* разработана модель многолучевого канала связи, включающая шесть лучей с различными временными задержками и интенсивностями. Проведено моделирование приема дискретной информации для разных методов модуляции: 16-КАМ (квадратурной амплитудной), 8-ФМ (многопозиционной фазовой) и 8-ЧМ (многопозиционной частотной) модуляциями. Выполнена оценка вероятности битовой ошибки в зависимости от отношения сигнал/шум и параметров многолучевого канала (временных задержек, интенсивностей отраженных лучей). Показано, что применение фильтров с инверсной ИХ позволяет значительно снизить вероятность битовой ошибки и улучшить качество связи. Оценено изменение величины BER при отклонениях параметров фильтра от идеальных.

Выводы. Результаты демонстрируют, что использование компенсационных фильтров эффективно для борьбы с многолучевыми искажениями, особенно в условиях сильной интерференции. Полученные данные могут быть использованы для проектирования и оптимизации современных систем связи, работающих в сложных условиях распространения сигналов.

Ключевые слова: многолучевый канал связи, импульсная характеристика, фильтр с инверсной импульсной характеристикой, многопозиционная модуляция, вероятность битовой ошибки, отношение сигнал/шум

Для цитирования: Полевода Ю.А., Куликов Г.В. Исследование эффективности компенсации многолучевости в каналах связи при использовании фильтров с инверсной импульсной характеристикой. *Russian Technological Journal*. 2026;14(1):31–42. https://doi.org/10.32362/2500-316X-2026-14-1-31-42, https://www.elibrary.ru/UDTTHY

Прозрачность финансовой деятельности: Авторы не имеют финансовой заинтересованности в представленных материалах или методах.

Авторы заявляют об отсутствии конфликта интересов.

INTRODUCTION

Modern communication systems face various challenges, one of which is data transmission in multipath environments. Multipath propagation, caused by signal reflection from various obstacles, can result in interference and degradation of the received signal, significantly reducing the quality of communication. In order to overcome this issue, several methods have been developed, such as: the use of directional antennas [1, 2], diversity reception [3–6], adaptive filtering [7, 8], and the selection of appropriate modulation techniques [9–12]. One key method used to mitigate the negative effects of multipath is through the use of impulse response (IR) filters which are inverse to the channel IR which allows delayed signals to be compensated [13–17]. This paper presents the results of modeling and analysis of the efficacy of these filters in a multipath communication channel when utilizing signals with various modulation techniques, such as: quadrature amplitude modulation (16-QAM, coherent detection); multi-position phase-shift keying (8-PSK, coherent detection); and multi-position frequency-shift keying (8-FSK, noncoherent detection).

The paper aims to evaluate the impact of multipath channel parameters (delay, reflected signal strength) and the filter on the bit error rate (BER) when receiving discrete signals, as well as to determine the energy gain from employing filters with inverse IR. For analysis, a multipath model was developed in the *Simulink*[1] environment, comprising six beams with distinct delays and intensities (discrete multipath).

MULTIPATH CHANNEL MODEL

An IR communication channel can be defined and its parameters estimated by means of a preliminary probing of the channel with specific form signals such as short δ-pulses, signals with frequency modulation, or signals encoded with specific pseudo-random sequences [18–23]. While this aspect is not detailed in the paper, it is assumed that the parameters of the IR channel have been determined accurately or with some degree of error. Such information in the model can be obtained by using a short probe pulse, the duration of which determines the lower limit of the range of possible beam delays. For instance, the duration of the probe pulse is chosen to be 1 ns.

A discrete multipath channel model (6 beams, including the direct path $s_{\text{drct}}(t)$) is created using the *MATLAB*/*Simulink* (trial version) and *Scilab Xcos*[2] software environments. The delays τ_k of the signals are 0 (for the direct path), 7, 14, 21, 28, and 33 ns, while the relative (relative to the average amplitude of the direct path signal) intensities μ_k of the delayed signals are 0.09, 0.08, 0.07, 0.06, and 0.05, respectively (Fig. 1, left). The values for delays are provided for illustrative purposes only and may be adjusted depending on the specific radio propagation conditions.

Therefore, the output of the multipath channel can be described as follows:

$$s(t) = s_{\text{drct}}(t) + \sum_{k=1}^{5} \mu_k s_{\text{drct}}(t - \tau_k) + n(t),$$

wherein $n(t)$ is white Gaussian noise (additive white Gaussian noise channel), t is the time.

The circuit of the filter with inverse IR consists of 6 branches, each with an amplification factor corresponding to the intensity and time delay (Fig. 1, right). In the portion which corresponds to delayed signals, the circuit acts as a mirror (in terms of polarity) of the communication channel mode.

BENCHMARKING FILTER WITH INVERSE IR

The benchmarking of a filter with inverse IR can be clearly seen when passing a single probe pulse through the channel. Figure 2a shows the oscillogram of the signal at the communication channel output showing 1 direct signal and 5 reflections, which corresponds to that of the IR channel.

[1] https://www.mathworks.com/products/simulink.html. Accessed February 15, 2025.

[2] https://www.scilab.org/software/xcos. Accessed April 05, 2025.

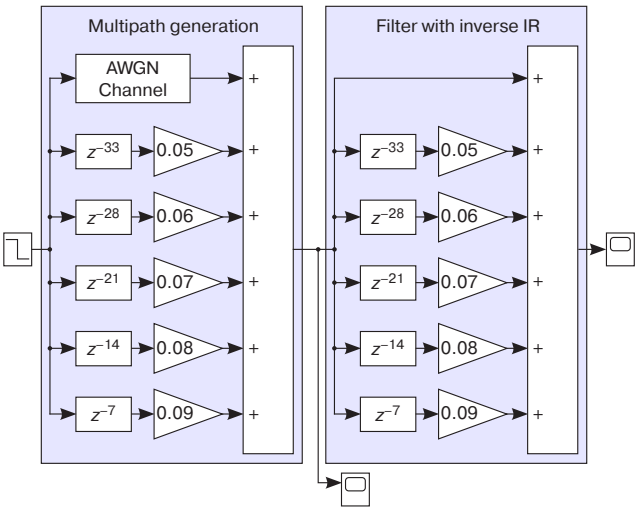

Fig. 1. Multipath signal generation and processing model.
z^{-1} is delay unit, where "−1" is beam delay time

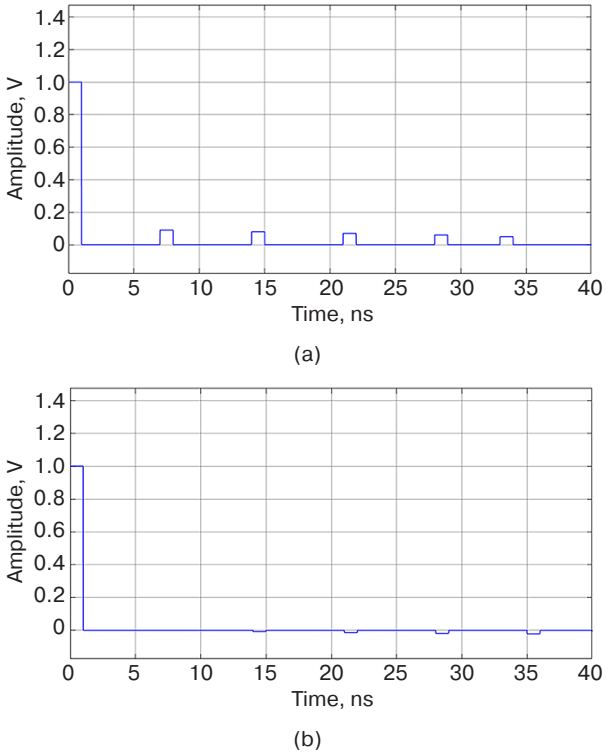

Fig. 2. Oscillograms: (a) IR; (b) signal at the output of the filter with inverse IR

Figure 2b shows the signal at the output of a filter with inverse IR. This demonstrates that the filter has compensated for delayed beam signals. However, instead of these signals, responses appear at time positions that are twice the time delay. This is easily explained by the characteristics of signal passage through the filter [24].

SIMULATION OF COMMUNICATION CHANNEL USING MULTIPOSITION SIGNALS

Energy gain analysis

The study analyzes the energy gain (in terms of signal-to-noise ratio, SNR) in relation to the relative intensity of a reflected beam for various modulation techniques: 16-QAM, 8-PSK, and 8-FSK. The modeling is conducted with one direct and one reflected beam, with a delay of 7 ns. The intensity of the reflected beam μ varies over a broad range, allowing for an assessment of the impact of both weak and strong reflections on bit error rates. For each modulation technique, the relationships between BER and SNR (E_b/N_0, where E_b is the energy per bit of information and N_0 is the noise power spectral density) are plotted (Fig. 3) both without the use (dashed lines) and with the use of the inverse IR filter (solid lines).

Figure 4 shows the results of calculating the energy gain for BER = 10^{-3}.

Figures 3 and 4 show that for a reflected beam intensity of μ = 0.3, the gain in the SNR (E_b/N_0), when using a filter with inverse IR, varies between 1 and 10 decibels, depending on the modulation scheme employed. The gain for the 16-QAM signal is approximately twice that of the 8-PSK signal, and more than 10 times that of the 8-FSK signal. This is due to the fact that the 8-FSK signal has the highest initial immunity to interference [11]. For example, with the reflected beam intensity of μ = 0.3 and SNR (E_b/N_0) of 9 dB, BER without a filter is approximately 10^{-3} for 8-FSK. It is more than one order of magnitude higher for 8-PSK and twice as high for 16-QAM.

The relationship between BER and SNR

The next stage of the study involves modeling a communication channel with 1 direct beam and 5 reflected beams, each with varying delays (7, 14, 21, 28, and 33 ns) and intensities (for 16-QAM and 8-PSK, μ = 0.09, 0.08, 0.07, 0.06, and 0.05 relative to the average amplitude of the direct signal beam, and for 8-FSK, μ = 0.2, 0.3, 0.4, 0.5, and 0.6). The simulation results are BER as a function of SNR (E_b/N_0) for various numbers of beams (Figs. 5–7), with (solid lines) and without (dashed lines).

Figures 5 and 7 show that for any number of received signals, the filter with inverse IR compensates for multipath interference for all signal types, thus reducing BER. For example, with SNR of 10 dB for 16-QAM and 8-PSK signals with 5 received reflections, BER is reduced approximately by a factor of 7. For 8-FSK signal which has higher noise immunity. More intense reflections are used in the simulations, thus the improvement is less significant than when compared to 16-QAM and 8-PSK signals.

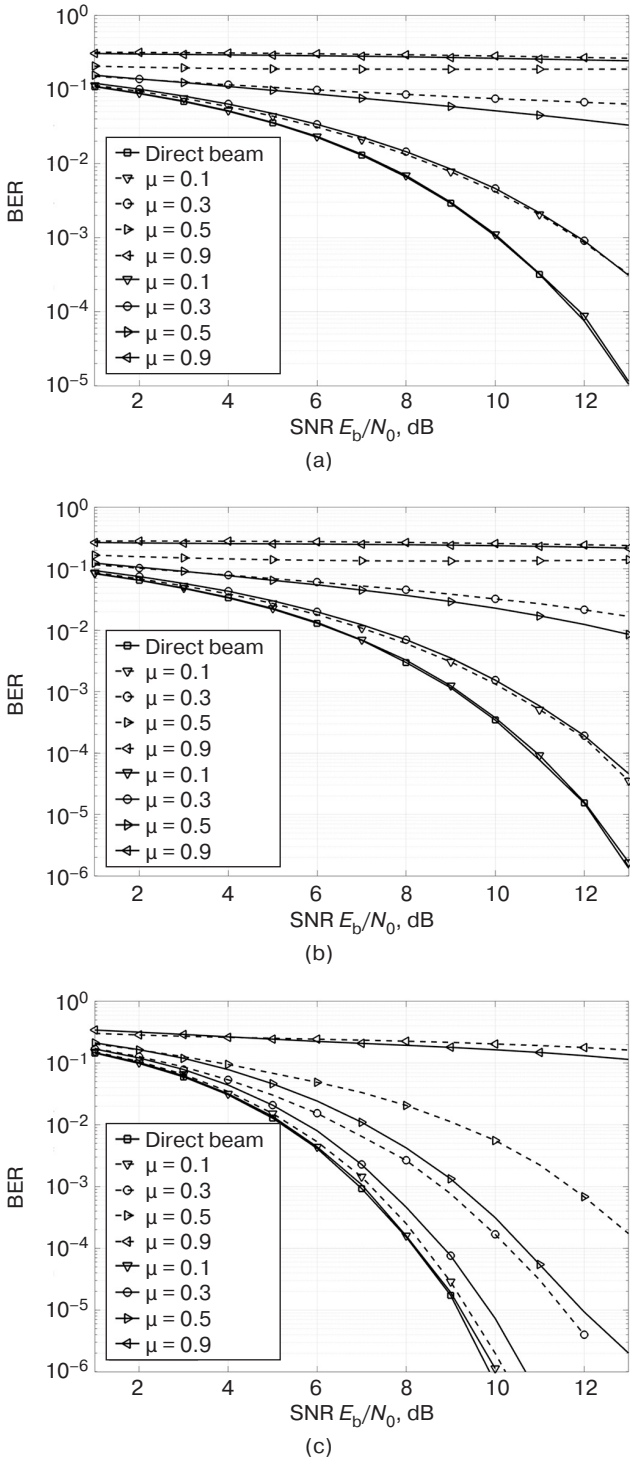

Fig. 3. BER dependency on SNR when receiving signals with one direct and one reflected beam:
(a) 16-QAM;
(b) 8-PSK;
and (c) 8-FSK

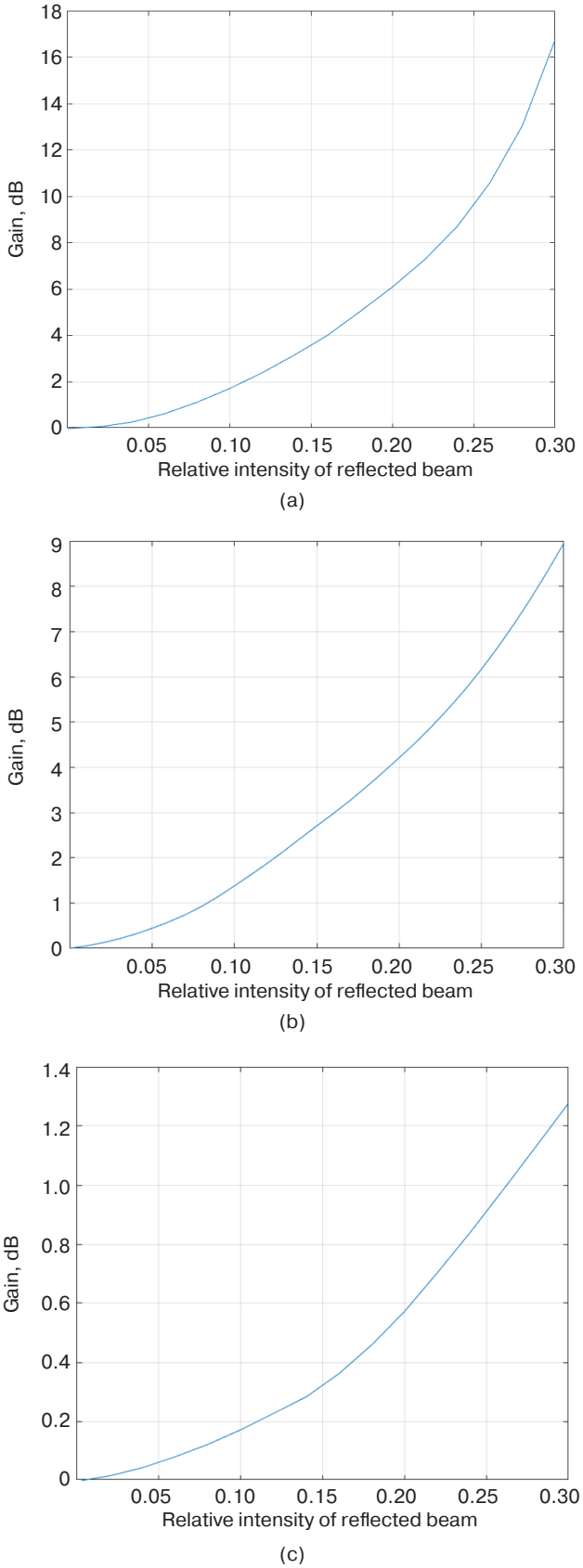

Fig. 4. Results of calculating the energy gain for:
(a) 16-QAM;
(b) 8-PSK;
and (c) 8-FSK

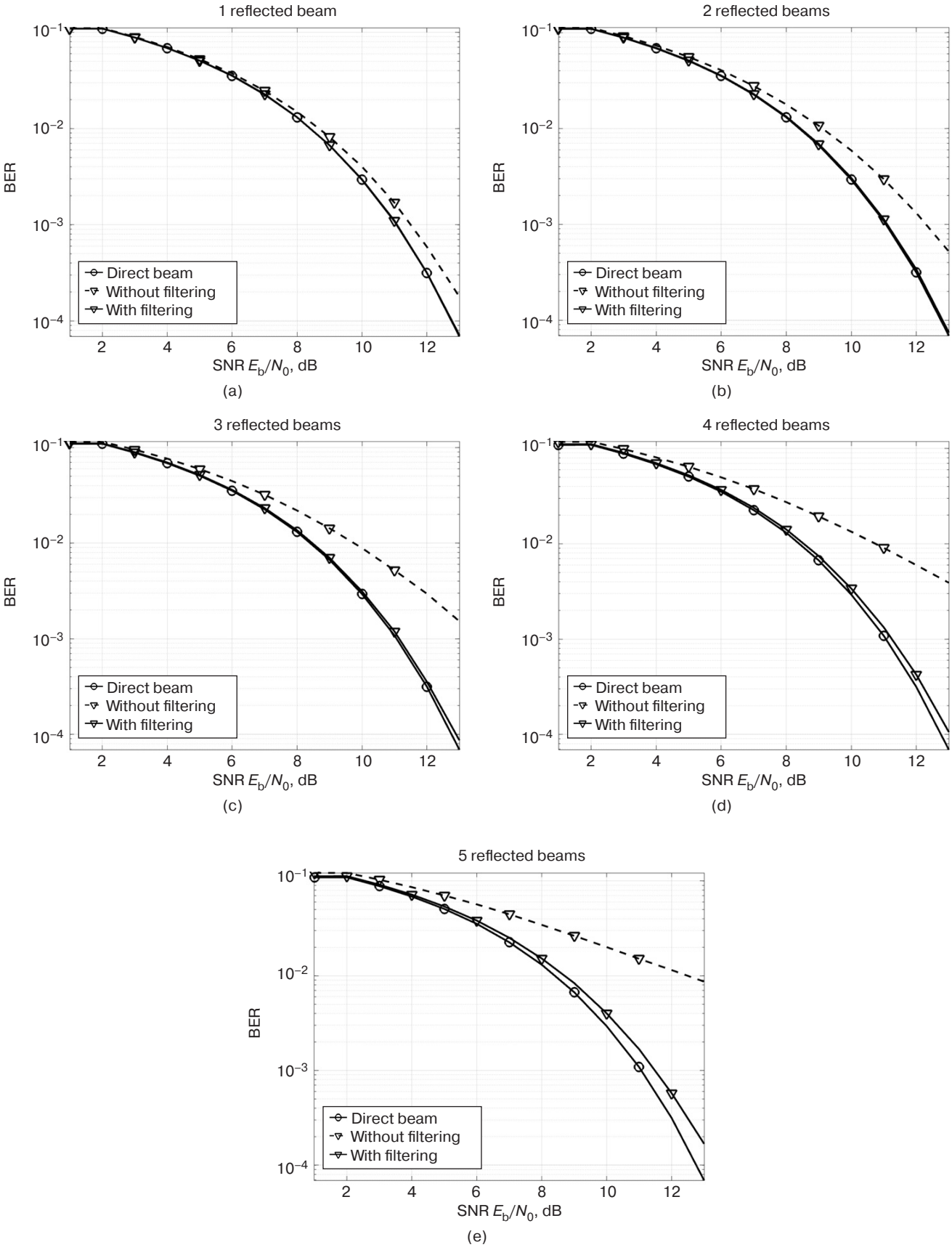

Fig. 5. BER dependence on SNR at different number of beams for 16-QAM

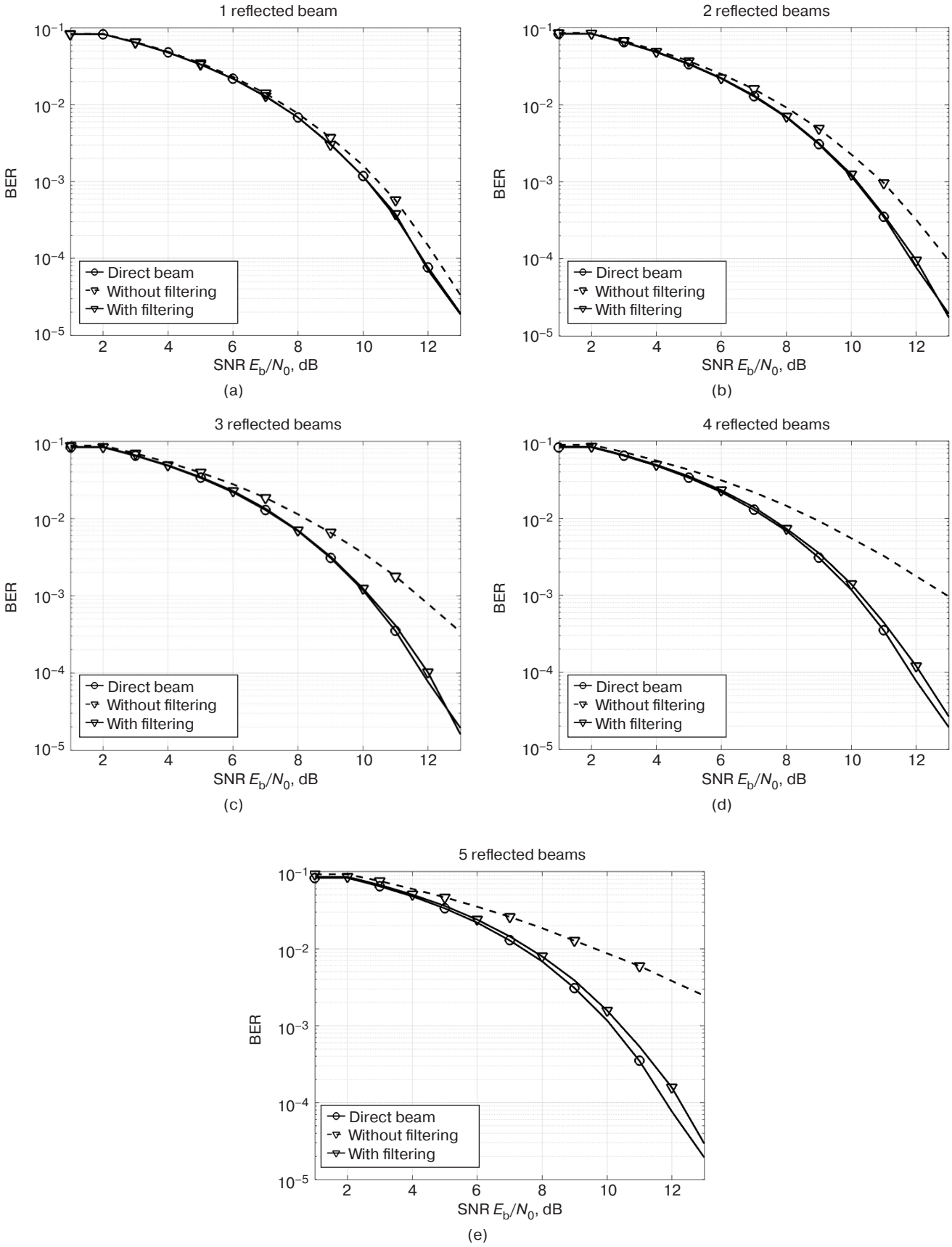

Fig. 6. BER dependence on SNR at different number of beams for 8-PSK

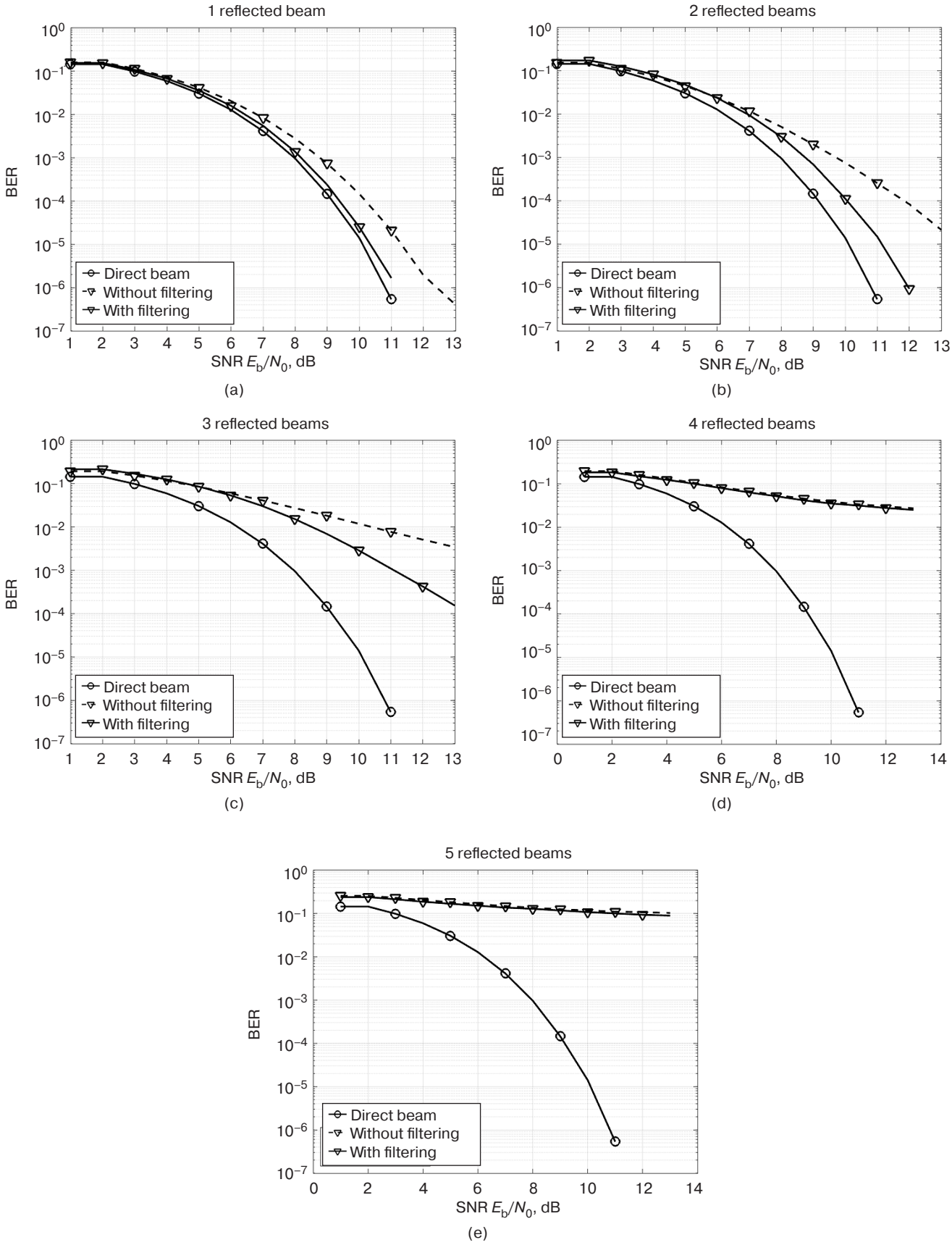

Fig. 7. BER dependence on SNR at different number of beams for 8-FSK

The impact of parameter inaccuracy in the filter with inverse IR

The performance of the filter with inverse IR depends on the precision of its parameter settings, including gain coefficients and time delays within the branches. Under real-world conditions, these parameters can deviate from their calculated values due to variations in the signal transmission environment, inaccuracies in channel estimation, or errors in adaptive algorithms. Therefore, it is essential to assess how parameter deviations in the filter with inverse IR affect communication quality and BER.

In order to evaluate this, a scenario is selected with a channel comprising a direct and delayed signal, with a relative power of 0.2 and a time delay of 21 ns at SNR of 10 dB.

Figure 8 presents graphs of the relationship between BER and deviation of the gain in the filter branch, normalized to a nominal value of 0.2, for 16-QAM, 8-PSK, and 8-FSK signals.

From the results obtained, it can be concluded that the correct operation of the filter is maintained within a fairly broad range of gain variations in the filter section. Therefore, even if the gain deviates by 1.5 times the nominal value specified by the reflected beam level, BER will increase approximately twofold. If the gain deviates two times, BER will increase by an order of magnitude for all signals under consideration.

Figure 9 shows graphs of the relationship between BER and the deviation of the delay in the filter branch, normalized to a nominal value of 21 ns, for 16-QAM, 8-PSK (at the reflected beam intensity of $\mu = 0.2$), and 8-FSK (at the reflected beam intensity of $\mu = 0.5$).

The graphs in Figs. 9a and 9b (for 16-QAM and 8-PSK, respectively) have a characteristic appearance which can be explained by the use of a complex envelope in the signal representation model. This results in a lower "plateau" along the normalized delay time axis, with a duration determined by the channel symbol duration, during which the information component of the signal phase remains constant. When the delay deviates beyond the boundaries of this "plateau," BER sharply increases. For the 8-FSK model, BER cannot be accurately estimated when the delay deviates from the nominal value by less than 5% due to certain software limitations. Nevertheless, the results indicate that the filter is operating correctly within a very narrow range around the nominal delay value. It can be said that an accuracy of approximately 1% is required for proper operation.

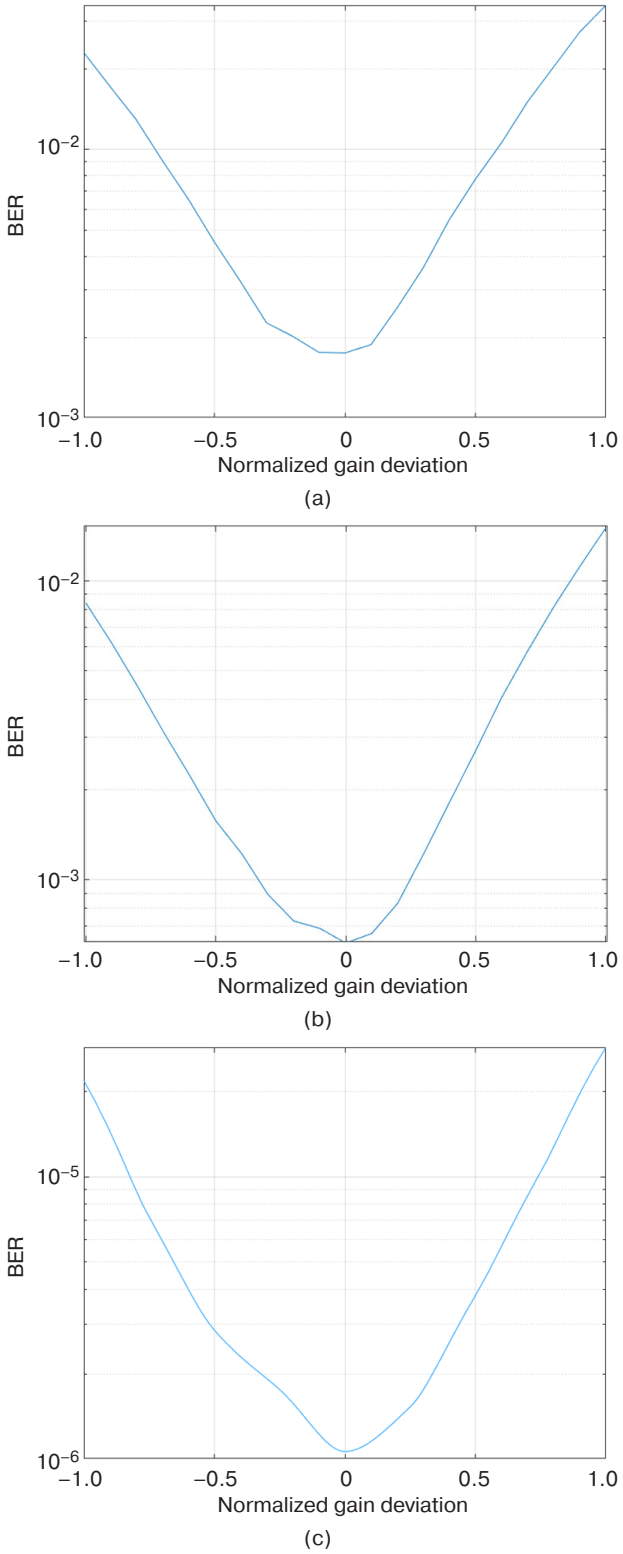

Fig. 8. BER dependence on the normalized gain deviation in the filter branch for signals:
(a) 16-QAM;
(b) 8-PSK;
and (c) 8-FSK

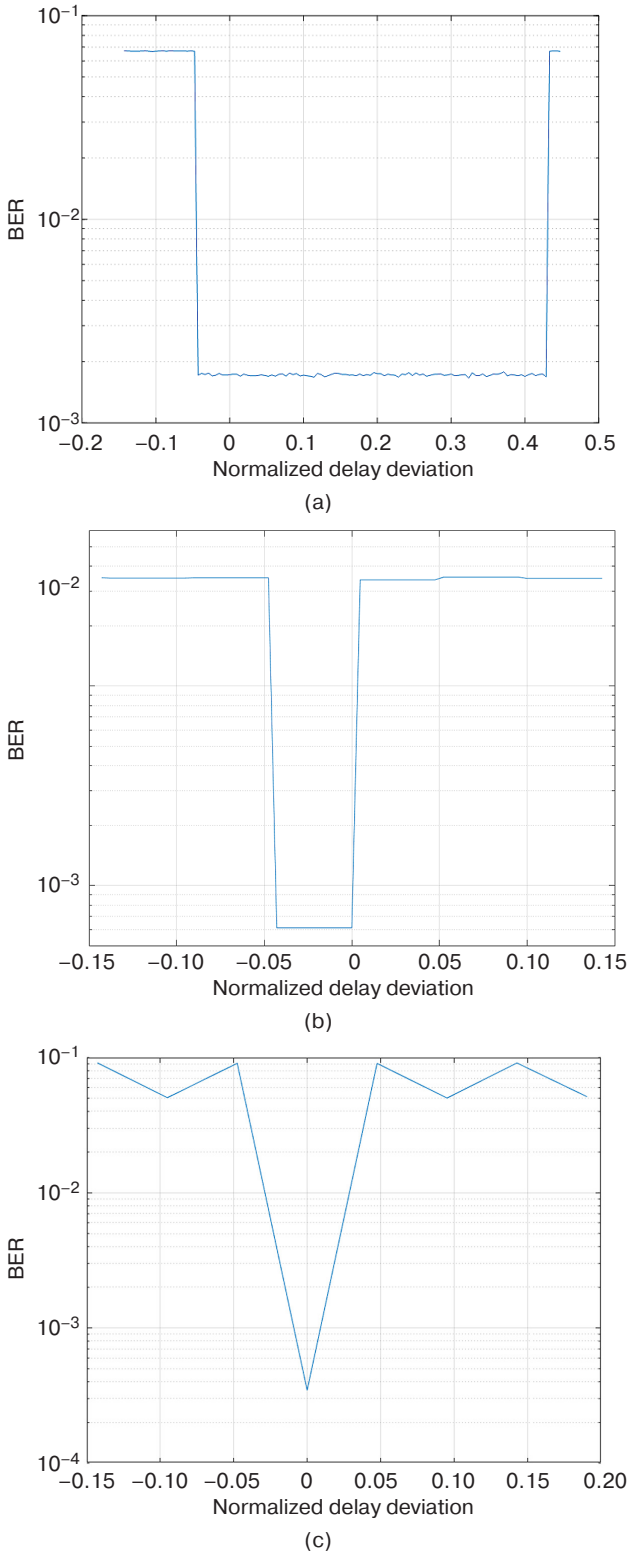

Fig. 9. BER dependence on the normalized delay deviation in filter branch for signals:
(a) 16-QAM;
(b) 8-PSK;
and (c) 8-FSK

CONCLUSIONS

The paper presents the results of an investigation into the efficiency of the filter with inverse IR to that of the communication channel with a discrete multipath at the reception of signals with multi-position types of modulation, such as 16-QAM, 8-PSK, and 8-FSK. Based on mathematical modeling in the *Simulink* environment, the impact of channel parameters and filter parameters on BER is explored.

The use of such compensation filters offers a substantial energy advantage in terms of SNR, which varies depending on the modulation type from units to tens of decibels, making them particularly promising for high-speed communication systems. It was ascertained that the filter continues to function with deviations in the branch gains up to 1.5 times the nominal value, although it is highly sensitive to the accuracy of time delays, with a permissible deviation of 1%.

The efficiency of the filter is also dependent on the number and intensity of beams. Therefore, the upper limit of applicability can be considered to be the value of μ, which is slightly greater than 0.5. When $\mu \to 0.9$, the filter becomes ineffective due to the high level of response at time positions that are twice the time delay (Fig. 2).

Therefore, the use of filters with inverse IR to that of the communication channel is an effective method for combating multipath distortion, significantly improving communication quality and gain. The results obtained confirm the potential of this approach in increasing the reliability and capacity of modern telecommunication systems.

Future research will focus on developing adaptive algorithms aimed at determining the IR of the communication channel and automatically determining parameters for a filter with inverse IR.

Authors' contribution

All authors contributed equally to the research work.

REFERENCES

1. Kubanov V.P., Ruzhnikov V.A., Spodobaev M.Yu., Spodobaev Yu.M. *Osnovy teorii antenn i rasprostraneniya radiovoln* (*Fundamentals of the Theory of Antennas and Radio Wave Propagation*). Samara: OFORT; 2016, 258 p. (In Russ.).
2. Vendik I.B., Vendik O.G., Kozlov D.S., Munina I.V. *Diagrammoobrazovanie v antennykh reshetkakh* (*Diagram Formation in Antenna Arrays*). Moscow: Fizmatlit; 2020, 112 p. (In Russ.).
3. Proakis J. *Digital Communications.* N.Y.: McGraw-Hill Publ.; 2001, 1002 p.
4. Nazarov S.N., Shagarova A.A. Techniques of diversed reception in systems of mobile communication and broadband access. *Avtomatizatsiya protsessov upravleniya = Automation of Control Processes*. 2010;3:88–94 (in Russ.). https://elibrary.ru/muonlj
5. Krinitsky G.V., Leonova M.D., Yurasova E.N. Multipath mitigation techniques in satellite navigation for precise landing. *Nauchnyi vestnik MGTU GA = Civil Aviation High Technologies*. 2015;222:98–102 (in Russ.).
6. Kulikov G.V., Polevoda Yu.A., Kostin M.S. Use of spatially distributed in-phase antenna to increase the noise immunity of signal reception. *Russian Technological Journal.* 2023;11(6):39–46. https://doi.org/10.32362/2500-316X-2023-11-6-39-46
7. Widrow B., Stearns S.D. *Adaptive Signal Processing*. Prentice-Hall; 1985, 474 p.
8. Fal'ko A.I. *Adaptivnyi priem signalov* (*Adaptive Reception of Signals*): Monograph. Novosibirsk: SibGUTI; 2015, 328 p. (In Russ.).
9. Fuqin Xiong. *Digital Modulation Techniques.* 2nd ed. Boston, London: Artech House, Inc.; 2006, 1039 p.
10. Sklar B., Harris F.J. *Digital Communications: Fundamentals and Applications.* 3rd ed. Pearson Education, Inc.; 2021, 1105 p.
11. Troitskaya A.E., Polevoda Yu.A., Kulikov G.V. Noise immunity of signal reception with multiple frequency-shift keying against retransmitted interference. *Russian Technological Journal.* 2024;12(5):33–41. https://doi.org/10.32362/2500-316X-2024-12-5-33-41
12. Ermolaev V.T., Flaksman A.G. *Teoreticheskie osnovy obrabotki signalov v besprovodnykh sistemakh svyazi* (*Theoretical Bases of Signal Processing in Wireless Communication Systems*): Monograph. Nizhny Novgorod: N.I. Lobachevsky NNGU; 2011, 368 p. (In Russ.).
13. Golubev A.G., Molchanov P.A. Estimation algorithms for impulse response of multibeam communication channel with transformation of the working frequency band. *Nauchno-tekhnicheskiye vedomosti SPbGPU. Fiziko-matematicheskiye nauki = St. Petersburg Polytechnic University Journal. Physics and Mathematics*. 2014;1(189):150–156 (in Russ.).
14. Nechaev Yu.B., Malyutin A.A. Methods for estimating the multipath channel parameters using the iterative reception algorithms. *Teoriya i tekhnika radiosvyazi = Radio Communication Theory and Technology.* 2009;2:13–25 (in Russ.). https://www.elibrary.ru/mwnirh
15. Nechaev Yu.B., Malyutin A.A., Radko P.N. Interference immunity of iterative reception algorithms in multipath channels with not precisely defined parameters. *Teoriya i tekhnika radiosvyazi = Radio Communication Theory and Technology.* 2009;4:23–28 (in Russ.). https://www.elibrary.ru/muukjn
16. Korennoi A.V., Mezhuev A.M., Revin V.S. Adaptive algorithm receiving multipath signals in the high frequency communication channel based on the estimation of its impulse response. *Zhurnal Sibirskogo federal'nogo universiteta. Seriya: Tekhnika i tekhnologii = Journal of Siberian Federal University. Engineering & Technologies*. 2017;10(2):200–210 (in Russ.). https://www.elibrary.ru/yhssll
17. Anikin A.S. Impulse responses variability of the terrestrial paths of propagation of centimeter radio waves in ten-second intervals. *Doklady Tomskogo gosudarstvennogo universiteta sistem upravleniya i radioehlektroniki* (*Doklady TUSUR*) = *Proceedings of TUSUR University.* 2017;20(2):10–14 (in Russ.). https://doi.org/10.21293/1818-0442-2017-20-2-10-14, https://www.elibrary.ru/zgqmap
18. Kolmonen V.-M., Kivinen J., Vuokko L., Vainikainen P. 5.3-GHz MIMO Radio channel sounder. *IEEE Trans. Instrum. Meas*. 2006;55(4):1263–1269. https://doi.org/10.1109/TIM.2006.877724
19. Molina-Garcia-Pardo J.-M., Rodriguez J.-V., Juan-Llacer L. MIMO Channel Sounder Based on Two Network Analyzers. *IEEE Trans. Instrum. Meas*. 2008;57(9):2052–2058. https://doi.org/10.1109/TIM.2008.922091
20. Kalachikov A.A., Shchelkunov N.S. Methods of MIMO radio channel sounding. *Vestnik SibGUTI = The Herald of Siberian State University of Telecommunication and Information Science*. 2015;3(31):66–72 (in Russ.). https://www.elibrary.ru/vnvxfb
21. Farina A. Simultaneous measurement of impulse response and distortion with a swept-sine technique. *Audio Engineering Society. AES Convention Papers Forum*. February 2000. Papers Number 5093, 21 p. Available from URL: https://www.researchgate.net/publication/2456363_Simultaneous_Measurement_of_Impulse_Response_and_Distortion_With_a_Swept-Sine_Technique. Accessed February 15, 2025.
22. Khaliullin R.F., Sulimov A.I. Simulation of the impulse response estimation for a MIMO radio system with multipath effect. *Radiotekhnika = Radioengineering*. 2023;87(12):99–109 (in Russ.). https://doi.org/10.18127/j00338486-202312-11, https://www.elibrary.ru/pteaii
23. Khaliullin R.F., Sulimov A.I., Galiev A.A. Using software-defined radio for estimation of impulse response of multipath channel. *In: Radio Wave Propagation: Proceedings of the 28th All-Russian Open Scientific Conference*, Yoshkar-Ola, May 16–19, 2023. Yoshkar-Ola: Volga State Technological University; 2023. P. 261–264 (in Russ.). https://www.elibrary.ru/qivpqk
24. Kulikov G.V., Polevoda Yu.A., Chistyakov E.A. Methods of adaptive rejection of signal audio interference. In: *Space Technologies – 2024: Proceedings of the International Interdepartmental Scientific and Production Conference.* Moscow: RTU MIREA; 2024. P. 230–235 (in Russ.). https://www.elibrary.ru/yriksc

СПИСОК ЛИТЕРАТУРЫ

1. Кубанов В.П., Ружников В.А., Сподобаев М.Ю., Сподобаев Ю.М. *Основы теории антенн и распространения радиоволн.* Самара: ОФОРТ; 2016, 258 с.
2. Вендик И.Б., Вендик О.Г., Козлов Д.С., Мунина И.В. *Диаграммообразование в антенных решетках.* М.: Физматлит; 2020, 112 с.
3. Proakis J. *Digital Communications.* N.Y.: McGraw-Hill Publ.; 2001, 1002 p.
4. Назаров С.Н., Шагарова А.А. Методы разнесенного приема в системах подвижной связи и широкополосного доступа. *Автоматизация процессов управления*. 2010;3:88–94. https://elibrary.ru/muonlj

5. Криницкий Г.В., Леонова М.Д., Юрасова Е.Н. Методы снижения влияния многолучевости на качество спутниковой навигации для обеспечения точного захода на посадку. *Научный вестник МГТУ ГА*. 2015;222:98–102.
6. Куликов Г.В., Полевода Ю.А., Костин М.С. Использование пространственно-распределенной синфазной антенны для повышения помехоустойчивости приема сигналов. *Russian Technological Journal.* 2023;11(6):39–46. https://doi.org/10.32362/2500-316X-2023-11-6-39-46
7. Widrow B., Stearns S.D. *Adaptive Signal Processing*. Prentice-Hall; 1985, 474 p.
8. Фалько А.И. *Адаптивный прием сигналов*: монография. Новосибирск: СибГУТИ; 2015, 328 с.
9. Fuqin Xiong. *Digital Modulation Techniques.* 2nd ed. Boston, London: Artech House, Inc.; 2006, 1039 p.
10. Sklar B., Harris F.J. *Digital Communications: Fundamentals and Applications.* 3rd ed. Pearson Education, Inc.; 2021, 1105 p.
11. Троицкая А.Е., Полевода Ю.А., Куликов Г.В. Помехоустойчивость приема сигналов с многопозиционной частотной манипуляцией на фоне ретранслированной помехи. *Russian Technological Journal.* 2024;12(5):33–41. https://doi.org/10.32362/2500-316X-2024-12-5-33-41
12. Ермолаев В.Т., Флаксман А.Г. *Теоретические основы обработки сигналов в беспроводных системах связи*: монография. Нижний Новгород: Изд-во ННГУ им. Н.И. Лобачевского; 2011, 368 с.
13. Голубев А.Г., Молчанов П.А. Алгоритмы оценивания импульсной характеристики многолучевого канала связи с трансформацией рабочего диапазона частот. *Научно-технические ведомости СПбГПУ. Физико-математические науки*. 2024;1(189):150–156.
14. Нечаев Ю.Б., Малютин А.А. Методы оценки параметров многолучевого канала связи при итеративных алгоритмах приема. *Теория и техника радиосвязи*. 2009;2:13–25. https://www.elibrary.ru/mwnirh
15. Нечаев Ю.Б., Малютин А.А., Радько П.Н. Помехоустойчивость итеративных алгоритмов приема в многолучевых каналах с неточно известными параметрами. *Теория и техника радиосвязи*. 2009;4:23–28. https://www.elibrary.ru/muukjn
16. Коренной А.В., Межуев А.М., Ревин В.С. Адаптивный алгоритм приема многолучевых сигналов в декаметровом канале связи на основе оценки его импульсной характеристики. *Журнал Сибирского федерального университета. Серия: Техника и технологии*. 2017;10(2):200–210. https://www.elibrary.ru/yhssll
17. Аникин А.С. Изменчивость импульсных реакций сухопутных трасс распространения сантиметровых радиоволн в десятисекундных интервалах. *Доклады Томского государственного университета систем управления и радиоэлектроники* (*Доклады ТУСУР*). 2017;20(2):10–14. https://doi.org/10.21293/1818-0442-2017-20-2-10-14, https://www.elibrary.ru/zgqmap
18. Kolmonen V.-M., Kivinen J., Vuokko L., Vainikainen P. 5.3-GHz MIMO Radio channel sounder. *IEEE Trans. Instrum. Meas*. 2006;55(4):1263–1269. https://doi.org/10.1109/TIM.2006.877724
19. Molina-Garcia-Pardo J.-M., Rodriguez J.-V., Juan-Llacer L. MIMO Channel Sounder Based on Two Network Analyzers. *IEEE Trans. Instrum. Meas*. 2008;57(9):2052–2058. https://doi.org/10.1109/TIM.2008.922091
20. Калачиков А.А., Щелкунов Н.С. Методы зондирования радиоканала MIMO. *Вестник СибГУТИ*. 2015;3(31):66–72. https://www.elibrary.ru/vnvxfb
21. Farina A. Simultaneous measurement of impulse response and distortion with a swept-sine technique. *Audio Engineering Society*. *AES Convention Papers Forum*. February 2000. Papers Number 5093, 21 p. URL: https://www.researchgate.net/publication/2456363_Simultaneous_Measurement_of_Impulse_Response_and_Distortion_With_a_Swept-Sine_Technique. Дата обращения 15.02.2025. / Accessed February 15, 2025.
22. Халиуллин Р.Ф., Сулимов А.И. Моделирование оценки импульсной характеристики MIMO-радиосистемы с многолучевым эффектом. *Радиотехника*. 2023;87(12):99–109. https://www.elibrary.ru/pteaii
23. Халиуллин Р.Ф., Сулимов А.И., Галиев А.А. Применение программно-определяемого радио для определения импульсной характеристики многолучевого радиоканала. В сб.: *Распространение радиоволн: сборник докладов XXVIII Всероссийской открытой научной конференции*, Йошкар-Ола, 16–19 мая 2023 г. Йошкар-Ола: Поволжский государственный технологический университет; 2023. С. 261–264. https://www.elibrary.ru/qivpqk
24. Полевода Ю.А., Куликов Г.В., Чистяков Е.А. Компенсация многолучевости в канале связи с КАМ сигналом. В сб.: *Космические технологии – 2024. Сборник научных статей Международной межведомственной научно-технической конференции.* М.: РТУ МИРЭА; 2024. С. 236–241. https://www.elibrary.ru/yriksc

About the Authors

Yuriy A. Polevoda, Postgraduate Student, Department of Radio Electronic Systems and Complexes, Institute of Radio Electronics and Informatics, MIREA – Russian Technological University (78, Vernadskogo pr., Moscow, 119454 Russia). E-mail: polevoda@mirea.ru. https://orcid.org/0009-0007-6327-9685

Gennady V. Kulikov, Dr. Sci. (Eng.), Professor, Department of Radio Electronic Systems and Complexes, Institute of Radio Electronics and Informatics, MIREA – Russian Technological University (78, Vernadskogo pr., Moscow, 119454 Russia). E-mail: kulikov@mirea.ru. Scopus Author ID 36930533000, RSCI SPIN-code 2844-8073, http://orcid.org/0000-0001-7964-6653

Об авторах

Полевода Юрий Александрович, аспирант, кафедра радиоэлектронных систем и комплексов, Институт радиоэлектроники и информатики, ФГБОУ ВО «МИРЭА – Российский технологический университет» (119454, Россия, Москва, пр-т Вернадского, д. 78). E-mail: polevoda@mirea.ru. https://orcid.org/0009-0007-6327-9685

Куликов Геннадий Валентинович, д.т.н., профессор, кафедра радиоэлектронных систем и комплексов, Институт радиоэлектроники и информатики, ФГБОУ ВО «МИРЭА – Российский технологический университет» (119454, Россия, Москва, пр-т Вернадского, д. 78). E-mail: kulikov@mirea.ru. Scopus Author ID 36930533000, SPIN-код РИНЦ 2844-8073, http://orcid.org/0000-0001-7964-6653

Translated from Russian into English by Kirill V. Nazarov
Edited for English language and spelling by Dr. David Mossop

Micro- and nanoelectronics. Condensed matter physics
Микро- и наноэлектроника. Физика конденсированного состояния

UDC 539.87
https://doi.org/10.32362/2500-316X-2026-14-1-43-54
EDN AYEFUG

RESEARCH ARTICLE

Fabrication of two-dimensional semiconductors on the surface of ferroelectric films by means of gold-assisted mechanical exfoliation

Evgeny I. Zhemerov [@], Andrey A. Guskov, Elizaveta A. Bulavintseva, Dmitry S. Seregin, Sergei D. Lavrov

MIREA – Russian Technological University, Moscow, 119454 Russia
[@] Corresponding author, e-mail: zhemerov@mirea.ru

• **Submitted:** 02.06.2025 • **Revised:** 10.07.2025 • **Accepted:** 07.11.2025

Abstract

Objectives. The aim of this study is to develop and demonstrate an effective method for obtaining large-area, high-quality monolayers of molybdenum disulfide (MoS_2) on the surface of ferroelectric lead zirconate titanate (PZT) films which exhibit pronounced granularity and texturing. Conventional mechanical exfoliation techniques are inefficient for transferring two-dimensional materials onto nonplanar surfaces. This is due to local height variations and substrate granularity which hinder the formation of continuous monolayers and high-defect-density transferred structures. A particular challenge is the transfer onto functional substrates with surface topography characterized by heterogeneities ranging from tens of nanometers to micrometers.

Methods. A gold-assisted exfoliation (GAE) method was employed, including: magnetron sputtering of a 50 nm gold film; mechanical delamination of monolayers using thermally cleavable tape; and subsequent gold etching. The characterization was performed using X-ray diffraction, optical confocal microscopy, atomic force microscopy, and second harmonic generation techniques. The efficiency of the transfer process was compared for Si/SiO_2 and PZT substrates.

Results. MoS_2 crystallites with areas up to 3000 μm^2 were obtained on PZT and over 65000 μm^2 on standard Si/SiO_2 substrates, both of which exhibit minimal defect densities. Conventional mechanical exfoliation is shown to be unable to ensure transfer onto textured surfaces, whereas the GAE method preserves the monolayer character of the transferred crystallites even on nonplanar substrates.

Conclusions. This work demonstrates for the first time the possibility of obtaining large-area, high-quality MoS_2 monolayers on substrates with pronounced grainy and textured structures, such as ferroelectric PZT films, using the gold-assisted exfoliation method. The work also shows that gold-assisted exfoliation is an effective technique for fabricating extended two-dimensional films with controlled morphological and structural properties, including on substrates previously considered unsuitable for such applications.

Keywords: two-dimensional materials, molybdenum disulfide, gold-assisted exfoliation, ferroelectric thin films, lead zirconate titanate, mechanical exfoliation, nanostructures, FeFET

For citation: Zhemerov E.I., Guskov A.A., Bulavintseva E.A., Seregin D.S., Lavrov S.D. Fabrication of two-dimensional semiconductors on the surface of ferroelectric films by means of gold-assisted mechanical exfoliation. *Russian Technological Journal.* 2026;14(1):43–54. https://doi.org/10.32362/2500-316X-2026-14-1-43-54, https://www.elibrary.ru/AYEFUG

Financial disclosure: The authors have no financial or proprietary interest in any material or method mentioned.

The authors declare no conflicts of interest.

НАУЧНАЯ СТАТЬЯ

Создание двумерных полупроводников на поверхности сегнетоэлектрических пленок методом механической эксфолиации при помощи золота

Е.И. Жемеров [@], А.А. Гуськов, Е.А. Булавинцева, Д.С. Серегин, С.Д. Лавров

МИРЭА – Российский технологический университет, Москва, 119454 Россия
[@] Автор для переписки, e-mail: zhemerov@mirea.ru

• **Поступила:** 02.06.2025 • **Доработана:** 10.07.2025 • **Принята к опубликованию:** 07.11.2025

Резюме

Цели. Цель работы заключается в разработке и демонстрации эффективного метода получения протяженных и высококачественных монослоев дисульфида молибдена (MoS_2) на поверхности сегнетоэлектрических пленок цирконата-титаната свинца (ЦТС) с выраженной зернистой и текстурированной структурой. Стандартные методы механической эксфолиации оказываются неэффективными для переноса двумерных материалов на неровные поверхности из-за локальных перепадов высоты и зернистости подложки, что приводит к невозможности формирования протяженных монослоев и высокой плотности дефектов в переносимых структурах. Особую сложность представляет перенос на функциональные подложки с рельефом поверхности, характеризующимся неоднородностью на масштабах от десятков нанометров до микрометров.

Методы. Использован метод золото-ассистированной эксфолиации (gold-assisted exfoliation, GAE), включающий магнетронное напыление золотой пленки толщиной 50 нм, механическое отделение монослоев с помощью терморасщепляемого скотча и последующее травление золота. Характеризация проведена методами рентгеновской дифракции, оптической конфокальной микроскопии, атомно-силовой микроскопии и генерации второй оптической гармоники. Сравнение эффективности переноса выполнено на подложках кремния/оксида кремния (Si/SiO_2) и ЦТС.

Результаты. Получены кристаллиты MoS_2 площадью до 3000 мкм^2 на ЦТС и свыше 65000 мкм^2 – на стандартных подложках Si/SiO_2 при минимальной плотности дефектов. Показано, что стандартная механическая эксфолиация не обеспечивает перенос на текстурированные поверхности, тогда как GAE сохраняет монослойность переносимых кристаллитов даже на неровных подложках.

Выводы. Впервые продемонстрирована возможность получения протяженных и высококачественных монослоев MoS_2 на подложках с выраженной зернистой и текстурированной структурой, таких как сегнетоэлектрические пленки ЦТС, с помощью метода золото-ассистированной эксфолиации. Показано, что золото-ассистированная эксфолиация представляет собой эффективный метод для создания протяженных двумерных пленок с контролируемыми морфологическими и структурными характеристиками, в т.ч. на подложках, ранее считавшихся непригодными для подобных задач.

Ключевые слова: двумерные материалы, дисульфид молибдена, золото-ассистированная эксфолиация, сегнетоэлектрические пленки, цирконат-титанат свинца, механическая эксфолиация, наноструктуры, FeFET

Для цитирования: Жемеров Е.И., Гуськов А.А., Булавинцева Е.А., Серегин Д.С., Лавров С.Д. Создание двумерных полупроводников на поверхности сегнетоэлектрических пленок методом механической эксфолиации при помощи золота. *Russian Technological Journal*. 2026;14(1):43–54. https://doi.org/10.32362/2500-316X-2026-14-1-43-54, https://www.elibrary.ru/AYEFUG

Прозрачность финансовой деятельности: Авторы не имеют финансовой заинтересованности в представленных материалах или методах.

Авторы заявляют об отсутствии конфликта интересов.

INTRODUCTION

Over the past two decades, two-dimensional (2D) materials such as graphene, molybdenum disulfide, and hexagonal boron nitride have become the subject of intensive research due to their unique physical, optical, and electronic properties, fundamentally different from those of their bulk analogs [1, 2]. These properties are due to the quantum size effect, high anisotropy, increased specific surface area, and changes in the electronic structure upon going to atomically thin layers. 2D materials in particular exhibit unusual quantum phenomena such as the quantum Hall effect, strong fluorescence in MoS_2 monolayers, and ultra-high charge carrier mobility. This opens new horizons for fundamental research in condensed matter physics and materials science [3].

Thanks to these properties, two-dimensional materials are being considered as platforms for creating new generations of electronic, optoelectronic, energy, and sensor devices. However, the practical realization of their promise is closely linked to the ability to produce high-quality, defect-free, and extended-area monolayers, as well as their integration into modern micro- and nanoelectronic technologies. Until recently, the synthesis of such layers and their transfer to functional substrates was a serious technological challenge, significantly hindering both in-depth research into fundamental principles and the development of applied solutions.

There are several methods for producing two-dimensional materials, each with its own advantages and limitations. The most common approaches include mechanical exfoliation, liquid exfoliation, and chemical vapor deposition (CVD). Mechanical exfoliation, first used to synthesize graphene, remains the benchmark method for producing high-quality samples with low defect density [4]. However, its scalability is limited by small lateral dimensions. Liquid exfoliation enables the mass production of materials but leads to crystal fragmentation and contamination. Chemical vapor deposition enables the synthesis of large-area films, but the defect density in such materials often exceeds 10^{12}–10^{13} cm^{-2} [5].

One possible solution to the problem of creating layers with the desired characteristics is the gold-assisted exfoliation (GAE) method which has been relatively recently developed. This method combines the advantages of mechanical exfoliation and scalability, enabling the production of single crystals up to a centimeter in size [6–8], while the defect density in the resulting layers is minimal and can reach $\sim 3 \cdot 10^{11}$ cm^{-2} [9]. Thus, GAE is the preferred method for applications where high structural perfection and surface cleanliness are critical.

Despite significant progress in producing 2D materials, integrating high-quality 2D crystals into real devices still poses significant technological challenges. One of the key challenges in modern electronics is the creation of functional structures in which 2D layers are transferred onto substrates with distinct surface topography. These include such films as ferroelectric lead zirconate titanate ($Pb(Zr_{0.48}Ti_{0.52})O_3$, PZT) films used in ferroelectric field-effect transistor (FeFET) architectures and other memristor devices. However, standard mechanical exfoliation methods are ineffective for transferring 2D materials to such uneven or textured surfaces. Localized differences in height and substrate graininess dramatically reduce the contact area between the 2D crystal and the substrate, making it impossible to form extended and continuous monolayers. As a result, attempts to use classical approaches lead either to a complete absence of transfer or to the formation of highly fragmented and defective regions unsuitable for practical application.

In order to overcome these limitations, new methods must be developed to ensure selective and delicate transfer of 2D materials, even onto complex substrates with pronounced microroughness. One of the most promising solutions is the GAE method mentioned above. However, its application to textured ferroelectric films has remained largely unexplored to date. Given that such structures are essential for the implementation of modern FeFET and memristor devices, demonstrating the feasibility of efficient transfer of 2D materials onto PZT and similar surfaces is of fundamental and applied importance.

The main objective of this study is to experimentally demonstrate that gold-assisted exfoliation enables the formation of extended, high-quality monolayers of 2D materials not only on standard flat substrates, but also on functional ferroelectric films with distinct topography. This study compares the transfer efficiency

of SiO_2 and PZT, and analyzes the morphology, structural perfection, and area of the resulting crystallites. Particular attention is paid to the comparison with the results obtained using classical mechanical exfoliation. As this study shows, this does not, however, ensure the transfer of 2D materials onto uneven substrates. Thus, the results of this study not only expand our fundamental understanding of the mechanisms of interaction between 2D crystals and textured surfaces, but also open up new possibilities for integrating 2D materials into promising electronic and spintronic devices.

1. MATERIALS AND METHODS

1.1. Methodology for creating two-dimensional films

Molybdenum disulfide (MoS_2) was chosen as the two-dimensional semiconductor material for creating monolayers. This is due to two key factors: its widespread use in modern research; and its strong chemical interaction with gold [10]. Gold atoms, which possess vacant *d*-orbitals, effectively interact with the lone electron pairs of sulfur atoms, forming strong covalent bonds. This interaction ensures the high selectivity of the GAE method with respect to sulfur-containing compounds, making MoS_2 the optimal material for developing this technique.

In order to verify the developed method, experiments were conducted in two stages. In the first stage, a standard silicon/silicon oxide (Si/SiO_2) structure, traditionally used in mechanical exfoliation [11, 12], was used as a substrate for the formation of reference quasi-two-dimensional crystallites. In the second stage, the gold-assisted exfoliation technology was adapted for deposition onto a textured ferroelectric PZT film. This allowed for the applicability of the method for creating two-dimensional structures on functional materials with a non-uniform surface to be evaluated.

PZT films ($Pb(Zr_{0.48}Ti_{0.52})O_3$) were formed from a film-forming solution prepared by the sol–gel method using a complex of zirconium isopropoxide monosolvate ($Zr[OCH(CH_3)_2]_4(CH_3)_2CHOH$, Sigma-Aldrich, USA), titanium tetraisopropoxide ($Ti[O(CH_3)_2CH]_4$, Sigma-Aldrich) and lead acetate ($Pb(CH_3COO)_2$) synthesized from lead oxide (PbO, Sigma-Aldrich) according to a previously developed technique [13]. The PZT solution was applied layer by layer (6 layers, ~220 nm) by spin coating on platinized silicon substrates with the following structure: Pt (~150 nm)–TiO_2 (~10 nm)–SiO_2 (~300 nm)–Si (~800 μm). After spin coating (2500 rpm), each layer was dried for 5 min with an infrared lamp in pulsed mode at a temperature of ~200°C and annealed for 15 min at a temperature of 400°C in an SNOL 1.6.2.5.1/10-IZM muffle furnace (Termiks, Russia). After heat treatment of the sixth layer, the sample was crystallized for 10 min using an AS-One 150 fast annealing unit (Annealsys, France) at a temperature of 650°C (heating rate ~15°C/s).

The process of creating single-crystal samples involves five key steps which are detailed in Fig. 1. In the first step, a bulk molybdenum disulfide crystal is separated layer by layer using adhesive tape (e.g., silicone tape). This step enables the production of multilayer fragments with thicknesses ranging from a few nanometers to microns. In the second step, a 50-nm-thick gold film is deposited onto the pre-treated multilayer MoS_2 crystallites using a VUP-5 magnetron setup (Russia). The process is carried out in a vacuum chamber at a power of 100 W and an argon pressure of $5 \cdot 10^{-3}$ Torr. In the third step, thermal release tape (TRT) is tightly pressed onto the gold surface. After fixation, the tape is carefully peeled off from the original substrate, thus capturing the top MoS_2 layer along with the gold film. The Au–MoS_2 adhesive force exceeds the interlayer van der Waals bonds in MoS_2, enabling selective detachment of the monolayer. In the fourth step, the resulting TRT–Au–MoS_2 structure is transferred to a Si/SiO_2 substrate, in order for the MoS_2 layer to remain in contact with the substrate. The substrate is then heated on a hot plate at 130–150°C for 1–2 min. This weakens the adhesion of the TRT tape, enabling its removal without leaving a trace. In the final step, the gold film is removed by immersion in an etching solution (4 g KI + + 1 g I_2 in 40 mL H_2O) for 3–5 min at room temperature. MoS_2 demonstrates the chemical inertness to this reagent due to its covalent S–Mo–S structure. After the etching is complete, the surface is cleaned for 10 min with acetone to remove any remaining etchant, followed by a rinse with isopropyl alcohol. This procedure ensures the complete removal of contaminants and reagent residues, facilitating the formation of clean, high-quality 2D semiconductor monolayers with large lateral dimensions.

1.2. Research methods

X-ray diffraction was used to analyze the crystal structure, allowing us to determine interplanar spacings and structural symmetry. This is necessary, in order to verify the phase purity of bulk molybdenum disulfide and assess the quality of the PZT films, which served as the basis for creating the two-dimensional films. This approach allows us to confirm the material compliance with the specified characteristics and their suitability for further research.

Diffraction patterns were obtained using a DRON-8T diffractometer (Burevestnik, Russia) at a voltage of 40 kV and a current of 20 mA. Due to the limitations of the method, only bulk MoS_2 samples and polycrystalline

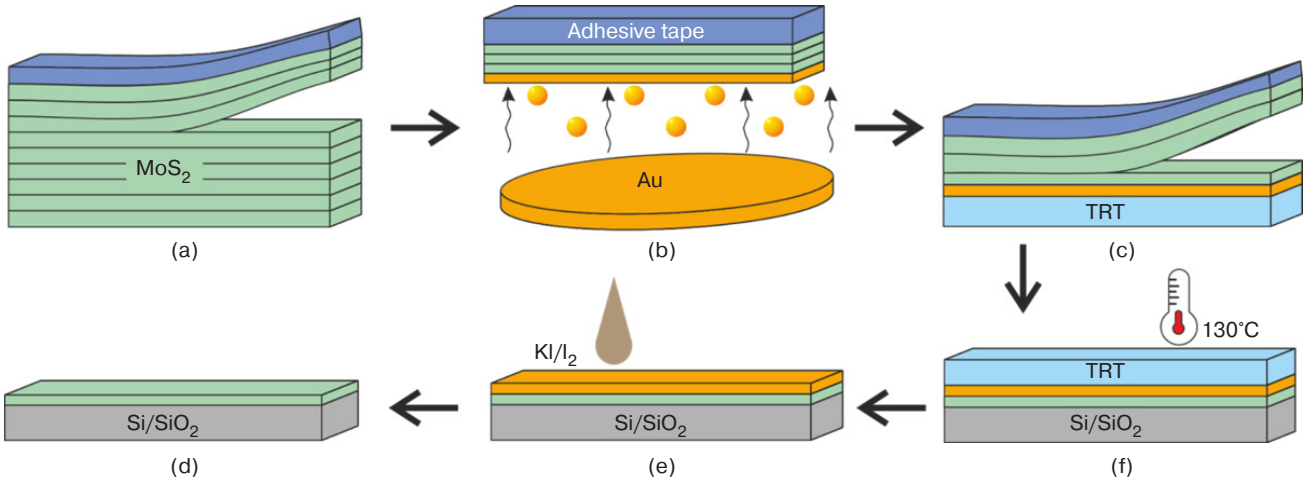

Fig. 1. Process of creating monolayer MoS_2 films:
(a) mechanical exfoliation of MoS_2; (b) magnetron sputtering of gold on MoS_2;
(c) application of TRT tape to gold and subsequent exfoliation of MoS_2; (d) removal of TRT tape by heating;
(e) etching of gold with a KI/I_2 solution; (f) the finished monolayer on a Si/SiO_2 substrate

PZT films were studied, since the small thickness of two-dimensional films significantly complicates the separation of the diffraction signal from the substrate.

Following GAE exfoliation, standard optical confocal microscopy was used to detect monolayer MoS_2 crystallites on the substrate surface. This approach is optimal for rapid preliminary analysis, enabling the determination of crystallite thickness, size, and the presence of defects [8]. An Alpha 300s+ optical microscope (WITec, Germany) with high-aperture objectives and color filters was used. This provides enhanced image contrast for monolayer crystallites, critical when working with atomically thin materials. This method effectively identifies promising areas for subsequent detailed study using other analytical methods.

Atomic force microscopy (AFM), which complements optical data, was used to accurately assess the topography of two-dimensional materials. Atomic force microscopy provides a three-dimensional image of the surface with a resolution of up to nanometers, enabling the detection of defects such as cracks, dislocations, and roughness. This is especially important for quality control of the resulting two-dimensional films and the assessment of the influence of the substrate on their morphology [14]. All measurements were performed using an Ntegra Prima scanning probe microscopy system (NT-MDT, Russia) in contact mode. Rigid probes of the Etalon series with a spring constant of 12 N/m were used, ensuring an optimal balance between resolution and the integrity of the studied samples.

The standard fluorescence microscopy-spectroscopy technique was not used in this study. This is due to the complete signal quenching caused by residual gold nanostructures after the GAE technique. Even very small amounts of gold (Au), retained on the substrate surface or near two-dimensional crystallites, act as effective nonradiative recombination centers. This is due to two main mechanisms of luminescence quenching. The first mechanism is the charge quenching effect: electron transfer from MoS_2 to Au leads to *p*-doping of the material and suppression of exciton luminescence. The second mechanism is resonant energy transfer: at distances less than 10 nm between Au and MoS_2 non-radiative energy transfer from excitons to plasmonic modes of gold occurs [15, 16]. In addition, this technique is not applicable to samples thicker than one monolayer [17].

For this reason, second harmonic generation (SHG) was additionally used to study structural symmetry, crystallographic orientation, and defects in two-dimensional materials. This nonlinear optical method is based on the conversion of two photons of exciting radiation into one photon with doubled frequency in non-centrosymmetric media. SHG is particularly effective for studying thin MoS_2 layers, since the signal intensity depends significantly on the number of layers and their polytype. In regions with broken crystal symmetry, including edges, defects, and transitions between domains, a significant enhancement of the non-linear response is observed, ensuring high sensitivity of the method to the structural features of two-dimensional crystallites.

The experimental setup used a TiF-DP 60 femto-second titanium:sapphire laser (Avesta, Russia) with a pulse duration of 20–60 fs and a repetition rate of 80 MHz. The femtosecond pulses provided high peak

power with low average power, enabling an intense nonlinear response without thermal damage to the sample. A modified WITec Alpha 300S+ confocal microscope was also used for precise sample positioning and scanning.

2. RESULTS

In order to characterize the crystal structure and phase composition of the starting materials, X-ray diffraction studies were carried out in the 2θ-scanning mode. The results are presented in Fig. 2. The diffraction pattern of the bulk MoS_2 crystal demonstrates clearly defined reflections (004), (006), and (008), indicating a high degree of crystallinity and a preferential orientation of the crystallites along the axis perpendicular to the plane of the layers. The nature of the diffraction pattern indicates a hexagonal structure of the 2H or 3R polytype of MoS_2, fully consistent with the literature data [18, 19]. Analysis of the diffraction pattern of the PZT film revealed the presence of characteristic peaks (100), (111), (002), (200), and (301), confirming the formation of the perovskite phase with a preferential orientation in the (111) plane [20]. The formation of the perovskite-like AVO_3 structure in PZT provides the emergence of ferroelectric properties. This is due to the displacement of Ti^{4+}/Zr^{4+} and Pb^{2+} cations from centrosymmetric positions in the oxygen octahedra, which disrupts the inversion symmetry of the crystal and creates spontaneous polarization [21]. The possibility of reorienting this polarization by an external electric field determines the ferroelectric behavior of the material, as confirmed by characteristic hysteresis loops in the polarization-electric field dependences [22]. The low-intensity reflections corresponding to the Pt and Si phases are associated with the multilayer structure of the substrate used. They do not affect the functional properties of the ferroelectric film. Quantitative analysis of the half-width of the diffraction lines indicates the absence of significant microstrains and structural defects in the studied materials, confirming their high crystalline perfection and structural homogeneity. These results indicate the suitability of the selected materials for further use as feedstock and functional substrate in the creation of heterostructures by gold-assisted exfoliation.

In order to analyze the influence of the surface parameters of the used substrates on the efficiency of the GAE technique, the surfaces of both substrates—Si/SiO_2 and PZT—were analyzed using the AFM technique. The resulting three-dimensional maps of the substrate surfaces are presented in Fig. 3. As can be clearly seen from the results obtained, PZT has significantly greater surface inhomogeneities due to the characteristics of grain growth during crystallization. PZT films obtained by the sol–gel method are characterized by the formation of a polycrystalline structure with pronounced grain boundaries, leading to the formation of a textured surface. Further analysis of the results obtained revealed that PZT has a roughness of about $1.090 \cdot 10^{-9}$ m, while for the Si/SiO_2 substrate this parameter is $5.073 \cdot 10^{-10}$ m.

Thus, the height differences on the PZT substrate surface are comparable to or even exceed the thickness of the 2D MoS_2 (films deposited on it (~0.7 nm for a monolayer), leading to a significant reduction in the contact area between the substrate and the film. Non-uniform contact between the materials negatively impacts the van der Waals forces responsible for MoS_2 adhesion to the surface. This in turn degrades the deposition quality of 2D crystallites and leads to the formation of defects at the interfaces between the 2D material and the substrate. All this reduces the efficiency of charge transfer and degrades the electronic performance of the devices.

After sample creation, several hundred two-dimensional MoS_2 crystallites were identified on the surfaces of the Si/SiO_2 and PZT substrates using

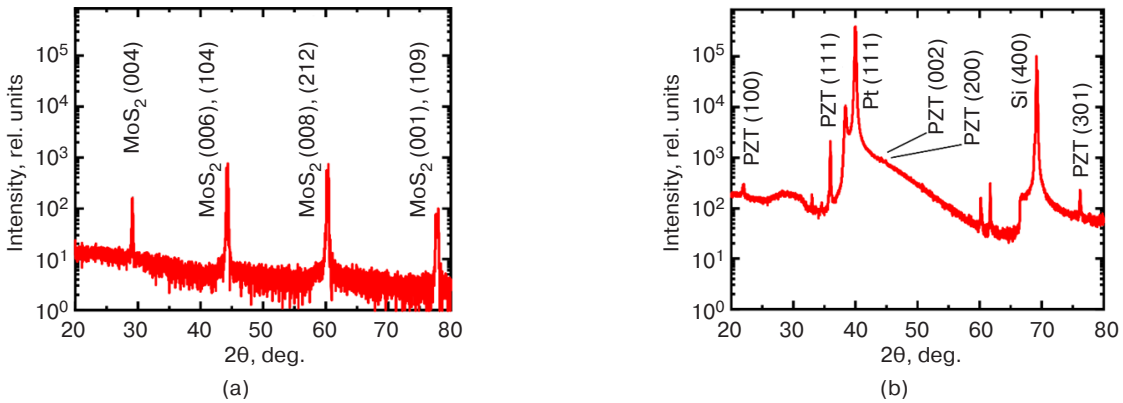

Fig. 2. Diffraction patterns of bulk MoS_2 (crystals (a) and PZT substrate (b)

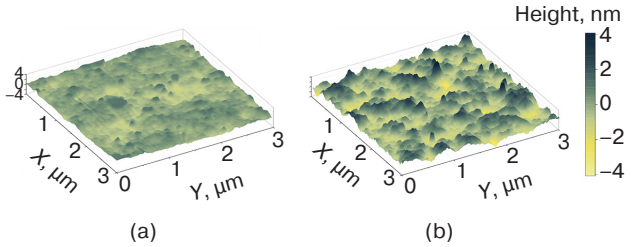

Fig. 3. Three-dimensional surface topography maps of the substrates obtained by AFM: (a) Si/SiO_2 and (b) polycrystalline PZT film

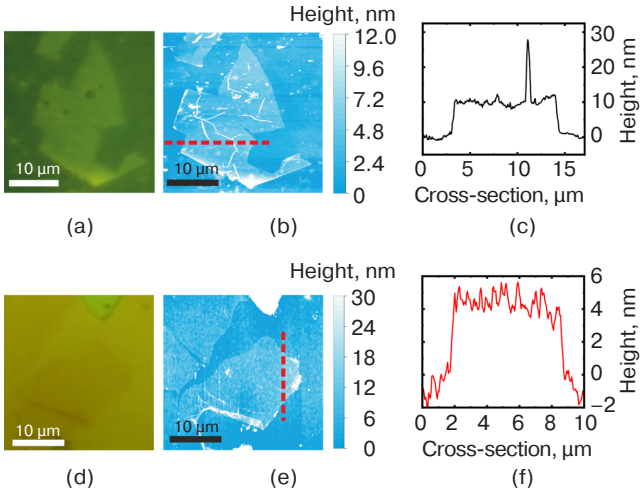

Fig. 4. Results of gold exfoliation: (a) Optical image of a region with MoS_2 crystallites on a Si/SiO_2 substrate; (b) AFM topography of a MoS_2 crystallite on a Si/SiO_2 substrate; (c) The height profile obtained from the section (red dashed line) shown in (b); (d) Optical image of a region with MoS_2 crystallites on a PZT substrate; (e) AFM topography of a MoS_2 crystallite on a PZT substrate; (f) The height profile obtained from the section (red dashed line) shown in (e)

confocal optical microscopy. Representative samples with typical morphological characteristics were selected for detailed analysis: an area of ~200 μm^2, the absence of visible defects, and a uniform distribution over the surface. Figures 4a and 4d show the crystallites for each substrate, selected as standards for the comparative study.

In order to determine the thickness and lateral dimensions of the crystallites, topographic maps were obtained using AFM (Figs. 4b and 4e). The thickness of the film on the Si/SiO_2 substrate was 5 nm, corresponding to ~8 monolayers of MoS_2 with an interlayer distance of 0.65 nm, while on PZT, a thickness of 8 nm (~12 layers) was recorded. The crystallite area was approximately 200 μm^2 for both crystallites.

The average surface roughness of the MoS_2 films was 2.53 nm for both substrates, significantly exceeding the values for the original substrates (0.51 nm for Si/SiO_2 and 1.09 nm for PZT). This increase in roughness is due to the appearance of pronounced morphological irregularities, primarily folds, which are clearly visible in the topographic maps and highlighted in red in Figs. 4c and 4f. The formation of folds is associated with the characteristics of mechanical transfer and the specific application of the GAE technique. In addition, foreign defects caused by residual materials after gold etching can be observed on the crystallite surface. These defects manifest themselves as local inclusions and can be detected both on the substrate and over the entire surface of the monolayer. It is important to note that the grain structure of the PZT substrate is partially visible through the MoS_2 surface, indicating non-uniform contact between the film and the substrate and the presence of regions where MoS_2 appears to be "suspended" above the surface.

Figure 5a shows a scanning electron microscopy (SEM) image of a MoS_2 crystallite on a Si/SiO_2 substrate where characteristic film folds (marked with arrows) formed during mechanical transfer are clearly visible. Topography analysis revealed that the fold height reaches 30 nm with an average length of 5 μm, consistent with the AFM data (Figs. 4b and 4e). Similar SEM measurements were not carried out for the PZT substrate due to the occurrence of local polarization reversal of the ferroelectric film under the

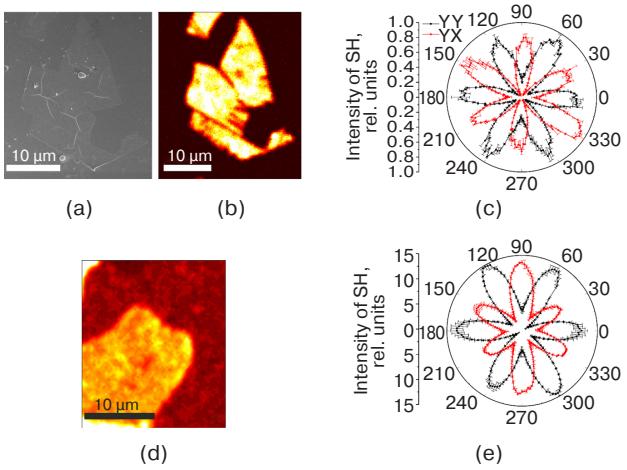

Fig. 5. SEM image of a MoS_2 crystallite on a Si/SiO_2 substrate (a); two-dimensional map of the second harmonic (SH) distribution in quasi-two-dimensional MoS_2 crystallites on Si/SiO_2 and PZT substrates (b), (d); azimuthal dependencies of the SH intensity in MoS_2 crystallites on Si/SiO_2 and PZT substrates (c), (e) in parallel (YY) and crossed (YX) combinations of pump radiation polarization and the selected SH field component

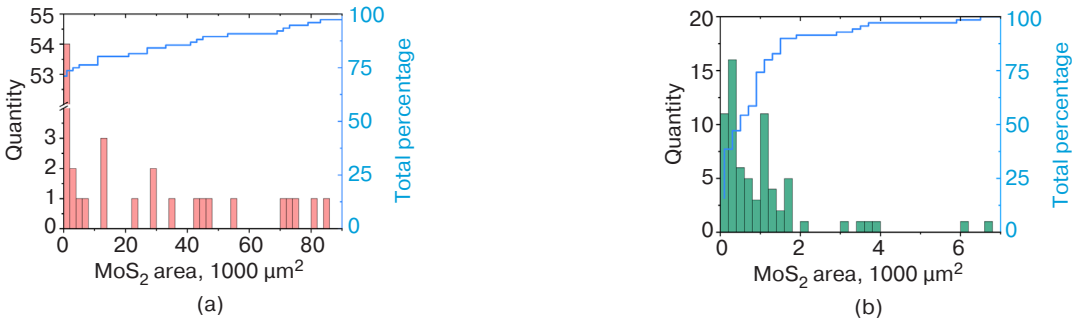

Fig. 6. Histogram of the area of two-dimensional MoS_2 crystallites on a substrate (a) Si/SiO_2 and (b) PZT

action of the electron beam which significantly distorts the distribution of the second optical harmonic [23]. It has been established experimentally that even short-term (~30 s) exposure to electrons with an energy of 5 kV leads to an irreversible change in the domain structure of PZT, which makes it impossible to correctly compare optical and electron microscopic data.

Spatial maps of the SHG intensity distribution obtained by scanning nonlinear microscopy (Figs. 5b and 5d) enable the reliable identification of morphological defects, including folds and cracks. A local increase in signal intensity is recorded in zones corresponding to such defects. This increase may be due to a violation of local centrosymmetry or to edge effects caused by an increase in nonlinear optical susceptibility near domain boundaries or at the edges of the crystalline region [24], as well as an increase in film thickness.

The six-beam azimuthal dependence of the second optical harmonic intensity in thin MoS_2 (Figs. 5c and 5e) is due to the crystallographic symmetry of the material. In the case of a non-centrosymmetric 3R polytype, as well as with an even number of layers, the structure is characterized by the point symmetry group C_{3v}. This leads to a pronounced six-beam dependence of the second harmonic intensity on the azimuthal rotation angle of the sample [25, 26]. In the experiment, the phases of the intensity maxima coincide at all flake points, indicating the single-crystal nature of the film, and the uniform orientation of the crystallographic axes.

A uniform SHG intensity distribution is observed in most of the MoS_2 film regions studied. This indicates a low density of morphological defects and high crystalline quality of the material. The uniformity of the signal confirms the absence of significant grain boundaries, folds, and cracks over the bulk of the flake, and also indicates a minimal influence of polytypism, in particular, the dominance of the non-centrosymmetric 3R polytype, which makes the largest contribution to the SHG signal.

In order to conduct an objective comparison of the efficiency of forming quasi-two-dimensional films on various substrates, a statistical analysis of the morphological parameters of over 300 created crystallites was performed. One of the key criteria in this case is the area distribution of individual crystallites, since this parameter determines the suitability of the material for further applications and directly depends on both the chosen exfoliation method and the substrate properties.

The area distribution histograms of quasi-two-dimensional MoS_2 crystallites obtained by the GAE method are shown in Fig. 6, demonstrating a significant difference between the Si/SiO_2 (Fig. 6a) and PZT (Fig. 6b) substrates. It is important to note that the statistical sample includes crystallites with an area greater than 0.2 μm^2 and a thickness less than or equal to 7 nm (~10 monolayers), corresponding to the transition region between quantum-well and bulk properties. The lower area threshold was chosen based on technological requirements. Smaller crystallites are unsuitable for the creation of functional devices due to limitations of lithography and the formation of electrode structures.

For Si/SiO_2 substrates, more than 25% of the visualized crystallites have an area exceeding 65000 μm^2, or four orders of magnitude higher than the typical results of conventional exfoliation (<0.5 μm^2) [27]. On the PZT substrate, the distribution is shifted towards the lower values. The area of the largest 25% of crystallites is only 3000 μm^2, associated with increased surface roughness (R_a = 1.09 nm) and, as a result, heterogeneous contact between the film and the substrate. It is fundamentally important that, when using standard mechanical exfoliation, not a single crystallite with an area greater than 1 μm^2 could be detected on the PZT.

Thus, the gold-assisted exfoliation method ensures the formation of extended and high-quality MoS_2 monolayers not only on standard but also on textured substrates, where other approaches prove ineffective.

CONCLUSIONS

For the first time this work demonstrates the possibility of producing extended, high-quality MoS_2 monolayers on substrates with a pronounced granular and textured structure, such as ferroelectric PZT films. The gold-assisted exfoliation method enables the formation of crystallites with an area of up to 3000 μm^2 on PZT and over 65000 μm^2 on standard Si/SiO_2 substrates. This is several orders of magnitude greater than the results achievable using traditional mechanical exfoliation where no crystallites larger than 1 μm^2 can be formed on textured substrates. The crystallinity and homogeneity of the resulting layers were confirmed by AFM and nonlinear optical microscopy.

The results obtained open up new prospects for integrating 2D semiconductors into functional devices such as FeFETs and memristors which require layer transfer onto complex and uneven substrates. The GAE technique can be extrapolated to a wide range of 2D materials and various types of functional surfaces. Thus, gold-assisted exfoliation represents an effective and reproducible tool for creating extended 2D films with controlled morphological and structural characteristics, including on substrates previously considered as unsuitable for such applications.

ACKNOWLEDGMENTS

The main results of the study were obtained with the support of the Russian Science Foundation (project No. 24-79-10304) in terms of developing a method for creating two-dimensional films, as well as the Ministry of Science and Higher Education of the Russian Federation (project No. FSFZ-2024-0047) in terms of experimental methods for studying the properties of the created structures.

Authors' contributions

E.I. Zhemerov—methodology development, literature review, conducting experiments, interpretation and generalization of results, preparation of the initial manuscript draft.

A.A. Guskov—methodology development, conducting experiments, interpretation and generalization of results, preparation of the initial manuscript draft and the article for publication.

E.A. Bulavintseva, **D.S. Seregin**—methodology development, sample preparation.

S.D. Lavrov—creation of research concept and methodology, preparation of the initial manuscript draft, manuscript text editing, general supervision.

All authors have read and approved the published version of the manuscript.

REFERENCES

1. Ziewer J., Ghosh A., Hanušová M., Pirker L., Frank O., Velický M., Grüning M., Huang F. Strain-Induced Decoupling Drives Gold-Assisted Exfoliation of Large-Area Monolayer 2D Crystals. *Adv. Mater*. 2025;37(14):2419184. https://doi.org/10.1002/adma.202419184
2. Rodríguez A., Çakıroğlu O., Li H., Carrascoso F., Mompean F., Garcia-Hernandez M., Munuera C., Castellanos-Gomez A. Improved Strain Transfer Efficiency in Large-Area Two-Dimensional MoS2 Obtained by Gold-Assisted Exfoliation. *J. Phys. Chem. Lett*. 2024;15(24):6355–6362. https://doi.org/10.1021/acs.jpclett.4c00855
3. Huang Y., Pan Y.-H., Yang R., Bao L.-H., Meng L., Luo H.-L., Cai Y.-Q., Liu G.-D., Zhao W.-J., Zhou Z., et al. Universal mechanical exfoliation of large-area 2D crystals. *Nat. Commun.* 2020;11(1):2453. https://doi.org/10.1038/s41467-020-16266-w
4. Ding S., Lin F., Jin C. Quantify point defects in monolayer tungsten diselenide. *Nanotechnology*. 2021;32(25):255701. https://doi.org/10.1088/1361-6528/abeeb2
5. Edelberg D., Rhodes D., Kerelsky A., Kim B., Wang J., Zangiabadi A., Kim C., Abhinandan A., Ardelean J., Scully M., et al. Approaching the Intrinsic Limit in Transition Metal Diselenides via Point Defect Control. *Nano Lett.* 2019;19(7):4371–4379. https://doi.org/10.1021/acs.nanolett.9b00985

6. Wu K., Wang H., Yang M., Li L., Sun Z., Hu G., Song Y., Han X., Guo J., Wu K., et al. Gold-Template-Assisted Mechanical Exfoliation of Large-Area 2D Layers Enables Efficient and Precise Construction of Moiré Superlattices. *Adv. Mater*. 2024;36(23):2313511. https://doi.org/10.1002/adma.202313511
7. Dai Y., Huang X., Han X., Guo J., Xu X., Wang L., Liu K., Song N., Wang Y., Huang Y. Recent Progress of Mechanical Exfoliation and the Application in the Study of 2DMaterials. In: Wee A., Yin X., Tang C.S. (Eds.). *Two-Dimensional Transition-Metal Dichalcogenides*. Wiley; 2024. P. 211–265. https://doi.org/10.1002/9783527838752.ch6
8. Panasci S.E., Schilirò E., Migliore F., Cannas M., Gelardi F.M., Roccaforte F., Giannazzo F., Agnello S. Substrate impact on the thickness dependence of vibrational and optical properties of large area MoS_2 produced by gold-assisted exfoliation. *Appl. Phys. Lett.* 2021;119(9):093103. https://doi.org/10.1063/5.0062106
9. Wan Y., Li E., Yu Z., Huang J.-K., Li M.-J., Chou A.-S., Lee Y.-T., Lee C.-J., Hsu H.-C., Zhan Q., et al. Low-defect-density WS_2 by hydroxide vapor phase deposition. *Nat. Commun*. 2022;13(1):4149. https://doi.org/10.1038/s41467-022-31886-0
10. Velický M., Donnelly G.E., Hendren W.R., McFarland S., Scullion D., DeBenedetti W.J.I., Correa G.C., Han Y., Wain A.J., Hines M.A., et al. Mechanism of Gold-Assisted Exfoliation of Centimeter-Sized Transition-Metal Dichalcogenide Monolayers. *ACS Nano*. 2018;12(10):10463–10472. https://doi.org/10.1021/acsnano.8b06101
11. Koenig S.P., Boddeti N.G., Dunn M.L., Bunch J.S Ultrastrong adhesion of graphene membranes. *Nature Nanotech*. 2011;6(9):543–546. https://doi.org/10.1038/nnano.2011.123
12. Huang Y., Sutter E., Shi N.N., Zheng J., Englund T.Y.D., Gao H.-J., Sutter P. Reliable Exfoliation of Large-Area High-Quality Flakes of Graphene and Other Two-Dimensional Materials. *ACS Nano*. 2015;9(11):10612–10620. https://doi.org/10.1021/acsnano.5b04258
13. Kotova N.M., Vorotilov K.A., Seregin D.S., Sigov A.S. Role of precursors in the formation of lead zirconate titanate thin films. *Inorg. Mater*. 2014;50:612–616. https://doi.org/10.1134/S0020168514060107
[Original Russian Text: Kotova N.M., Vorotilov K.A., Seregin D.S., Sigov A.S. Role of precursors in the formation of lead zirconate titanate thin films. *Neorganicheskie materialy*. 2014;50(6):661–666 (in Russ.).]
14. Brotons-Alcázar I., Terreblanche J.S., Giménez-Santamarina S., Gutiérrez-Finol G.M., Ryder K.S., Forment-Aliaga A., Coronado E. Atomic Force Microscopy beyond Topography: Chemical Sensing of 2D Material Surfaces through Adhesion Measurements. *ACS Appl. Mater. Interfaces*. 2024;16(15):19711–19719. https://doi.org/10.1021/acsami.3c19254
15. Mendez-Gonzalez D., Melle S., Calderón O.G., Laurenti M., Cabrera-Granado E., Egatz-Gómez A., López-Cabarcos E., Rubio-Retama J., Díaz E. Control of upconversion luminescence by gold nanoparticle size: from quenching to enhancement. *Nanoscale*. 2019;11(29):13832–13844. https://doi.org/10.1039/c9nr02039j
16. Bhanu U., Islam M.R., Tetard L., Khondaker S.I. Photoluminescence quenching in gold – MoS_2 hybrid nanoflakes. *Sci Rep*. 2014 Jul 4:4:5575. https://doi.org/10.1038/srep05575
17. Mak K.F., Lee C., Hone J., Shan J., Heinz T.F. Atomically Thin MoS_2: A New Direct-Gap Semiconductor. *Phys. Rev. Lett*. 2010;105(13):136805. https://doi.org/10.1103/physrevlett.105.136805
18. Srimuk P., Wang L., Budak Ö., Presser V. High-performance ion removal via zinc–air desalination. *Electrochem. Commun*. 2020;115:106713. https://doi.org/10.1016/j.elecom.2020.106713
19. Vasi S., Giofrè S.V., Perathoner S., Mallamace D., Abate S., Wanderlingh U. X-ray Characterizations of Exfoliated MoS_2 Produced by Microwave-Assisted Liquid-Phase Exfoliation. *Materials*. 2024;17(16):3887. https://doi.org/10.3390/ma17163887
20. Kim C.J., Yoon D.S., Lee J.S., Choi C.G., No K. A Study on the Microstructure of Preferred Orientation of Lead Zirconate Titanate (PZT) Thin Films. *J. Mater. Res*. 1997;12(4):1043–1047. https://doi.org/10.1557/JMR.1997.0145
21. Popescu D.G., Husanu M.A., Constantinou P.C., et al. Experimental Band Structure of $Pb(Zr,Ti)O_3$: Mechanism of Ferroelectric Stabilization. *Adv. Sci*. 2023;10(6):e2205476. https://doi.org/10.1002/advs.202205476
22. Beklešovas B., Iljinas A., Stankus V., et al. Structural, Morphologic, and Ferroelectric Properties of PZT Films Deposited through Layer-by-Layer Reactive DC Magnetron Sputtering. *Coatings*. 2022;12(6):717. https://doi.org/10.3390/coatings12060717
23. Kokhanchik L.S., Gainutdinov R.V., Lavrov S.D., Mishina E.D., Volk T.R. E-Beam Recording of Domain Structures on the Nonpolar Surface of $LiNbO_3$Crystals at Different SEM Voltages and their Investigation by PFM and SHG Microscopy. *Ferroelectrics*. 2015;480(1):49–57. https://doi.org/10.1080/00150193.2015.1012419
24. Mishina E.D., Sherstyuk N.E., Shestakova A.P., Lavrov S.D., Semin S.V., Sigov A.S., Mitioglu A., Anghel S., Kulyuk L. Edge effects in second-harmonic generation in nanoscale layers of transition-metal dichalcogenides. *Semiconductors*. 2015;49(6):791–796.
[Original Russian Text: Mishina E.D., Sherstyuk N.E., Shestakova A.P., Lavrov S.D., Semin S.V., Sigov A.S., Mitioglu A., Anghel S., Kulyuk L. Edge effects in second-harmonic generation in nanoscale layers of transition-metal dichalcogenides. *Fizika i Tekhnika Poluprovodnikov*. 2015;49(6):810–816 (in Russ.).]
25. Li Z.-Y., Cheng H.-Y., Kung S.-H., Yao H.-C., Inbaraj C.R.P., Sankar R., Ou M.-N., Chen Y.-F., Lee C.-C., Lin K.-H. Uniaxial Strain Dependence on Angle-Resolved Optical Second Harmonic Generation from a Few Layers of Indium Selenide. *Nanomaterials*. 2023;13(4):750. https://doi.org/10.3390/nano13040750
26. Li Y. Measurement of the Second-Order Nonlinear Susceptibility and Probing Symmetry Properties of Few-Layer MoS_2 and h-BN by Optical Second-Harmonic Generation. In: *Probing the Response of Two-Dimensional Crystals by Optical Spectroscopy*. Springer Theses; 2016. P. 45–54. https://doi.org/10.1007/978-3-319-25376-3_6

27. Desai S.B., Madhvapathy S.R., Amani M., Kiriya D., Hettick M., Tosun M., Zhou Y., Dubey M., Ager J.W., Chrzan D., et al. Gold-Mediated Exfoliation of Ultralarge Optoelectronically-Perfect Monolayers. *Adv. Mater.* 2016;28(21):4053–4058. https://doi.org/10.1002/adma.201506171

About the Authors

Evgeny I. Zhemerov, Student, Researcher Intern, Laboratory of Physics for Neuromorphic Computing Systems, Institute for Advanced Technologies and Industrial Programming, MIREA – Russian Technological University (78, Vernadskogo pr., Moscow, 119454 Russia). E-mail: zhemerov@mirea.ru. ResearcherID LLM-2528-2024, RSCI SPIN-code 6300-2743, https://orcid.org/0009-0002-0507-6242

Andrey A. Guskov, Graduate Student, Junior Researcher, Laboratory of Physics for Neuromorphic Computing Systems, Institute for Advanced Technologies and Industrial Programming, MIREA – Russian Technological University (78, Vernadskogo pr., Moscow, 119454 Russia). E-mail: guskov@mirea.ru. Scopus Author ID 57225969940, ResearcherID AAE-2479-2022, RSCI SPIN-code 8000-3575, https://orcid.org/0000-0002-8462-5811

Elizaveta A. Bulavintseva, Student, Researcher Intern, Laboratory of Physics for Neuromorphic Computing Systems, Institute for Advanced Technologies and Industrial Programming, MIREA – Russian Technological University (78, Vernadskogo pr., Moscow, 119454 Russia). E-mail: Liza12.07.2002@gmail.com. ResearcherID LLM-2612-2024, https://orcid.org/0009-0009-5310-3146

Dmitry S. Seregin, Cand. Sci. (Eng.), Head of the Department, Research and Education Center "Technology Center", Institute for Advanced Technologies and Industrial Programming, MIREA – Russian Technological University (78, Vernadskogo pr., Moscow, 119454 Russia). E-mail: d_seregin@mirea.ru. Scopus Author ID 55643557800, ResearcherID R-6023-2016, RSCI SPIN-code 4960-6761, https://orcid.org/0000-0002-6371-9632

Sergei D. Lavrov, Cand. Sci. (Phys.-Math.), Senior Researcher, Laboratory of Physics for Neuromorphic Computing Systems; Associate Professor, Department of Nanoelectronics, Institute for Advanced Technologies and Industrial Programming, MIREA – Russian Technological University (78, Vernadskogo pr., Moscow, 119454 Russia). E-mail: lavrov_s@mirea.ru. Scopus Author ID 55453548100, ResearcherID G-2912-2016, RSCI SPIN-code 5918-8994, https://orcid.org/0000-0002-9432-860X

Об авторах

Жемеров Евгений Игоревич, студент, стажер-исследователь, лаборатория физики для нейроморфных вычислительных систем, Институт перспективных технологий и индустриального программирования, ФГБОУ ВО «МИРЭА – Российский технологический университет» (119454, Россия, Москва, пр-т Вернадского, д. 78). E-mail: zhemerov@mirea.ru. ResearcherID LLM-2528-2024, SPIN-код РИНЦ 6300-2743, https://orcid.org/0009-0002-0507-6242

Гуськов Андрей Александрович, аспирант, младший научный сотрудник, лаборатория физики для нейроморфных вычислительных систем, Институт перспективных технологий и индустриального программирования, ФГБОУ ВО «МИРЭА – Российский технологический университет» (119454, Россия, Москва, пр-т Вернадского, д. 78). E-mail: guskov@mirea.ru. Scopus Author ID 57225969940, ResearcherID AAE-2479-2022, SPIN-код РИНЦ 8000-3575, https://orcid.org/0000-0002-8462-5811

Булавинцева Елизавета Александровна, студент, сотрудник лаборатории физики для нейроморфных вычислительных систем, Институт перспективных технологий и индустриального программирования, ФГБОУ ВО «МИРЭА – Российский технологический университет» (119454, Россия, Москва, пр-т Вернадского, д. 78). E-mail: Liza12.07.2002@gmail.com. ResearcherID LLM-2612-2024, https://orcid.org/0009-0009-5310-3146

Серегин Дмитрий Сергеевич, к.т.н., начальник отдела, Научно-образовательный центр «Технологический центр», Институт перспективных технологий и индустриального программирования, ФГБОУ ВО «МИРЭА – Российский технологический университет» (119454, Россия, Москва, пр-т Вернадского, д. 78). E-mail: d_seregin@mirea.ru. Scopus Author ID 55643557800, ResearcherID R-6023-2016, SPIN-код РИНЦ 4960-6761, https://orcid.org/0000-0002-6371-9632

Лавров Сергей Дмитриевич, к.ф.-м.н., старший научный сотрудник, лаборатория физики для нейроморфных вычислительных систем; доцент, кафедра наноэлектроники, Институт перспективных технологий и индустриального программирования, ФГБОУ ВО «МИРЭА – Российский технологический университет» (119454, Россия, Москва, пр-т Вернадского, д. 78). E-mail: lavrov_s@mirea.ru. Scopus Author ID 55453548100, ResearcherID G-2912-2016, SPIN-код РИНЦ 5918-8994, https://orcid.org/0000-0002-9432-860X

Translated from Russian into English by Lyudmila O. Bychkova
Edited for English language and spelling by Dr. David Mossop

Micro- and nanoelectronics. Condensed matter physics
Микро- и наноэлектроника. Физика конденсированного состояния

UDC 537.632
https://doi.org/10.32362/2500-316X-2026-14-1-55-63
EDN FDCWGD

RESEARCH ARTICLE

Specific features of temperature dependence of colossal and tunneling magnetoresistance in manganite films

Tatiana N. Bakhvalova [1], Alexey N. Yurasov [1], Maxim M. Yashin [1, @], Valentina A. Bessonova [2]

[1] *MIREA – Russian Technological University, Moscow, 119454 Russia*
[2] *Mikheev Institute of Metal Physics of the Ural Branch of the Russian Academy of Sciences, Yekaterinburg, 620108 Russia*
[@] *Corresponding author, e-mail: ihkamax@mail.ru*

• **Submitted:** 03.04.2025 • **Revised:** 15.04.2025 • **Accepted:** 20.11.2025

Abstract

Objectives. This work aims to theoretically and experimentally investigate the specific features of magnetoresistance temperature dependence in nanostructured films of doped manganites. The temperature dependence of electrical resistance for $La_{0.67}Ba_{0.33}MnO_3$ manganite films, grown by laser ablation on various dielectric substrates, is investigated over a wide temperature range.

Methods. Epitaxial $La_{0.67}Ba_{0.33}MnO_3$ films with a thickness of 80 nm were grown by pulsed laser ablation using an ArF excimer laser (a laser wavelength of 247 nm) on single-crystalline $SrTiO_3$ and $ZrO_2(Y_2O_3)$ substrates. The magnetoresistance properties were measured using a two-probe DC method. The measurements were conducted in magnetic fields up to 8 kOe applied in the film plane, across a temperature range of 80–350 K. To accomplish the research objectives, an empirical magnetoresistance model was applied in two distinct temperature regions: near the magnetic phase transition temperature and in the ground-state region.

Results. Empirical relations for temperature dependence of magnetoresistance for nanostructured $La_{0.67}Ba_{0.33}MnO_3$ films were established, encompassing both the Curie temperature region and the ground-state regime. Our studies revealed that the magnetoresistance of epitaxial single-crystalline $La_{0.67}Ba_{0.33}MnO_3$ films exhibits a sharp peak exclusively near the Curie temperature while remaining negligible in other temperature ranges. Conversely, $La_{0.67}Ba_{0.33}MnO_3$ films with a variant structure demonstrate significant low-temperature magnetoresistance. This effect arises from magnetic-field-induced modifications of the high-frequency conductivity, which results from spin-polarized electron tunneling across structural domain boundaries. A unified empirical model to describe various mechanisms of magnetoresistance in doped manganites is proposed.

Conclusions. For the first time, an empirical model to describe both the colossal and tunneling magnetoresistance in thin films of doped manganites has been developed. This model demonstrates excellent agreement between experimental and calculated data for $La_{0.67}Ba_{0.33}MnO_3$ films with and without a variant structure. The simulation results agree well with experimental data. The findings elucidate the understanding of magnetoresistance mechanisms, contribute to the development of the magnetorefractive effect theory for thin-film manganites, and inform new approaches for controlling charge carrier dynamics in strongly correlated magnetic oxides.

Keywords: manganites films, variant structure, colossal magnetoresistance, spin-dependent tunneling, magnetorefractive effect, structural domains

For citation: Bakhvalova T.N., Yurasov A.N., Yashin M.M., Bessonova V.A. Specific features of temperature dependence of colossal and tunneling magnetoresistance in manganite films. *Russian Technological Journal.* 2026;14(1):55–63. https://doi.org/10.32362/2500-316X-2026-14-1-55-63, https://www.elibrary.ru/FDCWGD

Financial disclosure: The authors have no financial or proprietary interest in any material or method mentioned.

The authors declare no conflicts of interest.

НАУЧНАЯ СТАТЬЯ

Особенности температурных зависимостей колоссального и туннельного магнитосопротивления в пленках манганитов

Т.Н. Бахвалова [1], А.Н. Юрасов [1], М.М. Яшин [1, @], В.А. Бессонова [2]

[1] *МИРЭА – Российский технологический университет, Москва, 119454 Россия*
[2] *Институт физики металлов им. М.Н. Михеева УрО РАН, Екатеринбург, 620108 Россия*
[@] *Автор для переписки, e-mail: ihkamax@mail.ru*

• **Поступила:** 03.04.2025 • **Доработана:** 15.04.2025 • **Принята к опубликованию:** 20.11.2025

Резюме

Цели. Целью работы является экспериментальное и теоретическое исследование особенностей температурных зависимостей магнитосопротивления в наноструктурированных пленках легированных манганитов. В широком температурном диапазоне изучено поведение электросопротивления пленок манганитов состава $La_{0.67}Ba_{0.33}MnO_3$, выращенных методом лазерной абляции на различных диэлектрических подложках.

Методы. Для достижения поставленной цели методом лазерной абляции с использованием импульсного эксимерного были выращены эпитаксиальные пленки $La_{0.67}Ba_{0.33}MnO_3$ толщиной 80 нм на монокристаллических подложках $SrTiO_3$ и $ZrO_2(Y_2O_3)$. Магнитосопротивление измерялось двухконтактным методом на постоянном токе в полях до 8 кЭ в плоскости образца и температурном интервале 80–350 K. Для достижения поставленной цели применялась эмпирическая модель магнитосопротивления в двух температурных областях: вблизи температуры магнитного фазового перехода и в области основного состояния.

Результаты. Построены эмпирические температурные зависимости магнитосопротивления для наноструктурированной пленки $La_{0.67}Ba_{0.33}MnO_3$, охватывающие как область температуры Кюри, так и область основного состояния. Показано, что в эпитаксиальной монокристаллической пленке $La_{0.67}Ba_{0.33}MnO_3$ магнитосопротивление имеет выраженный максимум вблизи температуры Кюри и пренебрежимо мало в других областях. В пленке $La_{0.67}Ba_{0.33}MnO_3$ с вариантной структурой имеется сильный низкотемпературный вклад в магнитосопротивление, связанный с изменением высокочастотной проводимости пленки во внешнем магнитном поле из-за процессов туннелирования спин-поляризованных электронов через границы структурных доменов. Предложена единая эмпирическая модель для описания различных механизмов магнитосопротивления в легированных манганитах.

Выводы. Впервые в рамках одной эмпирической модели проведено описание колоссального и туннельного магнитосопротивления для пленок легированных манганитов. Показано, что такая модель дает хорошее согласие экспериментальных и расчетных данных в пленке $La_{0.67}Ba_{0.33}MnO_3$ с вариантной структурой. Результаты моделирования хорошо согласуются с экспериментальными данными. Полученные данные могут способствовать пониманию механизмов магнитосопротивления и развитию теории магниторефрактивного эффекта для тонкопленочных манганитов, а также разработке новых подходов к управлению динамикой носителей заряда в сильно-коррелированных магнитных оксидах.

Ключевые слова: пленки манганитов, вариантная структура, колоссальное магнитосопротивление, туннелирование, магниторефрактивный эффект, структурные домены

Для цитирования: Бахвалова Т.Н., Юрасов А.Н., Яшин М.М., Бессонова В.А. Особенности температурных зависимостей колоссального и туннельного магнитосопротивления в пленках манганитов. *Russian Technological Journal*. 2026;14(1):55–63. https://doi.org/10.32362/2500-316X-2026-14-1-55-63, https://www.elibrary.ru/FDCWGD

Прозрачность финансовой деятельности: Авторы не имеют финансовой заинтересованности в представленных материалах или методах.

Авторы заявляют об отсутствии конфликта интересов.

INTRODUCTION

In modern physics, special attention is paid to the study of fundamental magnetic and transport properties of composite or nanostructured functional thin-film nanomaterials. Such materials form the basis of many current technological applications, from information carriers to sensor devices [1]. Doped lanthanum manganites are a promising class of substances exhibiting unusual properties [2–5] and possessing a number of unique characteristics. These include high spin polarization of charge carriers and magnetization, high sensitivity of static and optical conductivity to structural and magnetic phase transitions and external fields [2–5], e.g., metal-insulator transition, colossal magnetoresistance (MR) effect, giant magneto-transmittance, magnetorefractive effect (MRE), etc. [6–8]. These properties render doped lanthanum manganites potential candidates for use in spintronics and magneto-optical devices in the infrared (IR) range operating at room temperatures.

The magnetorefractive effect consists in a change in optical parameters (refractive indices, or more precisely, reflection and transmission coefficients) in a magnetic field. In heavily doped manganites, this is a high-frequency analogue of colossal MR in the IR range of the spectrum [2]. In manganite films, the MRE reaches gigantic values (10–20%); at the same time, its spectral and temperature dependence is quite intricate due to the contribution of not only delocalized charge carriers but also the magnetic and charge uniformity of the films, their thickness and MS value, as well as size effects, resonance phenomena, and defects ([2] and the references therein).

The physical properties of manganite films are determined by their composition and growth conditions, as well as by the type of substrate. Thus, the study [9] investigated $La_{2/3}Ba_{1/3}MnO_3$ films on $ZrO_2(Y_2O_3)$ substrates and found the formation of a variant (equivalent) structure during epitaxial growth of the film on a single-crystal substrate with significantly different crystal lattice parameters. This structure is formed by structural domains (variants) with nanoscale crystallites in the film bulk, separated by coherent high-angle boundaries with a thickness of ~0.4 nm. It should be noted that the fixed orientation of crystallites with a limited set of angles is a fundamental difference between films with a variant structure and polycrystalline samples with disoriented crystallites of different sizes in the film bulk. The nature and features of the variant structure were discussed in detail in [10].

Consequently, the domain structure of such films determines the appearance of an additional mechanism underlying the MR caused by the tunneling processes of spin-polarized charge carriers at the domain boundaries, which are most intense when the temperature approaches absolute zero. A comparative analysis of the optical, electrical, and magneto-optical properties of $La_{2/3}Ba_{1/3}MnO_3$ films with and without a variant structure allowed us to study the main features of the physical mechanisms responsible for the temperature and field dependence of MR and MRE in these films [2, 7–9]. To describe MRE as a response to colossal MR in manganites, the effective medium approximation [11], previously proposed for the analysis of tunneling processes at optical frequencies in various metallic nanocomposites and granular alloys [12], was successfully applied. However, the high susceptibility of the electrical properties of manganites to internal and external factors leads to difficulties in the theoretical description of the MR and MRE mechanisms. Indeed, the developed theory is applicable to purely metallic and tunnel conduction and is capable of considering the redistribution of the high- and low-conductivity phases; however, it fails to take into account the effects associated, e.g., with changes in the magnetic field concentration of charge carriers, absorption edges, effective mass of polarons [2], etc. Furthermore, there is currently no single model describing the coexistence of two MR mechanisms in films of doped manganites with significantly different temperature regions of existence.

This article presents the results of simulating the temperature dependence of MR in a $La_{0.67}Ba_{0.33}MnO_3$ (LBM) manganite film with a variant structure, in comparison with a film without a variant structure. It is shown that

the proposed empirical approach enables the main features to be taken into account, thus being useful when developing a general theory of MR in strongly correlated magnetoresistive magnetics.

EXPERIMENTAL

LBM epitaxial films with a thickness of d = 80 nm were grown by laser ablation using an excimer pulsed argon fluoride laser (ArF laser), with a laser wavelength of 247 nm and a frequency of about 9 Hz, on single-crystal $SrTiO_3$ (hereinafter referred to as STO) and $ZrO_2(Y_2O_3)$ (hereinafter referred to as YSZ (Y_2O_3 stabilized ZrO_2)) substrates, at a substrate temperature of 730 K and an oxygen pressure of 0.4 mbar. The thickness of the films was determined by exposure duration. According to scanning electron microscopy (SEM) data, the surface of the LBM/YSZ film has a multi-grain structure with an average crystallite size of 40–70 nm. This structure is formed by columnar oriented crystallites growing through the thickness of the film, which is fundamentally different from the island-like growth of thin LBM/STO epitaxial films. The synthesis method and the results of film sample testing are detailed in [9, 13].

The magnetoresistance of the films $\frac{\Delta\rho}{\rho} = [\rho_H - \rho_0]/\rho_0$, where ρ_H and ρ_0 are the values of the specific resistance in the presence and absence of a magnetic field, was measured using a two-contact method at direct current in fields up to 8 kE in the plane of the sample and in the temperature range of 80–50 K. The experimental temperature and field dependencies of the MR of the films are shown in Fig. 1. The magnetoresistance in epitaxial films of LBM manganites (without a variant structure) demonstrates a field and temperature dependence similar to that of bulk single crystals of the same composition. In the LBM/STO film, a pronounced maximum in the temperature dependence of the negative MR effect in the region of Curie temperature T_C = 305 K was observed. The presence of this maximum is associated with the suppression of magnetic moment fluctuations by the field, which are maximal in the region of magnetic phase transition. This maximum is characteristic of manganites with colossal MR [2, 14]. The field dependence of MR in this region shows a linear dependence without hysteresis and saturation in fields up to 8 kE (Fig. 1c). At the same time, for the LBM/YSZ film, the MR dependence on T shows only a shoulder near T_C against the background of a continuous increase in MR with decreasing temperature (Fig. 1a). The continuous increase in MR is associated with the tunneling of spin-polarized electrons through the boundaries of structural domains.

The maximum value of the tunnel MR obtained was approximately 27% at T = 13 K (not shown in the figure). Estimation of the degree of electron spin polarization P at $T \sim 0$ K using the expression $\frac{\Delta\rho}{\rho} = 2P^2/(1-P^2)$ gives a value of $P \approx 0.36$, which is close to the value of P for $La_{0.8}Ag_{0.1}MnO_{3+\delta}/ZrO_2(Y_2O_3)$ films with a variant structure [15]. The field dependence of low-temperature MR differs significantly (Fig. 1b). Thus, the negative MR sharply reaches saturation and gains almost 25% in magnetic fields greater than 2 kE, resulting in a butterfly-wing hysteresis characteristic of materials with tunnel MR with weak positive maxima in the fields of about 0.5 kE. The arrow in the figure indicates a feature associated with the colossal MR in the LBM/YSZ film. The hatched areas schematically reflect the regions of predominant contribution of the tunnel (I) and colossal (II) MR mechanisms, respectively. More detailed results of the analysis of the temperature and field dependence of MR and MRE in LBM films can be found in [9, 13, 16].

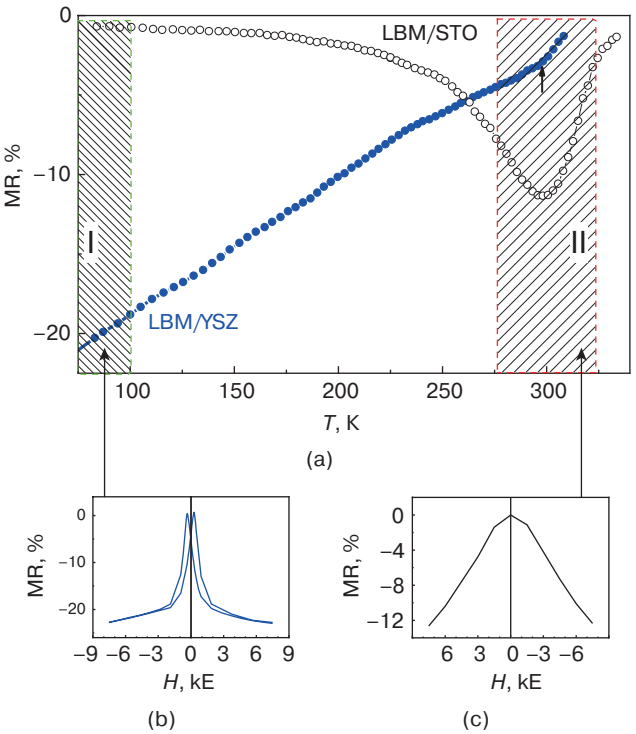

Fig. 1. Experimental characteristics:
(a) temperature dependence of MR for LBM/STO and LBM/YSZ films at H = 7.5 kE;
(b) and (c) are field dependencies of MR for LBM/YSZ and T = 80 K and LBM/STO films at $T = T_C$, respectively

SIMULATION RESULTS

The nanostructured LBM/YSZ film (with a variant structure) shows the presence of conductive ferromagnetic structural domains separated by weakly

conductive boundaries. When a constant external magnetic field is applied in the T_C region, a peculiarity associated with colossal MR in the domain volume is observed in the MR. At low temperatures, tunnel MR associated with charge carrier tunneling at domain boundaries is observed. In this regard, the peculiarities of the temperature behavior of MR in LBM/YSZ were considered in two main areas: near and well below the ferromagnetic ordering temperature (Curie temperature). At low temperatures, the MR(T) dependence has the form of a quasi-linear function T_{cr} ~ 250 K. Upon an increase in temperature, it takes the form of a film without a variant structure (LBM/STO) and is described by a second-order polynomial function (or, in the first approximation, a linear function). To account for these two contributions, the proposed mathematical model is complemented with the coefficients of α and β. In terms of its physical meaning, the coefficient α takes into account the contribution of low-temperature (tunnel) MR: α = 1 at $T < T_{cr}$ and α = 0 at $T > T_{cr}$. This condition is satisfied by the expression of the form:

$$\alpha = \frac{1}{1 + e^{\frac{T_{cr}}{T - T_{cr}}}}, \quad (1)$$

where T_{cr} is the critical temperature at which a change in the MR mechanism is observed. Similarly, we can obtain a formula for the coefficient β of the high-temperature (colossal) MR:

$$\beta = \frac{1}{1 + e^{\frac{T_{cr}}{T_{cr} - T}}}. \quad (2)$$

A similar approach was used to describe the MR in the LBM/STO film (without a variant structure). The low-temperature region of the MR has a weakly linear section with a zero output near T = 0 K. Above 250 K, the MR(T) dependence is described by a Gaussian function. A similar pattern was observed for $La_{0.7}Ca_{0.3}MnO_3$ films in [17].

The low-temperature region of the MR films was approximated as a quasi-linear section. The best match between the experimental and calculated curves is achieved by approximation with a second-order polynomial function (Fig. 2). However, the use of a polynomial significantly complicates the calculations; hence, a linear approximation was used. As a result, the general formula for describing the temperature dependence of MR (Δρ/ρ) can be represented as:

$$\frac{\Delta\rho}{\rho} = \alpha A_1 T + \beta \left(A_1 T_{cr} + B_1 e^{\frac{-(T - T_C)^2}{2\sigma^2}} \right), \quad (3)$$

where A_1 is a coefficient describing the slope of the temperature dependence curve and determined by the growth conditions and composition of the sample (the magnitude is small and amounts to ≈0.01, which is associated with a slight change in MR in the low-temperature region); B_1 is the MR value for a given film; σ is the root mean square deviation.

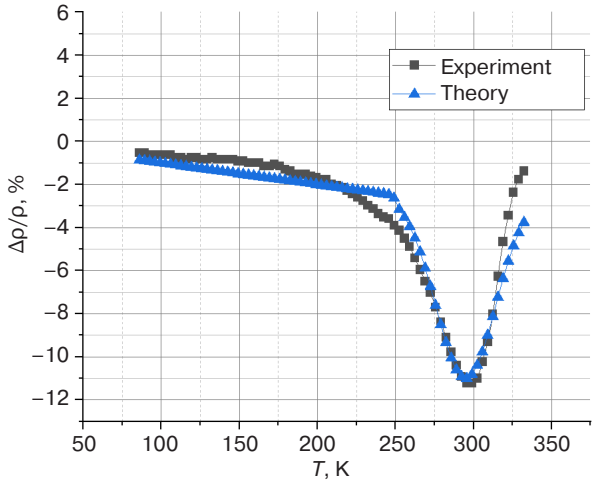

Fig. 2. Temperature dependence of MR (Δρ/ρ) for LBM/STO film: experiment and calculation

In LBM films with a variant structure, the differences between low-temperature and high-temperature regions are not extremely significant (Fig. 3). The presence of structural domains in the film leads to a noticeable change in the MR(T) curve and the absence of pronounced features near T_C. At the same time, the value of MR increases with a decrease in temperature, in contrast to films without a variant structure. A similar MR dependence was also observed for $(La_{0.65}Sr_{0.35})_{0.8}Mn_{1.2}O_{3\pm\delta}$ films with a variant structure [18]. In the low-temperature region, the dependence Δρ/ρ(T) is linear, becoming close to quadratic above the critical temperature (Fig. 3). In a first approximation, this feature near T_C can be considered insignificant. Then the dependence Δρ/ρ(T) will be quasi-linear. As a result, similar to the case considered earlier, we obtain a simplified expression for Δρ/ρ(T) for the LBM/YSZ film:

$$\frac{\Delta\rho}{\rho} = (\alpha + \beta)\left(A_0 + A_2 T\right), \quad (4)$$

where coefficient A_0 is the MR of the sample in terms of modulus (at T = 0 K), A_2 is the coefficient describing the slope of the curve (~0.086).

Thus, in doped LBM manganites, it became possible to account for the high- and low-temperature components of MR within a single empirical model. A simplified linear model that takes into account the critical temperature and characteristic values of colossal and

tunnel MR enables a good description of experimental data for both films with and without a variant structure. This model can be applied to explain the temperature characteristics of MR in a wide class of manganites of other compositions. The next step is to develop a theory of MRE in polycrystalline and composite manganite samples, taking into account the development of optical calculations of magnetic reflection [19, 20] and the results of this work. It is important to note that MRE, compared to the linear equatorial Kerr effect, is an even magnetization magneto-optical effect. In the IR region of the spectrum, taking into account interference effects [21, 22], the former can significantly exceed the latter, which makes MRE the most promising intensity effect from the point of view of fundamental and applied problems.

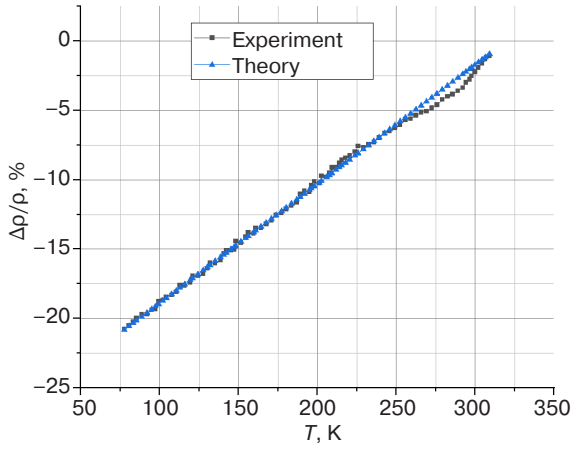

Fig. 3. Temperature dependence of MR (Δρ/ρ) for LBM/YSZ film: experiment and calculation

CONCLUSIONS

The work shows that in the LBM/STO film, the MR has a pronounced maximum near the Curie temperature and is negligible in other areas. In the LBM/YSZ film, a strong low-temperature contribution to MR is observed, associated with a change in the high-frequency conductivity of the film in an external magnetic field due to the tunneling of spin-polarized electrons through the boundaries of coherent structural domains. For the first time, a unified empirical model that takes into account different MR mechanisms is proposed. Such an approach provides good agreement between experimental and calculated data for doped manganites. The proposed empirical approach can be used to model spin transport processes in strongly correlated magnetoresistive magnets, including at optical frequencies in the form of MRE.

It should be noted that the wide temperature window of MR existence in a film with a variant structure is important from the point of view of possible practical applications.

ACKNOWLEDGMENTS

The study was supported by the "RTU MIREA Accelerator" program.

Authors' contributions

T.N. Bakhvalova—literature review, computer modeling, discussion of results, writing the text of the article.

A.N. Yurasov—model development, discussion of results, writing the text of the article, editing the article.

M.M. Yashin—computer modeling, discussion of results, writing the text of the article.

V.A. Bessonova—conducting the experiments.

REFERENCES

1. Ramirez A.P. Colossal magnetoresistance. *J. Phys.: Condens. Matter*. 1997;9(39):8171–8199. http://doi.org/10.1088/0953-8984/9/39/005
2. Granovsky A., Sukhorukov Yu., Gan'shina E., Telegin A. Magnetorefractive effect in magnetoresistive materials. In: *Magnetophotonics: From Theory to Applications.* Berlin Heidelberg: Springer; 2013. P. 107–133. http://doi.org/10.1007/978-3-642-35509-7_5
3. Gan'shina E., Loshkareva N., Sukhorukov Yu., et al. Optical and magneto-optical spectroscopy of manganites. *J. Magn. Magn. Mater*. 2006;300(1):62–66. https://doi.org/10.1016/j.jmmm.2005.10.033
4. Gorbenko O.Yu., Demin R.V., Kaul A.R., et al. Magnetic, electrical and crystallographic properties of thin $La_{1-x}Sr_xMnO_3$ films. *Phys. Solid State.* 1998;40(2):263–267. https://doi.org/10.1134/1.1130289
[Original Russian Text: Gorbenko O.Yu., Demin R.V., Kaul A.R., Koroleva L.I. Magnetic, electrical and crystallographic properties of thin $La_{1-x}Sr_xMnO_3$ films. *Fizika tverdogo tela* (*FTT*). 1998;40(2):290–294 (in Russ.).]
5. Bebenin N.G. Lanthanum manganites near the Curie temperature. *Phys. Metals Metallography.* 2004;98(1):78–85.
6. Bebenin N.G., Loshkareva N.N., Makhnev A.A., et al. Optical and magneto-optical properties of ferromagnetic $La_{1-x}Ba_xMnO_3$ single crystals. *J. Phys.: Condens. Matter*. 2010;22(9):096003. https://doi.org/10.1088/0953-8984/22/9/096003
7. Sukhorukov Yu.P., Telegin A.V., Bessonov V.D., et al. Magnetorefractive effect in the $La_{1-x}K_xMnO_3$ thin films grown by MOCVD. *J. Magn. Magn. Mater*. 2014;367:53–59. https://doi.org/10.1016/j.jmmm.2014.04.055
8. Telegin A., Sukhorukov Yu., Bessonov V. Optical response on the colossal magnetoresistance effect in manganites. *J. Supercond. Nov. Magn*. 2013;26(5):1437–1440. https://doi.org/10.1007/s10948-012-1867-8
9. Telegin A.V., Barsaume S., Bessonova V.A., et al. Magneto-optical response to tunnel magnetoresistance in manganite films with a variant structure. *J. Magn. Magn. Mater*. 2018;459:317–321. https://doi.org/10.1016/j.jmmm.2017.10.006
10. Kaul A.R., Gorbenko O.Yu., Kamenev A.A. The role of heteroepitaxy in the development of new thin-film oxide-based functional materials. *Russ. Chem. Rev*. 2004;73(9):861–880. https://doi.org/10.1070/RC2004v073n09ABEH000919
[Original Russian Text: Kaul A.R., Gorbenko O.Yu., Kamenev A.A. The role of heteroepitaxy in the development of new thin-film oxide-based functional materials. *Uspekhi khimii.* 2004;73(9):932–939 (in Russ.).]

11. Yurasov A.N., Telegin A.V., Sukhorukov Yu.P. Model of magnetorefractive effect in manganites within the effective medium theory. *Phys. Solid State*. 2016;58(4):674–677. https://doi.org/10.1134/S1063783416040326
[Original Russian Text: Yurasov A.N., Telegin A.V., Sukhorukov Yu.P. Model of magnetorefractive effect in manganites within the effective medium theory. *Fizika tverdogo tela* (*FTT*). 2016;58(4):656–660 (in Russ.).]
12. Bykov I.V., Gan'shina E.A., Granovskii A.B., et al. Magnetorefractive effect in granular alloys with tunnel magnetoresistance. *Phys. Solid State*. 2005;47(2):281–286. https://doi.org/10.1134/1.1866407
[Original Russian Text: Bykov I.V., Gan'shina E.A., Granovskii A.B., Gushchin V.S., Kozlov A.A., Masumoto T., Onuma S. Magnetorefractive effect in granular alloys with tunnel magnetoresistance. *Fizika tverdogo tela* (*FTT*). 2005;47(2):268–273 (in Russ.).]
13. Telegin A.V., Sukhorukov Yu.P., Nosov A.P., et al. Magnetoreflection and magnetooptical Kerr effect in $La_{2/3}Ba_{1/3}MNO_3$ films at room temperature. *Phys. Solid State*. 2017;59(2):292–297. https://doi.org/10.1134/S1063783417020305
[Original Russian Text: Telegin A.V., Sukhorukov Yu.P., Nosov A.P., Bessonova V.A., Gan'shina E.A. Magnetoreflection and magnetooptical Kerr effect in $La_{2/3}Ba_{1/3}MNO_3$ films at room temperature. *Fizika tverdogo tela* (*FTT*). 2017;59(2):284–289 (in Russ.). https://doi.org/10.21883/FTT.2017.02.44049.303]
14. Nagaev E.L. Lanthanum manganites and other giant magnetoresistance magnetic conductors. *Phys. Usp*. 1996;39(8): 781–805. https://doi.org/10.1070/PU1996v039n08ABEH000161
[Original Russian Text: Nagaev E.L. Lanthanum manganites and other giant magnetoresistance magnetic conductors. *Uspekhi fizicheskikh nauk*. 1996;166(8):833–858 (in Russ.). https://doi.org/10.3367/UFNr.0166.199608b.0833]
15. Sukhorukov Yu.P., Telegin A.V., Gan'shina E.A., et al. Tunneling of spin-polarized charge carriers in $La_{0.8}Ag_{0.1}MnO_{3+\delta}$ film with variant structure: Magnetotransport and magnetooptical data. *Tech. Phys. Lett.* 2005;31(6):484–487. https://doi.org/10.1134/1.1969772
[Original Russian Text: Sukhorukov Yu.P., Telegin A.V., Gan'shina E.A., Lokareva N.N., Kaul' A.R., Gorbenko O.Yu., Mostovshchikova E.N., Mel'nikov O.V., Vinogradov A.N. Tunneling of spin-polarized charge carriers in $La_{0.8}Ag_{0.1}MnO_{3+\delta}$ film with variant structure: Magnetotransport and magnetooptical data. *Pis'ma v Zhurnal tekhnicheskoi fiziki*. 2005;31(11): 78–87 (in Russ.).]
16. Bessonova V.A., Telegin A.V., Nosov A.P., et al. Features of absorption of thin films $La_{0.69}Ba_{0.31}MnO_{3-d}$ obtained using the method of pulsed laser deposition. *Opt. Spectroscopy*. 2022;130(9):1097–1103. http://doi.org/10.21883/EOS.2022.09.54826.3223-22
[Original Russian Text: Bessonova V.A., Telegin A.V., Nosov A.P., Sukhorukov Yu.P. Features of absorption of thin films $La_{0.69}Ba_{0.31}MnO_{3-d}$ obtained using the method of pulsed laser deposition. *Optika i spektroskopiya.* 2022;130(9):1365–1371 (in Russ.). https://doi.org/10.21883/OS.2022.09.53296.3223-22]
17. Granovskii A.B., Sukhorukov Y.P., Telegin A.V., et al. Giant magnetorefractive effect in $La_{0.7}Ca_{0.3}MnO_3$ films. *J. Exp. Theor. Phys*. 2011;112(1):77–86. https://doi.org/10.1134/S106377611005105X
[Original Russian Text: Granovskii A.B., Sukhorukov Yu.P., Telegin A.V., Bessonov V.D., Gan'shina E.A., Kaul' A.R., Korsakov I.E., Gorbenko O.Yu., Gonzales Kh. Giant magnetorefractive effect in $La_{0.7}Ca_{0.3}MnO_3$ films. *Zhurnal Eksperimental'noi i Teoreticheskoi Fiziki*. 2011;139(1):90–100 (in Russ.).]
18. Akimov G.Ya., Prilipko S.Yu., Revenko Yu.F., Timchenko V.M. Specific physical properties of nanocrystalline $(La_{0.65}Sr_{0.35})_{0.8}Mn_{1.2}O_{3\pm Delta}$ samples obtained by cold isostatic pressing. *Phys. Solid State.* 2009;51(4):770–772. https://doi.org/10.1134/S1063783409040210
[Original Russian Text: Akimov G.Ya., Prilipko S.Yu., Revenko Yu.F., Timchenko V.M. Features of physical properties of nanocrystalline samples of $(La_{0.65}Sr_{0.35})_{0.8}Mn_{1.2}O_{3\pm Delta}$ obtained using cold isostatic pressing. *Fizika tverdogo tela* (*FTT*). 2009;51(4):727–728 (in Russ.).]
19. Yurasov A.N., Sayfulina D.A., Bakhvalova T.N. Magnetorefractive effect in metallic Co/Pt nanostructures. *Russian Technological Journal*. 2024;12(2):57–66. https://doi.org/10.32362/2500-316X-2024-12-2-57-66
20. Gladyshev I.V. Reflection of light from multilayer structures, including both coherent and incoherent layers. In: *Optical Technologies, Materials and Systems* (*Optotech 2024*): *Conference Proceedings.* Moscow: 2024. P. 520–525 (in Russ.).
21. Gladyshev I.V., Yurasov A.N., Yashin M.M. Contribution of interference to the magneto-optical transverse Kerr effect in white light. *Russian Technological Journal.* 2024;12(6):59–68. https://doi.org/10.32362/2500-316X-2024-12-6-59-68
22. Gan'shina E.A., Garshin V.V., Perova N.N., et al. Magneto-optical Kerr Spectroscopy of Nanocomposites. *J. Exp. Theor. Phys*. 2023;137(4):572–581. https://doi.org/10.1134/S1063776123100151
[Original Russian Text: Gan'shina E.A., Garshin V.V., Perova N.N., Pripechenkov I.M., Yurasov A.N., Yashin M.M., Ryl'kov V.V., Granovskii A.B. Magneto-optical Kerr Spectroscopy of Nanocomposites. *Zhurnal Eksperimental'noi i Teoreticheskoi Fiziki*. 2023;164(4):662–672 (in Russ.). https://doi.org/10.31857/S0044451023100188]

СПИСОК ЛИТЕРАТУРЫ

1. Ramirez A.P. Colossal magnetoresistance. *J. Phys.: Condens. Matter*. 1997;9(39):8171–8199. http://doi.org/10.1088/0953-8984/9/39/005
2. Granovsky A., Sukhorukov Yu., Gan'shina E., Telegin A. Magnetorefractive effect in magnetoresistive materials. In: *Magnetophotonics: From Theory to Applications.* Berlin Heidelberg: Springer; 2013. P. 107–133. http://doi.org/10.1007/978-3-642-35509-7_5
3. Gan'shina E., Loshkareva N., Sukhorukov Yu., et al. Optical and magneto-optical spectroscopy of manganites. *J. Magn. Magn. Mater*. 2006;300(1):62–66. https://doi.org/10.1016/j.jmmm.2005.10.033
4. Горбенко О.Ю., Демин Р.В., Кауль А.Р., Королева Л.И. Магнитные, электрические и кристаллографические свойства тонких пленок $La_{1-x}Sr_xMnO_3$. *Физика твердого тела* (*ФТТ*). 1998;40(2):290–294.

5. Bebenin N.G. Lanthanum manganites near the Curie temperature. *Phys. Metals Metallography.* 2004;98(1):78–85.
6. Bebenin N.G., Loshkareva N.N., Makhnev A.A., et al. Optical and magneto-optical properties of ferromagnetic $La_{1-x}Ba_xMnO_3$ single crystals. *J. Phys.: Condens. Matter*. 2010;22(9):096003. https://doi.org/10.1088/0953-8984/22/9/096003
7. Sukhorukov Yu.P., Telegin A.V., Bessonov V.D., et al. Magnetorefractive effect in the $La_{1-x}K_xMnO_3$ thin films grown by MOCVD. *J. Magn. Magn. Mater*. 2014;367:53–59. https://doi.org/10.1016/j.jmmm.2014.04.055
8. Telegin A., Sukhorukov Yu., Bessonov V. Optical response on the colossal magnetoresistance effect in manganites. *J. Supercond. Nov. Magn*. 2013;26(5):1437–1440. https://doi.org/10.1007/s10948-012-1867-8
9. Telegin A.V., Barsaume S., Bessonova V.A., et al. Magneto-optical response to tunnel magnetoresistance in manganite films with a variant structure. *J. Magn. Magn. Mater*. 2018;459:317–321. https://doi.org/10.1016/j.jmmm.2017.10.006
10. Кауль А.Р., Горбенко О.Ю., Каменев А.А. Роль гетероэпитаксии в разработке новых тонкопленочных функциональных материалов на основе оксидов. *Успехи химии*. 2004;73(9):932–939.
11. Юрасов А.Н., Телегин А.В., Сухоруков Ю.П. Модель магниторефрактивного эффекта в манганитах в рамках теории эффективной среды. *Физика твердого тела* (*ФТТ*). 2016;58(4):656–660.
12. Быков И.В., Ганьшина Е.А., Грановский А.Б., Гущин В.С., Козлов А.А., Масумото Т., Онума С. Магниторефрактивный эффект в гранулированных сплавах с туннельным магнитосопротивлением. *Физика твердого тела* (*ФТТ*). 2005;47(2):268–273.
13. Телегин А.В., Сухоруков Ю.П., Носов А.П., Бессонова В.А., Ганьшина Е.А. Магнитоотражение и магнитооптический эффект Керра в пленках $La_{2/3}Ba_{1/3}MNO_3$ при комнатной температуре. *Физика твердого тела* (*ФТТ*). 2017;59(2):284–289. https://doi.org/10.21883/FTT.2017.02.44049.303
14. Нагаев Э.Л. Манганиты лантана и другие магнитные проводники с гигантским магнитосопротивлением. *Успехи физ. наук* (*УФН*). 1996;166(8):833–858. https://doi.org/10.3367/UFNr.0166.199608b.0833
15. Сухоруков Ю.П., Телегин А.В., Ганьшина Е.А., Локарева Н.Н., Кауль А.Р., Горбенко О.Ю., Мостовщикова Е.Н., Мельников О.В., Виноградов А.Н. Туннелирование спин-поляризованных носителей заряда в пленках $La_{0.8}Ag_{0.1}MnO_{3+d}$ с вариантной структурой: магнетотранспортные и магнетооптические данные. *Письма в ЖТФ*. 2005;31(11):78–87.
16. Бессонова В.А., Телегин А.В., Носов А.П., Сухоруков Ю.П. Особенности поглощения тонких пленок $La_{0.69}Ba_{0.31}MnO_{3-d}$, полученных методом импульсного лазерного осаждения. *Оптика и спектроскопия*. 2022;130(9):1365–1371. https://doi.org/10.21883/OS.2022.09.53296.3223-22
17. Грановский А.Б., Сухоруков Ю.П., Телегин А.В., Бессонов В.Д., Ганьшина Е.А., Кауль А.Р., Корсаков И.Е., Горбенко О.Ю., Гонзалес Х. Гигантский магниторефрактивный эффект в пленках $La_{0.7}Ca_{0.3}MnO_3$. *Журнал экспериментальной и теоретической физики*. 2011;139(1):90–100.
18. Акимов Г.Я., Прилипко С.Ю., Ревенко Ю.Ф., Тимченко В.М. Особенности физических свойств нанокристаллических образцов $(La_{0.65}Sr_{0.35})_{0.8}Mn_{1.2}O_{3\pm Delta}$, полученных с использованием холодного изостатического прессования. *Физика твердого тела* (*ФТТ*). 2009;51(4):727–728.
19. Юрасов А.Н., Сайфулина Д.А., Бахвалова Т.Н. Магниторефрактивный эффект в металлических наноструктурах Co/Pt. *Russian Technological Journal*. 2024;12(2):57–66. https://doi.org/10.32362/2500-316X-2024-12-2-57-66
20. Гладышев И.В. Отражение света от многослойных структур, включающих как когерентные, так и некогерентные слои. В сб.: *Оптические технологии, материалы и системы* (*Optomex 2024*): *Сборник докладов конференции*. Москва: 2024. С. 520–525. https://www.elibrary.ru/otpmij
21. Гладышев И.В., Юрасов А.Н., Яшин М.М. Вклад интерференции в магнитооптический экваториальный эффект Керра в белом свете. *Russian Technological Journal*. 2024;12(6):59–68. https://doi.org/10.32362/2500-316X-2024-12-6-59-68
22. Ганьшина Е.А., Гаршин В.В., Перова Н.Н., Припеченков И.М., Юрасов А.Н., Яшин М.М., Рыльков В.В., Грановский А.Б. Магнитооптическая керр-спектроскопия нанокомпозитов. *Журнал экспериментальной и теоретической физики*. 2023;164(4):662–672. https://doi.org/10.31857/S0044451023100188

About the Authors

Tatiana N. Bakhvalova, Lecturer, Department of Nanoelectronics, Institute for Advanced Technologies and Industrial Programming, MIREA – Russian Technological University (78, Vernadskogo pr., Moscow, 119454 Russia). E-mail: bahvalova@mirea.ru. ResearcherID ITW-2747-2023, Scopus Author ID 35145196400, https://orcid.org/0000-0001-7595-785X

Alexey N. Yurasov, Dr. Sci. (Phys.-Math.), Professor, Department of Nanoelectronics, Institute for Advanced Technologies and Industrial Programming, MIREA – Russian Technological University (78, Vernadskogo pr., Moscow, 119454 Russia). E-mail: alexey_yurasov@mail.ru. ResearcherID M-3113-2016, Scopus Authors ID 6602974416, RSCI SPIN-code 4259-8885, https://orcid.org/0000-0002-9104-3529

Maxim M. Yashin, Cand. Sci. (Phys.–Math.), Associate Professor, Department of Nanoelectronics, Institute for Advanced Technologies and Industrial Programming, MIREA – Russian Technological University (78, Vernadskogo pr., Moscow, 119454 Russia). E-mail: ihkamax@mail.ru. ResearcherID G-6809-2017, Scopus Author ID 57210607470, RSCI SPIN-code 2438-6135, https://orcid.org/0000-0001-8022-9355

Valentina A. Bessonova, Junior Researcher, M.N. Mikheev Institute of Metal Physics of Ural Branch of Russian Academy of Sciences (IMP UB RAS) (18, S. Kovalevskaya ul., Yekaterinburg, 620108 Russia). E-mail: valentina.a.bessonova@mail.ru. Scopus Author ID 55510248600, ResearcherID K-5887-2013, RSCI SPIN-code 7874-2518, https://orcid.org/0000-0002-2163-4913

Об авторах

Бахвалова Татьяна Николаевна, преподаватель, кафедра наноэлектроники, Институт перспективных технологий и индустриального программирования, ФГБОУ ВО «МИРЭА – Российский технологический университет» (119454, Россия, Москва, пр-т Вернадского, д. 78). E-mail: bahvalova@mirea.ru. ResearcherID ITW-2747-2023, Scopus Author ID 35145196400, https://orcid.org/0000-0001-7595-785X

Юрасов Алексей Николаевич, д.ф.-м.н., профессор, кафедра наноэлектроники, Институт перспективных технологий и индустриального программирования, ФГБОУ ВО «МИРЭА – Российский технологический университет» (119454, Россия, Москва, пр-т Вернадского, д. 78). E-mail: alexey_yurasov@mail.ru. ResearcherID M-3113-2016, Scopus Authors ID 6602974416, SPIN-код РИНЦ 4259-8885, https://orcid.org/0000-0002-9104-3529

Яшин Максим Михайлович, к.ф.-м.н., доцент, кафедра наноэлектроники, Институт перспективных технологий и индустриального программирования, ФГБОУ ВО «МИРЭА – Российский технологический университет» (119454, Россия, Москва, пр-т Вернадского, д. 78). E-mail: ihkamax@mail.ru. ResearcherID G-6809-2017, Scopus Author ID 57210607470, SPIN-код РИНЦ 2438-6135, https://orcid.org/0000-0001-8022-9355

Бессонова Валентина Анатольевна, младший научный сотрудник, ФГБУН «Институт физики металлов имени М.Н. Михеева Уральского отделения Российской академии наук» (ИФМ УрО РАН) (620108, Россия, Екатеринбург, ул. Софьи Ковалевской, д. 18). E-mail: valentina.a.bessonova@mail.ru. Scopus Author ID 55510248600, ResearcherID K-5887-2013, SPIN-код РИНЦ 7874-2518, https://orcid.org/0000-0002-2163-4913

Translated from Russian into English by Lyudmila O. Bychkova
Edited for English language and spelling by Dr. David Mossop

Mathematical modeling

Математическое моделирование

UDC 531.32
https://doi.org/10.32362/2500-316X-2026-14-1-64-81
EDN JUUJON

RESEARCH ARTICLE

Mathematical modeling of the orbital motion of an artificial satellite of the Moon using Delaunay variables

Olga V. Meshkova, Albina V. Shatina @

MIREA – Russian Technological University, Moscow, 119454 Russia
@ *Corresponding author, e-mail: shatina_av@mail.ru*

• **Submitted:** 19.05.2025 • **Revised:** 10.07.2025 • **Accepted:** 07.11.2025

Abstract

Objectives. This work aims to derive and study the system of equations of orbital motion of an artificial satellite of the Moon (ASM) in the gravitational field of an attracting planet using Delaunay variables. This will ensure a reduction in computational complexity when modeling long-term trajectories, as well as provide an analysis of stationary orbits of the Moon taking into account the gravitational influence of the Earth as a third body.

Methods. The study uses analytical mechanics, asymptotic methods, in particular, the averaging method, methods of stability theory, numerical methods for integrating systems of ordinary differential equations.

Results. The Hamiltonian and equations of motion of the ASM in canonical Delaunay variables are obtained. Averaged and non-averaged systems of equations of motion of the ASM are derived in the form of autonomous systems of ordinary differential equations with respect to the following orbital parameters: semi-major axis, eccentricity, inclination, longitude of the ascending node, longitude of the pericenter from the ascending node, and true anomalies. A closed system of differential equations of the second order with respect to the orbital eccentricity and the pericenter longitude from the ascending node is obtained. Its stationary solutions are found, their stability is investigated, and conditions for the existence of stationary motions are determined depending on the value of the constant of the first integral of the averaged system of equations. Integral curves and phase portraits were constructed to demonstrate the interrelationship of orbital parameters. A comparative analysis was conducted using JPL Horizons[1] data and previously published works.

Conclusions. The method developed enables the design of trajectories for future lunar missions to be optimized (e.g., Artemis, Luna-Glob), thus providing a balance between accuracy and computational efficiency. The results confirm the prospects of using Delaunay variables for analyzing long-term orbital dynamics in gravitational fields of complex configuration.

Keywords: artificial satellite of the Moon, gravitational field of the attracting center, Hamiltonian, canonical Delaunay variables, system of equations of orbital motion, orbital parameters

[1] JPL Horizons is an online service from the National Aeronautics and Space Administration (USA) that provides access to key data about the solar system and enables the calculation of precise trajectories of objects in it. https://ssd.jpl.nasa.gov/horizons/. Accessed March 04, 2025.

For citation: Meshkova O.V., Shatina A.V. Mathematical modeling of the orbital motion of an artificial satellite of the Moon using Delaunay variables. *Russian Technological Journal.* 2026;14(1):64–81. https://doi.org/10.32362/2500-316X-2026-14-1-64-81, https://www.elibrary.ru/JUUJON

Financial disclosure: The authors have no financial or proprietary interest in any material or method mentioned.

The authors declare no conflicts of interest.

НАУЧНАЯ СТАТЬЯ

Математическое моделирование орбитального движения искусственного спутника Луны с использованием переменных Делоне

О.В. Мешкова, А.В. Шатина @

МИРЭА – Российский технологический университет, Москва, 119454 Россия
@ *Автор для переписки, e-mail: shatina_av@mail.ru*

• **Поступила:** 19.05.2025 • **Доработана:** 10.07.2025 • **Принята к опубликованию:** 07.11.2025

Резюме

Цели. Целью работы является вывод и исследование системы уравнений орбитального движения искусственного спутника Луны (ИСЛ) в гравитационном поле притягивающей планеты в переменных Делоне, обеспечивающей снижение вычислительной сложности при моделировании долгосрочных траекторий, а также анализ стационарных орбит Луны с учетом гравитационного влияния Земли как третьего тела.

Методы. Используются методы аналитической механики, асимптотические методы, в частности, метод усреднения, методы теории устойчивости, численные методы для интегрирования систем обыкновенных дифференциальных уравнений.

Результаты. Получены гамильтониан и уравнения движения ИСЛ в канонических переменных Делоне, на основе которых выведены усредненная и неусредненная системы уравнений движения ИСЛ в виде автономных систем обыкновенных дифференциальных уравнений относительно следующих параметров орбиты: большой полуоси, эксцентриситета, наклонения, долготы восходящего узла, долготы перицентра от восходящего узла, истинных аномалий. Получена замкнутая система дифференциальных уравнений второго порядка относительно эксцентриситета орбиты и долготы перицентра от восходящего узла. Найдены ее стационарные решения, исследована их устойчивость, определены условия для существования стационарных движений в зависимости от значения константы первого интеграла усредненной системы уравнений. Построены интегральные кривые и фазовые портреты, демонстрирующие взаимосвязь параметров орбиты. Проведен сравнительный анализ с данными JPL Horizons[2] и ранее опубликованными работами.

Выводы. Разработанный метод позволяет оптимизировать проектирование траекторий для будущих лунных миссий (например, Artemis, «Луна-Глоб»), обеспечивая баланс между точностью и вычислительной эффективностью. Результаты подтверждают перспективность использования переменных Делоне для анализа долгосрочной орбитальной динамики в гравитационных полях сложной конфигурации.

Ключевые слова: искусственный спутник Луны, гравитационное поле притягивающего центра, гамильтониан, канонические переменные Делоне, система уравнений орбитального движения, параметры орбиты

[2] JPL Horizons – онлайн-сервис Национального управления по аэронавтике и исследованию космического пространства (США), который предоставляет доступ к ключевым данным о Солнечной системе и позволяет вычислять точные траектории объектов в ней. https://ssd.jpl.nasa.gov/horizons/. Дата обращения 04.03.2025. [JPL Horizons is an online service from the National Aeronautics and Space Administration (USA) that provides access to key data about the solar system and enables the calculation of precise trajectories of objects in it. https://ssd.jpl.nasa.gov/horizons/. Accessed March 04, 2025.]

Для цитирования: Мешкова О.В., Шатина А.В. Математическое моделирование орбитального движения искусственного спутника Луны с использованием переменных Делоне. *Russian Technological Journal*. 2026;14(1):64–81. https://doi.org/10.32362/2500-316X-2026-14-1-64-81, https://www.elibrary.ru/JUUJON

Прозрачность финансовой деятельности: Авторы не имеют финансовой заинтересованности в представленных материалах или методах.

Авторы заявляют об отсутствии конфликта интересов.

INTRODUCTION

The mathematical modeling of the orbital motion of an artificial satellite of the Moon (ASM) is one of the most pressing problems in space research. The relevance of this work is enhanced by the growing interest in long-term lunar projects, such as: the Artemis program (Artemis National Aeronautics and Space Administration, USA, 2022) [1]; the Chang'E-5 and Chang'E-6 missions (China National Space Administration, China, 2020 and 2024) [2, 3]; Chandrayaan-3 (Indian Space Research Organization, India, 2023) [4, 5]; and the Russian lunar program [6] which includes the deployment of an orbital station. In the context of the intensification of the lunar program in Russia, including the launch of new missions and research projects, accurate models of satellite motion are becoming especially necessary. The Moon is considered not only as an object of scientific study, but also as a potential base for further space research [6].

Although orbital motion around the Moon obeys Kepler's laws, significant deviations from the idealized model are explained by the influence of external disturbances. The fundamentals of analyzing such disturbances are laid out in the works of Laplace and Lagrange who proposed methods for solving the equations of motion for many-body systems[3].

In the 1960s, studies of the evolution of planetary satellite orbits with a twice-averaged perturbation function were carried out. A detailed study of this problem began with the discovery of a new first integral of the averaged system of equations. This discovery was made almost simultaneously in 1961 by the Soviet scientist M.L. Lidov [7] and the American scientist Y. Kozai [8] and was called the Lidov–Kozai effect. Subsequently, a picture of the evolution of a satellite's orbital motion, based on this effect, was developed in the works of M.A. Vashkovyak [9, 10]. Lidov was the first to conduct a thorough study of the influence of gravitational perturbations on the motion of satellites in systems with several bodies. In his works [7, 11], he considered the effects caused by the gravity of a third body which lead to long-period changes in orbital parameters. In addition, he proposed methods for simplifying complex equations of motion for practical application.

In turn, T.A. Eli [12] focused on numerical modeling of the orbital motion of lunar satellites taking into account significant external disturbances. In studies published in the early 2000s, he considered both short-term and long-term changes in orbital parameters under the influence of the gravity of the Earth, the Sun, and the Moon's mascons. Eli T.A. showed that for satellites in low lunar orbits (Low Lunar Orbit, LLO), the main influence is exerted by gravitational anomalies of the Moon, whereas for satellites in high lunar orbits (High Lunar Orbit, HLO), disturbances from the Earth and the Sun dominate.

In recent years, significant progress has been made in modeling lunar gravity anomalies. Study [13] demonstrated the use of high-order spherical harmonics to account for mascons, critical for low lunar orbits. Work [14] is devoted to the analysis of orbital stability within the framework of the Artemis mission, in which the authors use hybrid methods (analytical and numerical) to predict long-term evolution. In 2022, machine learning algorithms were proposed in [15], in the aims of accelerating the calculations of orbital perturbations especially relevant for real-time problems. In addition, the Chandrayaan-3 mission [4, 5] provided new data on the dynamics of highly elliptical orbits, confirming theoretical models. Work [16] proposed an approach to the design of frozen low lunar orbits based on the sequential application of non-gradient methods, Bayesian optimization and the Nelder–Mead method.

The motion of a lunar satellite is subject to various perturbations, including the gravitational influences of the Earth, the Sun, and other celestial bodies, the non-sphericity of the Moon, the influence of mascons (mass concentrations) in its lithosphere, solar radiation pressure, interactions with the space environment, and others. This article will focus on the system of equations for the spatial perturbation of the ASM motion caused by the Earth's gravitational field. This is the primary perturbation for satellites in high orbits.

Modern trajectory calculation systems rely on highly complex numerical methods which require significant resources. The proposed model, based on satellite orbital motion equations in Delaunay variables, provides comparable accuracy while reducing computation time. This makes the method promising for preliminary orbital analysis during the mission design phase.

[3] Lagrange J.-L. *Mécanique Analytique*. Paris: Veuve Desaint, 1788.

1. TASK STATEMENT. HAMILTONIAN

Let us consider a model problem of the motion of a celestial body–satellite system in the gravitational field of an attracting center. The celestial body, satellite, and attracting center will be modeled by material points P, S, O with the masses m_2, m_3, m_1, respectively (Fig. 1). We will assume that $m_3 \ll m_2 \ll m_1$. The radius vector of the center of mass C_0 of the celestial body–satellite system is denoted by the vector $\mathbf{R}_1$, and the relative position of points P and S is denoted by the vector $\mathbf{R}_2$, i.e., $\mathbf{R}_1 = \overline{OC_0}$, $\mathbf{R}_2 = \overline{PS}$. We will assume that $|\mathbf{R}_1| \gg |\mathbf{R}_2|$.

Let us introduce the inertial coordinate system $OXYZ$ and the Koenig axes $C_0\xi_1\xi_2\xi_3$. The radius vectors of the points P and S are expressed through $\mathbf{R}_1$, $\mathbf{R}_2$ as follows:

$$\overline{OP} = \mathbf{R}_1 - \frac{m_3}{m_2+m_3}\mathbf{R}_2, \quad \overline{OS} = \mathbf{R}_1 + \frac{m_2}{m_2+m_3}\mathbf{R}_2. \quad (1.1)$$

The kinetic energy of the celestial body—satellite system is determined by the equity:

$$T = \frac{1}{2}m_2\left(\frac{d}{dt}\overline{OP}\right)^2 + \frac{1}{2}m_3\left(\frac{d}{dt}\overline{OS}\right)^2.$$

Taking into account relations (1.1), we obtain:

$$T = \frac{1}{2}(m_2+m_3)\dot{\mathbf{R}}_1^2 + \frac{1}{2}m_r\dot{\mathbf{R}}_2^2, \quad m_r = \frac{m_2m_3}{m_2+m_3}, \quad (1.2)$$

m_r is the attached mass.

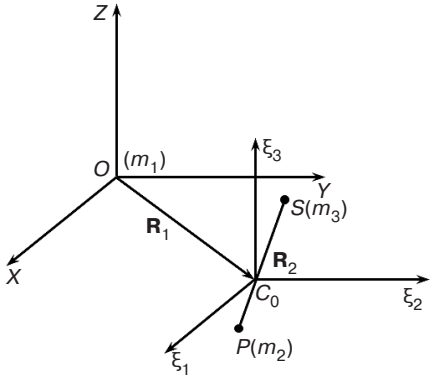

Fig. 1. Celestial body–satellite system

The potential energy of mutual attraction forces in the given problem is represented as:

$$\Pi = -\frac{fm_1m_2}{\left|\mathbf{R}_1 - \frac{m_3}{m_2+m_3}\mathbf{R}_2\right|} - \frac{fm_1m_3}{\left|\mathbf{R}_1 + \frac{m_2}{m_2+m_3}\mathbf{R}_2\right|} - \frac{fm_2m_3}{|\mathbf{R}_2|}, \quad (1.3)$$

where $f = 6.672\cdot10^{-11}\,\mathrm{m^3kg^{-1}s^{-2}}$ is the universal gravitational constant.

Given that the distance between the celestial body and the satellite is small compared to the length of the radius vector of the center of mass C_0, and using the formulas for the generating function of Legendre polynomials $P_n(x)$ [17], while retaining the second-order terms of smallness in R_2/R_1, we can transform expression (1.3). The potential (1.3) will take the following form:

$$\Pi = -\frac{fm_1(m_2+m_3)}{R_1} - \frac{fm_2m_3}{R_2} - \frac{fm_1m_r}{2R_1}\left(3\cos^2\psi_{12} - 1\right)\frac{R_2^2}{R_1^2}. \quad (1.4)$$

Here $R_1 = |\mathbf{R}_1|$, $R_2 = |\mathbf{R}_2|$, ψ_{12} is the angle between vectors $\mathbf{R}_1$, $\mathbf{R}_2$.

As a basic task, let us consider the motion of satellite S_0 with mass m (material point) in the gravitational field of the attracting center Q. In this case, the satellite moves along a Keplerian orbit—one of the conic sections. Let us focus on the case of an elliptical orbit.

The following parameters are used to determine the position of a satellite in the orbit: a is the semi-major axis of the ellipse; e is the eccentricity; i is the inclination of the satellite's orbit; h is the longitude of the ascending node (angle between Qx and the line QN_1 of the intersection of the plane of the satellite's orbit with the plane Qxy); g is the longitude of the pericenter π from the ascending node (the point of the satellite's orbit closest to the center Q); ϑ is the true anomaly, the angle between the direction to the pericenter π and the vector $\mathbf{R}$, $\mathbf{G} = \mathbf{R}\times m\dot{\mathbf{R}}$ is the momentum vector of the point S_0 (Fig. 2).

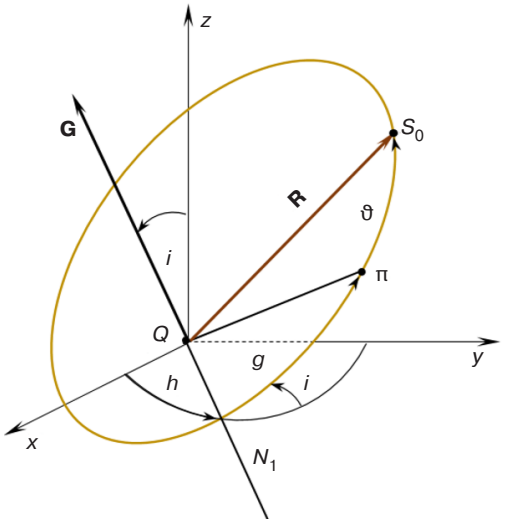

Fig. 2. Satellite orbit elements

The values *h, i, g, e, n, a* in the undisturbed problem remain constant, and the true anomaly ϑ is a function of time:

$$\dot{\vartheta} = \frac{\left(1+e\cos\vartheta\right)^2}{\left(1-e^2\right)^{3/2}} n,\ n = \sqrt{\frac{f_0}{a^3}},$$

$f_0 = fM_0$, where M_0 is the mass of the center of attraction.

Kinetic and potential energies in this case are expressed as:

$$T = \frac{1}{2} m\dot{\mathbf{R}}^2,\ \Pi = -\frac{f_0 m}{R}. \qquad (1.5)$$

In celestial mechanics, canonical Delaunay variables *L*, *G*, *H*, *l*, *g*, *h* are used to describe the orbital motion of celestial bodies. These variables are related to the modulus *R* of the satellite's radius vector and elements *a*, *e*, *i* by the following equations [18–20]:

$$L = m\sqrt{f_0 a},\ G = m\sqrt{f_0 a\left(1-e^2\right)},$$
$$H = m\sqrt{f_0 a\left(1-e^2\right)}\cos i,$$
$$R = \frac{G^2}{f_0 m^2\left(1+e\cos\vartheta\right)}.$$

Here *g*, *h*, *i*, ϑ are the previously defined orbital parameters, *l* is the mean anomaly. The dependence of the true anomaly ϑ on the variables *l*, *L*, *G* is implicitly expressed using the eccentric anomaly *w* through the following relationships:

$$\cos w = \frac{e+\cos\vartheta}{1+e\cos\vartheta},\ l = w - e\sin w.$$

The Hamiltonian of the unperturbed problem with kinetic and potential energies (1.5) in Delaunay variables has a simple form:

$$\mathcal{H} = -\frac{f_0^2 m^3}{2L^2}.$$

Let us return to the task at hand with kinetic energy (1.2) and potential energy (1.4). We will describe the motion of the mechanical system using canonical variables Delaunay L_k, G_k, H_k, l_k, g_k, h_k, corresponding to the vector $\mathbf{R}_k$ (k = 1, 2). The Hamiltonian of the task, taking this into account, will take the form:

$$\mathcal{H} = -\frac{\left(fm_1\right)^2\left(m_2+m_3\right)^3}{2L_1^2} - \frac{f^2\left(m_2+m_3\right)^2 m_r^3}{2L_2^2} + \mathcal{H}_1, \qquad (1.6)$$

$$\mathcal{H}_1 = -\frac{1}{2}\frac{fm_1 m_r}{R_1}\left(3\cos^2\psi_{12}-1\right)\frac{R_2^2}{R_1^2}. \qquad (1.7)$$

In formula (1.7), the modules of the vectors $\mathbf{R}_1$, $\mathbf{R}_2$ are expressed in terms of Delaunay variables as follows (k = 1, 2):

$$R_1 = \frac{G_1^2}{fm_1\left(m_2+m_3\right)^2\left(1+e_1\cos\vartheta_1\right)},$$

$$R_2 = \frac{G_2^2}{f\left(m_2+m_3\right)m_r^2\left(1+e_2\cos\vartheta_2\right)}, \qquad (1.8)$$

$$e_k = \sqrt{1-\frac{G_k^2}{L_k^2}}.$$

At the same time, there are equalities:

$$\cos w_k = \frac{e_k+\cos\vartheta_k}{1+e_k\cos\vartheta_k},\ l_k = w_k - e_k\sin w_k,\ k = 1,2.$$

For large orbital semi-axes and cosine of the inclination angle, expressions using Delaunay variables have the following form:

$$a_1 = \frac{L_1^2}{fm_1\left(m_2+m_3\right)^2},\ a_2 = \frac{L_2^2}{f\left(m_2+m_3\right)m_r^2},$$
$$\cos i_2 = \frac{H_2}{G_2}. \qquad (1.9)$$

Due to the conditions of the problem, we can assume that points *P* and *S* do not affect the motion of the center of mass C_0, i.e., point C_0 moves along an undisturbed Keplerian elliptical orbit in the *OXY* plane. Let us write out vectors $\mathbf{R}_1$, $\mathbf{R}_2$ in the inertial coordinate system *OXYZ*.

$$\mathbf{R}_1 = R_1\boldsymbol{\eta}_1,\ \boldsymbol{\eta}_1 = (\cos(g_1+\vartheta_1),\ \sin(g_1+\vartheta_1),\ 0),$$

$$R_1 = \frac{a_1\left(1-e_1^2\right)}{1+e_1\cos\vartheta_1},\ \dot{\vartheta}_1 = \frac{\left(1+e_1\cos\vartheta_1\right)^2}{\left(1-e_1^2\right)^{3/2}} n_1,$$
$$n_1 = \sqrt{\frac{fm_1}{a_1^3}}. \qquad (1.10)$$

$$\mathbf{R}_2 = R_2\boldsymbol{\eta}_2,\ \boldsymbol{\eta}_2 = (\eta_{2x},\ \eta_{2y},\ \eta_{2z},),$$
$$\eta_{2x} = \cos h_2\cos(g_2+\vartheta_2) - \sin h_2\cos i_2\sin(g_2+\vartheta_2),$$
$$\eta_{2y} = \sin h_2\cos(g_2+\vartheta_2) + \cos h_2\cos i_2\sin(g_2+\vartheta_2), \qquad (1.11)$$
$$\eta_{2z} = \sin i_2\sin(g_2+\vartheta_2).$$

In the limited setting under consideration, the first term on the right-hand side of formula (1.6) is a constant. Therefore, we can write the Hamiltonian of the problem in the form:

$$\mathcal{H} = -\frac{f^2\left(m_2+m_3\right)^2 m_r^3}{2L_2^2} + \mathcal{H}_1. \tag{1.12}$$

Taking into account (1.7)–(1.11), the perturbing part of the Hamiltonian $\mathcal{H}_1$ in formula (1.12) will take the following form:

$$\mathcal{H}_1 = \frac{f^2 m_1^4 G_2^4 \left(m_2+m_3\right)^4 \left(1+e_1\cos\vartheta_1\right)^3}{2G_1^6 m_r^3 \left(1+e_2\cos\vartheta_2\right)^2}\left(1-3\cos^2\psi_{12}\right), \tag{1.13}$$

$$\cos\psi_{12} = (\boldsymbol{\eta}_1, \boldsymbol{\eta}_2) = \cos(g_1+\vartheta_1)[\cos h_2\cos(g_2+\vartheta_2) - \sin h_2\cos i_2\sin(g_2+\vartheta_2)] +$$

$$+ \sin(g_1+\vartheta_1)[\sin h_2\cos(g_2+\vartheta_2) + \cos h_2\cos i_2\sin(g_2+\vartheta_2)].$$

2. EVOLUTION OF SATELLITE ORBITAL MOTION

Let us perform the procedure of averaging the Hamiltonian over the "fast" angular variables—the mean anomalies l_1, l_2:

$$\langle * \rangle_{l_1,l_2} = \frac{1}{(2\pi)^2}\int_0^{2\pi}\int_0^{2\pi}(*)\,dl_1\,dl_2 = \frac{1}{(2\pi)^2}\int_0^{2\pi}\int_0^{2\pi}(*)\frac{\left(1-e_1^2\right)^{3/2}}{\left(1+e_1\cos\vartheta_1\right)^2}\cdot\frac{\left(1-e_2^2\right)^{3/2}}{\left(1+e_2\cos\vartheta_2\right)^2}\,d\vartheta_1\,d\vartheta_2.$$

The perturbing part of the Hamiltonian (1.13) will take the following form as a result of the averaging procedure:

$$\langle \mathcal{H}_1 \rangle_{l_1,l_2} = \frac{f^2 m_1^4\left(m_2+m_3\right)^4}{16 m_r^3}\cdot\frac{L_2^4}{G_1^3 L_1^3}\left\{2\left(1-3\cos^2 i_2\right)+3e_2^2\left(1-3\cos^2 i_2-5\cos\left(2g_2\right)\sin^2 i_2\right)\right\}. \tag{2.1}$$

Expressing eccentricity e_2 and inclination i_2 through the variables L_2, G_2, H_2 according to formulas (1.8), (1.9) and taking into account formulas (1.12), (2.1), we will move on to the averaged Hamiltonian in Delaunay variables:

$$\langle \mathcal{H} \rangle_{l_1,l_2} = -\frac{f^2\left(m_2+m_3\right)^2 m_r^3}{2L_2^2} + \frac{f^2 m_1^4\left(m_2+m_3\right)^4}{16 m_r^3}\cdot\frac{L_2^4}{G_1^3 L_1^3}\left\{\left(1-3\frac{H_2^2}{G_2^2}\right)\left(5-3\frac{G_2^2}{L_2^2}\right)-15\cos\left(2g_2\right)\left(1-\frac{H_2^2}{G_2^2}\right)\left(1-\frac{G_2^2}{L_2^2}\right)\right\}. \tag{2.2}$$

Thus, we obtain an average representation of the Hamiltonian in terms of fast angular variables. The averaged equations of motion are written as a system of canonical equations:

$$\dot{L}_2 = -\frac{\partial\langle\mathcal{H}_1\rangle_{l_1,l_2}}{\partial l_2},\ \dot{G}_2 = -\frac{\partial\langle\mathcal{H}_1\rangle_{l_1,l_2}}{\partial g_2},\ \dot{H}_2 = -\frac{\partial\langle\mathcal{H}_1\rangle_{l_1,l_2}}{\partial h_2},\ \dot{i}_2 = \frac{\partial\langle\mathcal{H}_1\rangle_{l_1,l_2}}{\partial L_2} + \frac{f^2\left(m_2+m_3\right)^2 m_r^3}{L_2^3},$$
$$\dot{g}_2 = \frac{\partial\langle\mathcal{H}_1\rangle_{l_1,l_2}}{\partial G_2},\quad \dot{h}_2 = \frac{\partial\langle\mathcal{H}_1\rangle_{l_1,l_2}}{\partial H_2}. \tag{2.3}$$

Taking into account formula (2.2), the evolutionary system of equations of motion of the satellite in Delaunay variables (2.3) has the form:

$$\dot{L}_2 = 0,\ \dot{H}_2 = 0,$$

$$\dot{G}_2 = -\frac{15 f^2 m_1^4\left(m_2+m_3\right)^4}{8 m_r^3}\cdot\frac{L_2^4}{G_1^3 L_1^3}\left(1-\frac{H_2^2}{G_2^2}\right)\left(1-\frac{G_2^2}{L_2^2}\right)\sin\left(2g_2\right),$$

$$\dot{g}_2 = \frac{6f^2 m_1^4 \left(m_2+m_3\right)^4}{16 m_r^3} \cdot \frac{L_2^4}{G_1^3 L_1^3 G_2} \left\{ 5\frac{H_2^2}{G_2^2}\left(1-\cos\left(2g_2\right)\right) - \frac{G_2^2}{L_2^2}\left(1-5\cos\left(2g_2\right)\right) \right\},$$

$$\dot{h}_2 = \frac{-6f^2 m_1^4 \left(m_2+m_3\right)^4}{16 m_r^3 G_2} \cdot \frac{L_2^4}{G_1^3 L_1^3} \left(\frac{H_2}{G_2}\right) \left\{ 2 + \left(1-\frac{G_2^2}{L_2^2}\right)\left(3-5\cos\left(2g_2\right)\right) \right\},$$

$$\dot{l}_2 = \frac{f^2\left(m_2+m_3\right)^2 m_r^3}{L_2^3} + \frac{f^2 m_1^4 \left(m_2+m_3\right)^4}{16 m_r^3 G_1^3 L_1^3} 2L_2^3 \left\{ \left(1-3\frac{H_2^2}{G_2^2}\right)\left(10-3\frac{G_2^2}{L_2^2}\right) - 15\cos\left(2g_2\right)\left(1-\frac{H_2^2}{G_2^2}\right)\left(2-\frac{G_2^2}{L_2^2}\right) \right\}.$$

Using the following inverse ratios $H_2^2/G_2^2 = \cos^2 i_2$, $1-(H_2^2/G_2^2) = \sin^2 i_2$, $G_2^2/L_2^2 = 1-e_2^2$, obtained from equations (1.8) and (1.9), we derive an averaged system of equations for the satellite's motion in Delaunay variables (relative to "slow" variables):

$$\dot{L}_2 = 0,\ \dot{H}_2 = 0,$$

$$\dot{G}_2 = -\frac{15 f m_1 m_r}{8} \cdot \frac{a_2^2 e_2^2}{a_1^3\left(1-e_1^2\right)^{3/2}} \sin^2 i_2 \sin\left(2g_2\right),$$

$$\dot{l}_2 = \frac{\sqrt{f\left(m_2+m_3\right)}}{a_2^{3/2}} + \frac{m_1\sqrt{f}}{8\sqrt{\left(m_2+m_3\right)}} \cdot \frac{a_2^{3/2}}{a_1^3\left(1-e_1^2\right)^{3/2}} \left\{ \left(-2+3\sin^2 i_2\right)\left(7+3e_2^2\right) - 15\cos\left(2g_2\right)\sin^2 i_2\left(1+e_2^2\right) \right\}, \quad (2.4)$$

$$\dot{g}_2 = \frac{3m_1\sqrt{f}}{8\sqrt{\left(m_2+m_3\right)}} \cdot \frac{a_2^{3/2}}{a_1^3\left(1-e_1^2\right)^{3/2}\sqrt{\left(1-e_2^2\right)}} \left\{ 4 + e_2^2\left(1-5\cos\left(2g_2\right)\right) - 5\sin^2 i_2\left(1-\cos\left(2g_2\right)\right) \right\},$$

$$\dot{h}_2 = \frac{-3m_1\sqrt{f}}{8\sqrt{\left(m_2+m_3\right)}} \cdot \frac{a_2^{3/2}}{a_1^3\left(1-e_1^2\right)^{3/2}\sqrt{\left(1-e_2^2\right)}} \cos i_2 \left\{ 2 + e_2^2\left(3-5\cos\left(2g_2\right)\right) \right\}.$$

Next, we will perform transformations in the evolutionary system of equations of motion to transition to a form that depends on the variables e_2, i_2, g_2, h_2, and also perform a transition to dimensionless time $\tau = n_2 t$, $n_2 = \sqrt{f\left(m_2+m_3\right)a_2^{-3}}$. The final system takes the form:

$$a_2' = 0,$$

$$e_2' = \frac{15\mu a_0^3}{8} \cdot \frac{e_2\sqrt{1-e_2^2}}{\left(1-e_1^2\right)^{3/2}} \sin^2 i_2 \sin\left(2g_2\right),$$

$$i_2' = \frac{-15\mu}{16} \cdot \frac{a_0^3 e_2^2}{\sqrt{1-e_2^2}\left(1-e_1^2\right)^{3/2}} \sin\left(2i_2\right)\sin\left(2g_2\right),$$

$$l_2' = 1 + \frac{\mu}{8} \cdot \frac{a_0^3}{\left(1-e_1^2\right)^{3/2}} \left\{ \left(-2+3\sin^2 i_2\right)\left(7+3e_2^2\right) - 15\cos\left(2g_2\right)\sin^2 i_2\left(1+e_2^2\right) \right\}, \quad (2.5)$$

$$g_2' = \frac{3\mu}{8} \cdot \frac{a_0^3}{\left(1-e_1^2\right)^{3/2}\sqrt{1-e_2^2}} \left\{ 4 + e_2^2\left(1-5\cos\left(2g_2\right)\right) - 5\sin^2 i_2\left(1-\cos\left(2g_2\right)\right) \right\},$$

$$h_2' = \frac{-3\mu}{8} \cdot \frac{a_0^3}{\left(1-e_1^2\right)^{3/2}\sqrt{1-e_2^2}} \cos i_2 \left\{ 2 + e_2^2\left(3-5\cos\left(2g_2\right)\right) \right\},$$

where $\mu = \frac{m_1}{m_2 + m_3}$, $a_0^3 = \frac{a_2^3}{a_1^3}$ is the mass ratio (the ratio of the mass of the attracting center to the sum of the masses of the celestial body and the satellite) and the axial ratio (the ratio of the semi-major axes of the orbits), respectively.

Note that the value of the major semi-axis a_2 does not change over time. Furthermore, the right-hand sides of the system of equations (2.5) depend only on three variables: eccentricity e_2, orbital inclination i_2, and longitude of the pericenter g_2. Therefore, the 2nd, 3rd, and 5th equations of the system are separated from the rest of the equations, and the 4th and 6th equations can be integrated after the functions $e_2(\tau)$, $i_2(\tau)$, $g_2(\tau)$ are found. The angular variable l_2 is "fast." This variable was averaged. Therefore, it can be excluded from consideration. The system is reduced to four basic equations:

$$
\begin{aligned}
e_2' &= \frac{15k}{8} \cdot \frac{e_2\sqrt{1-e_2^2}}{\left(1-e_1^2\right)^{\frac{3}{2}}} \sin^2 i_2 \sin\left(2g_2\right), \\
i_2' &= \frac{-15k}{16} \cdot \frac{e_2^2}{\sqrt{1-e_2^2}\left(1-e_1^2\right)^{\frac{3}{2}}} \sin\left(2i_2\right)\sin\left(2g_2\right), \\
g_2' &= \frac{3k}{8} \cdot \frac{1}{\left(1-e_1^2\right)^{\frac{3}{2}}\sqrt{1-e_2^2}} \left\{4 + e_2^2\left(1-5\cos\left(2g_2\right)\right) - 5\sin^2 i_2\left(1-\cos\left(2g_2\right)\right)\right\}, \\
h_2' &= \frac{-3k}{8} \cdot \frac{\cos i_2}{\left(1-e_1^2\right)^{\frac{3}{2}}\sqrt{1-e_2^2}} \left\{2 + e_2^2\left(3-5\cos\left(2g_2\right)\right)\right\},
\end{aligned}
\tag{2.6}
$$

where $k = \mu a_0^3$.

The resulting system (2.6), with an accuracy up to a constant factor responsible for the choice of dimensionless time, coincides with the system of equations obtained by M.L. Lidov [7, 8], if we neglect the perturbations caused by the eccentricity of the Moon's gravitational field. The system of equations (2.6) has first integrals [7, 8]:

$$\cos^2 i_2\left(1-e_2^2\right) = C, \tag{2.7}$$

$$e_2^2\left(\frac{2}{5} - \sin^2 g_2 \sin^2 i_2\right) = D. \tag{2.8}$$

From the resulting ratio (2.7), it follows that as the value of e_2 increases, the value of i_2 will decrease, and *vice versa*. Let us move on to the parameters of the system (2.6):

$m_1 = 5.9736 \cdot 10^{24}$ kg is the mass of the Earth,

$m_2 = 7.349 \cdot 10^{22}$ kg is the mass of the Moon,

$m_3 = 10^3$ kg is the mass of the satellite,

$$\mu = \frac{m_1}{m_2 + m_3} = \frac{5.9736 \cdot 10^{24}}{7.349 \cdot 10^{22} + 10^3} \approx 81.28453.$$

As a first approximation, we can assume that the Moon moves in an elliptical orbit with eccentricity $e_1 = 0.0549$ and a semi-major axis of the geocentric orbit $a_1 = 384400 \cdot 10^3$ m.

We will consider lunar orbits with altitudes ranging from 500 to 20000 km (310 to 12430 miles), where the Earth's gravity has the greatest effect and causes orbital perturbations. Let $a_2 = 6500 \cdot 10^3$ m be the semi-major axis of the satellite's orbit, then:

$$a_0^3 = \frac{a_2^3}{a_1^3} = \frac{6500 \cdot 10^3}{379739 \cdot 10^3} \approx 0.017117, \quad k = \mu a_0^3 \approx 81.28453 \cdot 0.017117 \approx 1.39135.$$

We can integrate the resulting system (2.6) using the fourth-order Runge–Kutta method with a constant step size, setting the initial values: $e_{2_0} = 0.01$, $i_{2_0} = \frac{j\pi}{180}$, $g_{2_0} = 0$, $h_{2_0} = 0$, j = 30°, 45°, 60°, 85°, and on this basis we can construct integral curves. The resulting graphs (Fig. 3) clearly demonstrate compliance with the relationship of the first integral (2.7) of the system under consideration. The change in the value of eccentricity (the degree of ellipticity of the orbit) and the inclination angle (the angle between the orbital plane and a certain reference plane) on the graph can be either gradual or abrupt.

3. STATIONARY SOLUTIONS OF THE EVOLUTIONARY SYSTEM OF MOTION EQUATIONS OF THE ASM

Frozen orbits around the Moon, natural satellites, or asteroids are of great interest, since a number of space missions aim to fly around such bodies. Frozen orbits are those in which changes in inclination, eccentricity, and longitude of the pericenter from the ascending node are minimized. In order to define such orbits, we will determine stationary solutions to the first three equations (2.6), determined by the conditions:

$$e_2' = 0,\ i_2' = 0,\ g_2' = 0. \tag{3.1}$$

Since elliptical orbits are being considered, we will limit the values of eccentricity e_2 to the interval [0; 1):

$$0 \le e_2 < 1. \tag{3.2}$$

Considering integral (2.7), we obtain a closed autonomous system of the second order with respect to g_2, e_2:

$$\begin{gathered} e_2' = 5k_1 e_2 \sqrt{1-e_2^2}\left(1-e_2^2-C\right)\sin\left(2g_2\right), \\ g_2' = \frac{k_1}{\left(1-e_2^2\right)^{3/2}}\left\{\left(1-e_2^2\right)\left(4+e_2^2-5e_2^2\cos\left(2g_2\right)\right)-5\left(1-e_2^2-C\right)\left(1-\cos\left(2g_2\right)\right)\right\}. \end{gathered} \tag{3.3}$$

Here

$$k_1 = \frac{3k}{8\left(1-e_1^2\right)^{3/2}}.$$

Let us find stationary solutions to system (3.3) by setting its right-hand sides equal to zero. Taking into account condition (3.2), we obtain the following system of equations:

$$\begin{gathered} e_2\left(1-e_2^2-C\right)\sin\left(2g_2\right)=0, \\ \left(1-e_2^2\right)\left(4+e_2^2-5e_2^2\cos\left(2g_2\right)\right)-5\left(1-e_2^2-C\right)\left(1-\cos\left(2g_2\right)\right)=0. \end{gathered} \tag{3.4}$$

Note that according to equality (2.7), the value of the constant C is limited by the interval [0; 1].

From the first equation of system (3.4), it follows that either $e_2 = 0$, or $1-e_2^2-C=0$, or $\sin(2g_2) = 0$. In the case $e_2 = 0$ from the second equation of system (3.4), we obtain:

$$\cos\left(2g_2\right) = \frac{1-5C}{5\left(1-C\right)}. \tag{3.5}$$

Equation (3.5) has a solution under the condition $0 \le C \le 0.6$. Therefore, with the specified values of the parameter C we obtain the first series of stationary solutions:

$$e_2^* = 0,\ \ g_2^* = \pm\frac{1}{2}\arccos\frac{1-5C}{5\left(1-C\right)} + \pi m,\ m \in \mathbb{Z}\ \left(C \in [0;\, 0.6]\right). \tag{3.6}$$

If $1-e_2^2-C=0$, then from the second equation of system (3.4) we obtain:

$$\cos\left(2g_2\right) = 1 + \frac{4C}{5\left(1-C\right)}.$$

Given the restrictions imposed on the constant C, the latter equality is possible if $C = 0$. But then $e_2 = 1$. Thus we come at a contradiction with (3.2).

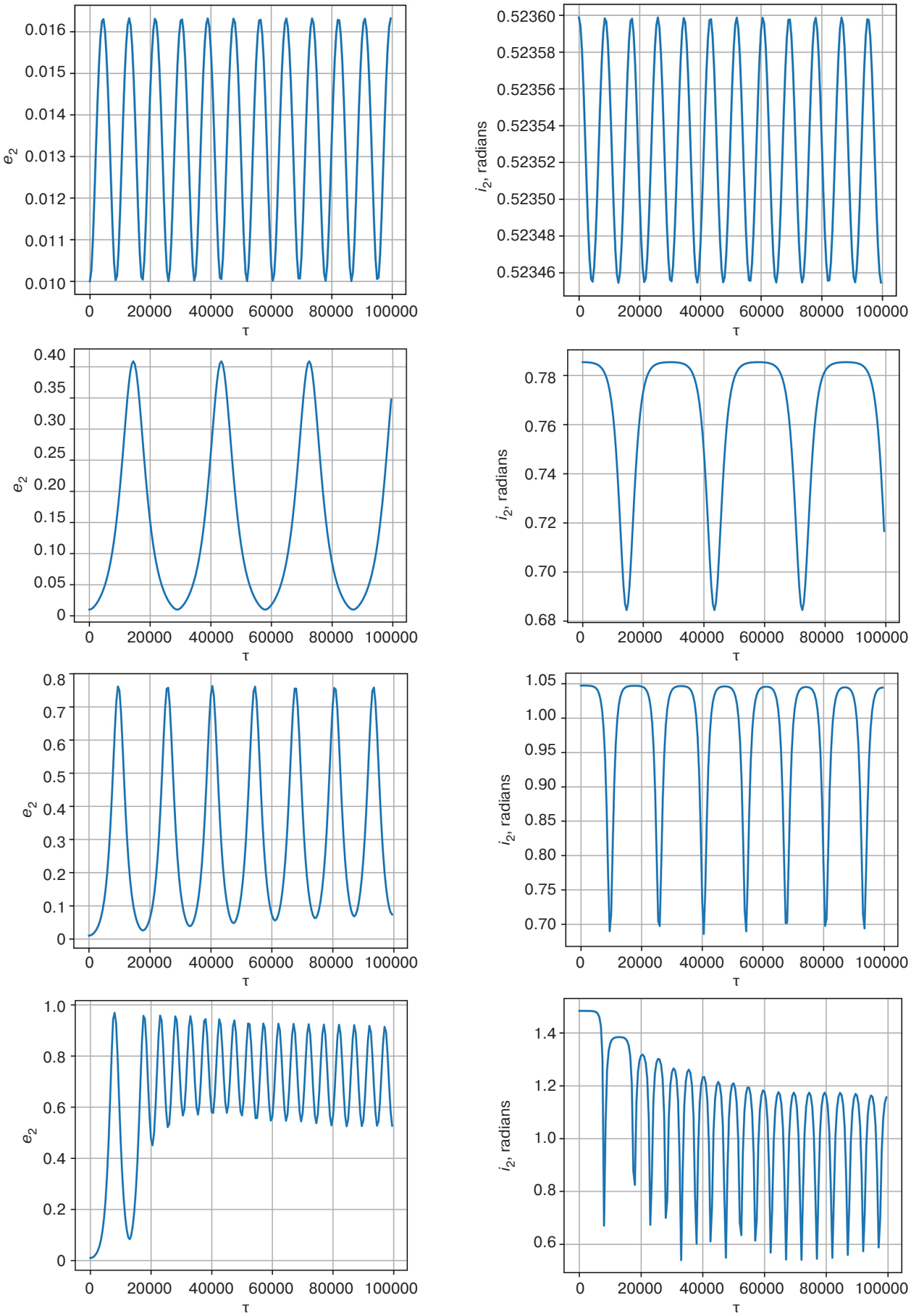

Fig. 3. Integral curves of the averaged system of equations (2.6) $e_2(\tau)$ and $i_2(\tau)$ at i_{2_0} = π/6, π/4, π/3, 85π/180

If $\sin(2g_2) = 0$, then either $\cos(2g_2) = 1$, or $\cos(2g_2) = -1$. If $\cos(2g_2) = 1$, then from the second equation of system (3.4) we obtain $e_2 = 1$, therefore this case is not suitable. If $\cos(2g_2) = -1$, then from the second equation of system (3.4) it follows that:

$$e_2^2 = 1 - \sqrt{\frac{5C}{3}}.$$

This equality is possible under the condition: $0 < C \le 0.6$. Thus, we obtained another series of stationary solutions:

$$e_2^* = \sqrt{1 - \sqrt{\frac{5C}{3}}}, \quad g_2^* = \frac{\pi}{2} + \pi m, \ m \in \mathbb{Z} \ \left(C \in (0;\, 0.6]\right). \tag{3.7}$$

Let us investigate the stability of stationary solutions based on a perturbed system of first-order equations. We can denote $e_2 = e_2^* + x_1$, $g_2 = g_2^* + x_2$, and further denote the right-hand sides of the system of equations (3.3) respectively as $F_1(e_2, g_2)$, $F_2(e_2, g_2)$. Then the perturbed system of equations of the first approximation will be written as:

$$x_1' = a_{11}x_1 + a_{12}x_2, \quad x_2' = a_{21}x_1 + a_{22}x_2,$$
$$a_{11} = \frac{\partial F_1\left(e_2^*, g_2^*\right)}{\partial e_2}, \ a_{12} = \frac{\partial F_1\left(e_2^*, g_2^*\right)}{\partial g_2}, \ a_{21} = \frac{\partial F_2\left(e_2^*, g_2^*\right)}{\partial e_2}, \ a_{22} = \frac{\partial F_2\left(e_2^*, g_2^*\right)}{\partial g_2}. \tag{3.8}$$

The partial derivatives of the right-hand sides of the evolutionary system of equations (3.3) are of the form:

$$\frac{\partial F_1\left(e_2, g_2\right)}{\partial e_2} = \frac{5k_1 \sin(2g_2)}{\sqrt{1-e_2^2}}\left\{\left(1-e_2^2\right)\left(1-3e_2^2-C\right) - e_2^2\left(1-e_2^2-C\right)\right\},$$

$$\frac{\partial F_1\left(e_2, g_2\right)}{\partial g_2} = 10k_1 e_2 \sqrt{1-e_2^2}\left(1-e_2^2-C\right)\cos\left(2g_2\right),$$

$$\frac{\partial F_2\left(e_2, g_2\right)}{\partial e_2} = \frac{3e_2 F_2\left(e_2, g_2\right)}{1-e_2^2} + \frac{4k_1 e_2}{\sqrt{1-e_2^2}}\left(1-5\cos\left(2g_2\right)\right),$$

$$\frac{\partial F_2\left(e_2, g_2\right)}{\partial g_2} = \frac{10k_1 \sin(2g_2)}{\left(1-e_2^2\right)^{3/2}}\left(C - \left(1-e_2^2\right)^2\right).$$

For the stationary solution (3.6), the coefficients a_{ij} on the right-hand sides of equations (3.8) are as follows:

$$a_{11} = 5k_1 \sin(2g_2^*)(1-C), \ a_{12} = 0, \ a_{21} = 0, \ a_{22} = -2a_{11}.$$

The roots of the characteristic equation are real and of different signs (the type of singular point is a saddle point). Consequently, the stationary solution (3.6) is unstable.

For the stationary solution (3.7), we obtain:

$$a_{11} = 0, \ a_{12} = -10k_1 e_2^* \sqrt{1-e_2^{*2}}\left(\sqrt{\frac{5C}{3}} - C\right) < 0, \ a_{21} = \frac{24k_1 e_2^*}{\sqrt{1-e_2^{*2}}} > 0, \ a_{22} = 0.$$

The roots of the characteristic equation $\lambda^2 - a_{12}a_{21} = 0$ are purely imaginary. Therefore, in the first approximation, the stationary solution is stable (the type of singular point is a center).

Figures 4–7 show phase portraits of the system of equations (3.3) for different values of the constant C.

We can see that the nature of the change in eccentricity is oscillatory. With regard to the evolution of the argument of perihelion, its change demonstrates either a system of open trajectories of a monotonic nature or a system of closed trajectories of an oscillatory nature surrounding the equilibrium positions. According to the analytical study, when $C > 0.6$ the system of equations (3.3) has no stationary solutions. This case is shown in Fig. 7. Here, the changes in eccentricity are oscillatory, and the longitude of the pericenter changes monotonically.

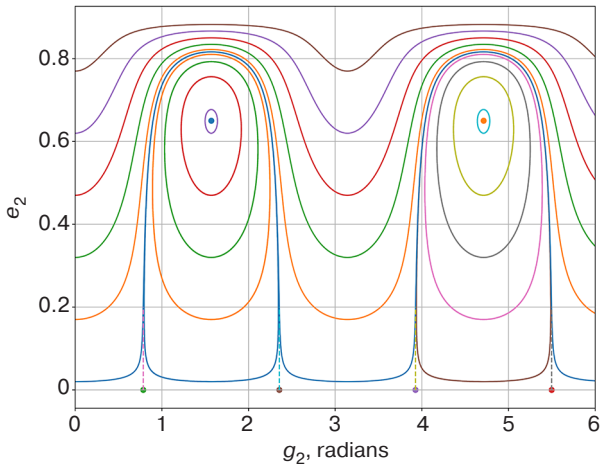

Fig. 4. Phase portrait of the system of equations (3.3) at $C = 0.2$

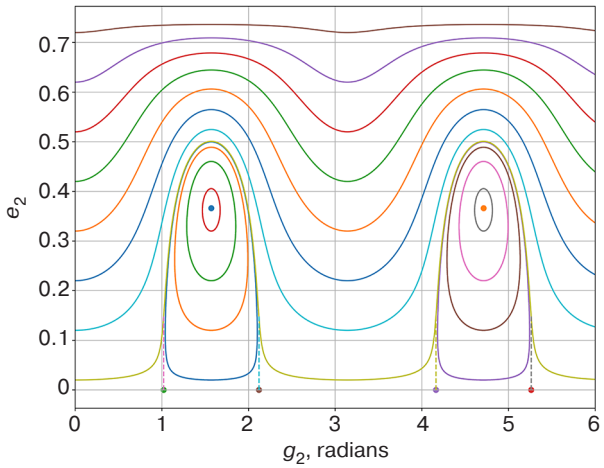

Fig. 5. Phase portrait of the system of equations (3.3) at $C = 0.45$

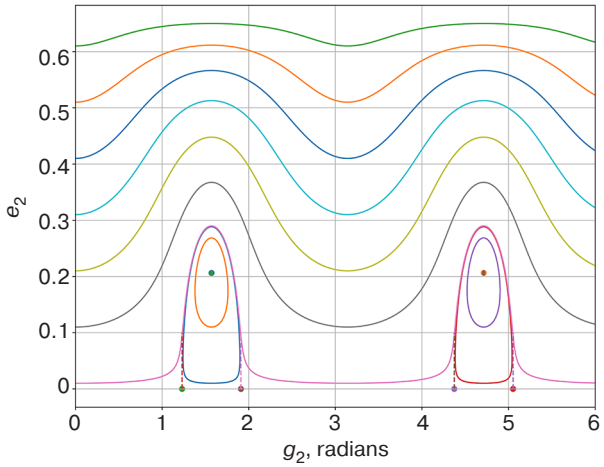

Fig. 6. Phase portrait of the system of equations (3.3) at $C = 0.55$

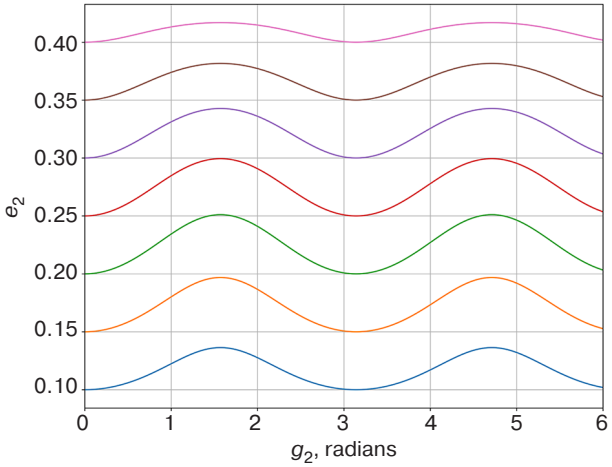

Fig. 7. Phase portrait of the system of equations (3.3) at $C = 0.8$

4. UNMEDIATED EQUATIONS OF SATELLITE MOTION FOR THE EXCITED TASK

Let us derive the unaveraged system of equations of motion for the ASM. The Hamiltonian of the problem has the form:

$$\mathcal{H} = -\frac{f^2\left(m_2+m_3\right)^2 m_r^3}{2L_2^2} + \mathcal{H}_1,\ \mathcal{H}_1 = -\frac{1}{2}\cdot\frac{fm_1m_rR_2^2}{R_1^3}\left(3\Phi^2-1\right). \tag{4.1}$$

The summand $\mathcal{H}_1$ in the expression for the Hamiltonian depends on the Delaunay variables L_2, G_2, H_2, l_2, g_2, h_2 *via* $R_2 = R_2(L_2, G_2, l_2)$ according to (1.8) and Φ:

$$\Phi = \cos\psi_{12} = \cos\left(g_2+\vartheta_2\right)\cos\left(g_1+\vartheta_1-h_2\right) + \cos i_2 \sin\left(g_2+\vartheta_2\right)\sin\left(g_1+\vartheta_1-h_2\right). \tag{4.2}$$

The canonical equations of motion of a satellite in Delaunay variables are as follows:

$$\dot{L}_2 = -\frac{\partial\mathcal{H}_1}{\partial l_2},\ \dot{G}_2 = -\frac{\partial\mathcal{H}_1}{\partial g_2},\ \dot{H}_2 = -\frac{\partial\mathcal{H}_1}{\partial h_2},\ \dot{l}_2 = \frac{f^2\left(m_2+m_3\right)^2 m_r^3}{L_2^3} + \frac{\partial\mathcal{H}_1}{\partial L_2},\ \dot{g}_2 = \frac{\partial\mathcal{H}_1}{\partial G_2},\ \dot{h}_2 = \frac{\partial\mathcal{H}_1}{\partial H_2}. \tag{4.3}$$

After calculating the partial derivatives, we obtain:

$$\dot{L}_2 = \frac{fm_1m_\text{r}R_2^2}{R_1^3}\cdot\frac{\left(1+e_2\cos\vartheta_2\right)}{\left(1-e_2^2\right)^{3/2}}\left\{\left(3\Phi^2-1\right)e_2\sin\vartheta_2+3\left(1+e_2\cos\vartheta_2\right)\Phi\Phi_2\right\},$$

$$\dot{G}_2 = \frac{3fm_1m_rR_2^2}{R_1^3}\Phi\Phi_2,\ \dot{H}_2 = \frac{3fm_1m_rR_2^2}{R_1^3}\Phi\Phi_3,$$

$$\dot{l}_2 = n_2 - \frac{fm_1m_\text{r}R_2^2}{R_1^3L_2e_2}\left\{\left(2e_2-\cos\vartheta_2-e_2\cos^2\vartheta_2\right)\left(3\Phi^2-1\right)+3\Phi\Phi_2\sin\vartheta_2\left(2+e_2\cos\vartheta_2\right)\right\},$$

$$\dot{g}_2 = \frac{fm_1m_\text{r}R_2^2}{R_1^3e_2G_2}\left\{\left(1+e_2\cos\vartheta_2\right)\cos\vartheta_2\left(1-3\Phi^2\right)+3\Phi\Phi_2\sin\vartheta_2\left(2+e_2\cos\vartheta_2\right)+\right.$$

$$\left.+3\Phi e_2\cos i_2\sin\left(g_2+\vartheta_2\right)\sin\left(g_1+\vartheta_1-h_2\right)\right\},$$

$$\dot{h}_2 = -\frac{3fm_1m_\text{r}R_2^2}{R_1^3G_2}\Phi\sin\left(g_2+\vartheta_2\right)\sin\left(g_1+\vartheta_1-h_2\right). \qquad (4.4)$$

Here

$$n_2 = \frac{f^2\left(m_2+m_3\right)^2m_\text{r}^3}{L_2^3},$$

$$\Phi_2 = \frac{\partial\Phi}{\partial\vartheta_2} = -\sin\left(g_2+\vartheta_2\right)\cos\left(g_1+\vartheta_1-h_2\right)+\cos i_2\cos\left(g_2+\vartheta_2\right)\sin\left(g_1+\vartheta_1-h_2\right), \qquad (4.5)$$

$$\Phi_3 = \frac{\partial\Phi}{\partial h_2} = \cos\left(g_2+\vartheta_2\right)\sin\left(g_1+\vartheta_1-h_2\right)-\cos i_2\sin\left(g_2+\vartheta_2\right)\cos\left(g_1+\vartheta_1-h_2\right).$$

Thus, we obtain a system of equations (3.4) for the motion of a 6th-order satellite in Delaunay variables. The first equation with $\dot{L}_2$ is responsible for the change in total orbital action over time, the second with $\dot{G}_2$ is responsible for the change in total angular momentum over time, and the third with $\dot{H}_2$ is responsible for the change in azimuthal angular momentum over time. The remaining three equations are responsible for changes in the orbital elements: mean anomaly l_2, argument of pericenter g_2; and the longitude of ascending node h_2. Point C_0 moves along an undisturbed Keplerian elliptical orbit in the OXY plane. Therefore R_1, ϑ_1 in (4.4), (4.5) are given functions of time according to (1.10), and the longitude of the pericenter g_1, the semi-major axis a_1 and the eccentricity e_1 are constant values.

Let us make the transition to dimensionless variables n_{20}, e_2, i_2, g_2, ϑ_2, h_2, where

$$n_{20} = \frac{n_2}{n_1} = \frac{f^2\left(m_2+m_3\right)^2m_\text{r}^3}{L_2^3n_1},\ n_1 = \sqrt{\frac{fm_1}{a_1^3}}.$$

Furthermore, let us move on to dimensionless time $\tau = n_1t/(2\pi)$ the number of revolutions of the center of mass C_0 relative to point O. We will transform the right-hand sides of the equations of system (4.4), taking into account (1.10) and relying on the known relations for the Delaunay variables:

$$L_2 = m_\text{r}\sqrt{f\left(m_2+m_3\right)a_2},\ G_2 = m_r\sqrt{f\left(m_2+m_3\right)a_2\left(1-e_2^2\right)},$$

$$H_2 = m_\text{r}\sqrt{f\left(m_2+m_3\right)a_2\left(1-e_2^2\right)}\cos i_2. \qquad (4.6)$$

As a result, we obtain:

$$n_{20}' = -\frac{6\pi\sqrt{1-e_2^2}\left(1+e_1\cos\vartheta_1\right)^3}{\left(1-e_1^2\right)^3\left(1+e_2\cos\vartheta_2\right)}\left\{\left(3\Phi^2-1\right)e_2\sin\vartheta_2+3\left(1+e_2\cos\vartheta_2\right)\Phi\Phi_2\right\},$$

$$e_2' = \frac{2\pi\sqrt{\left(1-e_2^2\right)^3}\left(1+e_1\cos\vartheta_1\right)^3}{\left(1-e_1^2\right)^3\left(1+e_2\cos\vartheta_2\right)^2 n_{20}}\left\{\left(3\Phi^2-1\right)\sin\vartheta_2\left(1+e_2\cos\vartheta_2\right)+3\Phi\Phi_2\left(2\cos\vartheta_2+e_2\cos^2\vartheta_2+e_2\right)\right\},$$

$$i_2' = -\frac{6\pi\sqrt{\left(1-e_2^2\right)^3}\left(1+e_1\cos\vartheta_1\right)^3}{\left(1-e_1^2\right)^3\left(1+e_2\cos\vartheta_2\right)^2 n_{20}}\Phi\sin i_2\cos\left(g_2+\vartheta_2\right)\sin\left(g_1+\vartheta_1-h_2\right),$$

$$g_2' = \frac{2\pi\sqrt{\left(1-e_2^2\right)^3}\left(1+e_1\cos\vartheta_1\right)^3}{\left(1-e_1^2\right)^3\left(1+e_2\cos\vartheta_2\right)^2 e_2 n_{20}}\left\{\left(1+e_2\cos\vartheta_2\right)\cos\vartheta_2\left(1-3\Phi^2\right)+\right.$$

$$\left.+\,3\Phi\Phi_2\sin\vartheta_2\left(2+e_2\cos\vartheta_2\right)+3\Phi e_2\cos i_2\sin\left(g_2+\vartheta_2\right)\sin\left(g_1+\vartheta_1-h_2\right)\right\}, \qquad (4.7)$$

$$\vartheta_2' = \frac{2\pi\left(1+e_2\cos\vartheta_2\right)^2 n_{20}}{\left(1-e_2^2\right)^{3/2}}+$$

$$+\frac{2\pi\sqrt{\left(1-e_2^2\right)^3}\left(1+e_1\cos\vartheta_1\right)^3}{\left(1-e_1^2\right)^3\left(1+e_2\cos\vartheta_2\right)^2 e_2 n_{20}}\left\{\left(1+e_2\cos\vartheta_2\right)\cos\vartheta_2\left(3\Phi^2-1\right)-3\Phi\Phi_2\sin\vartheta_2\left(2+e_2\cos\vartheta_2\right)\right\},$$

$$h_2' = -\frac{6\pi\sqrt{\left(1-e_2^2\right)^3}\left(1+e_1\cos\vartheta_1\right)^3}{\left(1-e_1^2\right)^3\left(1+e_2\cos\vartheta_2\right)^2 n_{20}}\Phi\sin\left(g_2+\vartheta_2\right)\sin\left(g_1+\vartheta_1-h_2\right),$$

$$\vartheta_1' = \frac{2\pi\left(1+e_1\cos\vartheta_1\right)^2}{\left(1-e_1^2\right)^{3/2}}.$$

We will perform the numerical integration of the averaged and unaveraged systems of equations (2.6) and (4.7) and compare the obtained numerical results with the modern temporal variations of eccentricity and inclination presented in [12]. As initial values, following [12], for the averaged system of equations (2.6) we take (2.6)

$$e_2(0) = 0.61,\ i_2(0) = 55.9^\circ = 55.9\pi/180 \text{ rad},\ g_2(0) = \pi/2,\ h_2(0) = 0. \qquad (4.8)$$

Since a dimensionless time in system (2.6), $\tau = n_2 t$, $n_2 = \sqrt{f\left(m_2+m_3\right)a_2^{-3}}$ is used, therefore, in order to consider a double period $2T$ = 2.5 years or 2.5 · 365 days, the time range needs to be set: $\tau = \frac{2.5\cdot 365}{0.0874} \cong 10440.$ Figure 8 shows the integral curves of the averaged system of equations (2.6).

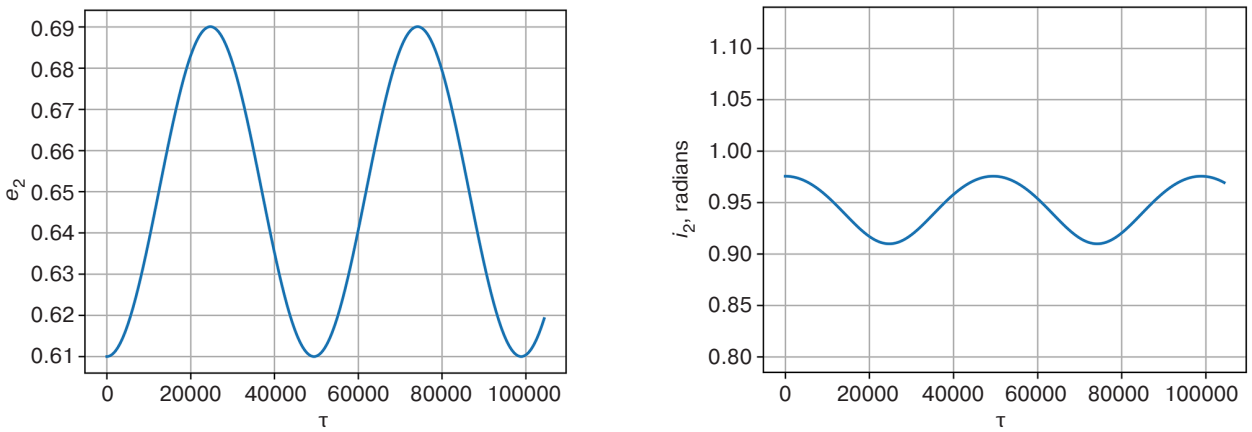

Fig. 8. Integral curves $e_2(\tau)$ and $i_2(\tau)$ of the averaged system of equations

We obtain the following predicted deviations of the average values of the elements: $\Delta e_2 \sim 0.08$, $\Delta i_2 \sim 3.7°(0.07$ rad), close to the results from [12]. This reflects the basic nature of the changes in the elements, while omitting short-period gravitational effects.

Next, we integrate the unaveraged system (4.7). In order to do this, we need to specify the initial values of the eccentricity, semi-major axis, longitude of the pericenter of the Moon's orbit, and the initial value of its true anomaly. The data was collected using the *Horizons System*[4] utility with the following parameters: target object is the Moon; coordinate center is the Earth; and time is 2009-07-15 01:00:00. Since [12] provides only 4 initial values (4.8), the remaining missing values of the true and mean anomaly were also collected using the *Horizons System* for the ASM operating at that time: LRO 2009-031A[5]. As a dimensionless time in the system (4.7), $\tau = n_1 t/(2\pi)$ is used. Therefore, in order to consider the double period $2T = 2.5$ years or $2.5 \cdot 365$ days, the time range needs to be set in $\tau^* = \dfrac{2.5 \cdot 365}{27.0632} \cong 34.$

Figure 9 shows the integral curves $e_2(t)$ and $i_2(t)$ of the averaged and non-averaged systems of equations. Figure 10 shows the integral curves of the systems of equations (2.6) and (4.7) with the same initial conditions in the plane (g_2, e_2), which are generally similar to the analogous curves presented in [12]. A characteristic steady oscillatory motion is observed, the length of the pericenter depends on the eccentricity in accordance with the periodic law. A change in the eccentricity e_2 is noted in the range from 0.61 to 0.69, which is relatively similar to $\Delta e \sim 0.09$ in the work [12].

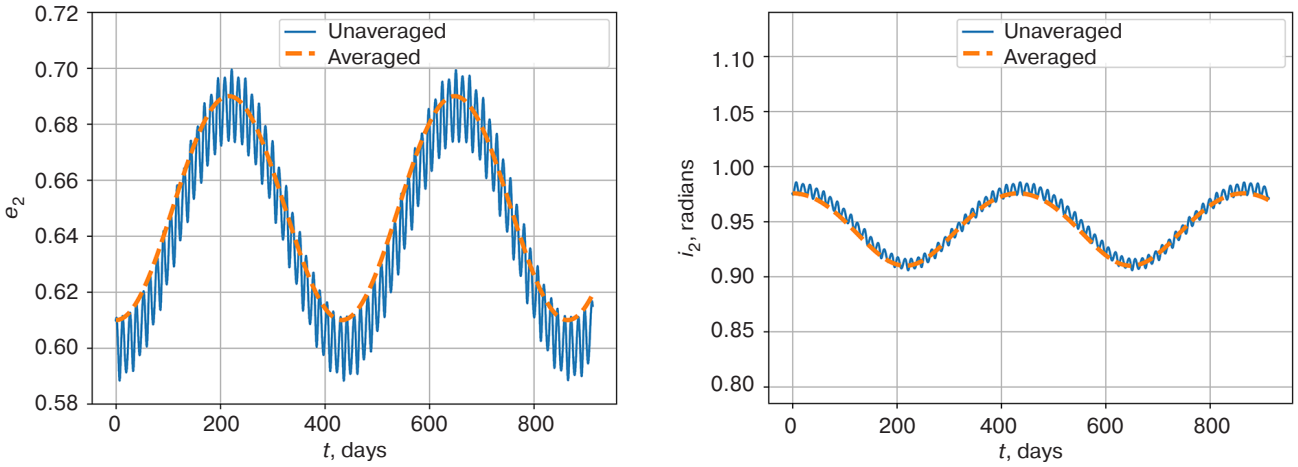

Fig. 9. Integral curves $e_2(t)$ and $i_2(t)$ of averaged and unaveraged systems of equations of satellite orbital motion

The graphs obtained also show periodic behavior and the main period, as in the averaged model, but with high-frequency oscillations superimposed upon it. The total amplitude of the oscillations corresponds to the amplitude of the averaged line, while the instantaneous values of eccentricity and inclination deviate from the averaged value. The averaged system is a "smoothed" version of the unaveraged system. The integral curves of the unaveraged system of equations contain more details and information about short-term changes in orbital elements. The averaged system can be useful for long-term forecasting and analysis of general trends. The unaveraged system is necessary for accurate modeling and prediction of satellite behavior over short time intervals. Although more difficult to analyze, the unaveraged system provides a more complete picture of satellite behavior.

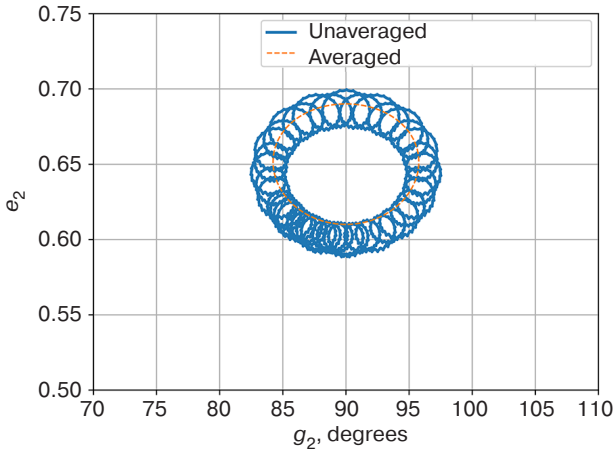

Fig. 10. Integral curves of averaged and unaveraged systems of equations of satellite orbital motion in a plane (g_2, e_2)

[4] https://ssd.jpl.nasa.gov/horizons/#api. Accessed February 04, 2025.

[5] Lunar Reconnaissance Orbiter is a robotic spacecraft orbiting the Moon. Launched on June 18, 2009. https://www.n2yo.com/satellite/?s=35315. Accessed February 04, 2025.

CONCLUSIONS

As a result of the study, averaged and unaveraged systems of equations of motion for the ASM were derived, taking into account the perturbation caused by the Earth's gravitational field, based on the system of equations of motion of the satellite in Delaunay canonical variables, enabling to track the change in its orbital parameters over time.

Stationary solutions of the averaged system of equations were found, and their stability was investigated. Conditions for the existence of "frozen" orbits were obtained, in which changes in inclination, eccentricity, and longitude of the pericenter from the ascending node are minimized. Phase portraits were constructed for the averaged system of equations at various values of the problem parameter which depends on the initial values of the inclination and eccentricity of the orbit. Integral curves of the non-averaged system of equations were also constructed.

It should be noted that the study takes into account the influence of the main factor on the satellite's orbit—external gravitational disturbance. Further study of this issue may enable a more accurate description of the motion of satellites around celestial bodies. The study has practical significance for the development and planning of space missions related to the exploration of the Moon and its vicinity. The equations obtained can be used to more accurately predict the orbital motion of satellites and determine the optimal parameters of their orbits.

ACKNOWLEDGMENTS

The work was carried out as part of the initiative research work of the Department of Higher Mathematics of the Institute of Artificial Intelligence at RTU MIREA (No. 192-III(VM)).

Authors' contribution

All authors contributed equally to the research work.

REFERENCES

1. Woodard M., Folta D.C., Woodfork D.W. ARTEMIS The First Mission to the Lunar Libration Orbits. In: *Conference: Internation Symposium on Space Flight Dynamics*. 2009. Available from URL: https://www.researchgate.net/publication/235990349. Accessed February 04, 2025.
2. Li C., Hu H., Yang M.-F., et al. Characteristics of the lunar samples returned by the Chang'E-5 mission. *Natl. Sci. Rev.* 2022;9(2):nwab188. https://doi.org/10.1093/nsr/nwab188
3. Li C., Hu H., Yang M.-F., et al. Nature of the lunar far-side samples returned by the Chang'E-6 mission. *Natl. Sci. Rev.* 2024;11(11):nwae328. https://doi.org/10.1093/nsr/nwae328
4. Mathavaraj S., Negi K. Chandrayaan-3 Trajectory Design: Injection to Successful Landing. *J. Spacecraft Rockets*. 2025;62(1):159–166. https://doi.org/10.2514/1.A35980
5. Kanu N.J., Gupta E., Verma N.J. An insight into India's Moon mission – Chandrayan-3: The first nation to land on the southernmost polar region of the Moon. *Planet. Space Sci.* 2024;242(5):105864. https://doi.org/10.1016/j.pss.2024.105864
6. Zelenyi L.M., Mitrofanov I.G., Tret'yakov V.I., Litvak M.L., Kalashnikov D.V., Surov A.V., Prokhorov V.G. Scientific program for the study of the spacecraft "Luna-25". In: *Automatic Spacecraft of the New Generation "Luna-25" – from Research to the Development of Lunar Resources*: in 2 v. Khimki; 2023. P. 8–28 (in Russ.). https://elibrary.ru/lggmqz
7. Lidov M.L. The evolution of orbits of artificial satellites of planets under the action of gravitational perturbations of external bodies. *Planet. Space Sci*. 1962;9(10):719–759. https://doi.org/10.1016/0032-0633(62)90129-0
   [Original Russian Text: Lidov M.L. The evolution of orbits of artificial satellites of planets under the action of gravitational perturbations of external bodies. *Iskusstvennye Sputniki Zemli*. 1961;8:5–45 (in Russ.).]
8. Kozai Y. Secular perturbations of asteroids with high inclination and eccentricity. *The Astronomical Journal*. 1962;67(9):591–598.
9. Vashkov'yak M.A., Teslenko N.M. Refined model for the evolution of distant satellite orbits. *Astron. Lett.* 2009;35(12):850–865. https://doi.org/10.1134/S1063773709120056
   [Original Russian Text: Vashkov'yak M.A., Teslenko N.M. Refined model for the evolution of distant satellite orbits. *Pis'ma v Astronomicheskii zhurnal.* 2009;35(12):934–950 (in Russ.). https://elibrary.ru/kygisd]
10. Vashkov'yak M.A. Constructive analytical solution of the evolution hill problem. *Sol. Syst. Res.* 2010;44(6):527–540. https://doi.org/10.1134/S0038094610060067
    [Original Russian Text: Vashkov'yak M.A. Constructive analytical solution of the evolution hill problem. *Astronomicheskii Vestnik.* 2010;44(6):560–573 (in Russ.). https://elibrary.ru/nbsuhf]
11. Lidov M.L. On the approximate analysis of the evolution of artificial satellite orbits. In: *Problemy dvizheniya iskusstvennykh nebesnykh tel* (*Problems of the Motion of Artificial Celestial Bodies*). Moscow: USSR Academy of Sciences; 1963. P. 119–134 (in Russ.).
12. Ely T.A. Stable Constellations of Frozen Elliptical Inclined Lunar Orbits. *J. Astronaut. Sci*. 2005;53(3):301–316. https://doi.org/10.1007/BF03546355

13. Goossens S., Sabaka T.J., Wieczorek M.A., Neumann G.A., Mazarico E., Lemoine F.G., et al. High-resolution gravity field models from GRAIL data and implications for models of the density structure of the Moon's crust. *Journal of Geophysical Research: Planets* (*JGR Planets*). 2020;125(2):e2019JE006086. https://doi.org/10.1029/2019JE006086
14. Folta D.C., Pavlak T.A., Haapala A.F., Howell K.C., Woodard M.A. Earth–Moon libration point orbit stationkeeping: Theory, modeling, and operations. *Acta Astronautica*. 2013;94(1):421–433. https://doi.org/10.1016/j.actaastro.2013.01.022
15. Jadala G., Meedinti G.N., Delhibabu R. Satellite Orbit Prediction Using a Machine Learning Approach. *ICAI Workshops*. 2022. P. 28–46.
16. Ovchinnikov M., Shirobokov M., Trofimov S. Lunar Satellite Constellations in Frozen Low Orbits. *Aerospace*. 2024;11(11):918. https://doi.org/10.3390/aerospace11110918
17. Aksenov E.P. *Spetsial'nye funktsii v nebesnoi mekhanike* (*Special Functions in Celestial Mechanics*). Moscow: Nauka; 1986, 320 p. (In Russ.).
18. Duboshin G.N. *Nebesnaya mekhanika. Osnovnye zadachi i metody* (*Celestial Mechanics. Basic Problems and Methods*). Moscow: Nauka; 1975, 800 p. (In Russ.).
19. Murray C., Dermott S. *Dinamika Solnechnoi sistemy* (*Solar System Dynamics*); transl. from Engl. Moscow: Fizmatlit; 2010, 588 p. (In Russ.). ISBN 978-5-9221-1121-8
[Murray C.D., Dermott S.F. *Solar System Dynamics*. Cambridge University Press; 1999, 592 p.]
20. Vil'ke V.G. *Mekhanika sistem material'nykh tochek i tverdykh tel* (*Mechanics of Systems of Material Points and Rigid Bodies*). Moscow: Fizmatlit; 2013, 268 p. (In Russ.). ISBN 978-5-9221-1481-3

СПИСОК ЛИТЕРАТУРЫ

1. Woodard M., Folta D.C., Woodfork D.W. ARTEMIS The First Mission to the Lunar Libration Orbits. In: *Conference: Internation Symposium on Space Flight Dynamics*. 2009. URL: https://www.researchgate.net/publication/235990349. Дата обращения 04.02.2025. / Accessed February 04, 2025.
2. Li C., Hu H., Yang M.-F., et al. Characteristics of the lunar samples returned by the Chang'E-5 mission. *Natl. Sci. Rev*. 2022;9(2):nwab188. https://doi.org/10.1093/nsr/nwab188
3. Li C., Hu H., Yang M.-F., et al. Nature of the lunar far-side samples returned by the Chang'E-6 mission. *Natl. Sci. Rev*. 2024;11(11):nwae328. https://doi.org/10.1093/nsr/nwae328
4. Mathavaraj S., Negi K. Chandrayaan-3 Trajectory Design: Injection to Successful Landing. *J. Spacecraft Rockets*. 2025;62(1):159–166. https://doi.org/10.2514/1.A35980
5. Kanu N.J., Gupta E., Verma N.J. An insight into India's Moon mission – Chandrayan-3: The first nation to land on the southernmost polar region of the Moon. *Planet. Space Sci.* 2024;242(5):105864. https://doi.org/10.1016/j.pss.2024.105864
6. Зеленый Л.М., Митрофанов И.Г., Третьяков В.И., Литвак М.Л., Калашников Д.В., Суров А.В., Прохоров В.Г. Научная программа исследований космического аппарата «Луна-25». В кн.: *Автоматический космический аппарат нового поколения «Луна-25» – от исследования к освоению лунных ресурсов*: в 2 т. Химки: Научно-производственное объединение им. С.А. Лавочкина; 2023. С. 8–28. https://elibrary.ru/lggmqz
7. Лидов М.Л. Эволюция орбит искусственных спутников планет под действием гравитационных возмущений внешних тел. *Искусственные спутники Земли*. 1961;8:5–45.
8. Kozai Y. Secular perturbations of asteroids with high inclination and eccentricity. *The Astronomical Journal*. 1962;67(9):591–598.
9. Вашковьяк М.А., Тесленко Н.М. Уточненная модель эволюции далеких спутниковых орбит. *Письма в Астрономический журнал*. 2009;35(12):934–950. https://elibrary.ru/kygisd
10. Вашковьяк М.А. Конструктивно-аналитическое решение эволюционной задачи Хилла. *Астрономический вестник*. 2010;44(6):560–573. https://elibrary.ru/nbsuhf
11. Лидов М.Л. О приближенном анализе эволюции орбит искусственных спутников. В кн.: *Проблемы движения искусственных небесных тел*. М.: Изд-во АН СССР; 1963. С. 119–134.
12. Ely T.A. Stable Constellations of Frozen Elliptical Inclined Lunar Orbits. *J. Astronaut. Sci*. 2005;53(3):301–316. https://doi.org/10.1007/BF03546355
13. Goossens S., Sabaka T.J., Wieczorek M.A., Neumann G.A., Mazarico E., Lemoine F.G., et al. High-resolution gravity field models from GRAIL data and implications for models of the density structure of the Moon's crust. *Journal of Geophysical Research: Planets* (*JGR Planets*). 2020;125(2):e2019JE006086. https://doi.org/10.1029/2019JE006086
14. Folta D.C., Pavlak T.A., Haapala A.F., Howell K.C., Woodard M.A. Earth–Moon libration point orbit stationkeeping: Theory, modeling, and operations. *Acta Astronautica*. 2013;94(1):421–433. https://doi.org/10.1016/j.actaastro.2013.01.022
15. Jadala G., Meedinti G.N., Delhibabu R. Satellite Orbit Prediction Using a Machine Learning Approach. *ICAI Workshops*. 2022. P. 28–46.
16. Ovchinnikov M., Shirobokov M., Trofimov S. Lunar Satellite Constellations in Frozen Low Orbits. *Aerospace*. 2024;11(11):918. https://doi.org/10.3390/aerospace11110918
17. Аксенов Е.П. *Специальные функции в небесной механике*. М.: Наука; 1986, 320 с.
18. Дубошин Г.Н. *Небесная механика. Основные задачи и методы*. М.: Наука; 1975, 800 с.
19. Мюррей К., Дермотт С. *Динамика Солнечной системы*: пер. с англ. М.: Физматлит; 2010, 588 с. ISBN 978-5-9221-1121-8
20. Вильке В.Г. *Механика систем материальных точек и твердых тел*. М.: Физматлит; 2013, 268 с. ISBN 978-5-9221-1481-3

About the Authors

Olga V. Meshkova, Master Student, Department of Higher Mathematics, Institute of Artificial Intelligence, MIREA – Russian Technological University (78, Vernadskogo pr., Moscow, 119454 Russia). E-mail: oxn.lar5@yandex.ru. https://orcid.org/0009-0002-2917-1025

Albina V. Shatina, Dr. Sci. (Phys.-Math.), Docent, Head of the Department of Higher Mathematics, Institute of Artificial Intelligence, MIREA – Russian Technological University (78, Vernadskogo pr., Moscow, 119454 Russia). E-mail: shatina_av@mail.ru. Scopus Author ID 6506958326, RSCI SPIN-code 8714-6450, https://orcid.org/0000-0001-5016-5899

Об авторах

Мешкова Ольга Вячеславовна, магистрант, кафедра высшей математики, Институт искусственного интеллекта, ФГБОУ ВО «МИРЭА – Российский технологический университет» (119454, Россия, Москва, пр-т Вернадского, д. 78). E-mail: oxn.lar5@yandex.ru . https://orcid.org/0009-0002-2917-1025

Шатина Альбина Викторовна, д.ф.-м.н., доцент, заведующая кафедрой высшей математики, Институт искусственного интеллекта, ФГБОУ ВО «МИРЭА – Российский технологический университет» (119454, Россия, Москва, пр-т Вернадского, д. 78). E-mail: shatina_av@mail.ru. Scopus Author ID 6506958326, SPIN-код РИНЦ 8714-6450, https://orcid.org/0000-0001-5016-5899

Translated from Russian into English by Lyudmila O. Bychkova
Edited for English language and spelling by Dr. David Mossop

Mathematical modeling

Математическое моделирование

UDC 004.8, 004.852
https://doi.org/10.32362/2500-316X-2026-14-1-82-90
EDN KCUBAG

RESEARCH ARTICLE

Feature space transformation in the support vector method

Aleksey V. Fedorov [@], **Denis V. Parfenov**

MIREA – Russian Technological University, Moscow, 119454 Russia
[@] *Corresponding author, e-mail: fedorov_av@mirea.ru*

• **Submitted:** 22.05.2025 • **Revised:** 02.07.2025 • **Accepted:** 10.11.2025

Abstract

Objectives. This study focuses on the development and investigation of a generalized nonlinear Support Vector Machine (SVM) method incorporating an adaptive transformation of the feature space. Its aim is to improve computational efficiency while maintaining high classification accuracy. The binary classification problem is used as a case study. The main objective of the research is to quantitatively evaluate the performance of the proposed approach when compared to classical SVM models using fixed kernel functions, and to analyze how the transformation parameters affect classification quality.

Methods. The proposed approach involves a preliminary transformation of the input data using a learnable nonlinear mapping with a fixed structure. This mapping is implemented as a composition of elementary functions and is parameterized by a limited number of trainable weights which allows control over model complexity. A linear SVM with L2 regularization is applied after the transformation. The model is trained using conventional, unconstrained numerical optimization methods. The classification quality is evaluated using the Accuracy metric averaged over 10-fold cross-validation. The work also studies the behavior of the model with varying feature space dimensionality. In addition, computational complexity is analyzed in terms of the number of operations and inference time required on test datasets.

Results. Numerical experiments demonstrate that the proposed model significantly reduces classification time when compared to a polynomial-kernel SVM, while maintaining a comparable level of accuracy. The runtime analysis confirms that the proposed approach scales much better than traditional kernel methods. At the same time, the structure of the model remains interpretable and can be further adapted to the specifics of the application domain.

Conclusions. The method developed provides an efficient alternative to traditional kernel-based algorithms. Through the use of a parameterized transformation of the feature space, the method enables adaptability, interpretability, and scalability, making it promising for practical applications in machine learning tasks.

Keywords: classification, feature space transformation, nonlinear mapping, nonlinear support vector machine, kernel functions, computational complexity

For citation: Fedorov A.V., Parfenov D.V. Feature space transformation in the support vector method. *Russian Technological Journal.* 2026;14(1):82–90. https://doi.org/10.32362/2500-316X-2026-14-1-82-90, https://www.elibrary.ru/KCUBAG

Financial disclosure: The authors have no financial or proprietary interest in any material or method mentioned.

The authors declare no conflicts of interest.

НАУЧНАЯ СТАТЬЯ

Трансформация пространства признаков в методе опорных векторов

А.В. Федоров [@], **Д.В. Парфенов**

МИРЭА – Российский технологический университет, Москва, 119454 Россия
[@] *Автор для переписки, e-mail: fedorov_av@mirea.ru*

• **Поступила:** 22.05.2025 • **Доработана:** 02.07.2025 • **Принята к опубликованию:** 10.11.2025

Резюме

Цели. Работа посвящена разработке и исследованию обобщенного нелинейного метода опорных векторов (support vector machine, SVM) с использованием адаптивной трансформации пространства признаков, направленного на улучшение вычислительной эффективности при сохранении высокого качества классификации. В качестве задачи-примера рассматривается двухклассовая классификация. Целью исследования является количественная оценка производительности предложенного подхода в сравнении с классическими SVM-моделями, использующими фиксированные ядровые функции, а также изучение влияния параметров трансформации на качество классификации.

Методы. Предлагается модифицированный подход, при котором входные данные предварительно преобразуются с помощью обучаемого нелинейного отображения фиксированной структуры. Это отображение реализуется в виде композиции элементарных функций и параметризуется ограниченным числом обучаемых весов, что обеспечивает контроль над сложностью модели. После трансформации применяется линейный SVM с L2-регуляризацией. Для обучения модели используются стандартные методы численной оптимизации без ограничений. Качество классификации оценивается с помощью метрики точности (Accuracy), усредненной по результатам 10-кратной перекрестной валидации. Рассматривается поведение модели при изменении размерности признакового пространства. Проводится анализ вычислительной сложности по числу операций и времени применения модели на тестовых выборках.

Результаты. Численные эксперименты показали, что предложенная модель позволяет существенно сократить время классификации по сравнению с SVM с полиномиальным ядром, обеспечивая при этом сопоставимое качество. Анализ временных затрат подтвердил, что предложенный подход масштабируется значительно лучше, чем классические ядровые методы. При этом структура модели сохраняет интерпретируемость и может быть дополнительно адаптирована под особенности предметной области.

Выводы. Разработанный метод представляет собой эффективную альтернативу классическим ядровым алгоритмам. Благодаря параметризуемому отображению признакового пространства он обеспечивает адаптивность, интерпретируемость и масштабируемость, что делает его перспективным для практического применения в задачах машинного обучения.

Ключевые слова: классификация, преобразование признакового пространства, нелинейное отображение, нелинейный метод опорных векторов, функции ядра, вычислительная сложность

Для цитирования: Федоров А.В. Парфенов Д.В. Трансформация пространства признаков в методе опорных векторов. *Russian Technological Journal*. 2026;14(1):82–90. https://doi.org/10.32362/2500-316X-2026-14-1-82-90, https://www.elibrary.ru/KCUBAG

Прозрачность финансовой деятельности: Авторы не имеют финансовой заинтересованности в представленных материалах или методах.

Авторы заявляют об отсутствии конфликта интересов.

INTRODUCTION

A fundamental problem in machine learning (ML) is addressing the challenge of classifying linearly inseparable data. A traditional method for tackling this involves employing a generalized nonlinear support vector machine (SVM) with kernel functions. These kernels facilitate the computation of scalar products in a transformed space which offers improved geometric properties for class separation [1]. However, this approach has certain limitations. The commonly used kernels often have a limited number of parameters, restricting their flexibility. Furthermore, the variety of kernels utilized in practice is relatively small, which reduces the adaptability of the model.

The paper introduces an alternative approach which differs from traditional kernel methods by enabling the direct optimization of nonlinear transformation parameters within the feature space during SVM training. The proposed transformation is divided into two stages. Initially, the input features undergo a linear mapping defined by a matrix containing trainable coefficients. Subsequently, one-dimensional nonlinear transformations, executed through polynomials with trainable coefficients, are applied to each component of the resulting vector. This approach offers the flexibility to tailor the characteristic space to specific data needs while preserving high computational efficiency.

The primary benefit of the proposed model lies in its considerable reduction in computational costs when utilizing the pre-trained model, compared to approaches reliant on kernel functions. In traditional SVMs which use kernel functions, the computational complexity depends heavily on the number of support vectors. In real-world scenarios these can be quite large, thereby substantially increasing classification time. In contrast, the proposed approach performs data transformation with a fixed computational complexity determined solely by the dimensions of the input and output spaces and the selected polynomial order. This feature makes the method especially efficient for processing large datasets.

Recent efforts have focused on enhancing the effectiveness and flexibility of classification techniques in ML applications. For example, study [2] presents a robust SVM model enhanced with a customized optimization approach to ensure resistance against noise in the data. Research [3] establishes the theoretical basis for multiscale, adaptive feature extraction, proposing it as a viable alternative to traditional kernel-based approaches. Study [4] investigates the geometric interpretation of adaptable feature transformations in neural networks, in line with the idea of a parametrizable representation of feature spaces. Furthermore, study [5] introduces a method involving the diagonal expansion of parameters within a Hilbert space endowed with a reproducing kernel. This facilitates the simultaneous training of both the feature structures and the kernel parameters. Finally, the adaptive law-based transformation (ALT) method discussed in [6] is designed for adaptive feature transformations, specifically targeting time series classification. It bears conceptual similarities to the approach presented in this paper.

1. TRANSFORMATION OF THE FEATURE SPACE

As previously mentioned, each object in the original dataset, denoted as $\mathbf{x} \in \mathbb{R}^n$ (where n represents the dimensionality of the original space), is transformed through the $m \times n$ matrix $\mathbf{A}$. The resultant vector $\tilde{\mathbf{x}} \in \mathbb{R}^m$ is then calculated using the following equation:

$$\tilde{\mathbf{x}} = \mathbf{A}\mathbf{x} = \begin{bmatrix} a_{11} & a_{12} & \dots & a_{1n} \\ a_{21} & a_{22} & \dots & a_{2n} \\ \dots & \dots & \dots & \dots \\ a_{m1} & a_{m2} & \dots & a_{mn} \end{bmatrix} \begin{bmatrix} x_1 \\ x_2 \\ \dots \\ x_n \end{bmatrix}.$$

The dimension m, chosen by the user, specifies the number of features in the transformed space, influencing whether the data space is expanded or reduced. Matrix $\mathbf{A}$ contains trainable parameters, enabling adjustments to align the linear transformation with the specific data structure.

For each element in the resultant vector $\tilde{\mathbf{x}} = (\tilde{x}_1, \tilde{x}_2, ..., \tilde{x}_m)^{\mathrm{T}}$, a nonlinear function is applied in the form of polynomial $p_i(\tilde{x}_i)$ of degree d, where $i = \overline{1,m}$. The resultant vector, $\tilde{\tilde{\mathbf{x}}} \in \mathbb{R}^m$, is then calculated as follows:

$$\tilde{\tilde{\mathbf{x}}} = \begin{bmatrix} p_1(\tilde{x}_1) \\ p_2(\tilde{x}_2) \\ \dots \\ p_3(\tilde{x}_m) \end{bmatrix}.$$

The polynomials $p_i(\cdot)$ may vary for each coordinate, providing high flexibility within the model. The general form of polynomial $p_i(\tilde{x})$ is defined as follows:

$$p_i(\tilde{x}) = c_{i1}\tilde{x} + c_{i2}\tilde{x}^2 + \dots + c_{id}\tilde{x}^d,$$

wherein c_{ij} represents trainable parameters, and d denotes the fixed-degree polynomial.

The inclusion of nonlinear functions enables the adjustment of the feature space geometry, facilitating a more effective separation of classes. A key aspect of the proposed classifier model lies in the simultaneous training of both the feature space transformation parameters and the support vector method.

The objective of training the model can be outlined as follows:

$$\frac{1}{2}\|\mathbf{w}\|^2 + C\sum_{i=1}^{N}\max\left(1 - y_i\left(\left\langle \mathbf{w}, \Phi_{\mathbf{A},\mathbf{P}}(\mathbf{x}_i)\right\rangle + b\right), 0\right)^2 \to \min_{\mathbf{w},b,\mathbf{A},\mathbf{P}}.$$

Here, $\mathbf{x}_i \in \mathbb{R}^n$ represents the input vectors; $y_i \in \{-1; +1\}$ are the associated class labels. $\Phi_{\mathbf{A},\mathbf{P}}(\mathbf{x})$ represents the original vector $\mathbf{x}$ after the linear transformation $\mathbf{A}$ and the application of polynomial functions p_i; $\mathbf{A}$ and $\mathbf{P}$ are transformation parameters for the linear and polynomial operations, respectively; $\mathbf{w}$ and b are linear classifier parameters. C represents the penalty weight assigned to deviations, while N indicates the total number of training samples included in the dataset.

The proposed approach incorporates L2 regularization [7, 8], crucial for stabilizing the training process and mitigating the risk of overtraining. This regularization is applied not only to the parameters of the linear transformation matrix but also to the coefficients of the polynomial mapping. By employing L2 regularization, the growth of weight norms is restricted, thereby decreasing the probability of overtraining. Numerical experiments have demonstrated that this regularization technique supports effective learning outcomes. Consequently, the objective function has the following form:

$$\sum_{i=1}^{N}\max\left(1 - y_i\left(\left\langle \mathbf{w}, \Phi_{\mathbf{A},\mathbf{P}}(\mathbf{x}_i)\right\rangle + b\right), 0\right)^2 + \\ + \frac{1}{2C}\|\mathbf{w}\|^2 + \lambda_1\|\mathbf{A}\|^2 + \lambda_2\|\mathbf{P}\|^2 \to \min_{\mathbf{w},b,\mathbf{A},\mathbf{P}}, \quad (1)$$

wherein λ_1 and λ_2 are regularization coefficients.

In order to address problem (1), an optimization method without BFGS[1] constraints is utilized [9], provided through the *Optim.jl* package[2]. The gradients of the objective function are computed using automatic differentiation based on dual numbers [10, 11], facilitated by the *ForwardDiff.jl* package.

2. BENCHMARKING

Benchmarking involves evaluating the performance of the classifier using datasets from the Curated Classification Benchmark OpenML-CC18 [12]. These datasets are specifically curated for comparing various ML algorithms. Table 1 provides an overview of the datasets utilized, highlighting their key attributes such as the number of objects, the dimension of the feature space, and concise descriptive details.

All tasks involve binary classification, meaning each task contains exactly two categories.

In order to evaluate model performance, 10-fold cross-validation [13] is implemented, ensuring a more dependable measurement of classifier quality.

Table 1. Overview of dataset characteristics

No.	Dataset	Number of objects	Dimension	Summary
1	blood-transfusion-service-center	748	4	Prediction of blood donation behavior in the future is required (2 categories)
2	phoneme	5404	5	Classification of speech sounds into two categories is required (2 categories)
3	diabetes	768	8	Detection of diabetes presence or absence is required (2 categories)
4	qsar-biodeg	1055	41	Prediction of chemical biodegradability is required (2 categories)
5	kc1	2109	21	Detection of the software module errors is required (2 categories)
6	pc1	1109	21	The task is similar to kc1 that involves classifying software components into “with errors” and “no errors” categories (2 categories)

[1] The Broyden–Fletcher–Goldfarb–Shanno algorithm.

[2] *Optim.jl Documentation. Optim.jl* is Julia optimization library. https://julianlsolvers.github.io/Optim.jl/stable/. Accessed July 07, 2025.

Employing multiple datasets facilitates testing the ability of the model to generalize across diverse inputs. Additionally, using a standardized test dataset ensures comparability with existing methods and published research, providing an objective analysis of the model's strengths and weaknesses.

Prior to training the classifier, all data is subjected to preliminary normalization processes, such as centering and scaling. These steps are essential for enhancing model stability and improving its generalization capabilities. Combined with 10-fold cross-validation and testing across diverse samples, these measures ensure an objective and reliable evaluation of the classifier's quality (Accuracy) [14].

The results of testing this classifier model with adaptive feature space transformation are presented in Table 2.

The proposed model is evaluated against the SVM method utilizing a polynomial kernel, as referenced in studies [15, 16]. In the case of SVM with polynomial kernels, classification takes place within an implicitly defined higher-dimensional space, in which the scalar product is computed directly via the kernel function, thus eliminating the need for explicit construction of the feature transformation. Conversely, the proposed method differentiates itself by explicitly constructing a nonlinear mapping of the original space. This is then subjected to linear separation through the support vector method.

It should be noted that SVM with a polynomial kernel is often regarded as a viable benchmark model. This is because, while the polynomial kernel typically delivers slightly lower classification performance when compared to more advanced kernels such as the radial basis function (RBF), it offers notable computational efficiency. This makes it a practical trade-off between classification accuracy and computational demands. The proposed approach achieves performance comparable to that of the SVM with a polynomial kernel, while simultaneously offering even greater computational efficiency.

Evaluation tests have been conducted where the parameters of the polynomial kernel are selected using a random search strategy over a predefined grid of values. The parameter selection process employs 10-fold cross-validation, ensuring careful optimization of the kernel hyperparameters and facilitating an accurate comparison across models. The test results for the SVM with a polynomial kernel are presented in Table 3.

Table 2. Classifier model testing results

No.	Dataset	Output space dimension (m)	Polynomial degree (d)	Accuracy, %
1	blood-transfusion-service-center	4	3	79.29
2	phoneme	5	3	83.33
3	diabetes	8	3	77.47
4	qsar-biodeg	41	3	85.97
5	kc1	21	3	84.45
6	pc1	21	3	92.24

Table 3. Testing results for SVM with a polynomial kernel

No.	Dataset	Degree (d)	Accuracy, %	Number of support vectors
1	blood-transfusion-service-center	3	77.14	367
2	phoneme	3	83.81	2,074
3	diabetes	2	76.95	397
4	qsar-biodeg	2	86.24	429
5	kc1	3	84.69	643
6	pc1	3	93.06	158

Table 4. Accuracy comparison between the proposed model and SVM with a polynomial kernel

No.	Dataset	Accuracy, %	
		Offered model	Polynomial kernel
1	blood-transfusion-service-center	79.29	77.14
2	phoneme	83.33	83.81
3	diabetes	77.47	76.95
4	qsar-biodeg	85.97	86.24
5	kc1	84.45	84.69
6	pc1	92.24	93.06

Table 4 presents a comparison of the classification accuracy of the proposed model and the SVM with a polynomial kernel on each dataset.

As shown in Table 4, the proposed classifier achieves an accuracy level similar to that of the SVM with a polynomial kernel. This highlights the flexibility of the model and its capacity to adapt effectively to the dataset characteristics.

3. ANALYSIS OF COMPUTATIONAL COMPLEXITY

In many ML tasks, the focus extends beyond just achieving high model accuracy: it also evaluates its computational complexity during classification. This becomes particularly critical in scenarios which demand rapid data processing, such as real-time systems used for object detection, data flow analysis, or diagnostics. Additionally, limited computational resources pose a significant challenge, especially when working with low-power devices such as mobile phones, embedded systems, or microcontrollers. These devices often lack sufficient memory, energy, or processing capabilities, making complex models impractical for deployment. Therefore, when selecting a model, it is crucial to account for its complexity and performance relative to the capabilities of the targeted hardware.

After training the proposed model, the resulting classifier (decision function) is as follows:

$$f(\mathbf{x}) = \left\langle \mathbf{w}, \Phi_{\mathbf{A},\mathbf{P}}(\mathbf{x}) \right\rangle + b.$$

The transformation $\Phi_{\mathbf{A},\mathbf{P}}(\mathbf{x})$ can be reduced to matrix multiplication and polynomial component transformation. Multiplying by matrix $\mathbf{A}$ involves $n \times m$ multiplication operations and $(n-1) \times m$ addition operations. Applying the polynomials $p_i(x)$ necessitates $d \times m$ multiplications along with $(d-1) \times m$ additions. Additionally, the shift dot product entails m more multiplication operations and m added additions.

Consequently, the classification of a single object involves $m \times (n + d + 1)$ multiplication operations and $m \times (n + d - 1)$ addition operations. Thus the computational complexity of the classification process remains independent of the number of support vectors. This represents a fundamental distinction between the proposed approach and the classical SVM, reliant on kernel functions and resolving the dual problem [17]. Leveraging an explicit parameterized features transformation $\Phi_{\mathbf{A},\mathbf{P}}(\mathbf{x})$, eliminates the need to transition to the dual problem, a hallmark of kernel tricks [15, 18]. This approach substantially reduces computational complexity, particularly in scenarios where resolving a dual problem results in a large number of support vectors, a common occurrence with noisy or high-dimensional datasets.

By applying kernel transformation, the dual minimization problem is addressed, leading to the following decision function:

$$f(\mathbf{x}) = \sum_{i=1}^{l} \alpha_i k(\mathbf{x}_i, \mathbf{x}) + b,$$

where $k(\mathbf{x}_i, \mathbf{x})$ represents the kernel function, while $\mathbf{x}_i$ denotes the support vectors.

The polynomial kernel is expressed as follows:

$$k(\mathbf{x}, \mathbf{x}') = \left(\left\langle \mathbf{x}, \mathbf{x}' \right\rangle + c\right)^d,$$

where c and d refer to the kernel parameters.

The calculation of the polynomial kernel involves $(n + d - 1) \times l$ multiplication operations when dealing with low powers ($d \in \{2; 3\}$), as well as $n \times l$ addition operations.

Here, n represents the space dimensionality (the length of vector x), d denotes the degree of the polynomial kernel, and l refers to the number of support vectors. In order to make a classification decision, the algorithm sums over all reference vectors, entailing l multiplication operations (where the kernel function value is multiplied by the coefficient α_i) and $l + 1$ addition operations. Consequently, the total number of basic operations required for classification is $l \times (n + d)$ multiplication operations and $l \times (n + 1) + 1$ addition operations.

In practical scenarios, the number of support vectors, l, is typically substantial, resulting in a significant rise in computational requirements. In order to preliminarily analyze the computational complexity of the proposed feature space transformation method in comparison to the conventional approach based on kernel functions, the following commonly observed relationships can be considered:

$$l \gg n, l \gg m, l \gg d, m \sim n, d < n.$$

An approach utilizing kernel functions typically demands considerably more calculations for classification purposes at the output stage. The findings are consolidated in Table 5, which outlines the total number of elementary operations necessary for object classification across all datasets.

The results demonstrate that the proposed model performs classification with substantially fewer arithmetic operations, such as additions and multiplications. Consequently, this method is more computationally efficient than when compared to using a polynomial kernel.

4. MODEL PERFORMANCE

The experiment evaluates the time taken to classify a single object from each dataset. The *BenchmarkTools.jl* package[3] is utilized to ensure precise runtime measurement, since it reduces the influence of background processes and provides an accurate

Table 5. Analysis of computational complexity between the proposed model and SVM with a polynomial kernel

No.	Dataset	Number of operations	
		Offered model	Polynomial kernel
1	blood-transfusion-service-center	56	4405
2	phoneme	80	29037
3	diabetes	176	7544
4	qsar-biodeg	3608	36466
5	kc1	1008	29579
6	pc1	1008	7269

Table 6. Performance comparison between the proposed model and SVM with a polynomial kernel

No.	Dataset	Performance, μs	
		Offered model	Polynomial kernel
1	blood-transfusion-service-center	0.356	7.75
2	phoneme	0.384	45.1
3	diabetes	0.422	11.3
4	qsar-biodeg	1.94	21.8
5	kc1	0.822	22.2
6	pc1	0.822	5.25

[3] *BenchmarkTools.jl* Documentation. *BenchmarkTools.jl* Manual. https://juliaci.github.io/BenchmarkTools.jl/stable/manual/. Accessed July 07, 2025.

estimation of computational costs. The measurements are conducted on pre-trained models, with classification times recorded in microseconds. The median runtime across all runs is chosen as the key metric, since it is less affected by outliers and effectively represents the typical model performance. A summary of the results is presented in Table 6 which facilitates a comparison of the classification speeds between the proposed model and the SVM with a polynomial kernel.

The experimental findings indicate that the proposed model provides significantly improved computational performance than when compared to an SVM using a polynomial kernel. For all datasets tested, the time taken to classify a single instance is noticeably shorter in the proposed model. This is in line with theoretical predictions regarding its computational complexity. In contrast to the polynomial kernel, which has a classification complexity depending on the number of support vectors, the proposed method has a fixed computational complexity, making it substantially more efficient for processing large datasets. Analysis of median runtime values reveals that this increase in classification speed is achieved without a notable decline in performance quality, thus positioning the proposed approach as a viable and competitive alternative to kernel-based techniques. Therefore, the experimental findings affirm that the proposed model presents a promising solution for tasks demanding high classification speed while preserving accuracy.

Additional experiments have been conducted using synthetic data, in order to investigate how classification time varies with the dimensionality of the feature space. For these experiments, the linear transformation matrix $\mathbf{A}$ is selected as a square matrix with the same number of rows and columns ($m = n$). This study allows the impact of dimensionality on computation time to be evaluated. The experiments are conducted on generated datasets with varying dimensions, and for each scenario, the median time required for classification of a single object is recorded. The results are visualized (see Figure) to show the increase in computation time as the dimension of the feature space increases.

The results demonstrate that for dimensions $n \leq 600$, the classification time grows at a moderate pace. This suggests that the proposed method can be effectively applied even to problems involving high-dimensional features. Consequently, the model maintains computational efficiency at medium to moderately high dimensions, making it well-suited for a broad spectrum of practical applications.

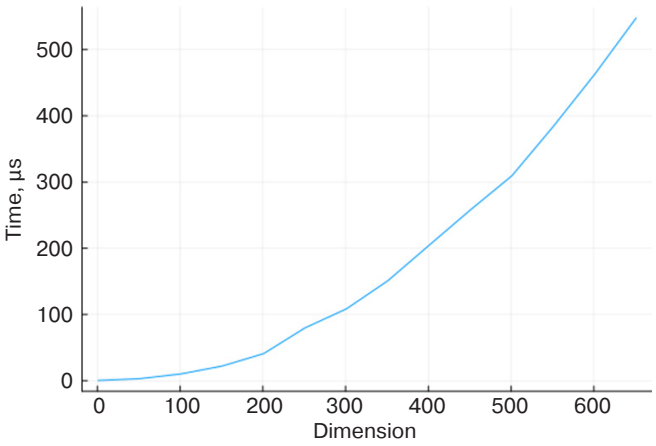

Figure. Classification time versus dimension plot

CONCLUSIONS

The paper introduces a method for transforming the feature space, aimed at effectively classifying linearly inseparable data. Unlike traditional kernel methods, this approach employs an explicit nonlinear feature mapping, with parameters optimized during the training process.

In order to evaluate the method performance, numerical experiments have been conducted. These include comparisons with classical kernel techniques in terms of classification accuracy and computational efficiency. The results demonstrate that the proposed model significantly outperforms SVM with a polynomial kernel in classification speed while maintaining comparable classification quality. Further analysis of runtime dependency on feature space dimensions reveals that for dimensions up to $n \leq 600$, the increase in classification time remains moderate. This indicates that the method is well-suited for handling high-dimensional data effectively.

In summary, the method developed presents a computationally efficient alternative to conventional kernel methods, offering a practical solution for tasks which demand high processing speed without compromising classification accuracy.

Authors' contributions

A.V. Fedorov—development of the model, its detailed study, and formulation of part of the method's idea.

D.V. Parfenov—problem statement, formulation of part of the method's idea, and overall supervision of the work.

REFERENCES

1. Vapnik V. *Statistical Learning Theory*. New York: Wiley; 1998, 736 p. ISBN 978-0-471-03003-4
2. Maggioni F., Spinelli A. A novel robust optimization model for nonlinear Support Vector Machine. *Computers & Operations Research*. 2024;157:105059.
3. Rubin N., Fischer K., Lindner J., Dahmen D., Seroussi I., Ringel Z., Krüger M., Helias M. From Kernels to Features: A Multi-Scale Adaptive Theory of Feature Learning. *arXiv* preprint arXiv:2402.03210. 2024. https://doi.org/10.48550/arXiv.2502.03210
4. LeJeune D., Alemohammad S. An Adaptive Tangent Feature Perspective of Neural Networks. In: *Proceedings of the 37th International Conference on Machine Learning* (*ICML*). 2024. Available from URL: https://proceedings.mlr.press/v234/lejeune24a/lejeune24a.pdf. Accessed July 07, 2025.
5. Li Y., Lin Q. Diagonal Over-parameterization in Reproducing Kernel Hilbert Spaces as an Adaptive Feature Model: Generalization and Adaptivity. *arXiv* preprint arXiv:2501.08679. 2025. https://arxiv.org/abs/2501.08679
6. Kurbucz M.T., Benkő Z., Varga L., et al. Adaptive Law-Based Transformation (ALT): A Fast and Transparent Feature Transformation Method for Time Series Classification. *arXiv* preprint arXiv:2501.09217. 2025. https://arxiv.org/abs/2501.09217
7. Tikhonov A.N., Arsenin V.Y. *Solutions of Ill-Posed Problems*. Washington, D.C.: W.H. Freeman and Co.; 1977, 258 p.
8. Bishop C.M. *Pattern Recognition and Machine Learning*. New York: Springer; 2006, 738 p.
9. Fletcher R. *Practical Methods of Optimization*. New York: John Wiley & Sons; 1987, 464 p.
10. Baydin A.G., Pearlmutter B.A., Radul A.A., Siskind J.M. Automatic differentiation in machine learning: a survey. *Journal of Machine Learning Research* (*JMLR*). 2018;18(153):1–43.
11. Fisher J. Automatic differentiation with dual numbers. *arXiv* preprint arXiv:2201.00024.
12. Bischl B., Casalicchio G., Feurer M., Hutter F., Lang M., Mantovani R.G., van Rijn J.N., Vanschoren J. OpenML Benchmarking Suites. *arXiv* preprint arXiv:1708.03731v2 [stat.ML], 2019. https://arxiv.org/abs/1708.03731v2
13. Kohavi R. A Study of Cross-Validation and Bootstrap for Accuracy Estimation and Model Selection. In: *Proceedings of Fourteenth International Joint Conference on Artificial Intelligence* (*IJCAI*). 1995;14(2):1137–1143.
14. Labatut V., Cherifi H. Accuracy Measures for the Comparison of Classifiers. *arXiv* preprint arXiv:1207.3790. https://doi.org/10.48550/arXiv.1207.3790
15. Schölkopf B., Smola A.J. *Learning with Kernels*. Cambridge: MIT Press; 2002, 300 p.
16. Hofmann T., Schölkopf B., Smola A.J. Kernel Methods in Machine Learning. *Ann. Statist*. 2008;36(3):1171–1220. https://doi.org/10.1214/009053607000000677
17. Boser B.E., Guyon I.M., Vapnik V. A Training Algorithm for Optimal Margin Classifiers. In: *Proceedings of the Fifth Annual Workshop on Computational Learning Theory* (*COLT*). 1992. P. 144–152. https://doi.org/10.1145/130385.130401
18. Cortes C., Vapnik V. Support-Vector Networks. *Mach. Learn*. 1995;20(3):273–297. https://doi.org/10.1007/BF00994018

About the Authors

Aleksey V. Fedorov, Postgraduate Student, Higher Mathematics Department, Institute of Artificial Intelligence, MIREA – Russian Technological University (78, Vernadskogo pr., Moscow, 119454 Russia). E-mail: fedorov_av@mirea.ru. https://orcid.org/0009-0003-2314-7400

Denis V. Parfenov, Cand. Sci. (Eng.), Associate Professor, Higher Mathematics Department, Institute of Artificial Intelligence, MIREA – Russian Technological University (78, Vernadskogo pr., Moscow, 119454 Russia). E-mail: parfenov@mirea.ru. Scopus Author ID 57217119805, RSCI SPIN-code 7463-3220, https://orcid.org/0009-0004-0905-3827

Об авторах

Федоров Алексей Викторович, аспирант, кафедра высшей математики, Институт искусственного интеллекта, ФГБОУ ВО «МИРЭА – Российский технологический университет» (119454, Россия, Москва, пр-т Вернадского, д. 78). E-mail: fedorov_av@mirea.ru. https://orcid.org/0009-0003-2314-7400

Парфенов Денис Васильевич, к.т.н., доцент, кафедра высшей математики, Институт искусственного интеллекта, ФГБОУ ВО «МИРЭА – Российский технологический университет» (119454, Россия, Москва, пр-т Вернадского, д. 78). E-mail: parfenov@mirea.ru. Scopus Author ID 57217119805, SPIN-код РИНЦ 7463-3220, https://orcid.org/0009-0004-0905-3827

Translated from Russian into English by Kirill V. Nazarov
Edited for English language and spelling by Dr. David Mossop

Mathematical modeling

Математическое моделирование

UDC 621.372.8
https://doi.org/10.32362/2500-316X-2026-14-1-91-102
EDN KVXGWT

RESEARCH ARTICLE

Modeling of surface waves in photonic crystal structures with a refractive index profile decreasing with distance from the surface

Sergey E. Savotchenko [@]

MIREA – Russian Technological University, Moscow, 119454 Russia
[@] *Corresponding author, e-mail: savotchenkose@mail.ru*

• **Submitted:** 27.11.2024 • **Revised:** 30.05.2025 • **Accepted:** 18.11.2025

Abstract

Objectives. Identification of the propagation patterns of surface waves in inhomogeneous and nonlinear crystal structures using mathematical models is an important fundamental problem in condensed matter physics, specifically waveguide optics. Models of waveguide structures used to establish an exact analytical solution are of particular significance. The aim of this work is to carry out a theoretical study of transversely polarized surface electric waves propagating along a photonic crystal with a certain refractive index profile.

Methods. The methods of mathematical physics, analysis, differential equations, and theory of special functions, as well as physical models of waveguide optics, were used in this study.

Results. A generalized hyperbolic permittivity profile was proposed to describe the spatially inhomogeneous distribution of the optical properties of a photonic crystal. This profile has a wide range of possibilities for varying its shape, allowing it to be used for a wide range of problems not limited to waveguide optics. An exact analytical solution of the wave equation with the selected permittivity profile was found in terms of the Whittaker function. Frequent cases of the generalized profile for which exact analytical solutions were indicated were also considered. These are expressed through the Whittaker and Macdonald functions. The study also describes surface transverse electric waves, where the field is localized near the surface of the photonic crystal and decreases with distance from it. The solution obtained also describes waveguide modes in which the field decreases with distance from the surface of the photonic crystal with oscillations. New features of surface wave localization were established. These were caused by a change in the parameters of the generalized hyperbolic profile modeling the dependence of the permittivity. It was also established that the maximum intensity of the surface wave is located in the photonic crystal.

Conclusions. The results of the description of the characteristics of surface waves obtained expand the theoretical concepts of waveguide optics. They can be useful in predicting the optical properties of various photonic crystal structures, as well as in designing various waveguide structures with the required dispersion-optical characteristics.

Keywords: inhomogeneous optical media, photonic crystal, surface waves, guided waves, waveguide modes

For citation: Savotchenko S.E. Modeling of surface waves in photonic crystal structures with a refractive index profile decreasing with distance from the surface. *Russian Technological Journal.* 2026;14(1):91–102. https://doi.org/10.32362/2500-316X-2026-14-1-91-102, https://www.elibrary.ru/KVXGWT

Financial disclosure: The author has no financial or proprietary interest in any material or method mentioned.

The author declares no conflicts of interest.

НАУЧНАЯ СТАТЬЯ

Моделирование поверхностных волн в фотонных кристаллических структурах с профилем показателя преломления, убывающим с расстоянием от поверхности

С.Е. Савотченко @

МИРЭА – Российский технологический университет, Москва, 119454 Россия
@ *Автор для переписки, e-mail: savotchenkose@mail.ru*

• **Поступила:** 27.11.2024 • **Доработана:** 30.05.2025 • **Принята к опубликованию:** 18.11.2025

Резюме

Цели. Выявление закономерностей распространения поверхностных волн в неоднородных и нелинейных кристаллических структурах на основе математических моделей является важной фундаментальной задачей в физике конденсированного состояния, относящейся к волноводной оптике. При этом особой важностью обладают такие модели волноводных структур, в которых удается найти точное аналитическое решение. Цель работы – теоретическое изучение поверхностных электрических волн поперечной поляризации, распространяющихся вдоль фотонного кристалла с определенной формой профиля показателя преломления.

Методы. Применены методы математической физики, анализа, дифференциальных уравнений и теории специальных функций, а также физические модели волноводной оптики.

Результаты. Для описания пространственно неоднородного распределения оптических свойств фотонного кристалла предложен обобщенный гиперболический профиль диэлектрической проницаемости, который обладает широкими возможностями вариации формы, что позволяет его использовать для широкого круга задач, не ограничиваясь волноводной оптикой. Найдено точное аналитическое решение волнового уравнения для выбранного профиля диэлектрической проницаемости, выражаемое через функцию Уиттекера. Рассмотрены частые случаи обобщенного профиля, для которого указаны точные аналитические решения, выражаемые через функции Уиттекера и Макдональда. Описаны поверхностные поперечные электрические волны, поле в которых локализовано вблизи поверхности фотонного кристалла и убывает при удалении от нее. Полученное решение также описывает волноводные моды, в которых поле убывает при удалении от поверхности фотонного кристалла с осцилляциями. Выявлены новые особенности локализации поверхностных волн, обусловленные изменением параметров обобщенного гиперболического профиля, моделирующего зависимость диэлектрической проницаемости. Установлено, что в линейной поверхностной волне максимум интенсивности расположен в фотонном кристалле.

Выводы. Полученные результаты описания характеристик поверхностных волн расширяют теоретические представления волноводной оптики. Они могут быть полезны для прогнозирования оптических свойств различных фотонных кристаллических структур, а также при проектировании различных волноводных структур с требуемыми дисперсионно-оптическими характеристиками.

Ключевые слова: неоднородные оптические среды, фотонный кристалл, поверхностные волны, управляемые волны, волноводные моды

Для цитирования: Савотченко С.Е. Моделирование поверхностных волн в фотонных кристаллических структурах с профилем показателя преломления, убывающим с расстоянием от поверхности. *Russian Technological Journal*. 2026;14(1):91–102. https://doi.org/10.32362/2500-316X-2026-14-1-91-102, https://www.elibrary.ru/KVXGWT

Прозрачность финансовой деятельности: Автор не имеет финансовой заинтересованности в представленных материалах или методах.

Автор заявляет об отсутствии конфликта интересов.

INTRODUCTION

The study of the properties of surface waves in crystals, including photonic heterostructures, by mathematical modeling is an important fundamental problem [1]. Of special significance are such models of waveguide structures which can be used to find an exact analytical solution.

When describing real crystals,the refractive index (or permittivity) profile which models the optical inhomogeneity is selected, in such a way that it best fits the experimental data. For example [2], the photonic band gap in one-dimensional exponentially graded photonic crystals was investigated using an exponential profile, in order to represent the change in refractive index between the initial and final boundaries of the graded layer. An exponential refractive index profile was also used to describe the properties of a new photonic crystal resonator structure [3]. A simple hyperbolic refractive index profile in the form $n \sim 1/x$, characterizing its decrease with distance x from the contact surface, was used in the description of photonic band gaps [4, 5]. It was also used in a new approach to achieve improved sensitivity characteristics of photonic crystal [6].

The problem of finding exact solutions to the wave equation in nonlinear and inhomogeneous media is associated with the choice of the refractive index (permittivity) profile in inhomogeneous media [7]. Many exactly integrable refractive index profiles are known [8–11]. However, there remain a significant number of problems involving the definition of explicit analytical expressions for surface waves. These are described not by solutions of individual equations, but by solutions of boundary-value problems of systems of equations in certain domains which satisfy the conjugation conditions at their boundaries [12–14].

This paper presents the results of a theoretical study of surface waves, or more precisely, transversely polarized electric waves propagating along a photonic crystal with a specific refractive index profile. A new exact analytical solution was obtained for this spatial dependence, which is a generalization of the hyperbolic profile [15]. It was used to describe new types of linear and nonlinear surface waves. Linear surface waves for a simple hyperbolic permittivity profile $\varepsilon \sim 1/x$ were recently described [16]. Nonlinear surface waves propagating along the contact of an inhomogeneous medium with such a profile with a nonlinear medium with step nonlinearity were also described [17]. In this work, surface waves with step nonlinearity were studied using a generalized hyperbolic permittivity profile. Such a profile has wide possibilities for varying its shape which allows its use for a wide range of problems not limited to waveguide optics [18].

1. MODEL OF A PHOTONIC CRYSTAL STRUCTURE WITH A VARIABLE REFRACTIVE INDEX

Let us consider a photonic crystal in which the refractive index decreases with distance from its surface. Such a decreasing profile can be achieved by injecting ions of specially selected impurities [5]. Ion implantation technologies are well developed and allow the formation of an ion distribution which will provide the desired spatial refractive index profile [2–6]. This paper considers models of hetero-structures made of nonmagnetic materials consisting of a photonic crystal in contact with a medium with uniform optical characteristics.

Let the Ox axis be perpendicular to the surface of the photonic crystal which is assumed to be flat. Then the crystal surface coincides with the plane $x = 0$. The Oy and Oz axes are located in this plane. The spatial distributions of the optical properties of the photonic heterostructure under consideration over the surface are assumed to be uniform. They change only in the direction transverse to the surface.

Let us consider only transverse monochromatic waves propagating along the surface of the crystal with the electric field strength component:

$$E_y(x,z) = u(x)e^{i(knz-\omega t)}, \quad (1)$$

wherein $u(x)$ is the transverse profile of the electric field strength, $k = 2\pi/\lambda$ is the wave number, λ is the wavelength, $n = ck/\omega$ is the effective refractive index, ω is the frequency, and c is the speed of light in a vacuum.

The equation for finding the transverse profile of the electric field strength has the following form [7]:

$$u''(x) + \{\varepsilon(x, I) - n^2\}k^2u(x) = 0. \quad (2)$$

Here, $\varepsilon(x, I)$ is the permittivity of the photonic hetero-structure which in general can reflect a nonlinear response in the form of a specific dependence on the electric field intensity $I = |u|^2$ (a model of nonlinearity of the medium). It also characterizes the optical inhomogeneity modeled by a dependence on the spatial coordinate (a spatial profile). The square of the permittivity determines the refractive index.

In the case under consideration, when the photonic crystal with the flat surface is in contact with the optically homogeneous medium with a nonlinear response (nonlinear medium) or without it (linear medium), the permittivity can be represented as follows [13]:

$$\varepsilon(x, I) = \begin{cases} \varepsilon_{\text{in}}(x), x > 0, \\ \varepsilon_{\text{ho}}(I), x < 0. \end{cases} \quad (3)$$

Here, $\varepsilon_{\text{in}}(x)$ models the inhomogeneity of the permittivity profile as a function of the coordinate in the direction perpendicular to the surface of the photonic crystal, and $\varepsilon_{\text{ho}}(I)$ models the nonlinear response of the optically homogeneous medium in contact with the photonic crystal.

If the transverse profile of the electric field strength is written as:

$$u(x) = \begin{cases} u_{\text{in}}(x), x > 0 \\ u_{\text{ho}}(I), x < 0, \end{cases} \quad (4)$$

wherein $u_{\text{in}}(x)$ and $u_{\text{ho}}(I)$ are the electric field strength profiles defined on the half-axes in the photonic crystal and in the optically homogeneous medium, respectively, then Eq. (2) is divided into two equations on the half-axes:

$$u''_{\text{in}}(x) + \{\varepsilon_{\text{in}}(x) - n^2\}k^2u_{\text{in}}(x) = 0, x > 0, \quad (5)$$

$$u''_{\text{ho}}(x) + \{\varepsilon_{\text{ho}}(I) - n^2\}k^2u_{\text{ho}}(x) = 0, x < 0. \quad (6)$$

The continuity of the field components on the surface of the photonic crystal determines the boundary conditions of conjugation at $x = 0$:

$$u_{\text{in}}(+0) = u_{\text{ho}}(-0), \quad (7)$$

$$u'_{\text{in}}(+0) = u'_{\text{ho}}(-0). \quad (8)$$

Finally, the following conditions should be added which follow from the requirement that the field disappears at infinity: $u_{\text{ho}}(x) \to 0$, $u_{\text{in}}(x) \to 0$ as $|x| \to \infty$.

As a result, a model is formulated as conjugation boundary-value problem (5)–(8). The continuous and everywhere bounded solutions can be used to describe the propagation of surface waves in photonic crystal structures.

2. MODELING OF A DESCENDING REFRACTIVE INDEX PROFILE OF A PHOTONIC CRYSTAL STRUCTURE

In order to find solutions in explicit form, a specific form of the permittivity profile $\varepsilon_{\text{in}}(x)$ and the model $\varepsilon_{\text{ho}}(I)$ of nonlinearity of the medium need to be selected. The inhomogeneity of the photonic crystal structure is often modeled using decreasing profiles [2–6]. They describe a decrease in the refractive index with increasing distance from the surface into the depth of the photonic structure. The following dependence is proposed:

$$\varepsilon_{\text{in}}(x) = e_0 + \frac{e_1}{x + h_1} + \frac{e_2}{(x + h_2)^2}, \quad (9)$$

wherein e_0, e_1, e_2, h_1, and h_2 are parameters of the spatial profile of the permittivity.

This form of the permittivity profile is a generalization of the hyperbolic profile considered earlier [15–17]. This can be obtained from expression (9) at $e_0 = e_2 = 0$.

Substitution of profile (9) into Eq. (5) leads to the following equation:

$$u''_{\text{in}}(x) + \left(e_0 + \frac{e_1}{x + h_1} + \frac{e_2}{(x + h_2)^2} - n^2\right)k^2u_{\text{in}}(x) = 0. \quad (10)$$

Using the definition of the Heun confluent function $H_c(q, \alpha, \gamma, \delta, e, z)$ as a solution $y(z)$ of the Heun confluent differential equation [19]

$$z(z-1)y'' + (\gamma(z-1) + \delta z + z(z-1)e)y' + (\alpha z - q)y = 0,$$

the general solution of Eq. (10) can be written with its help in the following form:

$$u_{\text{in}}(x) = (x + h_1)\mathrm{e}^{n_0kx}\left\{C_1(x + h_2)^{\frac{n_1+1}{2}}H_c \times \right.$$

$$\times\left(2kn_0(h_2 - h_1), n_1, 1, k^2e_1(h_2 - h_1), \frac{1}{2}, \frac{x + h_2}{h_2 - h_1}\right) +$$

$$+C_2(x + h_2)^{-\frac{n_1+1}{2}}H_c \times$$

$$\left.\times\left(2kn_0(h_2 - h_1), -n_1, 1, k^2e_1(h_2 - h_1), \frac{1}{2}, \frac{x + h_2}{h_2 - h_1}\right)\right\},$$

wherein $n_0 = \sqrt{n^2 - e_0}$, $n_1 = \frac{1}{2}\sqrt{1 - 4k^2e_2}$, and C_1 and C_2 are integration constants.

The analysis of such a solution is clearly very difficult. However, if it is assumed that $h_1 = h_2 = h$, then, for the profile:

$$\varepsilon_{in}(x) = e_0 + \frac{e_1}{x+h} + \frac{e_2}{(x+h)^2}. \quad (11)$$

Equation (10) has the following form:

$$u''_{in}(x) + \left(e_0 + \frac{e_1}{x+h} + \frac{e_2}{(x+h)^2} - n^2 \right) k^2 u_{in}(x) = 0. \quad (12)$$

Given this simplification, the general solution of Eq. (12) is expressed in terms of the Whittaker functions $W_{\mu,\nu}(z)$ and $M_{\mu,\nu}(z)$ as solutions $y(z)$ of the Whittaker differential equation [19]:

$$y'' + \left(\frac{\mu}{z} - \frac{1}{4} + \frac{1/4 - \nu^2}{z^2} \right) y = 0,$$

which is clearly simpler than the Heun differential equation.

Since a solution of the Whittaker equation which is bounded and decreases at infinity is the Whittaker function $W_{\mu,\nu}(z)$, then the transverse profile of the electric field strength in the photonic crystal structure determined by the solution of Eq. (10) can be written as follows:

$$u_{in}(x) = u_0 \frac{W_{\mu,\nu}(2n_0 k(x+h))}{W_{\mu,\nu}(2n_0 kh)}. \quad (13)$$

Here, u_0 is the value of the electric field strength on the surface of the photonic crystal, and the parameters of the Whittaker function are determined by the parameters of Eq. (11) as:

$$\mu = e_1 k / 2n_0 = e_1 k / 2\sqrt{n^2 - e_0},$$

$$\nu = n_1 = \sqrt{1 - 4k^2 e_2} / 2.$$

Hence, it follows that solution (13) exists under the conditions $n^2 > e_0$ and $k^2 > 1/4e_2$.

Thus, the spatial distribution of the electric field strength in the photonic crystal structure with the permittivity profile decreasing with distance from the surface according to generalized hyperbolic law (11) was obtained in explicit analytical form (12).

Note that the use of the generalized profile (11) allows the solution obtained (13) to be applied not only in the theory of waveguide optics, but also in quantum mechanics. Equation (12) can be considered as the stationary Schrödinger equation [18] with a generalized hyperbolic potential described by profile (11). Moreover, varying the values of the parameters of profile (11) enables significantly different forms of it to be obtained (Fig. 1). These are applicable in describing both monotonic (Fig. 1a) and nonmonotonic (Fig. 1b) potential barriers, as well as potential wells (Fig. 1c).

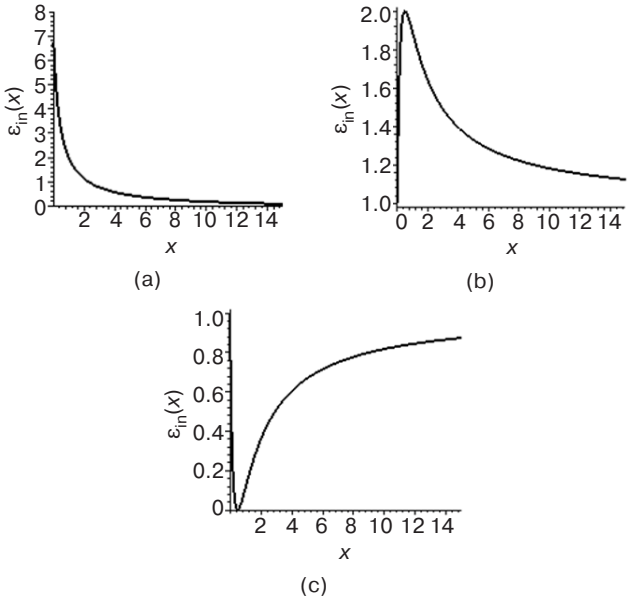

Fig. 1. Spatial profiles of permittivity (11) at various values of its parameters (in conventional dimensionless units): (a) $e_0 = -0.1$, $e_1 = 3$, and $e_2 = 0.2$; (b) $e_0 = -1$, $e_1 = 2$, and $e_2 = -1$; and (c) $e_0 = 1$, $e_1 = -2$, $e_2 = 1$, and $h = 0.5$

Let us consider special cases of profile (9).

1) $e_2 = 0$. In this case, profile (9) takes the form of a dependence decreasing according to a hyperbolic law:

$$\varepsilon_{in}(x) = e_0 + \frac{e_1}{x+h}, \quad (14)$$

and Eq. (12) is written as:

$$u''_{in}(x) + \left(e_0 + \frac{e_1}{x+h} - n^2 \right) k^2 u_{in}(x) = 0. \quad (15)$$

The general solution of Eq. (5) is expressed in terms of the Whittaker functions:

$$u_{in}(x) = C_1 W_{\mu,1/2}(2n_0 k(x+h)) + \\ + C_2 W_{\mu,1/2}(2n_0 k(x+h)), \quad (16)$$

wherein the parameters of the Whittaker functions are $\mu = e_1 k / 2n_0 = e_1 k / 2\sqrt{n^2 - e_0}$ and $\nu = 1/2$.

Since the description of surface waves requires that the solution should be bounded at infinity: $u_{in}(x) \to 0$ as $|x| \to \infty$, for further application of solution (16), it is necessary to set $C_2 = 0$. In order to satisfy conjugation condition (7) at the interface of the crystals, $C_1 = u_0 / W_{\mu,1/2}(2n_0kh)$, may be chosen. In this case, solution (16), which can be used to solve the boundary-value conjugation problem, takes the following form:

$$u_{in}(x) = u_0 \frac{W_{\mu,1/2}(2n_0k(x+h))}{W_{\mu,1/2}(2n_0kh)}. \quad (17)$$

2) $e_1 = 0$. In this case, profile (9) takes the form of a dependence decreasing according to a hyperbolic law:

$$\varepsilon_{in}(x) = e_0 + \frac{e_2}{(x+h)^2}, \quad (18)$$

and Eq. (12) is represented as:

$$u''_{in}(x) + \left(e_0 + \frac{e_2}{(x+h)^2} - n^2 \right) k^2 u_{in}(x) = 0. \quad (19)$$

The study found a general solution to Eq. (19):

$$u_{in}(x) = \sqrt{x+h} \times \\ \times \{C_1 I_\nu(2n_0k(x+h)) + C_2 K_\nu(2n_0k(x+h))\}. \quad (20)$$

Wherein $I_\nu(z)$ and $K_\nu(z)$ are modified cylindrical functions of the imaginary argument of the first and second kind, also called the Infeld and Macdonald functions, respectively, of the order $\nu = n_1 = \sqrt{1-4k^2e_2}\,/\,2$. These functions are linearly independent solutions of the modified Bessel differential equation [19]:

$$y'' + \frac{1}{z}y' - \left(1 + \frac{\nu^2}{z^2}\right) y = 0,$$

which is obviously simpler in comparison with both the Heun differential equation and the Whittaker differential equation.

Since the Infeld function is unbounded, $C_1 = 0$ needs to be set for the further application of solution (20). In order to satisfy conjugation condition (7) at the interface of the crystals, $C_2 = u_0\sqrt{h} / K_\nu(2n_0kh)$, can be chosen. In this case the solution (20), which can be used to solve the boundary-value conjugation problem, takes the following form:

$$u_{in}(x) = u_0 \sqrt{1 + \frac{x}{h}} \frac{K_\nu(2n_0k(x+h))}{K_\nu(2n_0kh)}. \quad (21)$$

It should be noted that solution (17) is such a special case of solution (13) obtained at $e_2 = 0$ in an obvious way, while solution (21) does not follow explicitly from solution (13) at $e_1 = 0$. However, its form is preferable for use in constructing a solution to the boundary-value conjugation problem in modeling surface waves. The Macdonald function contains one parameter less than the Whittaker function, which simplifies the analysis of the solution.

3. SURFACE WAVES ALONG A PHOTONIC CRYSTAL WITH A DECREASING REFRACTIVE INDEX

In the case under consideration, when the photonic crystal is in contact with air or with an optically homogeneous dielectric without a nonlinear response (linear medium), the permittivity in this half-space is assumed to be constant and independent of the field intensity: $\varepsilon_{ho}(I) = \varepsilon_0$.

As a result, the photonic crystal structure under consideration has a permittivity of:

$$\varepsilon(x, I) = \begin{cases} e_0 + \dfrac{e_1}{x+h} + \dfrac{e_2}{(x+h)^2}, & x > 0, \\ \varepsilon_0, & x < 0. \end{cases} \quad (22)$$

Then, taking into account the assumptions made, Eq. (6) describing the distribution of the field in a homogeneous medium is written as follows:

$$u''_{ho}(x) - q_0^2 u_{ho}(x) = 0, x < 0, \quad (23)$$

wherein $q_0^2 = k^2(n^2 - \varepsilon_0)$.

The solution of Eq. (15) decreasing at infinity has the following form:

$$u_{ho}(x) = u_0 e^{q_0 x}. \quad (24)$$

The surface wave is described by the solution of boundary-value conjugation problem (5)–(8). To find this solution, the parameters of obtained solutions (13) and (24) on the semi-axes need to be defined in such a way that they satisfy boundary conditions (7) and (8). Solutions (13) and (24) clearly satisfy continuity condition (7) on the surface of the photonic crystal. In order to satisfy the continuity condition of the derivatives, i.e., to ensure the smoothness of the transverse profile of the surface wave, solutions (13) and (24) are substituted into boundary condition (8). This gives the following dispersion equation:

$$q_0 = \frac{k}{n_0}(n_0^2 - e_1 / 2) - \frac{W_{\mu+1,\nu}(2n_0kh)}{hW_{\mu,\nu}(2n_0kh)}. \quad (25)$$

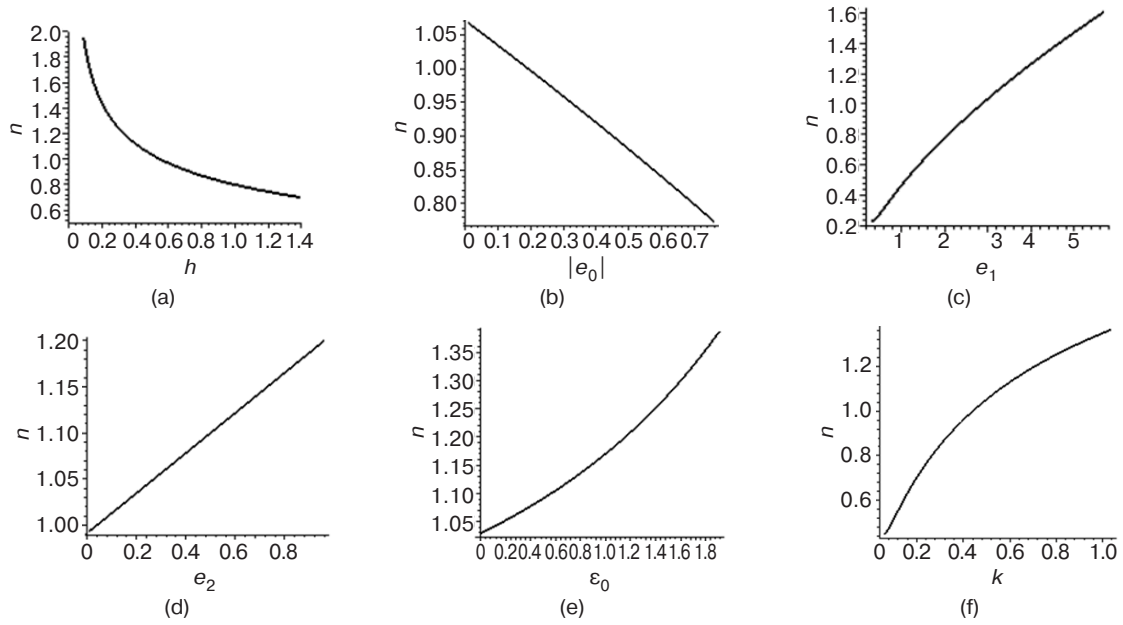

Fig. 2. Dependencies of the effective refractive index (in conventional dimensionless units):
(a) on h at $e_0 = -0.1$, $e_1 = 3$, $e_2 = 0.2$, $e_0 = 0.05$, and $k = 0.5$;
(b) on e_0 at $h = 0.5$, $e_1 = 3$, $e_2 = 0.2$, $e_0 = 0.05$, and $k = 0.5$;
(c) on e_1 at $h = 0.5$, $e_0 = -0.1$, $e_2 = 0.2$, $e_0 = 0.05$, and $k = 0.5$;
(d) on e_2 at $h = 0.5$, $e_0 = -0.1$, $e_1 = 3$, $e_0 = 0.05$, and $k = 0.5$;
(e) on e_0 at $h = 0.5$, $e_0 = -0.1$, $e_1 = 3$, $e_2 = 0.2$, and $k = 0.5$;
and (f) on k at $h = 0.5$, $e_0 = -0.1$, $e_1 = 3$, $e_2 = 0.2$, and $e_0 = 0.05$

The dispersion equation defines a continuous spectrum of values of the effective refractive index n as a function of the parameters of permittivity profile (22). Figure 2 presents the results of the numerical solution of dispersion Eq. (25). The effective refractive index increases with increasing parameters e_0, e_1, e_2, ε_0, and k and decreases only with increasing h.

Thus, the solution to boundary-value problem (5)–(8), describing a surface wave propagating along the surface of the photonic crystal, is obtained after substituting solutions (13) and (24) into the following expressions (4):

$$u(x) = u_0 \begin{cases} \dfrac{W_{\mu,\nu}(2n_0 k(x+h))}{W_{\mu,\nu}(2n_0 kh)}, & x > 0, \\ e^{q_0 x}, & x < 0. \end{cases} \qquad (26)$$

Figure 3 presents the transverse profiles of the electric field strength in surface wave (26).

The electric field is clearly localized in narrow regions near the surface on both sides, with the maximum intensity in the photonic crystal. The intensity can be higher in the photonic crystal than in the homogeneous dielectric, despite the fact that the field penetration depth in the photonic crystal may be less than that in the dielectric.

An increase in parameter h leads to an increase in the field localization width. The intensity maximum shifts into the depth of the photonic crystal, and its intensity increases (Fig. 3a). With a decrease in the parameter e_0 (an increase in its absolute value), the field penetration depth into the homogeneous dielectric increases and that into the photonic crystal decreases. The intensity maximum shifts toward the surface, and its intensity also decreases (Fig. 3b). An increase in the parameter e_1 leads to a decrease in the field localization width. The intensity of the maximum increases, and its position does not change (Fig. 3c). An increase in the parameter e_2 also leads to a decrease in the field localization width. However, the intensity of the maximum decreases, and its position shifts toward the surface (Fig. 3d). An increase in parameter ε_0 leads to almost the same effect, except that the field penetration depth into the homogeneous dielectric increases (Fig. 3d). An increase in the wavenumber (a decrease in the wavelength) leads to a decrease in the field localization width, the intensity of the maximum increases, and its position shifts slightly toward the surface (Fig. 3e).

The analysis shows that the field penetration depth into the photonic crystal decreases with increasing effective refractive index. Therefore, by adjusting the angle of incidence of the laser beam exciting the surface

wave, the field penetration depth into the photonic crystal can be varied.

An important point is that the solution (26) to the formulated boundary-value problem (5)–(8) obtained describes not only a surface wave, in which the electric field strength profile decreases fairly rapidly with increasing distance from the surface, but also waveguide modes, in which the electric field strength profile decreases with oscillations. Waveguide modes are excited at specific parameter values. Their characteristic profiles are shown in Fig. 4. The oscillation amplitudes of waveguide modes decrease as they approach the crystal surface. The order of a waveguide mode can be defined as the number of maxima of the intensity $I = |u|^2$ (the number of maxima and minima of the electric field strength).

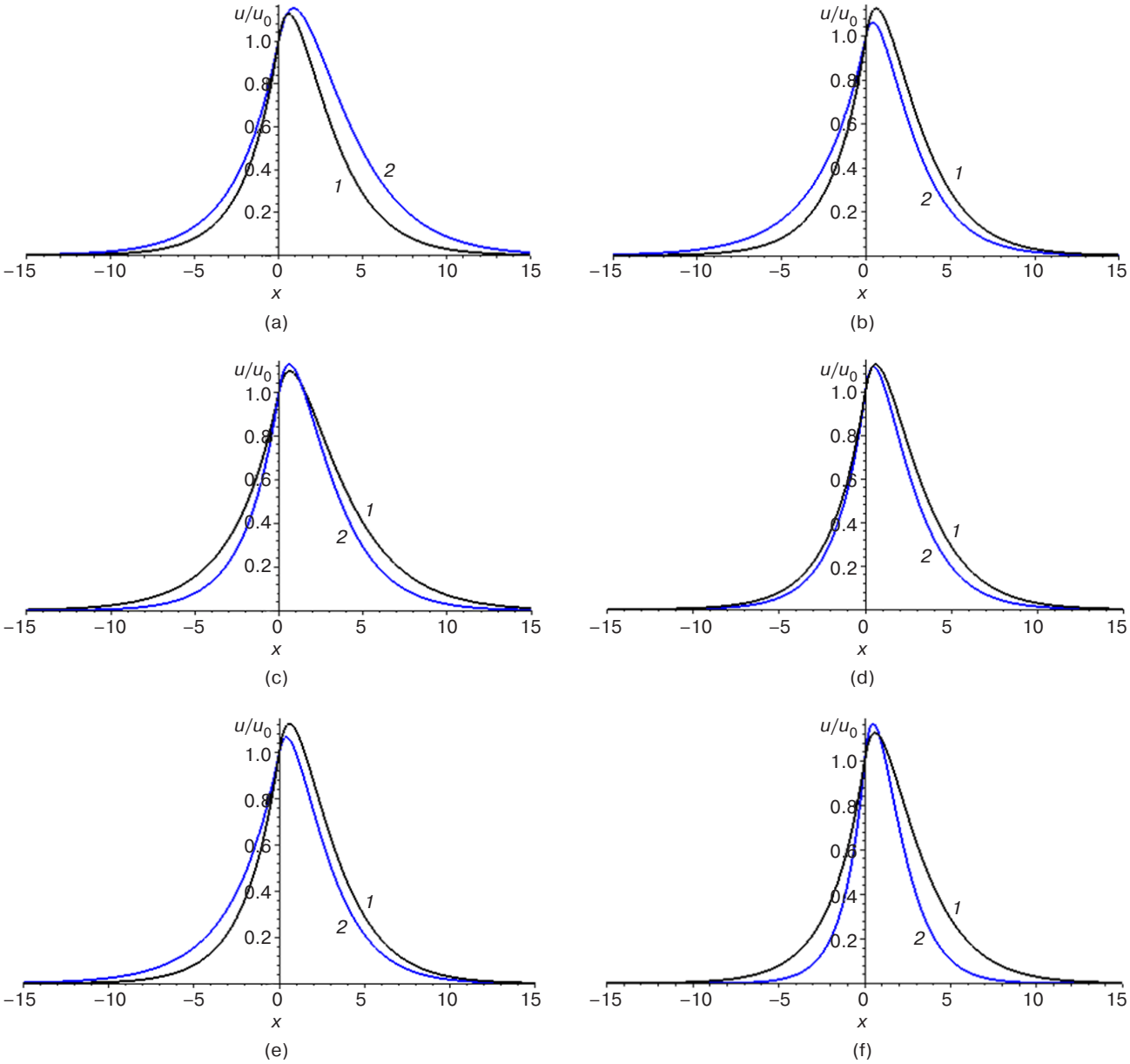

Fig. 3. Transverse profiles of the electric field strength in surface wave (26) at various values of the system parameters (in conventional dimensionless units):
(a) h = (*1*) 0.5 and (*2*) 0.9, $e_0 = -0.1$, $e_1 = 3$, $e_2 = 0.2$, $e_0 = 0.05$, and $k = 0.5$;
(b) $h = 0.5$, e_0 = (*1*) −0.1 and (*2*) −0.9, $e_1 = 3$, $e_2 = 0.2$, $e_0 = 0.05$, and $k = 0.5$;
(c) $h = 0.5$, $e_0 = -0.1$, e_1 = (*1*) 2 and (*2*) 3, $e_2 = 0.2$, $e_0 = 0.05$, and $k = 0.5$;
(d) $h = 0.5$, $e_0 = -0.1$, $e_1 = 3$, e_2 = (*1*) 0.2 and (*2*) 0.9, $e_0 = 0.05$, and $k = 0.5$;
(e) $h = 0.5$, $e_0 = -0.1$, $e_1 = 3$, $e_2 = 0.2$, e_0 = (*1*) 0.05 and (*2*) 0.5, and $k = 0.5$; and
(f) $h = 0.5$, $e_0 = -0.1$, $e_1 = 3$, $e_2 = 0.2$, $e_0 = 0.05$, and k = (*1*) 0.5 and (*2*) 0.7

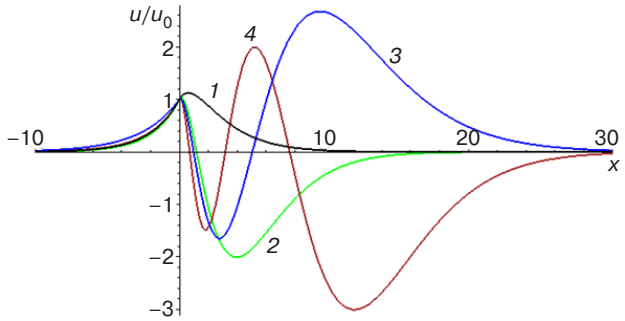

Fig. 4. Transverse profiles of the electric field strength of waveguide modes (26) at fixed values (in conventional dimensionless units) of $h = 0.5$, $e_0 = -0.1$, $e_2 = 0.2$, $e_0 = 0.05$, and $k = 0.5$ and various values of e_1 = (*1*) 3, (*2*) 9.1, (*3*) 10.1, and (*4*) 17.5

Let us now briefly consider a special case of profile (9) at $e_1 = 0$. Then the photonic crystal structure under consideration is characterized by a permittivity of:

$$\varepsilon(x, I) = \begin{cases} e_0 + \dfrac{e_2}{(x+h)^2}, x > 0, \\ \varepsilon_0, x < 0. \end{cases} \quad (27)$$

The mathematical description of the surface wave is now constructed from solutions (21) and (24). In order to find a solution to conjugation problem (5)–(8) in this case, the parameters of obtained solutions (21) and (24) on the semi-axes need to be defined, in such a way that they satisfy boundary conditions (7) and (8). Solutions (21) and (24) clearly satisfy continuity condition (7) on the surface of the photonic crystal. As a result, a solution to boundary-value conjugation problem (5)–(8) is obtained in the following form:

$$u(x) = u_0 \begin{cases} \sqrt{1 + \dfrac{x}{h}} \dfrac{K_\nu(2n_0k(x+h))}{K_\nu(2n_0kh)}, x > 0, \\ e^{q_0 x}, x < 0. \end{cases} \quad (28)$$

In a similar way, a dispersion equation is obtained:

$$\sqrt{\xi^2 - \varepsilon_0 (kh)^2} = \frac{1}{2} + \nu - \xi \frac{K_{\nu+1}(\xi)}{K_\nu(\xi)}, \quad (29)$$

wherein $\xi = n_0 kh$.

Dispersion Eq. (29) defines a continuous spectrum of values of the following effective refractive index:

$$n^2 = e_0 + (\xi / kh)^2, \quad (30)$$

wherein ξ is the positive root of Eq. (29).

A detailed analysis of solution (28) and the roots of the dispersion equation in the special case $e_0 = 0$ was given previously [20].

Thus, the exact analytical solutions of the boundary-value problem are obtained. In two cases using different functions, these solutions describe surface waves and waveguide modes propagating along a photonic crystal in contact with an optically homogeneous medium. The photonic crystal is characterized by the refractive index which decreases with distance from the contact surface in accordance with a generalized hyperbolic profile.

The formulated models and described characteristics of linear and nonlinear surface waves can be useful in predicting the optical properties of various photonic crystal structures, and multilayer composite optical structures [21, 22] used in optoelectronic engineering and photonics [23]. The results of this work can also be used in the design of various waveguide structures, including layered ones, with the required dispersion-optical characteristics.

CONCLUSIONS

This paper proposes models of photonic heterostructures with a spatial permittivity profile that allows for an exact analytical solution. A generalized hyperbolic profile was used to model this spatial distribution. Exact analytical solutions of the wave equation for the selected permittivity profiles were found. These are expressed in terms of the Whittaker and Macdonald functions.

A boundary-value problem was formulated to describe surface waves and waveguide modes propagating along the surface of the photonic crystal. This problem was solved using an exact solution for the generalized hyperbolic profile. Cases of contact between the photonic crystal and a homogeneous dielectric or a nonlinear optical medium were considered. Expressions were derived for surface transverse electric waves where the field is localized near the surface of the photonic crystal and decreases with distance from it.

A detailed analysis was made of the influence of the optical characteristics of the system for photonic crystal in contact with the homogeneous dielectric. This includes the parameters of the generalized hyperbolic permittivity profile, the permittivity of the homogeneous medium, and the wavenumber. A dispersion equation describing the dependence of the effective refractive index on the optical parameters of the system was derived and numerically analyzed. The study identified conditions for control parameters which allow for the localization of the electric field near the photonic crystal surface. It was shown that the solution to the boundary-value problem also describes waveguide modes, where the field decreases with oscillations with distance from the photonic crystal surface.

REFERENCES

1. Agrawal G.P. *Physics and Engineering of Graded-Index Media*. New York: Cambridge University Press; 2023, 348 p. https://doi.org/10.1017/9781009282086
2. Singh B.K., Bambole V., Tiwari S., Shukla K.K., Pandey P.C., Rastogi V. Photonic band gap consequences in one-dimensional exponential graded index photonic crystals. *Optik*. 2021;240:166854. https://doi.org/10.1016/j.ijleo.2021.166854
3. Dash D., Saini J., Goyal A.K., Massoud Y. Exponentially index modulated nanophotonic resonator for high-performance sensing applications. *Sci. Rep*. 2023;13(1):1431. https://doi.org/10.1038/s41598-023-28235-6
4. Singh B.K., Bijalwan A., Pandey P.C., Rastogi V. Photonic bandgaps engineering in double graded hyperbolic, exponential and linear index materials embedded one-dimensional photonic crystals. *Eng. Res. Express*. 2019;1(2):025004. https://doi.org/10.1088/2631-8695/ab48a0
5. Singh B.K., Bambole V., Rastogi V., Pandey P.C. Multi-channel photonic bandgap engineering in hyperbolic graded index materials embedded one-dimensional photonic crystals. *Opt. Laser Technol*. 2020;129(17):106293. https://doi.org/10.1016/j.optlastec.2020.106293
6. Dash D., Saini J. Hyperbolic Graded Index Biophotonic Cholesterol Sensor with Improved Sensitivity. *Progress In Electromagnetics Research M*. 2023;116:165–176. https://doi.org/10.2528/PIERM23032302
7. Chen C-L. *Foundations for Guided-Wave Optics.* New York: John Wiley & Sons Inc.; 2005, 462 p. https://doi.org/10.1002/0470042222
8. Lachance R.L., Belanger P.-A. Modes in divergent parabolic graded-index optical fibers. *Journal of Lightwave Technology* (*JLwT*). 1991;9(11):1425–1430. https://doi.org/10.1109/50.97628
9. Touam T., Yergeau F. Analytical solution for a linearly graded-index-profile planar waveguide. *Appl. Opt.* 1993;32(3): 309–312. https://doi.org/10.1364/AO.32.000309
10. Shvartsburg A.B. Dispersion of electromagnetic waves in stratified and nonstationary media (exactly solvable models). *Phys. Usp*. 2000;43(12):1201–1228. https://doi.org/10.1070/PU2000v043n12ABEH000827
[Original Russian Text: Shvartsburg A.B. Dispersion of electromagnetic waves in stratified and nonstationary media (exactly solvable models). *Uspekhi Fizicheskikh Nauk*. 2000;170(12):1297–1324 (in Russ.). https://doi.org/10.3367/UFNr.0170.200012b.1297]
11. Svendsen B.B., Söderström M., Carlens H., Dalarsson M. Analytical and Numerical Models for TE-Wave Absorption in a Graded-Index GNP-Treated Cell Substrate Inserted in a Waveguide. *Appl. Sci*. 2022;12(14):7097. https://doi.org/10.3390/app12147097
12. Almawgani A.H.M., Taya S.A., Hussein A.J., Colak I. Dispersion properties of a slab waveguide with a graded-index core layer and a nonlinear cladding using the WKB approximation method. *J. Opt. Soc. Am. B.* 2022;39(6):1606–1613. https://doi.org/10.1364/JOSAB.458569
13. Savotchenko S.E. Models of waveguides combining gradient and nonlinear optical layers. *Russian Technological Journal.* 2023;11(4):84–93 (in Russ.). https://doi.org/10.32362/2500-316X-2023-11-4-84-93
14. Savotchenko S.E. Models of symmetric three-layer waveguide structures with graded-index core and non-linear optical liners. *Russian Technological Journal.* 2024;12(5):77–89 (in Russ.). https://doi.org/10.32362/2500-316X-2024-12-5-77-89
15. Savotchenko S.E. Nonlinear surface waves propagating along an interface between the Kerr nonlinear and hyperbolic graded-index crystals. *J. Opt*. 2025;54:2363–2371. https://doi.org/10.1007/s12596-024-01907-w
16. Savotchenko S.E. New surface waves in a hyperbolic graded-index crystal. *Rom. Rep. Phys*. 2024;76(4):406. https://doi.org/10.59277/RomRepPhys.2024.76.406
17. Savotchenko S.E. Features of the surface wave propagation along the interface between the hyperbolic graded-index layer and nonlinear medium with a step change in the dielectric constant. *Phys. Lett. A.* 2024;524(11):129822. https://doi.org/10.1016/j.physleta.2024.129822
18. Kaplan I.G. *Intermolecular Interactions: Physical Picture, Computational Methods and Model Potentials*. Hoboken: John Wiley & Sons; 2006, 367 p. https://doi.org/10.1002/047086334X
19. Andrews G.E., Askey R., Roy R. *Special Functions*. UK: Cambridge University Press; 1999, 664 p. https://doi.org/10.1017/CBO9781107325937
20. Savotchenko S.E. Surface waves in a medium with spatial monotonic attenuation of the refractive index. *Rom. Rep. Phys*. 2025;77(1):402. https://doi.org/10.59277/RomRepPhys.2025.77.402
21. Yurasov A.N., Yashin M.M., Gladyshev I.V., Semyonova D.V., Gan'shina E.A., Kanazakova E.S. Influence of size effects and granule distribution by size on optical and magneto-optical properties of nanocomposites. *Russian Technological Journal.* 2021;9(3):49–57 (in Russ.). https://doi.org/10.32362/2500-316X-2021-9-3-49-57
22. Zhang X., Shao J., Yan C., Qin R., Lu Z., Geng H., Xu T., Ju L. A review on optoelectronic device applications of 2D transition metal carbides and nitrides. *Materials & Design*. 2021;200:109452. https://doi.org/10.1016/j.matdes.2021.109452
23. Santiago S. *Optoelectronics, Photonics and Sensors*. Prague: Czech Technical University of Prague; 2017, 40 p.

СПИСОК ЛИТЕРАТУРЫ

1. Agrawal G.P. *Physics and Engineering of Graded-Index Media*. New York: Cambridge University Press; 2023, 348 p. https://doi.org/10.1017/9781009282086
2. Singh B.K., Bambole V., Tiwari S., Shukla K.K., Pandey P.C., Rastogi V. Photonic band gap consequences in one-dimensional exponential graded index photonic crystals. *Optik*. 2021;240:166854. https://doi.org/10.1016/j.ijleo.2021.166854

3. Dash D., Saini J., Goyal A.K., Massoud Y. Exponentially index modulated nanophotonic resonator for high-performance sensing applications. *Sci. Rep*. 2023;13(1):1431. https://doi.org/10.1038/s41598-023-28235-6
4. Singh B.K., Bijalwan A., Pandey P.C., Rastogi V. Photonic bandgaps engineering in double graded hyperbolic, exponential and linear index materials embedded one-dimensional photonic crystals. *Eng. Res. Express*. 2019;1(2):025004. https://doi.org/10.1088/2631-8695/ab48a0
5. Singh B.K., Bambole V., Rastogi V., Pandey P.C. Multi-channel photonic bandgap engineering in hyperbolic graded index materials embedded one-dimensional photonic crystals. *Opt. Laser Technol*. 2020;129(17):106293. https://doi.org/10.1016/j.optlastec.2020.106293
6. Dash D., Saini J. Hyperbolic Graded Index Biophotonic Cholesterol Sensor with Improved Sensitivity. *Progress In Electromagnetics Research M*. 2023;116:165–176. https://doi.org/10.2528/PIERM23032302
7. Chen C-L. *Foundations for Guided-Wave Optics.* New York: John Wiley & Sons Inc.; 2005, 462 p. https://doi.org/10.1002/0470042222
8. Lachance R.L., Belanger P.-A. Modes in divergent parabolic graded-index optical fibers. *Journal of Lightwave Technology* (*JLwT*). 1991;9(11):1425–1430. https://doi.org/10.1109/50.97628
9. Touam T., Yergeau F. Analytical solution for a linearly graded-index-profile planar waveguide. *Appl. Opt.* 1993;32(3): 309–312. https://doi.org/10.1364/AO.32.000309
10. Шварцбург А.Б. Дисперсия электромагнитных волн в слоистых и нестационарных средах (точно решаемые модели). *Успехи физических наук* (*УФН*). 2000;170(12):1297–1324. https://doi.org/10.3367/UFNr.0170.200012b.1297
11. Svendsen B.B., Söderström M., Carlens H., Dalarsson M. Analytical and Numerical Models for TE-Wave Absorption in a Graded-Index GNP-Treated Cell Substrate Inserted in a Waveguide. *Appl. Sci*. 2022;12(14):7097. https://doi.org/10.3390/app12147097
12. Almawgani A.H.M., Taya S.A., Hussein A.J., Colak I. Dispersion properties of a slab waveguide *with* a graded-index core layer and a nonlinear cladding using the WKB approximation method. *J. Opt. Soc. Am. B.* 2022;39(6):1606–1613. https://doi.org/10.1364/JOSAB.458569
13. Савотченко С.Е. Модели волноводов, сочетающих градиентные и нелинейно-оптические слои. *Russian Technological Journal.* 2023;11(4):84–93. https://doi.org/10.32362/2500-316X-2023-11-4-84-93
14. Савотченко С.Е. Модели симметричных трехслойных волноводных структур с градиентной сердцевиной и нелинейно-оптическими обкладками. *Russian Technological Journal.* 2024;12(5):77–89. https://doi.org/10.32362/2500-316X-2024-12-5-77-89
15. Savotchenko S.E. Nonlinear surface waves propagating along an interface between the Kerr nonlinear and hyperbolic graded-index crystals. *J. Opt*. 2025;54:2363–2371. https://doi.org/10.1007/s12596-024-01907-w
16. Savotchenko S.E. New surface waves in a hyperbolic graded-index crystal. *Rom. Rep. Phys*. 2024;76(4):406. https://doi.org/10.59277/RomRepPhys.2024.76.406
17. Savotchenko S.E. Features of the surface wave propagation along the interface between the hyperbolic graded-index layer and nonlinear medium with a step change in the dielectric constant. *Phys. Lett. A.* 2024;524(11):129822. https://doi.org/10.1016/j.physleta.2024.129822
18. Kaplan I.G. *Intermolecular Interactions: Physical Picture, Computational Methods and Model Potentials*. Hoboken: John Wiley & Sons; 2006, 367 p. https://doi.org/10.1002/047086334X
19. Andrews G.E., Askey R., Roy R. *Special Functions*. UK: Cambridge University Press; 1999, 664 p. https://doi.org/10.1017/CBO9781107325937
20. Savotchenko S.E. Surface waves in a medium with spatial monotonic attenuation of the refractive index. *Rom. Rep. Phys*. 2025;77(1):402. https://doi.org/10.59277/RomRepPhys.2025.77.402
21. Юрасов А.Н., Яшин М.М., Гладышев И.В., Семенова Д.В., Ганьшина Е.А., Каназакова Е.С. Влияние размерных эффектов и распределения гранул по размерам на оптические и магнитооптические свойства нанокомпозитов. *Russian Technological Journal*. 2021;9(3):49–57. https://doi.org/10.32362/2500-316X-2021-9-3-49-57
22. Zhang X., Shao J., Yan C., Qin R., Lu Z., Geng H., Xu T., Ju L. A review on optoelectronic device applications of 2D transition metal carbides and nitrides. *Materials & Design*. 2021;200:109452. https://doi.org/10.1016/j.matdes.2021.109452
23. Santiago S. *Optoelectronics, Photonics and Sensors*. Prague: Czech Technical University of Prague; 2017, 40 p.

About the Author

Sergey E. Savotchenko, Dr. Sci. (Phys.-Math.), Associate Professor, Professor, High Mathematics Department, Institute for Advanced Technologies and Industrial Programming, MIREA – Russian Technological University (78, Vernadskogo pr., Moscow, 119454 Russia). E-mail: savotchenkose@mail.ru. Scopus Author ID 6603577988, RSCI SPIN-code 2552-4344, https://orcid.org/0000-0002-7158-9145

Об авторе

Савотченко Сергей Евгеньевич, д.ф.-м.н, доцент, профессор кафедры высшей математики, Институт перспективных технологий и индустриального программирования, ФГБОУ ВО «МИРЭА – Российский технологический университет» (119454, Россия, Москва, пр-т Вернадского, д. 78). E-mail: savotchenkose@mail.ru. Scopus Author ID 6603577988, SPIN-код РИНЦ 2552-4344, https://orcid.org/0000-0002-7158-9145

Translated from Russian into English by V. Glyanchenko
Edited for English language and spelling by Dr. David Mossop

Mathematical modeling

Математическое моделирование

UDC 004.023, 519.677
https://doi.org/10.32362/2500-316X-2026-14-1-103-112
EDN LDJQIL

RESEARCH ARTICLE

Experimental investigation of convergence characteristics of quasi-Newton algorithm on nonsmooth and nonconvex functions

Alexander V. Smirnov @

MIREA – Russian Technological University, Moscow, 119454 Russia
@ *Corresponding author, e-mail: av_smirnov@mirea.ru*

• **Submitted:** 02.04.2025 • **Revised:** 14.06.2025 • **Accepted:** 13.11.2025

Abstract

Objectives. The aim of the paper is to develop a methodology for studying the convergence of the quasi-Newton minimization algorithm (QNA) on nonsmooth and nonconvex objective functions (OF), as well as to conduct related numerical experiments.

Methods. The experiments were performed on a flexible OF capable of mimicking various patterns of value changes in different directions away from the minimum. A total of 18 OF instances with different landscape parameters were studied. For each example, 200 QNA searches were performed from random staring points, and all corresponding OF values were recorded. Then, the Expected Run Time (ERT) to reach a given threshold level of the OF was computed based on the data. The dependence of the achieved OF threshold on ERT was approximated separately for the segment in which all thresholds were achieved in all searches, and for a segment in which the thresholds were achieved, but not in all searches.

Results. The experiments show that, for the majority of cases in which all thresholds are achieved in all takes, a decrease in the OF follows the geometric progression law (linear convergence). However, in the second segment, convergence follows the power law. It was also found that the presence of anisotropy of the OF landscape and a loss of smoothness lead to convergence slowdown, and premature termination of search process before reaching the minimum with the required accuracy.

Conclusions. The study identifies patterns in the QNA convergence on the objective functions with different landscape parameters. Further advancement of the methodology would involve automating data collection and processing, as well as extending it to other types of optimization algorithms.

Keywords: quasi-Newton algorithm, objective function landscape, convex function, concave function, nonsmooth function, approximation, exponent, algorithm convergence

For citation: Smirnov A.V. Experimental investigation of convergence characteristics of quasi-Newton algorithm on nonsmooth and nonconvex functions. *Russian Technological Journal.* 2026;14(1):103–112. https://doi.org/10.32362/2500-316X-2026-14-1-103-112, https://www.elibrary.ru/LDJQIL

Financial disclosure: The author has no financial or proprietary interest in any material or method mentioned.

The author declares no conflicts of interest.

НАУЧНАЯ СТАТЬЯ

Экспериментальное исследование характеристик сходимости квазиньютоновского алгоритма на негладких и невыпуклых функциях

А.В. Смирнов [@]

МИРЭА – Российский технологический университет, Москва, 119454 Россия
[@] *Автор для переписки, e-mail: av_smirnov@mirea.ru*

• **Поступила:** 02.04.2025 • **Доработана:** 14.06.2025 • **Принята к опубликованию:** 13.11.2025

Резюме

Цели. Целью работы является разработка методики исследования характеристик сходимости квазиньютоновского алгоритма (КНА) на негладких и невыпуклых целевых функциях (ЦФ) и выполнение экспериментов по этой методике.

Методы. Эксперименты выполнялись на тестовой функции, обеспечивающей возможность задания различных законов изменения ее значений по разным направлениям от точки минимума. Всего исследованы 18 примеров ЦФ с разными параметрами рельефа. Для каждого примера выполнялись 200 стартов КНА из случайных точек и фиксировались все значения ЦФ, полученные в процессе поиска. Затем по этим данным вычислялись значения Expected Run Time (ERT) – ожидаемого времени достижения заданного порогового уровня ЦФ. Далее выполнялась аппроксимация зависимости достигнутого порога ЦФ от ERT отдельно для отрезка, в котором все пороги достигаются во всех стартах для этого примера, и для отрезка, в котором пороги достигаются, но не во всех стартах.

Результаты. Эксперименты показали, что в большинстве примеров для отрезка, в котором все пороги достигаются во всех стартах, имеет место убывание ЦФ по закону геометрической прогрессии (линейная сходимость), а во втором отрезке преобладает сходимость по степенному закону. Также установлено, что наличие анизотропии рельефа ЦФ и нарушений гладкости приводят к замедлению сходимости и завершению поиска до достижения минимума с требуемой точностью.

Выводы. Исследование позволило выявить закономерности в сходимости КНА на ЦФ с различными свойствами рельефа. Дальнейшее развитие методики должно включать автоматизацию сбора и обработки данных и распространение на другие виды алгоритмов поиска оптимальных решений.

Ключевые слова: квазиньютоновский алгоритм, рельеф целевой функции, выпуклая функция, вогнутая функция, негладкая функция, аппроксимация, показатель степени, сходимость алгоритма

Для цитирования: Смирнов А.В. Экспериментальное исследование характеристик сходимости квазиньютоновского алгоритма на негладких и невыпуклых функциях. *Russian Technological Journal*. 2026;14(1):103–112. https://doi.org/10.32362/2500-316X-2026-14-1-103-112, https://www.elibrary.ru/LDJQIL

Прозрачность финансовой деятельности: Автор не имеет финансовой заинтересованности в представленных материалах или методах.

Автор заявляет об отсутствии конфликта интересов.

INTRODUCTION

The paper considers the problem of finding the local extremum (LE) (minimum) $\mathbf{x}^*$ of the objective function (OF) $f(\mathbf{x})$ within a given search space Ω_X:

$$\mathbf{x}^* = \arg\min_{\mathbf{x}\in\Omega_X}(f(\mathbf{x})). \quad (1)$$

Quasi-Newton algorithms (QNA) can be an effective method for solving this problem. These algorithms use an approximation of the Hessian matrix (the matrix of second partial derivatives) based on the OF gradient which is only the first derivative. This allows the algorithm to determine the direction of the next step in the search process. It has been shown that for these algorithms to converge to the minimum, the function must be smooth and convex within the search space Ω_X [1, 2]. Software QNA implementations are available in widely used mathematical programming packages.

In cases where the conditions for smoothness and/or convexity of the objective function are not met, a rigorous analysis of the QNA is not available. Nevertheless, in practice, QNA has been successfully used to find local extrema of nonsmooth and/or nonconvex OFs in many cases. The conditions under which this application is successful, and the achievable results, have been little explored. At the same time, studies on the convergence conditions and rates of certain other search algorithms at such OFs are available [1–7]. However, these algorithms tend to converge more slowly than QNA.

The study [8] presents a theoretical analysis of the QNA performance for the function of a single variable, $f(x) = |x|$, with a loss of smoothness at the LE point. The analysis demonstrates that, in order to achieve the LE with an accuracy of no greater than a specified $\varepsilon > 0$, a logarithmic number of iterations ($\log_2(\varepsilon^{-1})$) is required. It has not been possible to perform theoretical analysis for the function $f(\mathbf{x}) = ||\mathbf{x}||$ with a search space dimension $ND > 1$. However, experimental results show that there is a linear convergence in the search process, with the OF value decreasing following the geometric progression law, in which the denominator approaches 1 as ND increases. The study uses only a specific type of the objective function with fixed landscape parameters, and results for other OF types may vary.

The study [9] presents the results of experimental investigations on QNA and a hybrid algorithm based on it, using a large range of test functions. However, the paper lacks sufficient information regarding the convergence characteristics, since only the final outcomes are provided: namely, the achieved LE values and the number of iterations. Additionally, there is a lack of information regarding the relationship between the number of iterations and the variation in the OF value within the LE.

A comparison of the performance of several algorithms, including QNA implementation, is conducted in [10]. This study utilizes a basic set of testing functions [11] and statistical indicators of convergence processes. However, this selection of testing functions does not permit a wide variation in the characteristics of the OF landscape in the LE vicinity, particularly with regard to convexity and asymmetry. In [12], experiments are conducted using QNA, and a testing function with the capability of adjusting certain features. However, convergence processes are not examined, and only the achieved OF values are recorded. Furthermore, it is possible to set only two distinct laws for modifying the OF during experiments in coordinates.

This study aims to develop a methodology and conduct experimental investigations into the convergence of QNA at various OF landscape parameters in the LE vicinity, including loss of smoothness, nonconvexity, anisotropy, and asymmetry across coordinates.

RESEARCH METHODS AND MATERIALS

Experimental research was conducted using the *MATLAB* software[1] implemented on the *GNU Octave* freeware platform[2]. The quasi-Newton algorithm within this software was implemented using the fminunc(..) function. However, this function only returns the final search result and the total number of the OF evaluations. In order to analyze convergence characteristics, all OF values calculated during the search process need to be obtained. In order to address this, a new function called QNLS_M(..) was developed. The simplified structure is shown in Fig. 1.

1. Input: **X** is a starting point; *Options* is the algorithm configuration.
2. Initialization of the Hessian **B** approximation by a diagonal matrix.
3. Calculation of the objective function *F* and its gradient **g** at the starting point.
4. Iterate the search until the completion condition is met.
   4.1. Determine the search direction, **s**, based on **B** and **g**.
   4.2. Find the appropriate step size, λ, using the linear search method.
   4.3. Move to the new point **X** = **X** + λ**s** and calculate the *F* and **g** values at this point.
   4.4. Calculate the **B** value using the BFGS[3] algorithm.
   4.5. Verify search completion conditions.
5. Output: **History** is the array containing the calculated OF values during the search in the order they were calculated, as well as the coordinates of the points where the calculations were performed.

Fig. 1. Structure of the QNLS_M (..) function implementing QNA

[1] https://www.mathworks.com/products/matlab.html. Accessed August 26, 2025.

[2] https://octave.org/. Accessed August 26, 2025.

[3] The Broyden–Fletcher–Goldfarb–Shanno (BFGS) algorithm is an iterative method for solving unconstrained nonlinear optimization problems.

This structure is standard, except for item 5 [1, 2]. In item 4, the linear search algorithm described in [8] is used. In item 4.4, a new approximation of the Hessian **B** is calculated when the condition for positive curvature of the objective function is met at this iteration. The finite difference method is used to calculate the gradient **g** and derivative in the direction of the linear search. In order to minimize the number of calculations of the OF, only one additional point with a bias $\Delta x_i = 10^{-8}$ is taken to estimate the partial derivative for each x_i coordinate.

Table 1 shows the search completion conditions, indicator values for the reasons for ExitFlag completion, and thresholds used in the experiments.

Table 1. Indicator values for the reasons of search completion

ExitFlag	Search completion condition
0	Maximum iteration limit of max_iter = 1000 is exceeded
1	First-order optimality criterion $\max(\|\mathbf{g}\|) \le$ g_tol $= 10^{-8}$ is met
2	Step size condition $\|\lambda\mathbf{s}\| \le$ min_step $= 10^{-12}$ is met
3	The number of consecutive iterations with a relative change in the OF less than ftol = 1.00001 has exceeded the specified threshold max_Nftol = 4
4	No step is found that does not result in an increase in the OF
5	The OF value is less than the specified threshold FuncTol $= 10^{-8}$

In the experiments, the test function TestLE6(**x**, **x***, **R**, **W**, **K**, *NS*) is used. The value at point **x** is calculated as in the following way. First, the bias from the given LE **x*** and the rotation of the coordinates given by the matrix **R** are performed:

$$\mathbf{z} = (\mathbf{x} - \mathbf{x}^*)^{\mathrm{T}}\,\mathbf{R}, \tag{2}$$

wherein T represents the transpose operation. Then, for coordinates with indices ranging from 1 to $ND - NS$ (where NS is an integer), the interpolation of the k coefficients and the exponent α is carried out, along with the calculation of a preliminary value of the function f:

$$k = \frac{1}{\|\mathbf{z}\|^2}\sum_{n=1}^{ND-NS}(K_{1n}z_n{}^2h(z_n) + K_{2n}z_n{}^2h(-z_n)),$$

$$\text{wherein } h(y) = \begin{cases} 1, y > 0, \\ 0, y \le 0, \end{cases} \tag{3}$$

$$\alpha = \frac{1}{\|\mathbf{z}\|^2}\sum_{n=1}^{ND-NS}(W_{1n}z_n{}^2h(z_n) + W_{2n}z_n{}^2h(-z_n)),$$

$$f = k\|\mathbf{z}\|^{\alpha}.$$

The variables K_{ij} and W_{ij} are elements of the matrices **K** and **W** which have dimensions of $2 \times ND$. They represent the values of coefficients and exponents, respectively, in the positive and negative directions for all coordinates in the search space. This algorithm, proposed in [13], allows for arbitrary setting of power function parameters for different coordinates and for smooth changes in these parameters in intermediate directions.

If $NS = 0$, then the final value of the function f is obtained. If $NS > 0$, a computation cycle is carried out for coordinates with indices n ranging from $ND - |NS| + 1$ to ND as follows:

$$f = f + \\ + \max\left[K_{1n}|z(n)|^{W_{1n}}\operatorname{sign}(z(n)), -K_{2n}|z(n)|^{W_{2n}}\operatorname{sign}(z(n))\right]. \tag{4}$$

If $NS < 0$, a series of operations are carried out at the specified indices, as follows:

$$f = \\ = \max\left[f, K_{1n}|z(n)|^{W_{1n}}\operatorname{sign}(z(n)), -K_{2n}|z(n)|^{W_{2n}}\operatorname{sign}(z(n))\right]. \tag{5}$$

As a result, lines originating from the LE point are generated, along which smoothness of the function is lost. For $NS = 0$, the smoothness can only be lost at the LE point **x***. By varying the combination of parameters, many well-known unimodal OFs, as well as functions with novel properties can be generated. Examples of graphs of the TestLE6(..) function for $ND = 2$ and various NS values are presented in Fig. 2. The other parameters of the function have the following values:

$$\mathbf{x}^* = \begin{pmatrix} 0 \\ 0 \end{pmatrix}, \quad \mathbf{W} = \begin{pmatrix} 1.5 & 0.5 \\ 0.75 & 1.0 \end{pmatrix}, \quad \mathbf{K} = \begin{pmatrix} 1 & 2 \\ 1 & 2 \end{pmatrix}.$$

Experimental studies were conducted in the form of individual tests, each consisting of 10 sets of 20 local extremum searches. The initial search points were randomly selected on a hypersphere with unit radius and center at **x***. In each test, various combinations of the **W**, **K**, and NS parameters were applied. At the start of each set of searches, the coordinate axes were rotated using a randomly generated and orthonormalized matrix **R**. During each search, the coordinates of all points were recorded where the OF calculation was performed, as well as the actual OF values.

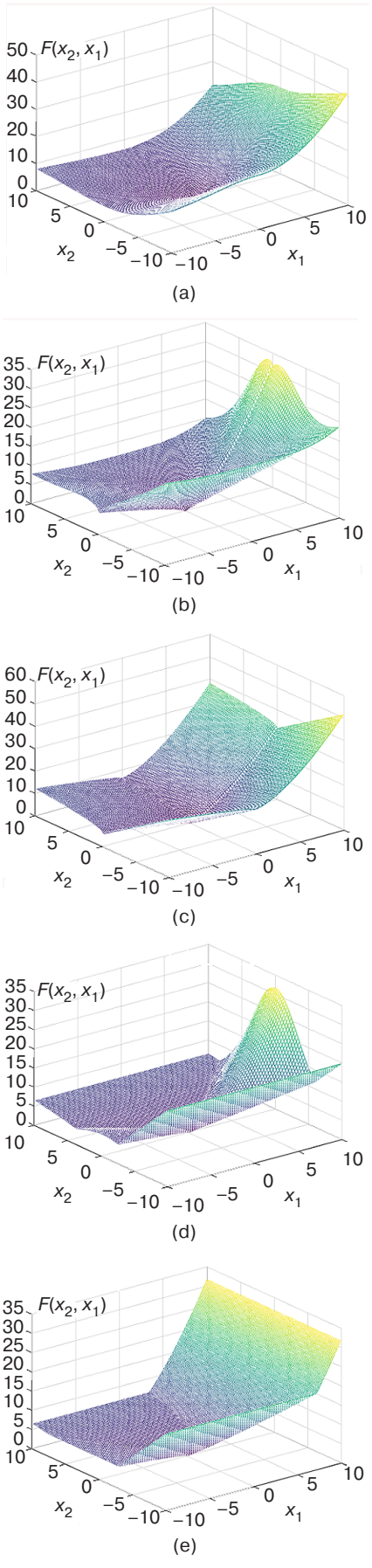

Fig. 2. Graphs of the TestLE6(..) function:
(a) *NS* = 0; (b) *NS* = 1; (c) *NS* = 2; (d) *NS* = −1; and (e) *NS* = −2

The expected time to reach a certain OF threshold was used as a characteristic to summarize the results of all tests. This is known in optimization literature as the Expected Run Time (ERT). This function can be defined as follows [14, 15].

Let us introduce a variable:

$$h = -\lg(f), \tag{6}$$

wherein f is the OF value. We define the scale of the threshold levels, as follows:

$$h_k = -2 + 0.02(k-1), \quad k = \overline{1,51}. \tag{7}$$

The corresponding OF thresholds, f_k, derived from (6), range from 10^2 to 10^{-8}. We define in the following way: $Nr_i(h_k)$ as the number of the OF computations performed during the ith search until threshold h_k is reached; and Ne_i as the total number of the OF computations until the ith search completes. Ir_k represents a subset of searches which reach the threshold h_k, with Inr_k denoting the number of these searches. Inr_k denotes a subset of searches that do not reach the threshold h_k. Then,

$$\mathrm{ERT}(h_k) = \frac{\sum\limits_{i \in Ir_k} Nr_i(h_k) + \sum\limits_{i \in Inr_k} Ne_i}{|\,Ir_k\,|}. \tag{8}$$

If the threshold h_k is not reached in any of the searches, the ERT(h_k) value becomes infinitely large.

We introduce the indicators determined by ERT, in order to compare the characteristics of the QNA operation. For this purpose, we define the following boundaries for the threshold scale:

h_{start} is the threshold value reached at the beginning of the experiment;

h_{all} is the maximum threshold value reached during the experiment;

h_{finish} is the highest threshold value achieved in at least one search during the experiment.

If $h_{\mathrm{all}} = 8$, which is the upper limit of the scale, then the value $h_{\mathrm{finish}} = h_{\mathrm{all}}$ is set.

In the segment $[h_{\mathrm{start}}, h_{\mathrm{all}}]$, we approximate the relationship between lg(f) and ERT using the *MATLAB/Octave regress*(..) function, as follows:

$$\lg(f) = b_{11} \cdot \mathrm{ERT} + b_{12} \cdot \lg(\mathrm{ERT}) + b_{13}. \tag{9}$$

We also calculate the determination coefficients for the first two terms.

If the segment $[h_{\mathrm{all}}, h_{\mathrm{finish}}]$ contains between 2 and 9 divisions on the threshold scale, then we perform approximation of the form (9) for the entire segment. We also define the coefficients b_{31}, b_{32}, and b_{33}, as well as the corresponding determination coefficients.

If this segment spans at least 9 divisions, it is divided into two subsegments, with the boundary of the second subsegment on the threshold scale denoted by h_b. Approximation of the form (9) is performed separately for each of these subsegments. In this case, coefficients for the first subsegment are denoted as b_{21}, b_{22}, and b_{23}, while coefficients for the second subsegment are b_{31}, b_{32}, and b_{33}. The value of h_b is determined by iterating through possible values within the $[h_{all}, h_{finish}]$ segment. Approximations for each subsegment are calculated and the value that minimizes the mean-square error of approximation is selected. Splitting the $[h_{all}, h_{finish}]$ segment allows for experiments to obtain more accurate approximations of the dependence of lg(f) on ERT in that segment.

Subsequently, by applying potentiation (9), we derive the following

$$f = \left(10^{b_{11}}\right)^{\mathrm{ERT}} \mathrm{ERT}^{b_{12}} \cdot 10^{b_{13}}. \qquad (10)$$

We denote $10^{b_{11}} = q_1$, $b_{12} = p_1$, $10^{b_{13}} = a_1$. Then (10) takes the following form:

$$f = a_1 \cdot q_1^{\mathrm{ERT}} \cdot \mathrm{ERT}^{p_1}. \qquad (11)$$

The second cofactor in (11) varies in accordance with the law of geometric progression, corresponding to linear convergence [1, 4]. The third cofactor follows a power function. Therefore, the values of q_1 and p_1 determine the laws and rates of convergence for the search on the segment $[h_{start}, h_{all}]$. Likewise, the values of q_3 and p_3 for the segment $[h_{all}, h_{finish}]$ can be determined if this interval is not divided; or the values of q_2 and p_2 for $[h_{all}, h_b]$, and the values of q_3 and p_3 for $[h_b, h_{finish}]$, if the interval $[h_{all}, h_{finish}]$ is split into two.

Segment boundaries and approximation coefficients for these segments can serve as indicators to compare the convergence of search algorithms for OF with different properties. In this method, instead of the OF value, the distance from the current point **x** to LE $\mathbf{x}^*$ can be used as an indicator of convergence [1, 5, 6]. The ERT(f) dependence can also be approximated, in order to obtain estimates for the number of the OF calculations required until a specified OF value is reached. This is another useful characteristic in certain cases [4, 7].

EXPERIMENTAL RESULTS

The parameters of the TestLE6(**x**, $\mathbf{x}^*$, **R**, **W**, **K**, *NS*) function, as determined in 18 tests, are presented in Table 2. The LE location is always set to the origin, $\mathbf{x}^* = \mathbf{0}$.

In tests 1–6, the space dimension $ND = 4$ and the OF is isotropic in all directions. In tests 1–3, the OF is convex. In test 4, it changes according to a linear law, and in tests 5 and 6, it is concave. In test 1, the objective function is smooth everywhere, while in tests 2–5, there is a loss of smoothness in the LE. Subsequent tests use the OFs from tests 2 and 5 as a basis, and modify any properties. Tests 7–10 introduce anisotropy in certain directions. Tests 11–14 increase the dimension of the space, while tests 15–18 create loss of smoothness on lines originating from the LE.

Let us now explain the introduction of anisotropy. The calculation procedure for **W** elements is as follows:

Table 2. Test function parameters in experiments

Test	*ND*	W_{max}	W_{min}	K_{max}	K_{min}	*NS*	Test	*ND*	W_{max}	W_{min}	K_{max}	K_{min}	*NS*
1	4	2.00	2.00	1	1	0	10	4	0.75	0.75	1	0.1	0
2	4	1.50	1.50	1	1	0	11	8	1.50	1.50	1	1	0
3	4	1.25	1.25	1	1	0	12	16	1.50	1.50	1	1	0
4	4	1.00	1.00	1	1	0	13	8	0.75	0.75	1	1	0
5	4	0.75	0.75	1	1	0	14	16	0.75	0.75	1	1	0
6	4	0.50	0.50	1	1	0	15	4	1.50	1.50	1	1	2
7	4	1.50	1.50	10	1	0	16	4	1.50	1.50	1	1	–2
8	4	1.50	0.75	1	1	0	17	4	0.75	0.75	1	1	2
9	4	1.50*	0.75*	1	1	0	18	4	0.75	0.75	1	1	–2

$$W_{1i} = W_{2i} = W_{\min} + \frac{(W_{\max} - W_{\min})(i-1)}{ND-1},\ i = \overline{1,ND}. \quad (12)$$

For $W_{\max} = W_{\min}$, we obtain $W_{1i} = W_{2i} = W_{\max}$, $i = \overline{1,ND}$, and the exponent of α in (5) is independent of direction. Similarly, values for the matrix **K** elements were determined. In test 9, a random permutation of the **W** row elements was also performed, for example:

$$W(\text{Test } 8) = \begin{pmatrix} 0.75 & 1 & 1.25 & 1.5 \\ 0.75 & 1 & 1.25 & 1.5 \end{pmatrix},$$

$$W(\text{Test } 9) = \begin{pmatrix} 1 & 1.25 & 1.5 & 0.75 \\ 0.75 & 1.5 & 1 & 1.25 \end{pmatrix}.$$

Table 3 shows the reasons for completion of the search in the experiments (Table 1). In the table, EF_1 (Exit Flag) represents the most frequently encountered reason in the certain test, while PEF_1 indicates the probability of that reason. Additionally, other reasons for termination encountered in the experiment, ranked in descending order by probability, are provided. This data indicates that if the function is convex at least along part of coordinates, i.e., if there is at least one element of the matrix **W** exceeding one, the search will reach a value of $f = 10^{-8}$. Otherwise, the search process terminates prematurely for other reasons.

Figures 3 and 4 show the ERT graphs obtained from the experiments, while Table 4 presents the approximation results for these dependencies. In order to enhance clarity, thresholds h_k are not used as the argument, but rather the corresponding f values obtained using (6), with the same index, for example, $f_{\text{all}} = 10^{-h\text{all}}$. The $\lg(f_{\text{start}})$ values are not included in the table. They can be inferred from the point at which the ERT increases. The approximation coefficients are presented in P/R^2 format, where P represents a value of q or p, and R^2 represents the corresponding determination coefficient. Only points where the ERT values are finite are shown in the graphs.

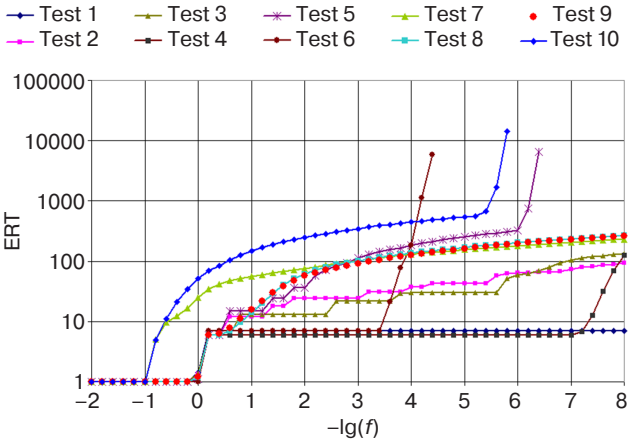

Fig. 3. ERT experiment graphs: tests 1–10

Let us proceed to analyzing the results of the experiments. For the isotropic quadratic function in test 1, the QNA algorithm accurately identifies the LE after the first iteration, illustrated by the horizontal line in Fig. 3. However, the approximation of the form (9) is highly inaccurate. The corresponding values in Table 4 are highlighted in bold.

Table 3. Statistics of search completion reasons in experiments

Test	EF_1	PEF_1	EF_2	PEF_2	Test	EF_1	PEF_1	EF_2	PEF_2	EF_3	PEF_3	EF_4	PEF_4
1	5	0.970	1	0.030	10	2	1.000	–	–	–	–	–	–
2	5	1.000	–	–	11	5	1.000	–	–	–	–	–	–
3	5	1.000	–	–	12	5	1.000	–	–	–	–	–	–
4	2	0.530	5	0.470	13	2	1.000	–	–	–	–	–	–
5	2	1.000	–	–	14	2	1.000	–	–	–	–	–	–
6	2	0.990	4	0.010	15	5	0.650	2	0.340	3	0.010	–	–
7	5	1.000	–	–	16	5	0.685	2	0.155	3	0.140	4	0.020
8	5	1.000	–	–	17	2	0.895	4	0.080	3	0.025	–	–
9	5	1.000	–	–	18	2	0.450	4	0.300	3	0.250	–	–

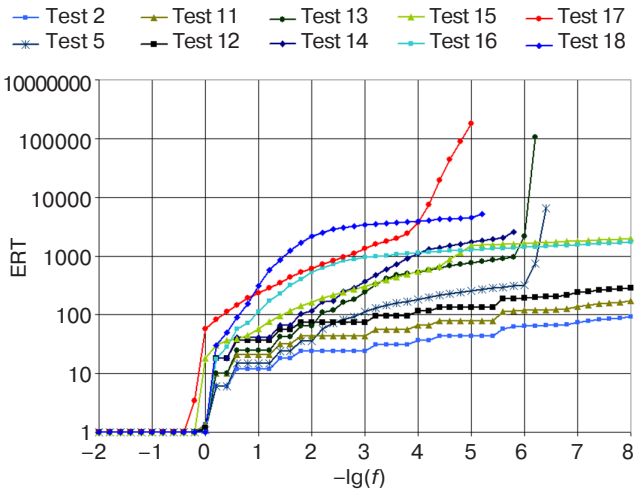

Fig. 4. ERT experiment graphs: tests 2, 5, and 11–18

In tests 4 and 6, with OF exponents of 1 and 0.5, respectively, the QNA also jumped to points with $f = f_{all}$ after the first iteration. On the $[f_{all}, f_{finish}]$ segments, the search slowed down and these sections can be approximated by a power law with good accuracy. There is no descent by geometric progression because $q_3 = 1.00$. In tests 2, 3, and 5 with exponents of 1.5, 1.25, and 0.75, respectively, no such jump in OF was observed. The $[f_{start}, f_{all}]$ segment in tests 2 and 5 can be accurately approximated by geometric progression.

In subsequent experiments, the OF parameters from tests 2 and 5 were altered. As can be seen from the graphs in Fig. 3, introducing the form (5) anisotropy into the OF, either by coefficient (tests 7 and 10) or by exponent (tests 8 and 9), resulted in an upward shift in ERT, i.e., a slowing down of the search. At the same time, random permutations of the degree indicators across the coordinates in test 9 did not alter ERT compared to test 8. In all experiments, the $[f_{start}, f_{all}]$ segment is approximated with high precision using

Table 4. ERT approximation results in experiments

Test	$\lg f_{all}$	$\lg f_b$	$\lg f_{finish}$	ERT(f_{all})	ERT(f_b)	ERT(f_{all})	q_1	p_1	q_2	p_2	q_3	p_3
1	−8.0	–	−8.0	7.00	–	–	**0.15/0.14**	**0.74/0.14**	–	–	–	–
2	−8.0	–	−8.0	93.2	–	–	0.84/0.96	−1.06/0.78	–	–	–	–
3	−8.0	–	−8.0	134	–	–	0.96/0.78	−3.39/0.87	–	–	–	–
4	−7.2	–	−8.0	6.77	–	126	**0.00/0.19**	**14.0/0.17**	–	–	1.00/0.94	−0.56/1.00
5	−5.8	–	−6.4	308	–	$6.56 \cdot 10^3$	0.97/0.96	−0.97/0.87	–	–	1.00/0.79	−0.58/0.94
6	−3.4	–	−4.4	7.00	–	$5.86 \cdot 10^3$	**0.00/0.30**	**66.7/0.29**	–	–	1.00/0.70	−0.33/0.98
7	−8.0	–	−8.0	232	–	–	0.91/1.00	0.057/0.72	–	–	–	–
8	−8.0	–	−8.0	270	–	–	0.94/1.00	−0.11/0.75	–	–	–	–
9	−8.0	–	−8.0	263	–	–	0.94/1.00	−0.28/0.76	–	–	–	–
10	−5.2	–	−5.8	563	–	$14.3 \cdot 10^3$	0.98/1.00	−0.26/0.73	–	–	1.00/0.80	−0.58/0.95
11	−8.0	–	−8.0	170	–	–	0.91/0.96	−0.84/0.74	–	–	–	–
12	−8.0	–	−8.0	290	–	–	0.94/0.96	−0.60/0.68	–	–	–	–
13	−5.8	–	−6.2	951	–	$106 \cdot 10^3$	0.99/0.92	−1.01/0.88	–	–	–	–
14	−4	−5.4	−5.8	1.11k	$1.96 \cdot 10^3$	$2.53 \cdot 10^3$	1.00/0.75	−1.04/0.88	1.00/0.99	−6.66/1.00	1.02/0.89	−52.4/0.90
15	−4.2	−5.2	−8.0	602	$1.53 \cdot 10^3$	$1.98 \cdot 10^3$	0.94/0.99	−0.39/0.83	1.07/0.86	−14.8/0.90	0.75/0.99	64.0/0.99
16	−0.8	−3.6	−8.0	71.9	$1.09 \cdot 10^3$	$1.73 \cdot 10^3$	0.98/0.98	−0.064/0.80	0.99/0.98	0.19/0.91	0.99/1.00	−11.4/1.00
17	−0.6	−3.8	−5.0	140	$2.45 \cdot 10^3$	$177 \cdot 10^3$	0.99/0.97	−0.33/0.84	1.00/0.94	−2.14/0.99	1.00/0.77	−0.61/0.99
18	−0.6	−3	−5.2	89.3	$3.40 \cdot 10^3$	$5.25 \cdot 10^3$	0.97/0.98	−0.894/0.80	1.00/0.99	−0.19/0.90	1.01/0.91	−51.3/0.94

geometric progression, whereas the $[f_{all}, f_{finish}]$ segment in test 10 is approximated using a power function.

The impact of the *ND* dimension of the search space is shown in Fig. 4 (tests 11–14). Expectedly, convergence slowed down with an increase in *ND*. Furthermore, for convex OF (tests 2, 11, and 12), a two-fold increase in *ND* leads to an equal upward shift in ERT on a logarithmic scale, while maintaining linear convergence. No clear patterns were observed for concave OF (tests 5, 13, and 14).

Introducing the loss of smoothness along the semi-infinite lines starting from the LE, in the case of a convex objective functions (tests 2, 15, and 16), results in a slowing down of the search process. This now reaches a limit of $f = 10^{-8}$ in not all tests. In the case of concave OFs (tests 5, 17, and 18), there is an increased minimum value, f_{all}, achieved at least once. In tests 15–18, the segment $[f_{start}, f_{all}]$ is approximated by a geometric progression with good accuracy. The power function contributes significantly to the approximation of the segments $[f_b, f_{finish}]$ and $[f_b, f_{finish}]$, as values for q_2 and q_3 are close to 1. However, uncommonly large values of $|p_2|$ and $|p_3|$ may occur in the results of some tests. This is due to gradual changes in ERT over the corresponding segments.

CONCLUSIONS

Based on the results of the experiments, it can be inferred that dividing the range of ERT thresholds into segments and approximating the function f(ERT) using the proposed form (9) for each segment allows certain patterns to be identified. The presence of convexity in at least some directions ensures a minimum threshold of $f = 10^{-8}$ to be achieved. In the case of segments $[f_{start}, f_{all}]$ which include the values of the OFs achieved in all searches, the convergence can be considered to be linear with a fairly high degree of accuracy. In the case of those segments $[f_{all}, f_{finish}]$, where the OF values are not achieved in all searches, convergence follows a power law of the ERT^p form.

Some results raise questions. In certain segments, the OF values are not achieved in all searches. This is understandable in cases where the OF is anisotropic, such as in tests 10 and 15–17. However, in tests 4–6 and 14, where the OF is isotropic, all starting points should yield the same search result. It is possible that the variation in the final search results in this case is due to random rounding errors in the QNA calculations.

These studies, of course, do not provide a complete understanding of the dependence of QNA convergence characteristics on OF landscape properties since within these studies, these properties vary separately and within limited ranges. In order to obtain a more comprehensive understanding, landscape properties need to be varied in various combinations over a wide range of parameter values. This would require a significant amount of experimentation and data analysis. The implementation of such an approach, presumably, could be achieved through the automation of experiment planning, data collection, and processing, including the use of artificial intelligence techniques.

Another area of interest is the expansion of the method to other types of algorithms aimed at finding an optimal solution, particularly population-based algorithms. This would allow for the comparison of convergence characteristics among different algorithms, essential for selecting the most effective algorithms for various problem types.

REFERENCES

1. Polyak B.T. *Vvedenie v optimizatsiyu* (*Introduction into Optimization*). Moscow: Nauka; 1983, 384 p. (In Russ.).
2. Nocedal J., Wright S. *Numerical Optimization*: 2nd ed. Springer; 2006, 684 p.
3. Dem'yanov V.F., Vasil'ev L.V. *Nedifferentsiruemaya optimizatsiya* (*Non-differentiable Optimization*). Moscow: Nauka; 1981, 384 p. (In Russ.).
4. Vorontsova E.A., Hilderbrand R.F., Gasnikov A.V., Stonyakin F.S. *Vypuklaya optimizatsiya* (*Convex Optimization*). Moscow: MPTI; 2021, 364 p. (In Russ.). ISBN 978-5-7417-0776-0
5. Puchinin S.M., Korolkov E.R., Stonyakin F.S., Alkousa M.S., Vyguzov A.A. Subgradient methods with B.T. Polyak-type step for quasiconvex minimization problems with inequality constraints and analogs of the sharp minimum. *Komp'yuternye issledovaniya i modelirovanie = Computer Research and Modeling*. 2024;16(1):105–122 (in Russ.). https://doi.org/10.20537/2076-7633-2024-16-1-105-122
6. Bento G.C., Mordukhovich B.S., Mota T.S., Nesterov Yu. Convergence of Descent Methods under Kurdyka-Lojasiewicz Properties. *arXiv. Preprint*. 2024. http://arxiv.org/pdf/2407.00812v1
7. Grimmer B., Jia Zh. Goldstein Stationarity in Lipschitz Constrained Optimization. *Optim. Lett*. 2025419:225–235. https://doi.org/10.1007/s11590-024-02158-1
8. Lewis A.S., Overton M.L. Nonsmooth optimization via quasi-Newton methods. *Math. Program.* 2013;141:135–163. https://doi.org/10.1007/s10107-012-0514-2
9. Tor A.H. Comparative numerical results on HANSO (Hybrid Algorithm for Nonsmooth Optimization). *arXiv. Preprint*. 2020. http://arxiv.org/pdf/2009.01037v1

10. Varelas K., Dahito M.-A. Benchmarking Multivariate Solvers of SciPy on the Noiseless Testbed. In: *GECCO 2019 Companion – The Genetic and Evolutionary Computation Conference*, Jul. 2019, Prague, Czech Republic. 2019. P. 1946–1954. https://doi.org/10.1145/3319619.3326891
11. Hansen N., Finck S., Ros R., Auger A. *Real-Parameter Black-Box Optimization Benchmarking 2009*: *Noiseless Functions Definitions*. [Research Report] RR-6829. INRIA; 2009. Available from URL: https://hal.inria.fr/inria-00362633v2. Accessed August 26, 2025.
12. Smirnov A.V. Investigation of influence of objective function valley ratio on the determination error of its minimum coordinates. *Russian Technological Journal.* 2023;11(5):57−67. https://doi.org/10.32362/2500-316X-2023-11-6-57-67
13. Smirnov A.V. The method of estimation of objective functions landscapes convexity during extremum search. *Russian Technological Journal.* 2025;13(2):121–131. https://doi.org/10.32362/2500-316X-2025-13-2-121-131
14. Hansen N., Auger A., Ros R., Mersmann O., Tusar T., Brockhoff D. COCO: A Platform for Comparing Continuous Optimizers in a Black-Box Setting. *Optim. Meth. Software.* 2021;36(1):114–144. https://doi.org/10.1080/10556788.2020.1808977
15. Wang H., Vermetten D., Ye. F., Doerr C., Back T. IOHanalyzer: Detailed Performance Analyses for Iterative Optimization Heuristics. *ACM Transaction on Evolutionary Learning and Optimization.* 2022;2(1):1–29. https://doi.org/10.1145/3510426

СПИСОК ЛИТЕРАТУРЫ

1. Поляк Б.Т. *Введение в оптимизацию*. М.: Наука; 1983, 384 с.
2. Nocedal J., Wright S. *Numerical Optimization*: 2nd ed. Springer; 2006, 684 p.
3. Демьянов В.Ф., Васильев Л.В. *Недифференцируемая оптимизация*. М.: Наука; 1981, 384 с.
4. Воронцова Е.А., Хильдебранд Р.Ф., Гасников А.В., Стонякин Ф.С. *Выпуклая оптимизация.* М.: МФТИ; 2021, 364 с. ISBN 978-5-7417-0776-0
5. Пучинин С.М., Корольков Е.Р., Стонякин Ф.С., Алкуса М.С., Выгузов А.А. Субградиентные методы с шагом типа Б.Т. Поляка для задач минимизации квазивыпуклых функций с ограничениями-неравенствами и аналогами острого минимума. *Компьютерные исследования и моделирование*. 2024;16(1):105–122. https://doi.org/10.20537/2076-7633-2024-16-1-105-122
6. Bento G.C., Mordukhovich B.S., Mota T.S., Nesterov Yu. Convergence of Descent Methods under Kurdyka-Lojasiewicz Properties. *arXiv. Preprint*. 2024. http://arxiv.org/pdf/2407.00812v1
7. Grimmer B., Jia Zh. Goldstein Stationarity in Lipschitz Constrained Optimization. *Optim. Lett*. 2025419:225–235. https://doi.org/10.1007/s11590-024-02158-1
8. Lewis A.S., Overton M.L. Nonsmooth optimization via quasi-Newton methods. *Math. Program.* 2013;141:135–163. https://doi.org/10.1007/s10107-012-0514-2
9. Tor A.H. Comparative numerical results on HANSO (Hybrid Algorithm for Nonsmooth Optimization). *arXiv. Preprint*. 2020. http://arxiv.org/pdf/2009.01037v1
10. Varelas K., Dahito M.-A. Benchmarking Multivariate Solvers of SciPy on the Noiseless Testbed. In: *GECCO 2019 Companion – The Genetic and Evolutionary Computation Conference*, Jul. 2019, Prague, Czech Republic. 2019. P. 1946–1954. https://doi.org/10.1145/3319619.3326891
11. Hansen N., Finck S., Ros R., Auger A. *Real-Parameter Black-Box Optimization Benchmarking 2009*: *Noiseless Functions Definitions*. [Research Report] RR-6829. INRIA; 2009. URL: https://hal.inria.fr/inria-00362633v2. Дата обращения 26.08.2025. / Accessed August 26, 2025.
12. Смирнов А.В. Исследование влияния степени овражности целевой функции на погрешность определения координат ее минимума. *Russian Technological Journal.* 2023;11(6):57−67. https://doi.org/10.32362/2500-316X-2023-11-6-57-67
13. Смирнов А.В. Метод оценки выпуклости рельефа целевых функций в процессе поиска экстремума. *Russian Technological Journal.* 2025;13(2):121–131. https://doi.org/10.32362/2500-316X-2025-13-2-121-131
14. Hansen N., Auger A., Ros R., Mersmann O., Tusar T., Brockhoff D. COCO: A Platform for Comparing Continuous Optimizers in a Black-Box Setting. *Optim. Meth. Software.* 2021;36(1):114–144. https://doi.org/10.1080/10556788.2020.1808977
15. Wang H., Vermetten D., Ye F., Doerr C., Back T. IOHanalyzer: Detailed Performance Analyses for Iterative Optimization Heuristics. *ACM Transaction on Evolutionary Learning and Optimization.* 2022;2(1):1–29. https://doi.org/10.1145/3510426

About the Author

Alexander V. Smirnov, Cand. Sci. (Eng.), Professor, Department of Telecommunications, Institute of Radio Electronics and Informatics, MIREA – Russian Technological University (78, Vernadskogo pr., Moscow, 119454 Russia). E-mail: av_smirnov@mirea.ru. Scopus Author ID 56380930700, RSCI SPIN-code 1616-0120, https://orcid.org/0000-0002-2696-8592

Об авторе

Смирнов Александр Витальевич, к.т.н., доцент, профессор кафедры телекоммуникаций, Институт радиоэлектроники и информатики, ФГБОУ ВО «МИРЭА – Российский технологический университет» (119454, Россия, Москва, пр-т Вернадского, д. 78). E-mail: av_smirnov@mirea.ru. Scopus Author ID 56380930700, SPIN-код РИНЦ 1616-0120, https://orcid.org/0000-0002-2696-8592

Translated from Russian into English by Kirill V. Nazarov
Edited for English language and spelling by Dr. David Mossop

Philosophical foundations of technology and society

Мировоззренческие основы технологии и общества

UDC 811.161.1
https://doi.org/10.32362/2500-316X-2026-14-1-113-126
EDN MMFNUT

RESEARCH ARTICLE

The communicative and aesthetic principle in teaching Russian as a foreign language to international students of technical specialties

Elena N. Tarasova [@], **Zhanna O. Moskvina**

MIREA – Russian Technological University, Moscow, 119454 Russia
[@] *Corresponding author, e-mail: tarasova_e@mirea.ru*

• **Submitted:** 23.04.2025 • **Revised:** 02.07.2025 • **Accepted:** 17.11.2025

Abstract

Objectives. In the context of the internationalization of higher education and the growing role of the Russian language as a means of professional communication in educational environments, the search for effective methodological solutions for teaching foreign students in technical disciplines has become particularly relevant. The aims of this study are twofold: to provide a scientific rationale for the methodological relevance of the communicative-aesthetic principle in teaching Russian as a foreign language to students of technical specialties; and to identify the impact of the communicative-aesthetic principle on the development of student speech culture and the formation of professional communication skills.

Methods. The methodological framework includes a comparative analysis of existing pedagogical approaches which incorporate communicative and aesthetic elements, along with classroom observation in multilingual technical university settings. In order to ensure objectivity in the findings, elements of both quantitative and qualitative analysis of student responses and speech production were used.

Results. The findings indicate that the application of the communicative-aesthetic principle enhances precision and motivation amongst students learning the Russian language aligned with literary norms. A number of observations were made including: increased interest in language learning; improved integration into the academic and cultural environment; and the development of speech aesthetics. All these factors contribute to the formation of a professionally relevant linguistic worldview.

Conclusions. The communicative-aesthetic principle can be considered as an effective methodological tool in teaching Russian as a foreign language in technical universities. Its implementation enhances the educational potential of speech instruction and fosters the integration of aesthetic components into professionally oriented communication. The practical significance of the study lies in the potential application of the developed methodological recommendations in educational programs and teaching materials. A promising area for further research is the creation of didactic resources aimed at developing professionally oriented speech and fostering creative thinking among students.

Keywords: communicative and aesthetic principle, teaching Russian as a foreign language, international students, technical specialties, speech culture, professional communication, methodological approaches, aesthetic perception of speech, student adaptation

For citation: Tarasova E.N., Moskvina Zh.O. The communicative and aesthetic principle in teaching Russian as a foreign language to international students of technical specialties. *Russian Technological Journal.* 2026;14(1):113–126. https://doi.org/10.32362/2500-316X-2026-14-1-113-126, https://www.elibrary.ru/MMFNUT

Financial disclosure: The authors have no financial or proprietary interest in any material or method mentioned.

The authors declare no conflicts of interest.

НАУЧНАЯ СТАТЬЯ

Коммуникативно-эстетический принцип в обучении иностранных студентов технических специальностей русскому языку

Е.Н. Тарасова [@], **Ж.О. Москвина**

МИРЭА – Российский технологический университет, Москва, 119454 Россия
[@] *Автор для переписки, e-mail: tarasova_e@mirea.ru*

• **Поступила:** 23.04.2025 • **Доработана:** 02.07.2025 • **Принята к опубликованию:** 17.11.2025

Резюме

Цели. В условиях интернационализации высшего образования и расширения присутствия русского языка как средства профессионального общения в образовательных пространствах особую актуальность приобретает поиск эффективных методических решений для обучения иностранных студентов технических специальностей. Целью настоящего исследования является научное обоснование методической значимости коммуникативно-эстетического принципа в обучении русскому языку иностранных студентов технического профиля и выявление влияния коммуникативно-эстетического принципа на развитие речевой культуры обучающихся и формирование навыков профессиональной коммуникации.

Методы. Методологическую основу исследования составили сравнительно-сопоставительный анализ существующих методических подходов, включающих элементы коммуникативной и эстетической направленности и наблюдение за учебным процессом в иноязычной аудитории в технических вузах. Для объективизации выводов применялись элементы количественно-качественного анализа ответов и речевых продуктов обучающихся.

Результаты. Полученные данные демонстрируют, что применение коммуникативно-эстетического принципа способствует более точному и мотивированному владению правильной и хорошей русской речью, ориентированной на литературные нормы. Отмечается повышение интереса студентов к языковому обучению, облегчение их интеграции в академическую и культурную среду, а также развитие речевого вкуса, что в совокупности способствует формированию профессионально релевантной языковой картины мира.

Выводы. Коммуникативно-эстетический принцип может рассматриваться как эффективное методическое средство при обучении русскому языку как иностранному в техническом вузе. Его применение усиливает воспитательный потенциал речевого обучения и создает условия для интеграции эстетического компонента в профессионально ориентированную коммуникацию. Практическая значимость исследования заключается в возможности использования разработанных методических рекомендаций при создании образовательных программ и учебных пособий. Перспективным направлением дальнейших исследований является разработка дидактических материалов, направленных на формирование профессионально ориентированной речи и стимулирование креативного мышления студентов.

Ключевые слова: коммуникативно-эстетический принцип, обучение русскому языку, иностранные студенты, технические специальности, речевая культура, профессиональная коммуникация, методические подходы, эстетическое восприятие речи, адаптация

Для цитирования: Тарасова Е.Н., Москвина Ж.О. Коммуникативно-эстетический принцип в обучении иностранных студентов технических специальностей русскому языку. *Russian Technological Journal*. 2026;14(1):113–126. https://doi.org/10.32362/2500-316X-2026-14-1-113-126, https://www.elibrary.ru/MMFNUT

Прозрачность финансовой деятельности: Авторы не имеют финансовой заинтересованности в представленных материалах или методах.

Авторы заявляют об отсутствии конфликта интересов.

INTRODUCTION

In modern approaches to foreign language teaching, including Russian as a foreign language (RFL), the development of foreign language communication skills plays a central role. They define the practical guidelines for the learning process. In a broad sense, "competence" can be interpreted as an individual's ability and willingness to perform certain types of activities [1]. In education, competence is most often understood as externally imposed requirements for the results of a student's training[1] [2]. Competency is understood as an internal personal development which arises as a result of mastering a set of competencies, ensuring the subject's ability to perform activities effectively[2].

Foreign language communication competence is understood as the ability to engage productively in verbal interaction in the given language of study in various meaningful communication situations, including the professional sphere [3]. Communicative competence includes a set of knowledge, practical skills, and speech experience necessary for the formation of a full-fledged ability to communicate in the language being studied[3].

Following the principle of professional orientation of RFL[4] training, the development of speech competence related to the educational and professional sphere begins at the pre-university stage. At this level, foreign students master not only the norms of standard literary language, but also elements of the scientific style of speech corresponding to their future professional specialization in the humanities, natural sciences, technical or technological[5] [4] sphere. This ensures that by the time they enter university (an advanced stage of education), students possess basic academic and professional communication skills [5].

In the subsequent stages of training, discipline-specific language tools need to be integrated to reflect the specifics of various professional sub-languages. This task is particularly important for students of technical specialties. Their professional communication requires specialized terminology and stable syntactic structures characteristic of the fields of engineering, physics, mathematics, and information technology. These features increase the requirements for methodological approaches and reinforce the relevance of applying integrative teaching principles, in particular, communicative-aesthetic principles [4]. By focusing on the activation of speech activity through artistic speech practices and theatrical forms of interpretation, the latter contribute to a deeper understanding of complex abstract concepts and the formation of a professionally oriented speech culture in students.

A.G. Volkova [5] notes that "children have changed, but teaching tools evolve slowly." The principle of consciousness plays a key role in organizing the learning process. This guides the way in which language units are taught on a comparative basis, helping to reduce the influence of interference from the native language. The construction of the teaching system involves a sequence of several stages: correction and articulation courses; an intensive conversation course; a text reproduction stage; transition to productive types of speech activity. Then speaking and writing [6]. It is here that new developments in the types and forms of testing student language levels can be appropriately introduced. Evaluating the cognitive, psychological, and motivational characteristics of foreign students in technical specialties is an important condition for the successful implementation of the communicative-aesthetic principle in teaching. The development of a special entrance test [7] enables potential difficulties

[1] *Pedagogical Terminology Dictionary*. https://voennaya-pedagogika.slovaronline.com/44-компетенция. Accessed March 18, 2025 (in Russ.).

[2] Zimnyaya I.A. Key competencies – a new paradigm for the outcomes of modern education. *Eidos.* 2006. No. 5. https://elibrary.ru/smmbix. Accessed March 20, 2025 (in Russ.).

[3] Khutorskoy A.V. Key competencies and educational standards. *Eidos.* 2002. No. 2. https://elibrary.ru/ztakqu. Accessed March 19, 2025 (in Russ.).

[4] Khutorskoy A.V. Key and subject-specific competency design technology. *Eidos.* 2005. No. 4. https://elibrary.ru/qlhzwi. Accessed April 01, 2025 (in Russ.).

[5] Order of the Ministry of Education and Science of the Russian Federation No. 1304 of October 3, 2014, "On the Approval of Requirements for the Implementation of Additional General Education Programs that Prepare Foreign Citizens and Stateless Persons for Professional Education Programs in Russian." https://brstu.ru/docs/podrazdeleniya-brgu/centr-dopolnitelnoi-podgotovki/inostr/Prikaz_1304.pdf. Accessed April 02, 2025 (in Russ.).

to be identified and the educational trajectory adapted, while taking into account the individual characteristics of students.

Of particular importance in this regard is the inclusion of theatrical elements in the educational process. This factor enables the simulation of professionally relevant situations through expressive speech, intonation, facial expressions, and contextual interaction. J. Gentsel emphasizes that the active involvement of students is a key factor in the success of teaching using this technology [8].

Consequently, the aestheticization of speech activity not only contributes to the development of linguistic competence. It also enables cognitive and emotional difficulties to be overcome when they arise in the teaching and learning of specialized terminology and communication formats characteristic of a technical professional environment.

OBJECTIVE SETTING

In the methodology of RFL teaching at the present stage, there is a transformation of the target orientations and the entire conceptual paradigm of language education. This vector of development is directed from a linguo-centric approach to a cognitive-discursive model which focuses on the assimilation of culture through language as a mediator of intercultural communication [9]. In this context, the aesthetic aspect of speech activity acquires the methodological status of a key parameter. Language performs not only informative and cognitive functions, but also serves as a representative of axiological dominants, national and cultural specifics, and the aesthetic norms of society [7].

The purpose of this article is to provide scientific justification for the methodological significance of the communicative-aesthetic principle in teaching Russian to foreign students of technical disciplines, and to identify its influence on the development of speech culture and professional communication skills. Another aim of the study is to identify effective teaching approaches which ensure not only the development of language skills, but also the aesthetic perception of language as a tool for intercultural and professional communication.

The methodological basis of the study consisted of a comparative analysis of methodological approaches, observation of the educational process, and a survey of foreign students.

Comparative analysis of methodological approaches has enables key features of the application of the communicative-aesthetic principle in teaching RFL to be identified. The analysis also defines its place in the system of modern linguistic and pedagogical concepts, justifying the need to integrate linguistic and aesthetic components into the process of developing professionally oriented speech competence.

Observation of the learning process was aimed at studying the dynamics of the speech skills and abilities of students in the context of applying the communicative-aesthetic principle. Particular attention was paid to analyzing the level of development of expressive speech means, compliance with literary norms, and the ability of students to use the Russian language in academic and professional communication.

The integration of the results of comparative analysis, observation, and questioning provided a comprehensive study of the methodological significance of the communicative-aesthetic principle. It enabled its influence on the development of speech culture and professional communication skills among foreign students to be objectively identified.

This paper presents a comprehensive review of the concepts of speech aesthetics and the communicative approach in teaching RFL. The review is based on the deductive-inductive method of analysis. The aim is to identify the relationship between the aesthetic characteristics of speech acts and the basic principles of the communicative approach, enabling an independent communicative-aesthetic principle to be substantiated and formulated in a way relevant to the methodology of teaching RFL.

The application of the communicative-aesthetic principle, implemented through the inclusion of artistic-pedagogical texts, dialogue fragments, role-playing situations, and theatrical elements in the content of teaching aids, is particularly relevant. Theatricalization not only activates the perception and comprehension of the text, but also enables the implementation of the principles of personalization, emotional involvement, and creative processing of the material [9]. This form of work strengthens the internal motivation of students, contributes to the formation of a sustained interest in the professional vocabulary being studied, and develops their expressive speech and interpretive abilities.

Justification for research and application of the communicative-aesthetic principle

The scientific justification for the methodological significance of the communicative-aesthetic principle in teaching Russian to foreign students of technical disciplines is based on the need for a comprehensive approach to the development of language competence. This also presupposes the unity of cognitive, cultural, and emotional-aesthetic components. The principle enables the educational process to be organized in such a way that language is perceived not only as a means of professional communication, but also as a cultural code that reflects the values of society.

The relevance of research and active application of the communicative-aesthetic principle in teaching

Russian to foreign students of technical specialties is defined by several interrelated factors.

Firstly, modern requirements for professional communication in technical disciplines involve not only the learning of terminology, but also the ability to express thoughts clearly, logically, and expressively. This is particularly important in the context of globalization of scientific and engineering interaction, in which the Russian language serves as a means of professional and academic communication. This principles needs to be carefully considered and introduced into widespread use [10].

Secondly, traditional approaches to teaching Russian at technical universities are mainly focused on developing pragmatic competence, while the aesthetic aspect of speech, related to expressiveness, coherence, and stylistic appropriateness of utterances, remains largely underestimated. At the same time, it is precisely this communicative-aesthetic principle which can ensure more effective assimilation of language norms and the development of speech skills appropriate to the professional and academic context [6].

Thirdly, the integration of the communicative-aesthetic principle into the methodology of RFL teaching for technical specialties contributes to the development of the ability of students to adapt their speech to various communicative situations. It also increases motivation to learn the language, and contributes to the formation of the linguistic personality of a specialist capable not only of perceiving and conveying information, but also doing so in accordance with the norms of academic and professional discursive culture [10].

DEGREE OF RESEARCH ON THE PROBLEM

The communicative approach is a system of principles which determine teaching strategy, but also reproduces models of natural speech interaction. As such it has replaced the grammar-translation method. Its introduction has led to a transformation in the process of teaching foreign languages. Instead of focusing on text analysis, extensive grammar exercises, mechanical memorization of dialogues and phrases, as well as strict control and correction of errors by the teacher, the main emphasis has shifted to the development of communication skills and the direct use of language in real communication. In Russian pedagogical science, the authors of works [6–14] and other researchers have made a significant contribution to the development of the communicative approach.

The concept of communicative competence has been developed in the works of many domestic and foreign scholars, such as [6–9, 12, 13] and others. Most researchers view communicative competence as a complex system which includes various specific competences (subcompetences). Among them are the authors of works [12, 14–17] and other researchers.

Linguistic (language) and pragmatic (speech, sociolinguistic, illocutionary) competences are considered to be two essential components of communicative competences[6,7] [14, 18–20]. Sub-competences have also been identified including: subject-specific (specialized, linguistic-professional, subject-thematic[8, 9], sociocultural[10] [13–15, 18–21]; intercultural [11–15, 19–22]; linguistic-country studies and linguistic-regional studies [13–15, 19]; strategic (compensatory); discursive [17–20]; and others).

The study of the aesthetics of language and speech has a long tradition, encompassing various academic disciplines: philosophy, linguistics, rhetoric, literary studies, and speech culture. Questions of expressiveness and aesthetic value in speech were considered as far back as antiquity [14, 15]. Aristotle, in his works on rhetoric and poetics, distinguished stylistic levels, while Cicero emphasized the role of harmony and elegance in speech. Socrates, in his Panegyric, offered recommendations on euphony and the appropriate use of metaphors. Ancient ideas continue to influence contemporary research on the aesthetics of language [23].

In the Russian tradition, M.V. Lomonosov paid special attention to the quality of speech, distinguishing between “pure” and “impure” speech. In Russian Grammar, he formulated the principles of euphony, logic, and accuracy, warning against excessive consonant clusters and vowel repetitions, which can complicate the perception of the text. Many of his ideas remain relevant in modern linguistics [16].

At the beginning of the 20th century in Russia, when there was active interest in linguistic purity and the improvement of speech aesthetics and speech culture in society, authors[11] [13, 17] contributed to the development of these issues. G.E. Sokolova is particularly noteworthy among contemporary researchers in the field of speech aesthetics education. She writes on the issue of teaching foreigners the basics of Russian speech aesthetics in the context of RFL teaching. In her works, she examines the

[6] Shchukin A.N. *Methods of teaching Russian as a foreign language*: academic textbook for higher education institutions. Moscow: Vysshaya Shkola; 2003. 334 p. (In Russ.).

[7] Balykhina T.M. *Methods of teaching Russian as a non-native* (*new*) *language:* academic textbook for teachers and students. Moscow: RUDN Publ.; 2007. 187 p. (In Russ.).

[8] Shchukin A.N. *Op. cit*.

[9] Riske I.E. *Developing sociocultural competence in senior students using English-language poetry*: Cand. Sci. Thesis (Pedagog.): 13.00.02. St. Petersburg: A.I. Herzen State Pedagogical University; 2000. 16 p. (In Russ.).

[10] *Ibid*.

[11] Vinokur G.O. *On the language of fiction literature*: Textbook for philology majors at universities. Moscow: Vysshaya Shkola; 1991. 448 p. (In Russ.).

historical aspects of language aesthetics, emphasizing their importance in forming the value-based attitude of students towards the Russian language. Particular attention is paid to literary texts as an effective means of assimilating the aesthetic norms of speech. The researcher emphasizes the need to integrate the aesthetic component into the learning process, which contributes not only to the development of language competence, but also to the understanding of the cultural codes of Russian speech [24].

The issue of the communicative-aesthetic principle in teaching Russian to foreign students has been studied in various aspects, but remains insufficiently developed in the context of teaching technical specialists.

E.A. Shesterina's research into the aesthetics of Russian speech (e.g., analysis of German speakers' perceptions) demonstrates the intercultural aspects of phonetic expressiveness perception. However, the results are only indirectly applicable to teaching methods for foreigners focused on technical specialties [25].

Analysis of scientific and academic sub-styles from the perspective of their aesthetic impact highlights the importance of speech aesthetics in scientific activity, while acknowledging that this area has not been sufficiently developed. The problem of scientific style aesthetics, which is important for technical specialties, remains unresolved[12].

The course "Ethics and Aesthetics of Speech"[13] is aimed at students in philology departments and covers the formation of ethical and aesthetic culture in a broad sense. Its approaches can be adapted for the teaching of Russian speech to technical specialists, but they require special methodological development.

The works of O.Yu. Koroleva and O.G. Filippova on the communicative aesthetics of primary school pupils illustrate the development of speech aesthetics in the educational process. However, the age group and cognitive context differs significantly from the tasks facing foreign students of technical specialties [26].

Matters of spoken language aesthetics [27], the didactic requirements for speech aesthetics [28], and the aesthetics and culture of Russian speech [29] are studied primarily from a general linguistic and methodological perspective, without specific reference to teaching Russian to foreign technical specialists [30].

Although studies of speech aesthetics in various aspects (phonetics, scientific speech, pedagogy) have been carried out, the communicative-aesthetic approach to teaching Russian to foreign students of technical specialties requires further development and systematization.

DISCUSSION

M.V. Lomonosov wrote: "Language formation occurs in a specific cultural environment, which determines its unique ways of expressing thought, national metaphors, and literary traditions. Without considering the aesthetic aspect, language learning is reduced to the mechanical mastery of vocabulary and grammar, which makes it difficult to understand the mentality of native speakers" [16]. In Russian, for example, emotionally expressive constructions, artistic means of expression, and idioms which reflect the characteristics of the national worldview play an important role. The works of M.V. Lomonosov state that communicative competence includes not only the transmission of information, but also the creation of aesthetically designed statements which correspond to the norms and traditions of native speakers.

Politeness, speech strategies, and text style vary significantly across cultures. The ignorance of these factors can lead to unnatural speech or even violations of communication norms. The aesthetic component helps in the assimilation of speech etiquette, while facilitating integration into the linguistic environment. In the Russian tradition, for example, imagery, aphorisms, and the use of proverbs and sayings are characteristics which enrich speech and make it more expressive [31].

Creative literature is an important tool for learning a language through culture. It reveals the characteristics of the national character, historical realities, and stylistics of speech, which contributes to the formation of the aesthetic perception of students and their ability to express themselves expressively. Thus, the inclusion of an aesthetic component in the process of teaching foreign languages enables a deeper understanding of the national worldview, the assimilation of cultural values and traditions of communication, making language learning more meaningful and effective [11].

The communicative approach to foreign language teaching aims to develop communicative competence: the ability to engage in speech activity in accordance with the goals and situation of communication [32]. It is characterized by flexibility and the absence of strictly prescribed methods which enables the modeling of real communicative situations [33].

The key principles of the approach include:

- functionality involving the selection and organization of material in accordance with speech functions;

[12] Vadzibov M.D. *Russian language and speech culture. Theoretical material and practical assignments*: academic textbook for bachelor's degree students in the humanities. Saratov: IPR Media; 2019, 207 p. ISBN 978-5-4497-0260-9. https://elibrary.ru/KAFNQS. Accessed April 01, 2025 (in Russ.).

[13] Magomedgadzieva P.N., Magomedova L. *Ethics and aesthetics of speech*: educational and methodological guide. Makhachkala: Dagestan State Pedagogical University; 2021, 54 p. (In Russ.).

- communication modeling, in which the teacher acts as an interlocutor and coordinator, encouraging students to interact;
- situationality which consists in creating communicative conditions for language practice;
- speech orientation, ensuring the use of language as a means of communication;
- the principle of novelty which involves constantly updating topics, tasks, and communication conditions, in order to increase motivation;
- individualization which takes into account the personal characteristics of learners [34–37].

The communicative approach makes language learning a process as close as possible to natural communication, ensuring the development of linguistic and sociocultural skills.

Based on the above information, we can derive the concept of the communicative-aesthetic principle in teaching RFL. It is based on a combination of the functional orientation of language and its aesthetic value and assumes that language acquisition occurs not only through the formation of communicative competence, but also through the development of the ability of learners to express themselves in a stylistically and culturally appropriate manner.

This principle stems from the idea that language is formed in a specific cultural environment and carries unique ways of expressing thoughts, metaphorical models, literary traditions, and means of artistic expression. Without taking the aesthetic aspect into account, language learning is reduced to the mechanical acquisition of vocabulary and grammar. This approach does little to contribute to a full understanding of the mentality of native speakers [16]. The communicative-aesthetic principle includes several key aspects:

1. Developing communication skills through speech aesthetics. The ability not only to convey information, but also to present it in accordance with the norms and traditions of native speakers. This includes politeness, speech strategies, stylistic variability, aphorisms, the use of proverbs, and other means of expression[14].
2. Situationality and communication modeling. Creating learning situations which reflect natural communication conditions in which learners can use language expressively and stylistically appropriately.
3. The role of creative literature. The use of literary texts as a means of studying not only the language, but also national worldview, history, and culture. This contributes to the formation of aesthetic perception of speech and skills for its expressive presentation [35].
4. Sociocultural adaptation through language. Learning the norms of speech etiquette acceptable in Russian-speaking society facilitates integration into the linguistic environment and makes speech natural and harmonious.
5. The aim of the communicative-aesthetic principle is to create conditions in which the Russian language is learned not only through mastering its functional aspects, but also through the aesthetic perception of speech, making the learning process meaningful, profound, and effective [38–42].

Teaching Russian to foreign students in technical fields requires an approach which includes not only the development of language skills, but also the formation of an aesthetic perception of language as a tool for intercultural and professional communication.

The aim of the communicative-aesthetic principle is to integrate the linguistic and aesthetic aspects of learning, contributing to the formation of professionally-oriented language competence. According to G.E. Sokolova, teaching foreign learners the aesthetics of the Russian language plays a key role in developing their ability to understand and master the language at a deeper level. This allows them not only to read and interpret works of Russian literature, but also to express their thoughts in Russian in accordance with the norms of speech etiquette [32].

The aesthetics of speech encompass many aspects, including expressiveness, clarity, accuracy, and harmony of linguistic expression. Developing these qualities in students contributes to the development of their communicative competence, and helps them avoid mechanical language acquisition. The inclusion of elements of literary texts and analysis of works by Russian classics allow students to develop creative thinking, emotional involvement, and interest in the Russian language [43, 44].

One effective method of implementing the communicative-aesthetic principle is the use of literary texts which reveal the beauty of the Russian language. Analysis of texts by K.G. Paustovsky, I.A. Bunin, and other authors, contributes to the formation of a Russian linguistic picture of the world among foreign students. It helps develop their speech ideal, and the ability to evaluate the aesthetic components of speech. The use of pre-text, intra-text, and post-text analysis allows students to consciously perceive speech patterns and use them in their own communication [45–47].

Incorporating aesthetic aspects into teaching helps students develop expressiveness, logical coherence, and persuasiveness in their statements. As G.E. Sokolova notes, studying the aesthetics of language helps students not only improve their oral and written

[14] A.N. Shchukin. *Foreign language teaching: theory and practice*: academic textbook for teachers and students. 2nd ed., revised and expanded. Moscow: Filomaths; 2004, 480 p. (In Russ.).

communication but also fosters a positive motivation for learning Russian. Developing artistic thinking and an emotional understanding of language makes learning more meaningful, and interactions with Russian speech culture more productive [24, 48].

FROM THE EXPERIENCE OF THE DEPARTMENT OF RUSSIAN LANGUAGE (AS A FOREIGN LANGUAGE)

The study places particular emphasis on identifying the influence of the communicative-aesthetic principle on the development of student speech culture and the improvement of their professional communication skills. The development of sustainable skills in expressive, acceptable, and culturally appropriate use of the Russian language facilitates the successful integration of students into the academic and professional environment. It also enhances their communicative competence, and develops their ability to interact interculturally [49].

One of the unique, practice-oriented embodiments of the communicative-aesthetic principle in RFL teaching is the work of the Postscriptum international student theater at MIREA – Russian Technological University. This theater, which brings together students from various countries, represents a multicultural educational space in which theatrical activity is used as effective tool for learning the Russian language as a means of intercultural and professional communication.

The theater's repertoire includes Russian and world classics, as well as contemporary plays, ensuring a rich content, cultural authenticity, and stylistic diversity in the curriculum. The immersive format of the performances involves students in the language environment, activating both receptive and productive speech skills. It contributes to the enhancement of pronunciation and intonation skills, dialogic speech, and expressive reading. Moreover, the theater serves not only as a form of extracurricular practice but also as a platform for developing language culture, emotional intelligence, and teamwork skills.

From a methodological perspective, the activities of Postscriptum theater allow us to consider artistic and verbal practice as an integrative didactic model, combining elements of role-playing, dramatization, and project-based learning. Participation in rehearsals and productions stimulates cognitive and emotional-aesthetic motivation, creates conditions for mastering the norms of literary language, and promotes a deeper understanding of cultural and linguistic realities [34].

The practical significance of theatrical learning lies in the potential for replicating this experience in educational institutions implementing RFL programs for students in engineering and technical fields. In the future, theater may serve as a basis for the creation of elective courses and original teaching aids aimed at integrating theatrical technologies into the development of professionally oriented language skills in international students.

CONCLUSIONS

The communicative-aesthetic principle is an important methodological element in teaching Russian to international students in technical fields. The aim is to integrate linguistic and cultural aspects which not only contributes to the development of professionally oriented language competence but also to a deeper understanding of the culture and traditions of native speakers. Incorporating aesthetic elements of the Russian language into the educational process not only improves language skills but also stimulates the interest of students in Russian literature and culture, making learning more profound and multifaceted.

The development and substantiation of the communicative-aesthetic principle meets modern educational practice requirements, providing a comprehensive approach to developing linguistic competence. It promotes a more complete understanding of language and its connection to culture and society, helping students not only successfully learn the Russian language but also adapt to the Russian-language academic and professional environment. This principle creates the conditions for developing expressive oral communication skills, emotional intelligence, and intercultural interaction skills, making the educational process more meaningful and harmonious.

The implementation of the communicative-aesthetic principle in RFL teaching, based on the practice of the Postscriptum international student theater at MIREA – Russian Technological University, has demonstrated its high level of effectiveness in teaching students majoring in technical fields. Theatrical activities as a multicultural educational platform, promote the active development of all components of verbal competence, foster a strong motivation for learning, and deepen integration into the oral environment.

The aestheticization of speech experience through artistic and speech practice ensures not only the improvement of language skills in accordance with literary norms, but also a deep understanding of cultural and linguistic realities, the emotional involvement of students in the process of learning a language, which in turn increases their motivation and contributes to successful academic adaptation.

Future research prospects include the development of areas related to the integration of dramatized learning into the development of professionally oriented speech in students in technical fields. Important objectives for

continued work will include increasing the amount of instructional time allocated to RFL mastering, as well as creating comprehensive teaching aids, including recommendations for teachers and practice-oriented assignments based on the implementation of the communicative-aesthetic principle.

Authors' contribution
All authors contributed equally to the research work.

REFERENCES

1. Azimov E.G., Shchukin A.N. *Novyi slovar' metodicheskikh terminov i ponyatii* (*teoriya i praktika obucheniya yazykam*) (*New Dictionary of Methodological Terms and Concepts* (*Theory and Practice of Language Teaching*)). Moscow: IKAR; 2010, 446 p. (In Russ.).
2. Abakumova N.N., Malkova I.Iu. *Kompetentnostnyi podkhod v obrazovanii: organizatsiya i diagnostika* (*Competence-Based Approach in Education: Organization and Diagnostics*). Tomsk: Tomsk State University; 2007, 368 p. (In Russ.). https://elibrary.ru/skchxt
3. Bolotov V.A., Serikov V.V., Serikov V.V. *Kompetentnostnaya model': ot idei k obrazovatel'noi paradigme* (*Competence Model: From Idea to Educational Paradigm*). *Pedagogika*. 2003;10:8–14 (in Russ.).
4. Shcherbenko L.R. On the role of professionally oriented texts in the formation of professional communicative competence of students in non-linguistic universities. *Mir Pedagogiki i Psikhologii*. 2022;11(76):229–233 (in Russ.). https://www.elibrary.ru/wukmqc
5. Volkova A.G. Organization of speaking clubs as a way of forming professional foreign language communicative competence of students. In: *Modern Trends in the Development of the System of Foreign Language Training in Non-Linguistic Universities: Regional Practice*. Krasnoyarsk: Krasnoyarsk State Agrarian University; 2022. P. 176–179 (in Russ.). https://www.elibrary.ru/tdrxjv
6. Passov E.I., Kuzovleva N.E. *Osnovy kommunikativnoi teorii i tekhnologii inoyazychnogo obrazovaniya* (*Bases of Communicative Theory and Foreign Language Teaching Techniques*). Moscow: Russkii yazyk. Kursy; 2010, 568 p. (In Russ.).
7. Kulaeva G.M. System for developing foreign students' ideas about the linguistic aesthetic ideal. In: *Russian Language: Problems of Functioning and Teaching Methodology at the Present Stage: Proceedings of the International Scientific and Practical Conference.* Penza; 2009. P. 233–235 (in Russ.). https://www.elibrary.ru/vmajmp
8. Genzel Ya. Teaching Russian as a Foreign Language by the Reproductive-Creative Method. *Russkii yazyk za rubezhom* = *Russian Language Abroad*. 1988;2:49–53 (in Russ.).
9. Passov E.I., Kuzovleva N.E. *Urok inostrannogo yazyka* (*Foreign Language Lesson*). Rostov-on-Don: Feniks; Moscow: Glossa-Press; 2010, 640 p. (In Russ.).
10. Vereshchagin E.M., Kostomarov V.G. *Yazyk i kultura* (*Language and Culture*). Moscow: Russkii yazyk; 1990, 247 p. (In Russ.).
11. Markova A.K. *Psikhologiya usvoeniya yazyka kak sredstva obshcheniya* (*Psychology of Language Acquisition as a Means of Communication*). Moscow: Pedagogika; 1974, 234 p. (In Russ.).
12. Shchepilova A.B. *Kommunikativno-kognitivnyi podkhod k obucheniyu frantsuzskomu yazyku kak vtoromu inostrannomu* (*Communicative-Cognitive Approach to Teaching French as a Second Foreign Language*). Moscow: Shkol'naya kniga; 2003, 488 p. (In Russ.).
13. Shcherba L.V. On the triple aspect of linguistic phenomena and experiments in linguistics. In: Zvegintsev V.A. (Ed.). *Istoriya yazykoznaniya 19 i 20 vekov v ocherkakh i izvlecheniyakh* (*History of Linguistics in the 19th and 20th Centuries in Essays and Extracts*). Moscow; 1960. P. 301–312 (in Russ.).
14. Shcherba L.V. *Yazykovaya sistema i rechevaya deyatel'nost'* (*Language System and Speech Activity*). Moscow: Editorial URSS; 2004, 344 p. (In Russ.).
15. Leont'ev A.A. *Osnovy psikholingvistiki* (*Fundamentals of Psycholinguistics*). Moscow: Smysl, St. Petersburg: Lan; 2003, 285 p. (In Russ.).
16. Lomonosov M.V. *Trudy po filologii 1739–1758 gg* (*Works on Philology*, *1739–1758*). Moscow–Leningrad; 1952, 996 p. (In Russ.).
17. Lunacharskii A.V. *Osnovy pozitivnoi ehstetiki* (*Fundamentals of Positive Aesthetics*). Moscow: URSS: Librokom; 2011, 189 p. (In Russ.).

18. Chuvaeva K.M. Forming communicative competence of international students in the course of Russian language at the initial stage of pre-university program. *Izvestiya Volgogradskogo gosudarstvennogo tekhnicheskogo universiteta. Seriya: Problemy sotsial'no-gumanitarnogo znaniya.* 2013;12(2(105)):69–73 (in Russ.). https://www.elibrary.ru/qbmiyn
19. Shokanova R.D., Tarasova E.N. Reproductive method in teaching Russian as a foreign language and its innovative aspects. *Russian Technological Journal.* 2021;9(3):98–107 (in Russ.). https://doi.org/10.32362/2500-316X-2021-9-3-98-107
20. Chernova N.I., Ivanova E.A., Bogush N.B., Katakhova N.V. Technology for determining non-humanities university students' cognitive-and-psychological characteristics. *Russian Technological Journal.* 2023;11(3):104–116. https://doi.org/10.32362/2500-316X-2023-11-3-104-116
21. Kulaeva G.M. The role of foreign students' ideas about the Russian linguistic aesthetic ideal in improving their language and communicative competence. In: *Russkii yazyk kak predmet obucheniya v vysshikh uchebnykh zavedeniyakh* (*Russian Language as a Subject of Teaching in Higher Education*). Lublin; 2013. P. 197–203 (in Russ.).
22. Dorfman O.V., Chernova O.E. Development of the communicative competence of students of technical universities as a strategy for teaching effective communication. *Litera*. 2022;4:27–35 (in Russ.). https://doi.org/10.25136/2409-8698.2022.4.37806, https://www.elibrary.ru/gmhglm
23. Bim I.L. Some current problems of modern foreign language teaching. *Inostrannye yazyki v shkole = Foreign Languages in School*. 2001;4:5–8 (in Russ.).
24. Sokolova G.E. Studying the history of the aesthetics of the Russian language and speech in classes with foreign students. *Nauka i shkola = Science and School*. 2019;6:208–219 (in Russ.). https://www.elibrary.ru/kksocb
25. Shesterina E.A. Aesthetic perception of the Russian sound speech by Germans (a case study of German internet forums). *Filologicheskie nauki v MGIMO = Linguistics & Polyglot Studies*. 2021;7(5):102–110 (in Russ.). https://doi.org/10.24833/2410-2423-2021-5-29-102-110, https://www.elibrary.ru/qprzyj
26. Koroleva O.Iu., Filippova O.G. Social situations of communication as a condition for the effective development of the communicative aesthetics of speech of younger schoolchildren. *Obrazovanie i vospitanie doshkol'nikov, shkol'nikov, molodezhi: teoriya i praktika*. 2024;2:43–50 (in Russ.). https://www.elibrary.ru/wirdjr
27. Multatuli V.M. The aesthetics of spoken language in the contemporary situation of the Russian language. *Vestnik Sankt-Peterburgskogo universiteta. Istoriya = Vestnik of St. Petersburg University. History*. 2006;1:73–82 (in Russ.). https://www.elibrary.ru/rttcnj
28. Vyatyutnev M.N. *Teoriya uchebnika russkogo yazyka kak inostrannogo* (*metodicheskie osnovy*) (*The Theory of the Textbook of Russian as a Foreign Language: Methodological Foundations*). Moscow: Russkii yazyak; 1984, 144 p. (In Russ.). https://www.elibrary.ru/sdihee
29. Dmitrieva L.I. Russian Speech: Aesthetics and Culture. *Nauchnyi al'manakh = Science Almanac*. 2017;8-1(34): 98–100 (in Russ.). https://www.elibrary.ru/zibyrj
30. Safonova V.V. *Izuchenie yazykov mezhdunarodnogo obshcheniya v kontekste dialoga kul'tur i tsivilizatsii* (*Studying Languages of International Communication in the Context of Dialogue of Cultures and Civilizations*). Voronezh: Istoki; 1996, 238 p. (In Russ.).
31. *Techniques & Principles in Language Teaching*. Oxford: Oxford University Press; 2011. P. 152, 161–164.
32. Sokolova G.E. Teaching the basics of speech aesthetics to foreign students in Russian language classes. In: *Modern Technologies in Teaching Russian: Proceedings of the International Scientific and Practical Conference.* Moscow: Moscow Pedagogical State University; 2020. P. 479–482 (in Russ.). https://www.elibrary.ru/qzanvb
33. Galperin P.Ia. New leaning opportunities, in particular, foreign languages. In: *Issues of Foreign Language Teaching Methodology in Non-Linguistic University Faculties.* Moscow: MGU Press; 1971. P. 50–57 (in Russ.).
34. Passov E.I. *Kommunikativnyi metod obucheniya inoyazychnomu govoreniyu* (*Communicative Method of Teaching Foreign Language Speaking*). Moscow: Prosveshchenie; 1991. P. 32–33 (in Russ.).
35. Galskova N.D., Gez N.I. *Teoriya obucheniya inostrannym yazykam. Lingvodidaktika i metodika* (*Theory of Teaching Foreign Languages. Linguodidactics and Methodology*). Moscow: Akademiya; 2013, 336 p. (In Russ.).
36. Brown G. *Speakers, Listeners and Communication*. *Explorations in Discourse Analysis*. Cambridge: Cambridge University Press; 1995, 261 p.
37. Brumfit G.F., Jonson K. *The Communicative Approach to Language Teaching*. Oxford: Oxford University Press; 1979, 243 p.
38. Goethals M. *Creative and Cognitive Foreign Language Learning. Int. J. Appl. Linguistics*. 1977;36(1):3–44. https://doi.org/10.1075/itl.36.01goe
39. Ter-Minasova S.G. *Yazyk i mezhkulturnaya kommunikatsiya* (*Language and Intercultural Communication*). Moscow: Slovo; 2000, 261 p. (In Russ.).
40. Tarasov E.F. *Iazyk kak sredstvo transliatsii kultury* (Language as a Means of Cultural Transmission). *Kulturologiia. Daidzhest* (*Culturology. Digest*). 2002;2:95–97 (in Russ.).
41. Kitaigorodskaya G.A. Communicative approach to developing a system of exercises (a brief historical overview). *Vestnik Moskovskogo universiteta. Seriya 19. Lingvistika i mezhkulturnaya kommunikatsiya = Moscow University Bulletin. Series 19. Linguistics and Intercultural Communication*. 2001;2:7–14 (in Russ.).
42. Kostomarov V.G. Language. Culture. Civilization. *Vestnik Moskovskogo universiteta. Seriya 20. Pedagogicheskoe obrazovanie = Lomonosov Pedagogical Education Journal*. 2007;2:93–102 (in Russ.). https://www.elibrary.ru/iceuel

43. Zhinkin N.N. Intellect, Language and Speech. In: R.A. Belova-David (Comp.). *Narushenie rechi u doshkol'nikov* (*Speech Disorders in Preschoolers*). Moscow: Prosveshchenie; 1972. P. 9–31 (in Russ.).
44. Ievleva Z.N. Grammatical content of communicative-oriented teaching of Russian as a foreign language. In: *Metodika prepodavaniya russkogo yazyka kak inostrannogo. Khrestomatiya* (*Methodology of Teaching Russian as a Foreign Language. Anthology*). Yekaterinburg: Ural State University; 2008. P. 14–36 (in Russ.).
45. Anisimova I.M. *Magiya obshcheniya. Istoriya i praktika ehtiketa* (*The Magic of Communication. History and Practice of Etiquette*). Moscow: Zvonnitsa-MG; 2004, 480 p. (In Russ.).
46. Abdraimov K.A. The aesthetics of speech, delivered didactic requirements. *Nauka i novye tekhnologii = Science and New Technologies*. 2013;1:276–279 (in Russ.). https://elibrary.ru/vzjrjd
47. Deikina A.D., Kulaeva G.M. Formation notions about aesthetic ideal in process of teaching Russian language as foreign language. *VESTNIK RUDN. Seriya "Voprosy obrazovaniya: yazyki i spetsial'nost'" = RUDN Journal of Language Education and Translingual Practices*. 2007;2:49–54 (in Russ.). https://elibrary.ru/mstkov
48. Sokolova G.E. Literary texts as a means of teaching foreign students aesthetics of the Russian language and speech. *Prepodavatel' XXI Vek. Russian Journal of Education*. 2021;4-1:240–247 (in Russ.). https://doi.org/10.31862/2073-9613-2021-4-240-247, https://elibrary.ru/wakhvb
49. Kononenko T.A., Lyashenko A.V., Pritula O.Yu., Belyaeva S.Yu. Aesthetics of Scientific Speech. *Student i nauka = Student and Science*. 2022;1(20):39–45 (in Russ.). https://elibrary.ru/osypou

СПИСОК ЛИТЕРАТУРЫ

1. Азимов Э.Г., Щукин А.Н. *Новый словарь методических терминов и понятий* (теория и практика обучения языкам). М.: ИКАР; 2010, 446 с.
2. Абакумова Н.Н., Малкова И.Ю. *Компетентностный подход в образовании: организация и диагностика.* Томск: Томский гос. ун-т; 2007, 368 с.
3. Болотов В.А., Сериков В.В. Компетентностная модель: от идеи к образовательной парадигме. *Педагогика*. 2003;10:8–14. https://elibrary.ru/skchxt
4. Щербенко Л.Р. О роли профессионально-ориентированных текстов в формировании профессиональной коммуникативной компетенции обучающихся неязыковых вузов. *Мир педагогики и психологии*. 2022;11(76):229–233. https://www.elibrary.ru/wukmqc
5. Volkova A.G. Organization of speaking clubs as a way of forming professional foreign language communicative competence of students. В сб.: *Современные тенденции развития системы подготовки обучающихся по иностранному языку в неязыковом вузе: региональная практика: Материалы всероссийской* (*национальной*) *научной конференции*, Красноярск, 10–11 ноября 2022 г. Красноярск: Красноярский государственный аграрный университет; 2022. P. 176–179. https://www.elibrary.ru/tdrxjv
6. Пассов Е.И., Кузовлева Н.Е. *Основы коммуникативной теории и технологии иноязычного образования*. М.: Русский язык. Курсы; 2010, 568 с.
7. Кулаева Г.М. Система работы по формированию представлений иностранных учащихся о языковом эстетическом идеале. В сб.: *Русский язык: проблемы функционирования и методики преподавания на современном этапе: Материалы Международной научно-практической конференции,* Пенза, 18–20 мая 2009 г. Пенза; 2009. С. 233–235. https://www.elibrary.ru/vmajmp
8. Генцель Я. Обучение русскому языку как иностранному репродуктивно-креативным методом. *Русский язык за рубежом*. 1988;2:49–53.
9. Пассов Е.И., Кузовлева Н.Е. *Урок иностранного языка*. Ростов-на-Дону: Феникс; М.: Глосса-Пресс; 2010, 640 с.
10. Верещагин Е.М., Костомаров В.Г. *Язык и культура.* М.: Русский язык; 1990, 247 с.
11. Маркова А.К. *Психология усвоения языка как средства общения*. М.: Педагогика; 1974, 239 с.
12. Щепилова А.В. *Коммуникативно-когнитивный подход к обучению французскому языку как второму иностранному*. М.: Школьная книга; 2003, 488 с.
13. Щерба Л.В. О трояком аспекте языковых явлений и об эксперименте в языкознании. В кн.: Звегинцев В.А. *История языкознания 19 и 20 веков в очерках и извлечениях.* М.; 1960. С. 301–312.
14. Щерба Л.В. *Языковая система и речевая деятельность*. М.: Едиториал УРСС; 2004, 344 с.
15. Леонтьев А.А. *Основы психолингвистики*. М.: Смысл; СПб.: Лань; 2003, 285 с.
16. Ломоносов М.В. *Труды по филологии* 1739–1758 гг. М.–Л.; 1952, 996 с.
17. Луначарский А.В. *Основы позитивной эстетики*. М.: URSS: Либроком; 2011, 189 с.
18. Чуваева К.М. Формирование коммуникативной компетенции иностранных учащихся в курсе русского языка на начальном этапе подготовки в вузах Российской Федерации. *Известия Волгоградского государственного технического университета. Серия: Проблемы социально-гуманитарного знания*. 2013;12(2(105)):69–73. https://www.elibrary.ru/qbmiyn
19. Шоканова Р.Д., Тарасова Е.Н. Репродуктивный метод в обучении иностранных студентов русскому языку и его инновационные аспекты. *Russian Technological Journal*. 2021;9(3):98–107. https://doi.org/10.32362/2500-316X-2021-9-3-98-107

20. Чернова Н.И., Иванова Е.А., Богуш Н.Б., Катахова Н.В. Технология определения когнитивно-психологических особенностей студентов негуманитарного вуза. *Russian Technological Journal.* 2023;11(3):104–116. https://doi.org/10.32362/2500-316X-2023-11-3-104-116
21. Кулаева Г.М. Роль представлений иностранных студентов о русском языковом эстетическом идеале в повышении уровня их языковой и коммуникативной компетенции. В кн.: *Ezyk rosyjski jako przedmiot nauczanie wszkole wyzszej* (*Русский язык как предмет обучения в высших учебных заведениях*). Lublin; 2013. С. 197–203.
22. Дорфман О.В., Чернова О.Е. Развитие коммуникативной компетенции студентов технических вузов как стратегия обучения эффективной коммуникации. *Litera.* 2022;4:27–35. https://doi.org/10.25136/2409-8698.2022.4.37806, https://www.elibrary.ru/gmhglm
23. Бим И.Л. Некоторые актуальные проблемы современного обучения иностранным языкам. *Иностранные языки в школе.* 2001;4:5–8.
24. Соколова Г.Е. Изучение истории эстетики русского языка и речи на занятиях с иностранными студентами. *Наука и школа*. 2019;6:208–219. https://www.elibrary.ru/kksocb
25. Шестерина Е.А. Представления немцев об эстетике звучания русской речи (на материале немецких интернет-форумов). *Филологические науки в МГИМО*. 2021;7(5(29)):102–110. https://doi.org/10.24833/2410-2423-2021-5-29-102-110, https://www.elibrary.ru/qprzyj
26. Королева О.Ю., Филиппова О.Г. Социальные ситуации общения как условие эффективности развития коммуникативной эстетики речи младших школьников. *Образование и воспитание дошкольников, школьников, молодежи: теория и практика.* 2024;2:43–50. https://www.elibrary.ru/wirdjr
27. Мультатули В.М. Эстетика разговорной речи к современной ситуации русского языка. *Вестник Санкт-Петербургского университета. История*. 2006;1:73–82. https://www.elibrary.ru/rttcnj
28. Вятютнев М.Н. *Теория учебника русского языка как иностранного* (методические основы). М.: Русский язык; 1984, 144 с. https://www.elibrary.ru/sdihee
29. Дмитриева Л.И. Русская речь: эстетика и культура. *Научный альманах*. 2017;8-1(34):98–100. https://www.elibrary.ru/zibyrj
30. Сафонова В.В. *Изучение языков международного общения в контексте диалога культур и цивилизаций*. Воронеж: Истоки; 1996, 238 с.
31. *Techniques & Principles in Language Teaching*. Oxford: Oxford University Press; 2011. P. 152, 161–164.
32. Соколова Г.Е. Обучение основам эстетики речи иностранных учащихся на занятиях по РКИ. В сб.: *Современные технологии в преподавании русского языка: сборник материалов Международной научно-практической конференции.* М.: Московский педагогический государственный университет; 2020. С. 479–482. https://www.elibrary.ru/qzanvb
33. Гальперин П.Я. Новые возможности обучения, в частности, иностранным языкам. В кн.: *Вопросы методики преподавания иностранных языков на неязыковых факультетах университетов*. М.: МГУ; 1971. С. 50–57.
34. Пассов Е.И. *Коммуникативный метод обучения иноязычному говорению*. М.: Просвещение; 1991. С. 32–33.
35. Гальскова Н.Д., Гез Н.И. *Теория обучения иностранным языкам. Лингводидактика и методика*. М.: Издательский центр «Академия»; 2013, 336 с.
36. Brown G. *Speakers, Listeners and Communication*. *Explorations in Discourse Analysis*. Cambridge: Cambridge University Press; 1995, 261 p.
37. Brumfit G.F., Jonson K. *The Communicative Approach to Language Teaching*. Oxford: Oxford University Press; 1979, 243 p.
38. Goethals M. *Creative and Cognitive Foreign Language Learning. Int. J. Appl. Linguistics*. 1977;36(1):3–44. https://doi.org/10.1075/itl.36.01goe
39. Тер-Минасова С.Г. *Язык и межкультурная коммуникация*. М.: Слово; 2000, 264 с. https://www.elibrary.ru/yqozjo
40. Тарасов Е.Ф. Язык как средство трансляции культуры. *Культурология. Дайджест*. 2002;2:95–97.
41. Китайгородская Г.А. Коммуникативный подход к созданию системы упражнений (небольшой исторический экскурс). *Вестник Московского университета.* Серия 19. *Лингвистика и межкультурная коммуникация*. 2001;2:7–14.
42. Костомаров В.Г. Язык. Культура. Цивилизация. *Вестник Московского университета. Серия 20. Педагогическое образование*. 2007;2:93–102. https://www.elibrary.ru/iceuel
43. Жинкин Н.Н. Интеллект, язык и речь. В кн.: сост. Р.А. Белова-Давид. *Нарушение речи у дошкольников.* М.: Просвещение; 1972. С. 9–31.
44. Иевлева З.Н. Грамматическое содержание коммуникативно-ориентированного обучения русскому языку как иностранному. В кн.: *Методика преподавания русского языка как иностранного*. *Хрестоматия*. Екатеринбург: УГУ им. М. Горького; 2008. С. 14–36.
45. Анисимова И.М. *Магия общения. История и практика этикета.* М.: Звонница-МГ; 2004, 480 с.
46. Абдраимов К.А. Эстетика речи и предъявляемые к ней дидактические требования. *Наука и новые технологии*. 2013;1:276–279. https://elibrary.ru/vzjrjd
47. Дейкина А.Д., Кулаева Г.М. Формирование представлений об эстетическом идеале в процессе обучения русскому языку как иностранному. *ВЕСТНИК РУДН. Серия «Вопросы образования: языки и специальность»*. 2007;2:49–54. https://elibrary.ru/mstkov

48. Соколова Г.Е. Художественные тексты как средство обучения эстетике русского языка и речи иностранных учащихся. *Преподаватель XXI век*. 2021;(4-1):240–247. https://doi.org/10.31862/2073-9613-2021-4-240-247, https://elibrary.ru/wakhvb
49. Кононенко Т.А., Ляшенко А.В., Притула О.Ю., Беляева С.Ю. Эстетика научной речи. *Студент и наука*. 2022;1(20):39–45. https://elibrary.ru/osypou

About the Authors

Elena N. Tarasova, Dr. Sci. (Ped.), Head of the Department of Russian Language (as a Foreign Language), Institute of International Education, MIREA – Russian Technological University (78, Vernadskogo pr., Moscow, 119454 Russia). E-mail: tarasova_e@mirea.ru. RSCI SPIN-code 6286-0426, https://orcid.org/0000-0002-2942-9586

Zhanna O. Moskvina, Cand. Sci. (Philol.), Associate Professor, Department of Russian Language (as a Foreign Language), Institute of International Education, MIREA – Russian Technological University (78, Vernadskogo pr., Moscow, 119454 Russia). E-mail: moskvina@mirea.ru. RSCI SPIN-code 7009-7666, https://orcid.org/0009-0002-0111-6681

Об авторах

Тарасова Елена Николаевна, д.пед.н., доцент, заведующая кафедрой русского языка (как иностранного), Институт международного образования, ФГБОУ ВО «МИРЭА – Российский технологический университет» (119454, Россия, Москва, пр-т Вернадского, д. 78). E-mail: tarasova_e@mirea.ru. SPIN-код РИНЦ 6286-0426, https://orcid.org/0000-0002-2942-9586

Москвина Жанна Олеговна, к.филол.н., доцент, кафедра русского языка (как иностранного), Институт международного образования, ФГБОУ ВО «МИРЭА – Российский технологический университет» (119454, Россия, Москва, пр-т Вернадского, д. 78). E-mail: moskvina@mirea.ru. SPIN-код РИНЦ 7009-7666, https://orcid.org/0009-0002-0111-6681

Translated from Russian into English by Lyudmila O. Bychkova
Edited for English language and spelling by Dr. David Mossop

MIREA – Russian Technological University.
78, Vernadskogo pr., Moscow, 119454 Russian Federation.
Publication date January 30, 2026.
Not for sale.

МИРЭА – Российский технологический университет.
119454, РФ, г. Москва, пр-т Вернадского, д. 78.
Дата опубликования 30.01.2026 г.
Не для продажи.

https://www.rtj-mirea.ru